proper name

A Field Study on the Water Use of a Dalea Scoparia Plant in the Northern Chihuahuan Desert

Submitted by

Barbara J. Kickham

In Partial Fulfillment of the Requirements for
the Degree of Master of Science in Hydrology

New Mexico Institute of Mining and Technology

Socorro, New Mexico

April, 1987

Table of Contents

LIST OF FIGURES

LIST OF TABLES

ACKNOWLEDGEMENTS

First of all I need to thank my advisor Daniel B. Stephens, Ph.D., who had the initial ideas for the research project and who kept me employed during most of my graduate study. I would like to extend another thank you to the New Mexico Bureau of Mines and Mineral Resources for the 1986 Summer Research Grant. Without the generous help of Warren Cox, James Mc Cord, Robert Knowlton, Jr., and of course the rest of my colleagues and friends at Tech, this thesis would have been infinitely more difficult to finish, and a lot less enjoyable. Thomas Duval was, and continues to be, a constant and unusual source of energy and insight. Extra special thanks go to my parents, Ed and Monica, because they have been with me through it all.

ABSTRACT

Water uptake by desert plants is highly relevant to groundwater recharge studies in arid climates. The amount of recharge, or drainage, that occurs beneath the zone of evaporation and root absorption is measureably affected by the extent of vegetation. The use of water by common desert vegetation has not been evaluated or quantified to a significant extent by previous investigations.

A field study was conducted to examine the evapotranspiration of a lavender bush (Dalea scoparia) on a sand dune at the Sevilleta National Wildlife Refuge near Socorro, New Mexico. The plant selected is isolated from adjacent vegetation. Depth to water in the area is approximately 20 meters below land surface. The site was equipped with nine neutron access tubes and 36 tensiometers placed on three transects radial to the canopy of the plant. Throughout the study period, March 1985 to June 1986, the soil surrounding the plant was monitored for changes in moisture content and soil-pressure gradients.

The moisture content and pressure-head measurements and meteorological data show that soil-water movement depends on precipitation, evaporation, root transpiration, and topography. The parameters which exert the dominant influence on soil-water movement vary seasonly. For example, significant soil-water movement toward the plant occurs in the spring and prior to blossom development. After rain events and during prolonged dry

periods, vertical components of soil-water movement dominate. Evidence from the study indicated that water withdrawal by roots was influenced by soil-moisture content and therefore was not uniform either spatially nor temporally.

The results of water balance around the edge of the plant canopy indicated that losses to evapotranspiration occur primarily between May and October. The water balance method proved to be inadequate for estimating the actual rate of evapotranspiration due to the time lag occurring between precipitation and infiltration. However, this method was successful in detecting seasonal variations in water use as well as estimating evapotranspiration over the entire year as a percent of precipitation.

INTRODUCTION

Desert plants experience extreme fluctuations in heat and soil-moisture storage and yet continue to thrive and flourish. Each physical aspect of a desert plant is in someway related to its survival mechanisms. Very few biological or hydrological studies have concentrated on the unique adaptive strategies of desert plants. Rather, a heavy emphasis has been placed on the consumptive water use of irrigated and nonirrigated croplands. Only recently have efforts been shifting towards trying to understand the effects of soil-water availability to plants under natural desert conditions.

Understanding the interaction between vegetation and soil-water, especially in semi-arid or arid climates, is important for many reasons. For instance, a study by Stephens and Knowlton (1986) determined that significant recharge is occuring in the desert near Socorro, New Mexico. However, one problem they felt should be addressed further, was the calculation of actual water loss to vegetation. Battelle-Pacific Northwest Laboratories (Kirkham and Gee, 1983) as part of a comprehensive study to locate a repository for radioactive waste, examined the relationships of vegetation, soil, and water. They concluded for the semi-arid study site near Richland, WA, that there was no "significant" water movement below the root zone. A similar study conducted by Los Alamos Laboratories (Perkins and De Poorter, 1985) concluded that plants impede the overall transport

of soluble toxic materials by reducing soil-moisture content. The degree to which toxic materials are immobilized at the surface is highly dependent on water content, maximum rooting depth, and soil type. In addition to the above reasons, interests are growing in preserving the desert in its natural state, increasing the amount of available water yield, and preventing further desertification of lands.

The intent of this paper is to show the relationships between a plant (Dalea scoparia) and the soil, water, and atmosphere surrounding it. Relatively short one year studies, such as this, may help to develop models to predict evapotranspiration over longer times and larger areas. Modeling efforts to date, have encountered many difficulties due to the large number of unknowns and high variability in plant water-use (Molz and Remson, 1971; Nimah and Hanks, 1973; Neuman et al., 1975; Narasimhan and Witherspoon, 1977). However, somewhat more success has been achieved in agricultural studies and with more data it may prove possible to apply these models to desert situations.

Water Uptake By Plant Roots

Knowledge of the processes by which plants obtain and use soil water is essential to understanding the interactions of soil, plant, water, and environment. The adaptations of desert plants to extreme fluctuations in water availability and tempera-

ture are particularly interesting. The tenuous existence of desert plants makes predicting their water use more difficult. Some questions that should be addressed include: how and why plants control transpiration rates, and what are the factors controlling water-use efficiency, root density, and root distribution. By combining soil physics and plant physiology we might obtain new insights into quantification of evapotranspiration.

Plant-Water Potential. The diffusion pressure, or potential, controls water movement within plant-cell walls and is dependent on the osmotic, matric, and turgor pressures (Hillel, 1980).

$$\psi_{diffusion} = \psi_{osmotic} + \psi_{matric} + \psi_{turgor} \qquad (1.1)$$

The osmotic pressure, created by the cell solution, affects water movement from soil to plant. In general, soil-water has a lower concentration than plant-water, hence water moves towards the roots. In extremely saline soils, a reverse osmotic potential may occur in which case plants lose water and wilt. The matric potential is the affinity of plant tissues for water which allows plants to imbibe water. The turgor pressure is the pressure exerted on the walls of cells, opposing the matric and osmotic potentials. The sum of these pressures must be low enough to maintain a gradient between leaf, root, and soil (figure 1).

Water Collection by Roots. The rate of water uptake by

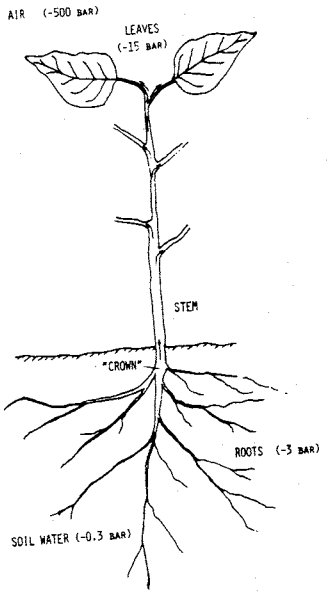

Figure 1. Schematic ilustration of the water potential from root to air (Hillel, 1980).

plant roots is controlled by the hydraulic properties of the soil, the pressure, or resistance, in the plant stem, and the density of roots (Gardner, 1964). For some grasses and in agricultural experiments the root density may be assumed to be uniform. In field situations it is more appropriate to divide the root structure into two separate regions. An upper region, which contains abundant lateral roots, is far more dense than the lower region. Following rainfalls, the lateral roots in the upper region deplete soil moisture before great losses occur due to evaporation and seepage. The lower root profile generally consists of one or more tap roots which draw water from deep regions when surface soil moisture is low (Gardner and Ehlig, 1963).

The governing flow equation for flow to a single root is

(Gardner, 1960)

$$\partial\theta/\partial t = 1/r\ \partial/\partial r(r\ D(\theta)\ \partial\theta/\partial r) \qquad (1.2)$$

where:

D = diffusivity [L^2/T]

r = radial distance from root axis [L]

t = time [T]

The assumptions of the equation are that the root has a uniform cylindrical geometry, an infinite length, and a constant water content surrounding it.

It has long been recognized that an individual root's ability to absorb water is not uniform along its length (Molz, 1971). The epidermis, cortex, and endodermis (outer layers of a root) do not have uniform permeability to water. The most permeable region along a root is actually the new growth just behind the root tip.

Recent experiments applying Computer Assisted Tomography (CAT) to x-ray attenuation have produced new evidence that water uptake does not occur uniformly over the entire root. This method is capable of measuring changes in water content to 0.006 g/cm^3 over distances of 1.5 mm. The findings of the study conducted on radish roots (Raphanus sativus cv long scarlet) showed that water uptake depends on soil-moisture and temperature which vary around the root (Hainsworth and Aylmore, 1986). The results of analytical solutions, based on equation 1.2, were compared to the results of the CAT method. Analytical solutions

were found unsatisfactory for detailing moisture content distribut around the root, primarily due to the assumption that a root has uniform permeability along its length.

Diffusivity varies significantly with water content and soil-suction therefore equation 1.2 is difficult to solve. An alternative approach is to consider the total water extracted, r_z [1/T], and integrate it through different soil depths containing various root densities (van Bavel et al., 1968).

$$r_z = \partial\theta/\partial t - \partial v/\partial z \tag{1.3}$$

where v = flux density [volume/time/area]

The cumulative water uptake per unit surface area of the root, R_z [L/T], may then be expressed

$$R_z = \int_0^z r_z \, dz \tag{1.4}$$

An accurate analysis of root distribution must incorporate changes both in time and space. The actual root density may not always be reflected by the soil-water gradients. Molz (1971) derived an "effective root distribution" to explain discrepancies between observed root distributions and water uptake patterns. Based on numerical and experimental work, he was able to quantify actual water uptake rates by combining data on soil-moisture loss and observed root distributions.

Transpiration. In all plant life there is a continuous

source of water which moves from the soil water at the roots to the vapor within the leaves. This water movement through the plant occurs due to the decreasing diffusion pressure inside plant cells from the roots to the leaves. On the surface of the leaves, water is evaporated off by way of transpiration through the stomates. The flow of water vapor through the plant membrane may be expressed (Wilkins, 1984)

$$q = \Delta\psi L_p \tag{1.5}$$

where:

q = flux of water [L/T]

$\Delta\psi$ = difference in effective water potential

L_p = hydraulic conductance [L/T]

The rate of plant transpiration varies through time and space, however, it does occur at nearly all times. Transpiration accounts for the loss of up to 98% of all water imbibed by plant roots, whereas photosynthetic activity requires only about 1% of the water taken up.

The factors affecting transpiration rates are primarily the stomatal condition and the gradient of diffusion pressure of water vapor within plant-cell walls. (Greulach, 1967). Transpiration occurs mainly through stomatal pores. The stomates will remain open as long as "guard cells" are turgid. As turgor pressure increases, thinner portions of the cell walls are stretched and thicker parts cup inward opening stomatal pores.

During dry soil conditions, a loss in turgor pressure will

close stomates, thereby reducing or stopping transpiration. The temperature within the plant-cell walls will increase, and permanent wilting (unrecoverable damage to plant tissue) occurs if the turgor pressure is not restored soon (Denmead and Shaw, 1962). By halting transpiration, and therefore water loss, pressure within the plant will increase. During the dry season, when temperature and solar radiation are maximum, many desert plants have been observed to temporarily cease transpiration (Whitford, 1986). This defense mechanism allows the plant to conserve a limited water supply without doing permanent internal damage to tissues.

Plants which are tolerant to conditions of water stress also have very slow growth rates. When soil-water content is low, photosynthesis is limited, as is the amount of carbon available for shoot growth (Whitford, 1986). With low water availability the gradient between the water tension in the stem and the water tension at the root-soil contact is reduced, thus decreasing the flux of water to the root. It has also been observed that plants subjected to limited soil water have more dense rooting structures than those with unlimited water supplies (Passiora, 1981). During drought, a greater number of roots are necessary to meet plant-water demands. Increasing the density of the root zone may also increase the permeability of the soil thereby making water more available to the plant. However, the increase in root growth with decreasing soil water is applicable only for water contents above the wilting point of the plant.

Location has a very pronounced effect on transpiration and soil-water use. For example, a plant located on the crest of a hillslope will have a much higher transpiration rate than the identical plant growing at the base (Sharp and Davies, 1985). A plant unprotected by adjacent vegetation or topography will transpire more than a protected plant due to the increased effects of wind and solar radiation. A plant exposed to afternoon sunlight experiences a vastly different set of atmospheric conditions than one protected from it. Cumulative solar radiation, air and soil temperature, relative humidity, and wind velocity are all factors that vary substantially within a 24 hour period and effect soil evaporation and water uptake by plant roots.

Related Research

Evapotranspiration of vegetation, both cultivated and wild, is difficult to quantify. Measuring the rate of uptake of soil water to plant roots depends on location, atmospheric conditions, and the physiology of the plant itself. Methods used to estimate evapotranspiration require a great deal of instrumentation and an extensive data base. Moreover, it is difficult to extend these estimates to other circumstances where environmental factors vary.

Many studies reviewed in the literature have utilized soil physical techniques to measure soil-water depletion. Depletion

includes deep percolation, root absorption, and evaporation. The focus of most studies is the moisture redistribution of irrigated plots. Using irrigated fields simplifies calculations because the initial moisture content is fairly uniform, a known volume of water is infiltrated, and the density of vegetation is fairly uniform throughout the site.

Agricultural Related Research. Research concerning plant transpiration and agricultural water needs began as a tool for scheduling irrigations. An early attempt to determine the transpiration of alfalfa was determined through the use of destructive sampling (Ogata et al., 1960). Soil moisture was found to be the limiting factor in the actual rate of transpiration. Decreases in soil moisture and pressure head in the root zone, as a result of evapotranspiration, caused an increased impedence of water flux through the soil to the plant roots.

A study conducted by van Bavel and others (1968a) concentrated on the problem of separating drainage and consumptive use of water in an irrigated sorghum plot. The problem they encountered was in extrapolating the soil moisture versus hydraulic conductivity curves for the very dry regions near the surface. Measurement of the hydraulic flux is dependent on an accurate determination of moisture, or pressure, versus hydraulic conductivity. However, the predicted root absorption rate versus depth produced the expected distribution. That is, the rate of water loss was initially highest near the surface and as soil moisture

was depleted, the hydraulic conductivity and flux decreased. It was concluded that the predicted root absorption rates were probably not the actual rates, but were proportional to them.

The influence of drying on the root growth of maize plants (Zea mays L.) was compared to similar well-watered plants (Sharp and Davies, 1985). The roots of the unwatered plants penetrated more deeply into the soil profile than did the well watered plants, without a corresponding increase in total dry root weight. Sharp and Davies (1985) observed that the zone of greatest water depletion moved downward in the unwatered columns in response to increased root proliferation in deeper soil layers. Although at a lower level than the watered plants, a constant leaf turgor was maintained in the unwatered plant throughout the first fifteen days of drying. By the eighteenth day, the unwatered plants experienced almost complete stomatal closure during mid-day. Water removal, deep in the soil, proved to be quite effective considering root and shoot growth continued throughout the soil drying period.

A three-year study conducted at the Agricultural Experiment Station near Las Cruces, New Mexico compared the growth of six legumes under different irrigation schemes (Tapia and Lugg, 1986). Overall the legumes under full irrigation developed more rapidly and had a larger yield than those growing under limited irrigation. Some of the legume species were not affected by limited irrigation when practiced only in the summer and fall. This was attributed to the fact that for some legumes primary

production occurs in the spring. For example, alfalfa (Medicago sativa L.) was greatly affected by limited irrigation whereas sainfoin (Onobrychis viciifolia Scop.), birdsfoot trefoil (Lotus corniculatus L.), and red clover (Trifolium pratense L.) were not.

The studies presented above represent the results of a few areas of agricultural research. Monitoring fully irrigated croplands indicates plant responses in idealized situations. The study of plants experiencing water stress, however, gives insight to the factors limiting plant growth and proliferation. Understanding the mechanisms by which desert plants survive, agriculturalists may be able to increase the efficiency of irrigation schedules.

Desert Plants in Natural Settings. Although there may exist a plethora of data related to the growth of agricultural crops the opposite is true of plants growing in natural settings. This may be attributed to the problems that arise in attempting to quantify and characterize the movement of soil water near plant roots. One of the primary problems is that it is difficult to isolate one plant because of the interaction of other rooting systems. Topography, the depth to the water table, degree to which there is protection from wind and sun, and the reflection off ground cover are all important considerations for evaluating water use.

In a study by Rice (1975), observations were made on the

diurnal changes in total head and water uptake for bermuda grass (Cynodon dactylon). The smallest hydraulic head values and largest water uptake rates were recorded during solar noon for the 10 cm depth. Afterwards, the soil pressures increased and water use by the plant decreased until just before dawn. Rooting depth was assummed to be 120 cm where the hydraulic gradient became unity, and there were no perceptible water losses other than deep drainage. Rice concluded from the data that the zone of maximum root density was at the 10 cm depth, however the effects of surface evaporation were probably greatest here also. No actual root density data was included in the study to confirm, or refute, the predicted root distribution. One point derived from this work is the importance of recording data at consistent times each week so that diurnal fluctuations do not interfere with observing seasonal changes in soil water.

Soil-moisture flux and evapotranspiration were calculated for a Chaparral stand during a period covering two water years (Scholl, 1976). In the first, an unusually dry year, 98% of precipitation was lost to evapotranspiration, whereas in the second, an unusally wet year, evapotranspiration accounted for only 80%. Very little seepage below the 180 cm depth was recorded during the dry year, however measurable seepage below the root zone (420 cm) was recorded during the wet year. Scoll attempted to predict root density and root distribution by examining total head and moisture content data.

A comparison of annual cheatgrass and perennial bluegrass

communities (Cline et al., 1977) illustrated the interaction of two different rooting structures. The annual grasses have shallower rooting profiles and shorter active growing seasons than do perennials. Plant growth of the annual cheatgrass community essentially ceased with the onset of summer and soil water below 0.5 m was not fully utilized. The cheatgrass, while being very efficient at extracting water in the shallow depths, still allowed the bluegrass to exploit moisture in the deeper soil layers. Therefore, perennial plants rooted below 0.5 m were relatively free from root competition by annual cheatgrass.

In arid and semi-arid areas, the availability of water is often the limiting factor in plant growth, and therefore water balance calculations are critical to understanding soil, water, and plant relationships. A study conducted in the northern Mojave Desert examined these relationships to quantify the annual net production of vegetation (Lane et al., 1983). The rate of evapotranspiration was used to estimate water use by perennial vegetation. Computed water use was multiplied by a water use efficiency factor (kilogram dry material produced per kilogram water) to estimate net production. Predicted and actual net production of vegetation agreed quite closely (r-squared = 83%, ie. 83% of the variance between the two parameters was explained) over an 8 year span. A linear relationship between predicted and observed transpiration rates was computed within a correlation coefficient of 90%. There were problems with this method in that an immense data base was necessary to calibrate the model and the

equations were site specific. It is difficult, and usually inaccurate, to use specific regression coefficients in regions with varying climate, soils, and vegetation.

Sammis (1974) conducted an intensive one year study on the micro-environment of a desert hackberry plant (Celtis pallida). The experiment resulted in some sensitive insights to plant responses, both diurnally and seasonally, to climatic and soil parameters. A group of plants were isolated by a plastic liner and monitored using neutron scattering, thermocouple psychrometers, and microclimatological equipment. Water potential in the plant xylem was measured using a pressure bomb system.

Water balancing of soil moisture was not sensitive enough to detect any differences in total water loss between the vegetated and the bare soil plots. The plants were only observed to alter the water use pattern. The main differences between the plots occurred after a rainfall event, when water was plentiful and transpiration rate was high.

Sammis applied a method first developed by Gardner and Ehlig (1963) to predict the evapotranspiration rates of the desert hackberry plant in situ according to:

$$Et = \frac{(\psi_l - \psi_{sm})}{R_{pl} + (b/K(\theta)} \qquad (1.6)$$

where,

ψ_l = leaf tissue potential [L]

ψ_{sm} = mean matric potential in the root zone [L]

b = lumped parameter including root radius, root density,

root depth, and outer boundary of root influence

$b/K(\theta)$ = soil resistance [T/L]

R_{pl} = lumped plant resistance term combining root cortex and xylem resistance [T/L]

This method requires data on soil potential, soil moisture, and unsaturated hydraulic conductivity. It also requires detailed information concerning the stomates, root and cover density, and transpirational demand of the plant. Under wet conditions, the approach agreed well with water balance estimates, but deviated greatly under water stress conditions. Water potential within the plant responded directly to atmospheric conditions, soil-moisture availability, and ultimately, plant metabolism. It was observed that the desert hackberry plant had the greatest transpiration rate when water was plentiful and actually changed physiologically when soil moisture was limited.

As part of the International Biology Program studies were conducted on actual evapotranspiration under semi-arid conditions (Evans and Thames, 1981). Four sites representing various trees, plants, and grasses were chosen in Arizona, Washington, and Utah. Water balance and lysimetric methods were used to estimate rates of evapotranspiration. The two methods were generally in good agreement. Discrepancies could probably be explained by spatial variability within the sites, timing of measurements with respect to precipitation events, and measurement errors. The highest evapotranspiration rates were calculated following

periods of precipitation. This probably corresponded to increases in evaporation from the soil surface rather than increases in transpiration. Average evapotranspiration rates were between 2-5 mm/day for creosote bush, salt bush, desert hackberry, sagebrush, and several grasses. Under extremely dry conditions (-10 to -50 bars) the evapotranspiration rate decreased to less than 0.1 mm/day illustrating the diverse ability of desert plants to survive varying soil-moisture conditions.

In recent years there has been a growing interest in the development of arid and semi-arid regions for urban and agricultural purposes. As a result, research interests concerning the responses of desert plants has increased. By examining vegetation growing under both controlled and natural settings abundant information may be obtained for a variety of soil-moisture conditions.

The following hydrologic study examined the water use pattern of a Dalea scoparia plant in an arid, sand dune environment. The study was conducted as part of an integrated study of ground-water recharge within the Sevilleta Wildlife Refuge. Research included an evaluation of the monthly soil-water balance using moisture content and pressure head data and an examination of the three-dimensional character of the flow of soil-water to the roots. The objectives of this work were to record the seasonal and topographic controls on a perennial desert plant in a natural setting.

SITE DESCRIPTION

The Desert Research Station of the New Mexico Institute of Mining and Technology Hydrology Group is located within the Sevilleta National Wildlife Refuge 24 km north of Socorro, New Mexico. The site occupies approximately 1.3 sq km and is 5 km west of Interstate 25 along the Rio Salado (figure 2). The Rio Salado is an ephemeral, braided stream with a braod, shallow channel. On-going research includes the use of soil physics, isotopic tracers, and meteorolgical data to study ground-water recharge rates, soil-hydraulic properties, stream-aquifer relations, and evapotranspiration rates.

Soil-physical techniques have been used to monitor soil-water flux through vegetated and unvegetated sites since January, 1983. Fifteen sites were instrumented with neutron access tubes and tensiometers to monitor the moisture content and matric potential of the soil (figure 3). Soil-water flux is recorded at the crest, mid-section, and base of a sand dune, and on flat, ancestral river bed deposits. These sites were chosen for their variable topography, vegetation, and soil type. The soil types include a variety of sands which do not vary significantly in their saturated hydraulic conductivities (Leavitt, 1987). The soil types found at the site were identified by Machette (1978) as shown is figure 3.

The principle vegetation and their common names were identified by Mr. Theodore Stans, Sevilleta Refuge Manager.

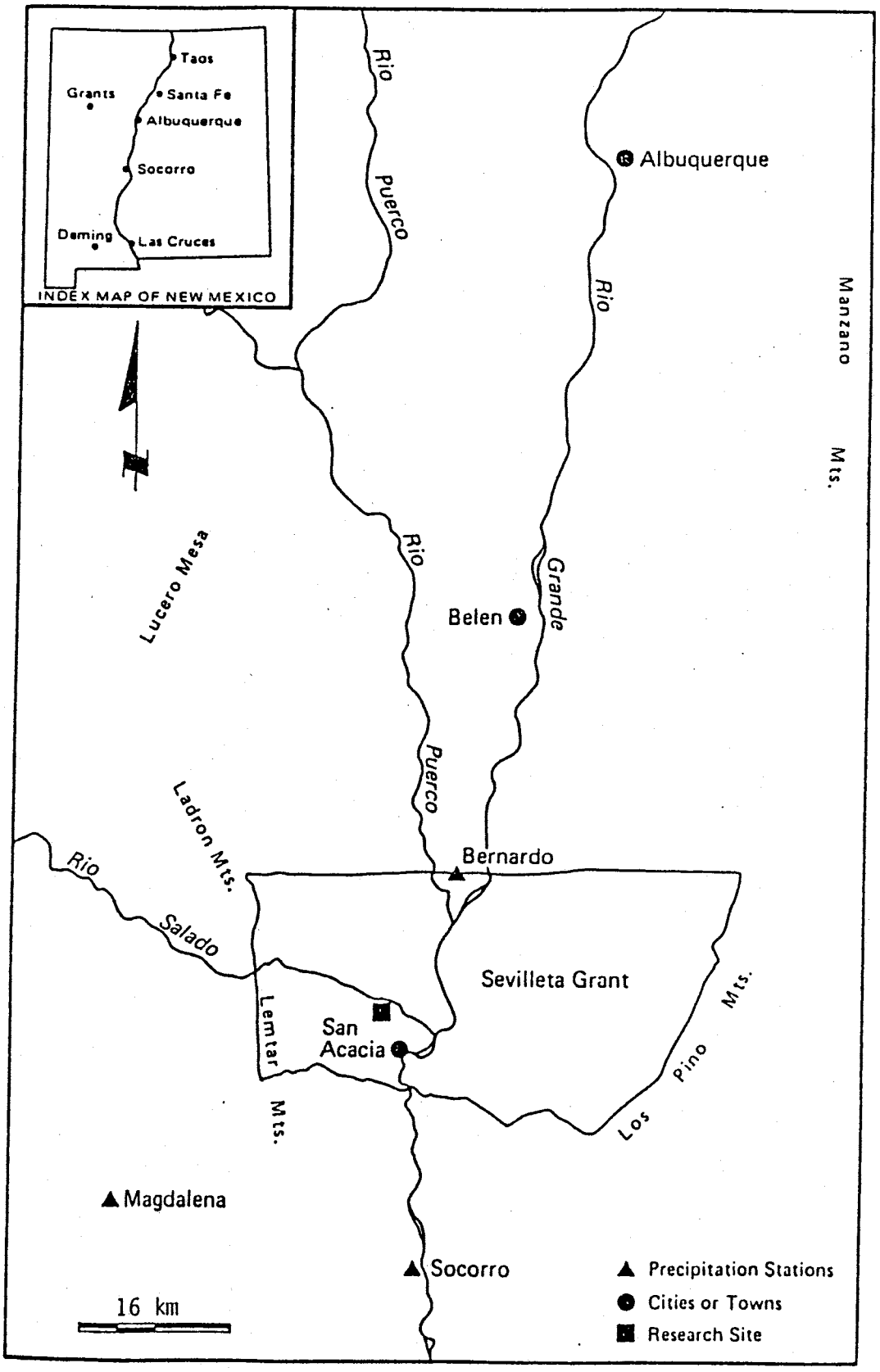

Figure 2. Research site location map.

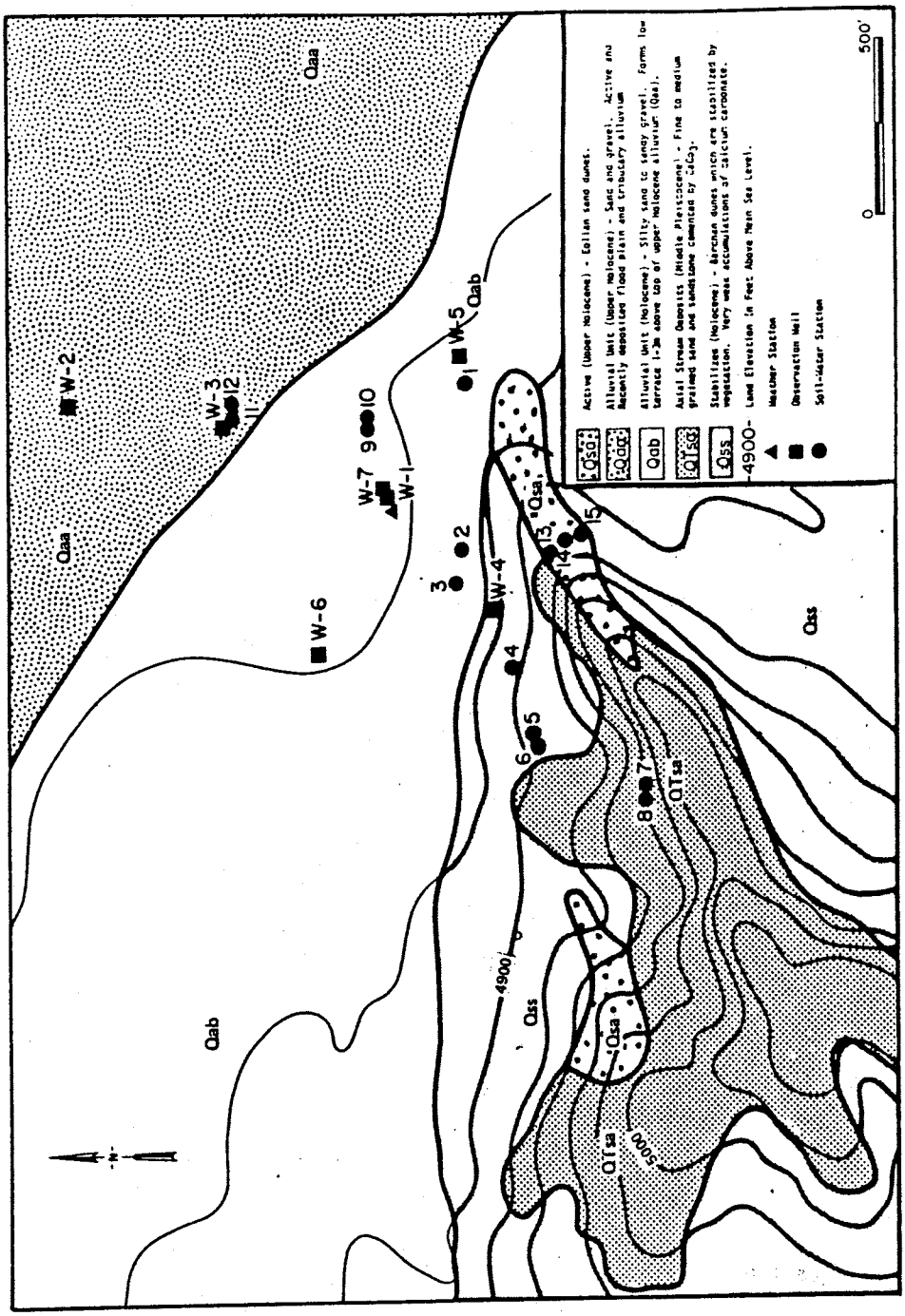

Figure 3. Station locations and soil types
(Plant located at station 15)

Grasses and cacti include: gramma grass, spectacle pod, night shade, desert willow, primrose, globe mallow, sand sage, bind weed, scorpion plant, indian rice grass, prickly pear, yucca, salt cedar, and juniper. Most of the plants and shrubs include: four-wing salt bush, snakeweed, sacatone, annual mustard, creosote bush, mesquite, and indigo bush.

The indigo bush (also known as a lavender bush, purple sage, broom dalea, or in Latin a Dalea scoparia) is the focus of this study. The Dalea scoparia plant (figure 4) under investigation is located near station 15 (figure 3) in the swale of an active, eolian, sand dune approximately 20 meters above the valley floor.

Typically, the Dalea scoparia plant flourishes in sandy soils. This plant maintains one, or with larger specimens, possibly 2 to 3, central tap roots. Notes taken on several root systems collected by the author found that the depth to which the tap roots extended was on the average about 3 - 4 times the height of the canopy. Lateral roots occur most frequently in the top one-third of the total rooting depth. The frequency of these lateral roots decreases very quickly with depth. Figure 5 is photo of a typical, although much smaller, Dalea scoparia plant. The roots extend laterally a distance perhaps equal to the width of the canopy in each direction. No root hairs were visible to the naked eye.

The Dalea scoparia is well suited to the extreme conditions of a desert environment. Near surface lateral roots allow fast water uptake during the rainy season. Intense thunderstorms,

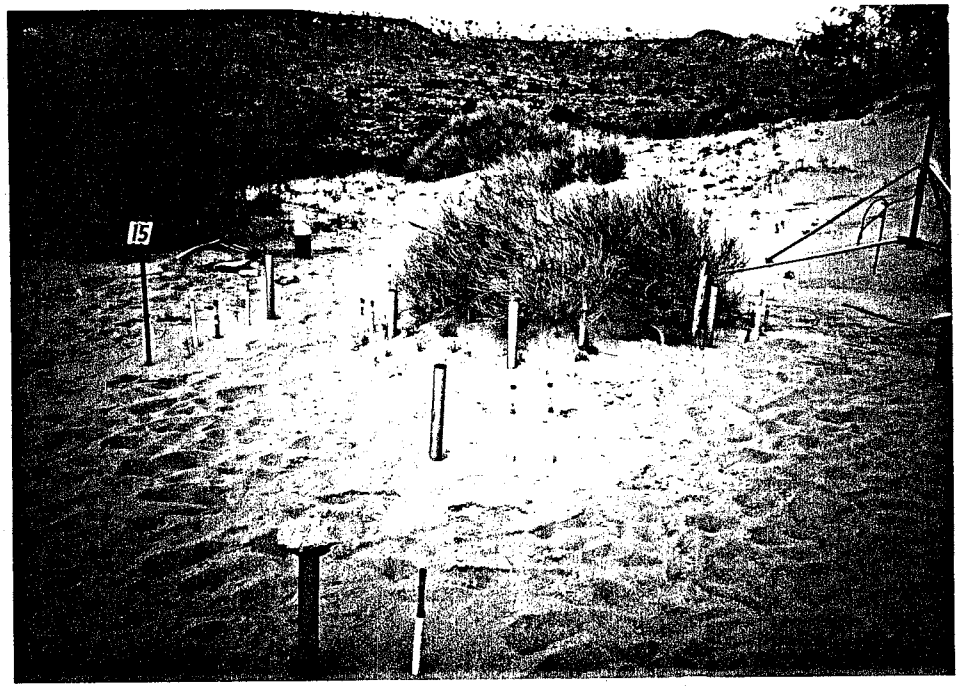

Figure 4. View of the Dalea scoparia plant and soil-water instrumentation.

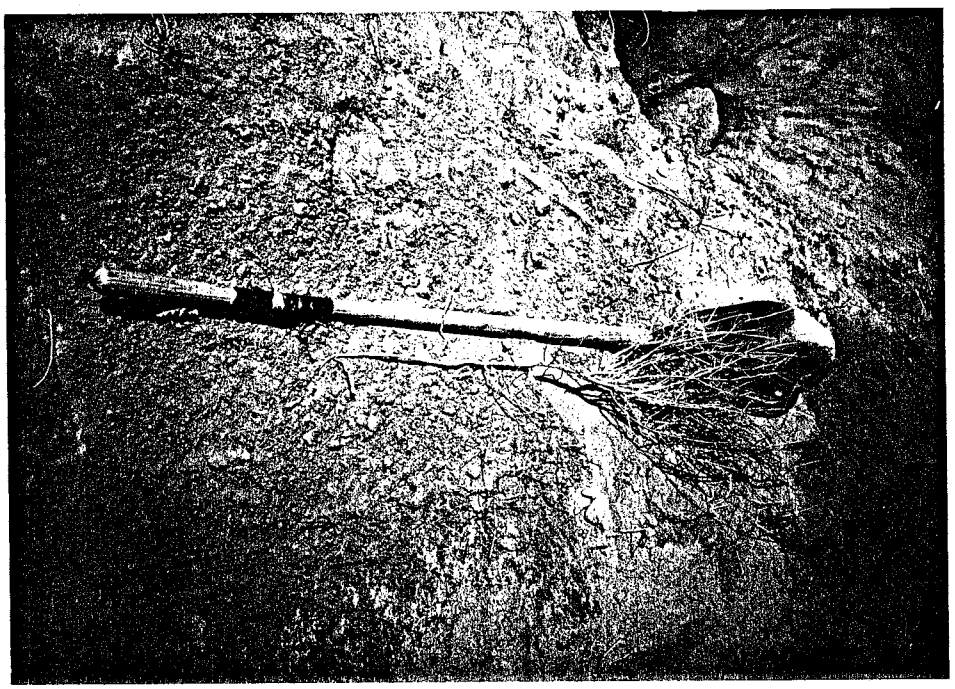

Figure 5. View of the roots (shovel handle) and canopy of a typical Dalea scoparia plant.

characteristic of the southwest, produce pulse inputs of precipitation though large initial losses occur due to evaporation. The deep tap root makes this plant efficient at using soil moisture below the zone of surface evaporation or water consumption by annuals. Due to the paucity of soil moisture the plant is unable to support a complex or dense root structure.

Laboratory analyses of core samples taken to a depth of 3.0 m characterize the soil as a uniform, medium to fine grained, subangular sand (appendix A). Table 1 summarizes some statistics calculated on soil samples collected near the plant. Particle-size versus the percent finer indicated only slightly coarser materials near the surface (figures 6a, b, c, d). Through visual inspection it was determined that the sand is approximately 88-93% quartz, 3-5% potassium feldspar, 3-5% mafics, and 1-2% muscovite. Saturated hydraulic conductivity ranges from 0.008 to 0.03 cm/s with an average value of 0.015 cm/s.

The site chosen for the investigation has some very unique aspects which make it particularly interesting. Some of these are:

1. The plant is isolated, at least on the land surface, from other vegetative influences. Calculated soil-moisture gradients may be assumed to represent the actual gradients induced solely by the plant being monitored.
2. The land surface is a significant distance above the water table. Expected fluctuations in the water table will not affect capillarity or matric potential in the study

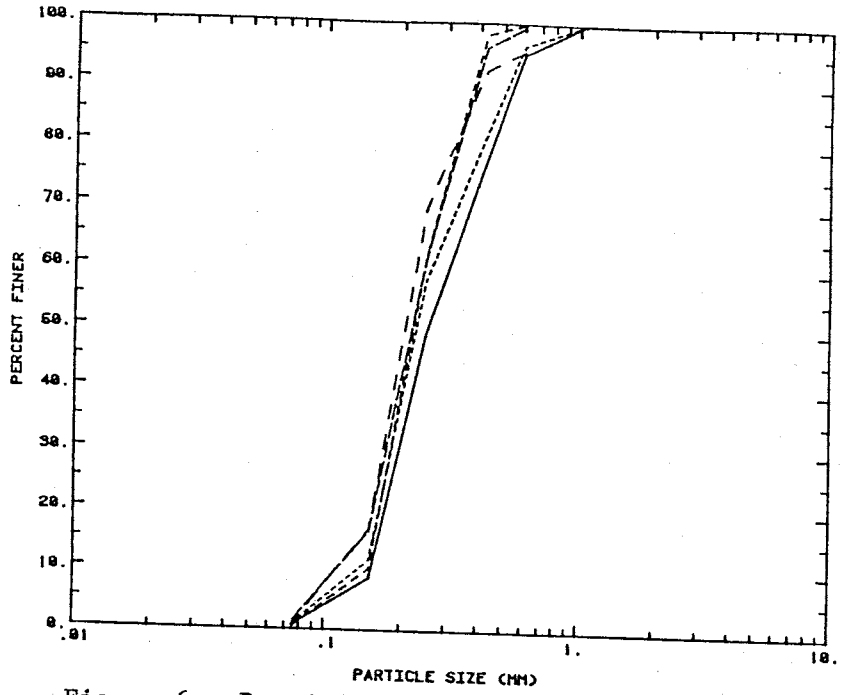

Figure 6a. Particle-size distribution for samples to the 1.5m depth; edge of plant canopy.

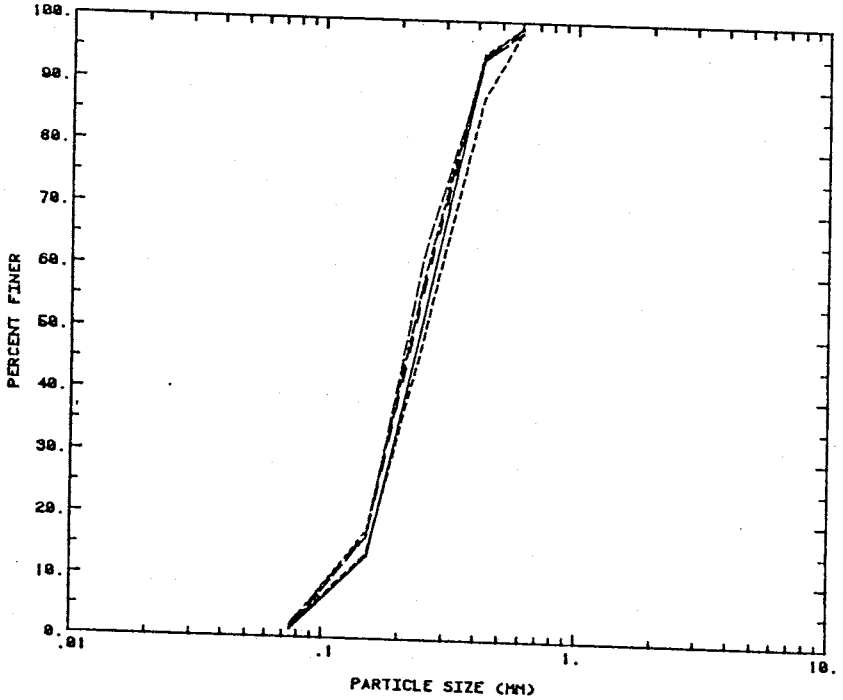

Figure 6b. Particle-size distribution for samples between 1.5 and 3m depth; edge of plant canopy.

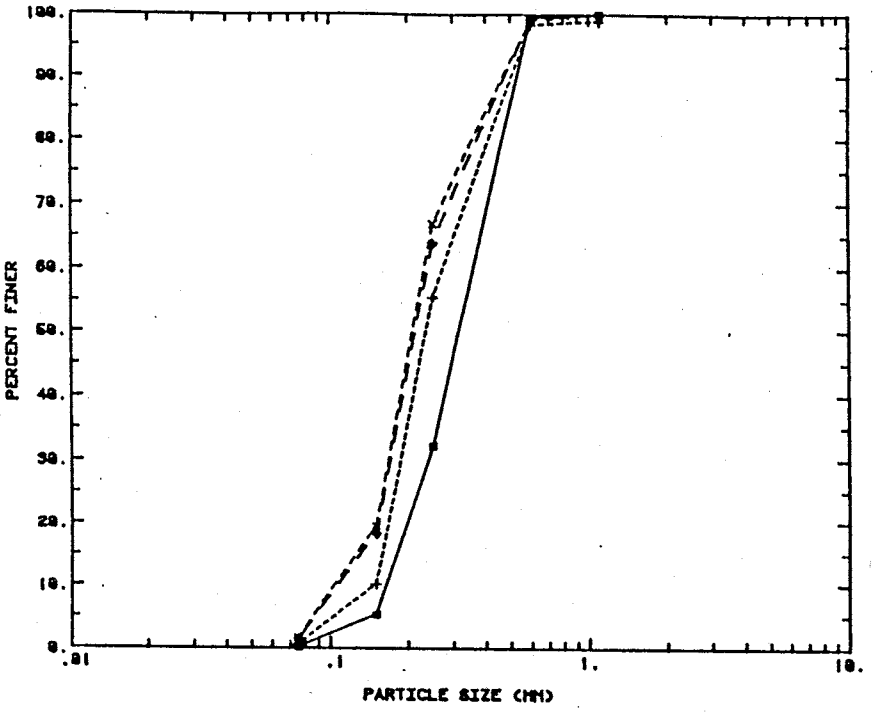

Figure 6c. Particle-size distribution for samples to the 1.5m depth; 1.15m from plant canopy.

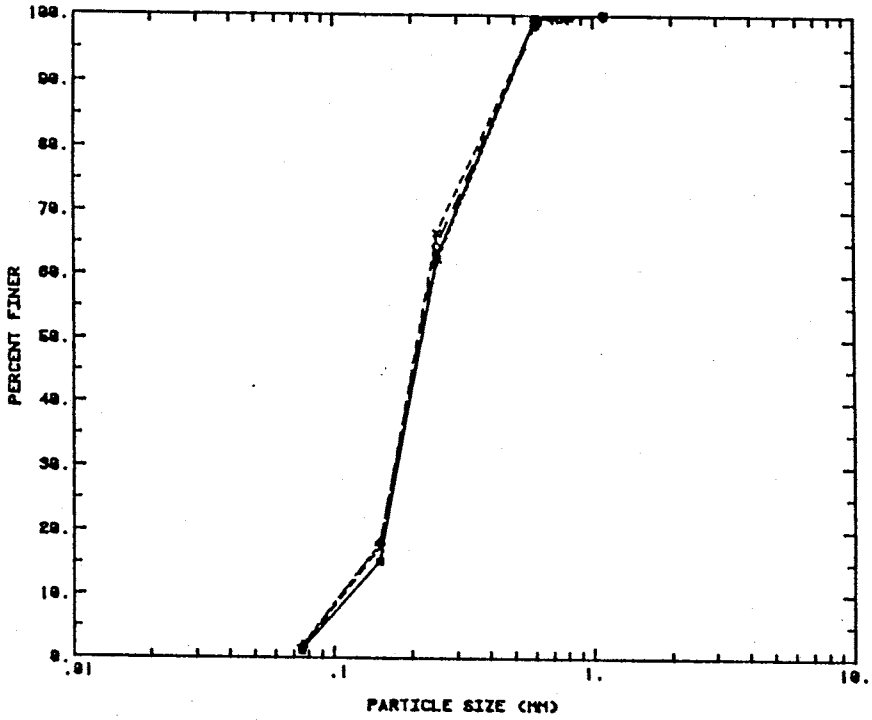

Figure 6d. Paticle-size distribution for samples between 1.5 and 3m depth; 1.15m from plant canopy.

Table 1. Summary of particle-size, saturated hydraulic conductivity, and residual moisture.

	Depth (cm)	Coeff of Curvature	Uniformity Coeff	10% Finer (mm)	K-sat (cm/s)	Residual Moisture (%)
East A	35	0.83	1.88	0.16	6.48E-02	3.34
	58	1.67	0.86	0.15	3.57E-02	4.47
	80	0.85	1.62	0.15	9.96E-03	4.79
	110	0.90	1.60	0.15	2.90E-02	5.39
	150	1.01	2.09	0.11	8.95E-02	4.72
	195	1.75	2.00	0.13	1.54E-01	
	212	1.44	2.50	0.10		5.60
	242	1.39	1.92	0.13		
	268	0.93	2.27	0.11	4.49E-02	5.11
	290	0.89	2.00	0.15		
	330	1.25	2.00	0.12		5.08
West C	30	1.12	2.04	0.16	1.03E-02	
	60	0.90	1.83	0.14	4.03E-03	
	90	0.89	2.00	0.12	1.84E-03	
	120	1.07	2.23	0.11	4.27E-03	
	150	0.91	1.89	0.13	2.62E-02	
	180	1.18	2.27	0.11	5.64E-02	
	270	2.00	2.00	0.11	1.01E-02	
	300	0.89	1.92	0.13	3.68E-02	

area.

3. The soil is uniform and infiltration rates are high. Runoff may be assumed to be negligble.

4. There is a relatively small topographic surface gradient. Topographic influence is small and lateral flow may be neglected.

5. The plant is located within close proximity to the weather station and access road. Measurements taken at the weather station at the base of the dune may be assumed to represent the conditions at the site. Collection of weekly and bi-weekly measurements may be done readily.

Site Instrumentation

Weather Station. A weather station is located at the base of the dune on which the study site is located just off of the access road (figure 7). The meteorological equipment includes: a tipping bucket rain gauge accurate to 0.02 cm; a hygrothermograph with temperature, relative humidity, and barometric pressure sensors; a mechanical pyranograph for measuring solar radiation; and standard class A evaporation pan equipped with a hook gauge accurate to 0.001 cm; and a totalizing anemometer for reading cumulative wind velocities.

Field Procedures. Soil-physical methods were used to monitor the soil-water flux in the immediate vicinity of the plant roots. The installation of monitoring equipment began during a hail storm in March, 1985, and data collection continued through July, 1986. Weekly measurements of moisture content and matric potential were taken through the month of August, 1986, with bi-weekly measurements beginning in September and continuing through the winter and spring. The layout of instrumentation is illustrated in figure 8. A full year of data collection allowed for a clearer understanding of the seasonal changes in soil moisture. Continued monitoring would not necessarily have been beneficial because tensiometers release small amounts of water which could affect the growth of plant roots. As a result,

Figure 7. Weather station.

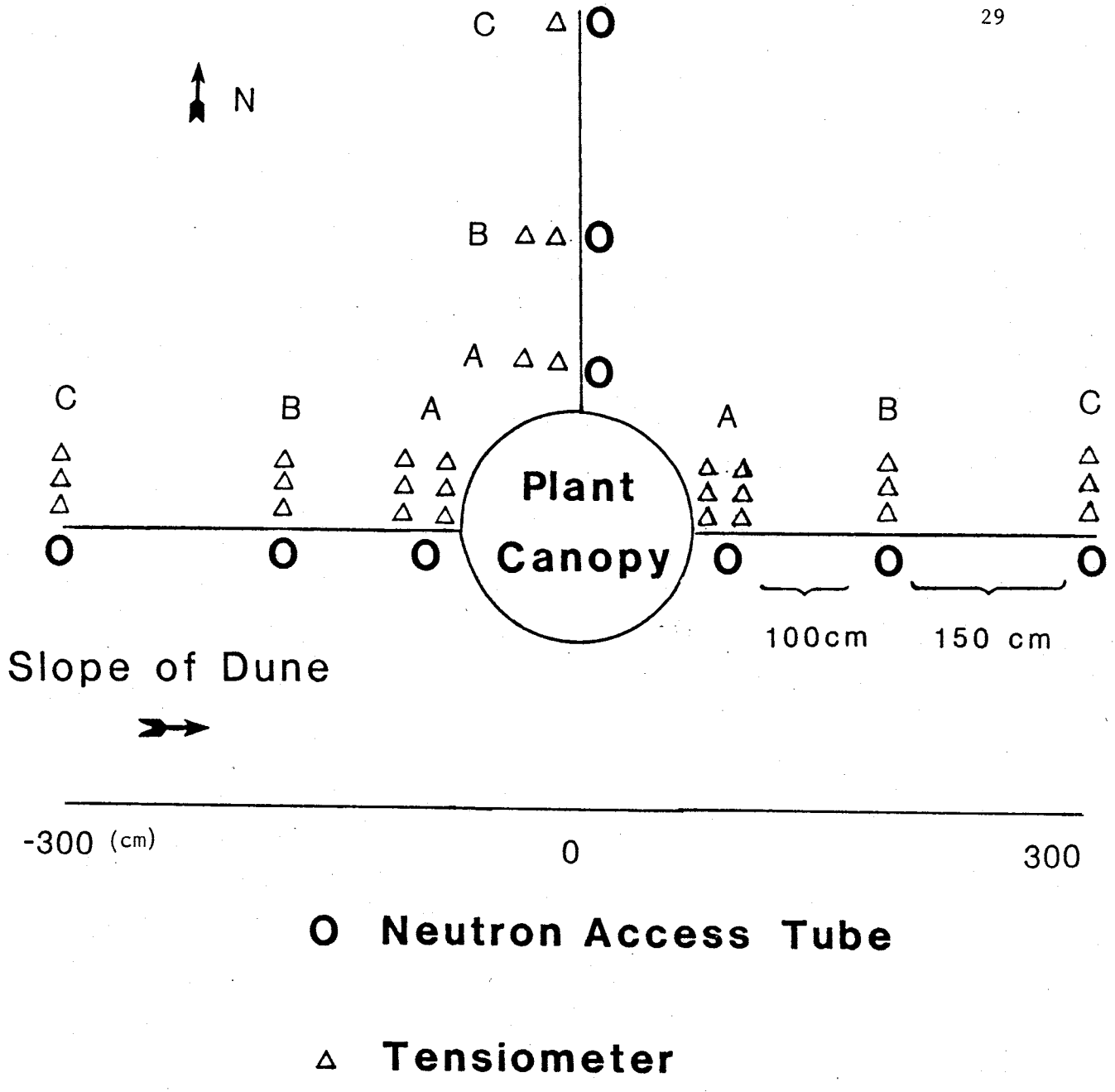

Figure 8. Layout of instrumentation

greater soil-water pressure heads might be recorded which would not be representative of undisturbed conditions.

Moisture Content Monitoring. Changes in moisture content were recorded with the use of neautron thermalization, or neutron scattering. This technique is fairly rapid, nondestructive, and allows for repeated measurements of the volumetric, or gravimetric, wetness of soil. The radius of influence for the neutron probe in low moisture contents is approximately 30 cm.

The neutron probe used at the site is manufactured by Campbell Pacific Nuclear, model 503. The radiation source consists of 50 millicuries of americium-241/beryllium. The neutron probe was calibrated for the specific site. Data obtained for the calibration are included in appendix C, page 14. Thin walled alluminum tubes, with 5 cm diameters, were installed to depths of 3 m to allow access for the neutron probe. The bottoms of the tubes were properly sealed to prevent soil from entering and to reduce condensation within the tubes. Holes for the access tubes were excavated by a hand auger with a 6 cm diameter. After inserting the tube, the annular space was backfilled with the same soil to ensure that proper contact between the soil and access tube was made. Volumetric soil samples were obtained for particle-size analyses and water content during the installation procedure (appendix A).

Measurement of Total Hydraulic Head. Matric potential was

monitored with the use of tensiometers. Nests of 3 - 4 tensiometers, ranging in depth between 30 and 240 cm were installed for determination of hydraulic gradient and pressure head. The tensiometers, contructed in the laboratory, consist of polyvinylchloride tubing, septum rubber stoppers, and porous ceramic cups. The porous cups have a 2.1 cm diameter, a 5.4 cm length, and are accurate to 1 bar of pressure. Installation of tensiometers was carefully done with the use of a hollow pipe and the hole was backfilled around the tensiometer to ensure good contact between the porous cup and the formation. The tensiometers were filled with distilled and de-aired water. During the winter months, a 50% solution of ethylene gylcol was used to prevent the possibility of the tensiometers freezing and cracking. Corrections were made for the density difference between distilled water and the ethylene glycol solution. The negative pressures in the soil were measured with the use of a portable field transducer (Tensiometer, Soil Moisture Systems, Las Cruces, NM).

METHODS OF ANALYSES

Hydrologic Processes Involved in Water Balance Evaluation

When attempting to determine the quantity and availability of soil water to plants there must be a thorough, quantitative description of the balance of water in the soil. Water balance is a transient state consisting of the summation of inflows, outflows, and storage changes of water within a given volume of soil. All of the soil-water flow processes (eg. infiltration, redistribution, drainage, evaporation, and uptake by plants) are interrelated and consequently are to be considered in all water balance calculations.

The water balance is, in effect, a statement of the law of conservation of matter. Matter cannot be created or destroyed, but can only change forms. In the root zone, the water balance may be seen graphically in figure 9 and is described by:

$$P - R - RO - I - ET = \int_0^z \int_{t_1}^{t_2} (d\theta/dt)\, dz\, dt \qquad (3.1)$$

where,

P = Precipitation

R = Recharge

RO = Runoff

I = Interflow

ET = Evapotranspiration

$$\int_0^z \int_{t_1}^{t_2} (d\theta/dt)\, dz\, dt = \text{Cumulative Changes in Storage}$$

All of these quantities are expressed as a volume of water per unit area, or equivalent depth units. The only term in equation 3.1 which was not determined through direct measurement was evapotranspiration. Each of the remaining variables was either assumed to be negligible or calculated using precipitation, moisture content, and soil-tension data collected in the field.

Factors which are considered in a balance of soil water depend on the location, scale of investigation, and period of observation. Comparing the magnitude of different components is also important. For example, thermally induced vapor flow in

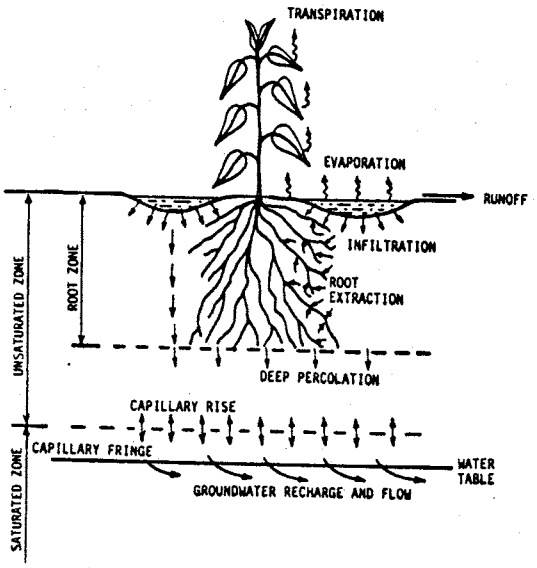

Figure 9. Schematic of water balance in the root zone (Hillel, 1980).

humic soil is probably insignificant in magnitude compared with other components of the water budget. However, it may play an important role in water transfer under desert conditions (Evans and Thames, 1981). Research investigating annual production, water use, or recharge predictions must consider the non-linear relationship of inflows and outflows. Following a precipitation event, a period of redistribution occurs and possible infiltration to the water table. The time required for deep percolation depends on intensity and periodicity of rainfalls.

After the initial flux of rainwater, drainage takes place increasingly slowly. Mathematically, the infiltration rate due to maintaining a constant moisture content at the land surface, may be expressed according to Philip's (1957) power series solution:

$$i(t) = 1/2st^{-\frac{1}{2}} + (A_2 + K_o) + 3/2A_3t^{\frac{1}{2}} + \ldots\ n/2\ A_n\ t^{n/2-1} \qquad (3.2)$$

where,

s = Sorptivity $[L/T^{1/2}]$

t = Time [T]

A_n = Empirical Constants

K_o = Saturated Hydraulic Conductivity [L/T]

Philip's solution pertains only to infiltration and does not describe the drainage or redistribution which follows a precipitation event. The infiltration rate goes to zero after rain ceases. The infiltrated pulse of water is pulled downward due to

capillary forces and gravity and is drawn upward due to evaporative demand in the forms of liquid and vapor transport. Over time the hydraulic gradient gradually diminishes and when the effect of surface soil evaporation is low the gradient approaches one. The flux through the soil eventually approaches the hydraulic conductivity of the initial moisture content.

A realistic rate of drainage, or recharge, to the water table can only be estimated because it is mainly dependent on soil hydraulic properties. Unsaturated hydraulic conductivity is very sensitive to small changes in moisture content in the dry zone. By combining the Darcy equation and the continuity equation, the general form of the flow equation is obtained. Richard's equation for one dimensional, vertical flow, in terms of pressure is expressed,

$$C(\psi)\ \partial\psi/\partial t = -\partial/\partial z\ (K(\psi)\ [\partial\psi/\partial z + 1]) \qquad (3.3)$$

Using this equation, the soil-water flux below the active root zone may be estimated. Unsaturated flow processes are often converted to terms of hydraulic diffusivity to simplify experimental and theoretical work. The flux of water may then be defined by wetness rather than soil pressures, and hydraulic diffusivity,

$$D(\theta) = K(\theta)\ d\psi/d\theta \qquad (3.4)$$

is used to rewrite the unsaturated flow equations using one dependent variable (θ) instead of two (θ and ψ).

$$\partial\theta/\partial t = \partial/\partial z\ D(\theta)\ [\partial\theta/\partial z + \partial K(\theta)/\partial z] \quad (3.5)$$

Runoff occurs if rain intensity exceeds the infiltration capacity. It also occurs as saturated overland flow if the water table is raised to the ground surface. No evidence of runoff, such as rills or other erosional features, were observed during the study period and the water table is estimated to be 20 m below the surface. Furthermore, laboratory analyses of the saturated hydraulic conductivity of the dune sand (appendix B) indicate a high infiltration capacity.

The interflow, or through flow, term in equation 3.1 was assumed negligible when considering the very small slope (0.024) across the site. Lateral flow does occur on a slope when streamlines penetrate a more permeable layer below a less permeable layer (Zaslavsky and Sinai, 1981). In general, water content, increases with depth on the dune and therefore so does hydraulic conductivity. As a result some error is involved in assuming vertical flow. Exactly how much error is difficult to estimate, but by examining the three-dimensional flow field this question may be addressed.

Precipitation was measured by means of a tipping bucket rain gauge located at the weather station in the flats below the dune. The accuracy of the gauge is estimated to be 0.02 cm. Recorded precipitation varies noticeably between Socorro, Bernardo, and the Sevilleta Wildlife Refuge which are only separated by 40 km. A great deal of variability in rainfall has been observed

even within the Sevilleta Wildlife Refuge. Part of this variation may be explained by the fact that different types of rain gauges are used. To simplify matters only the rain gauge at the Sevilleta weather station was used in this study. Precipitation data, along with average wind speeds and evaporation rates, may be found in appendix D.

Vapor transport induced by thermal gradients might be a factor to consider in the balance of soil water. Fukuda (1956) studied the diurnal pattern of changes in soil moisture, air temperature, relative humidity, and vapor pressure in loamy and sandy field plots. Water vapor in pores depends on diffusion, evaporation, and condensation processes. Fukuda found that evaporation was first observed at the surface, and as daytime temperatures increased, so did the depth of the evaporation front. With lower nighttime temperatures, condensation followed the same path as evaporation, first occurring at the surface, and then occurring at increasingly greater depths. However, this phenomenon was only observed at the near surface (0 - 30 cm) and it is assumed that this would not contribute significantly to the total soil-water balance.

The term, in equation 1, describing cumulative storage changes represents the total change in soil water within the root zone. This is calculated by integrating the change in wetness over depth and time. Storage changes indicate net losses or gains to the system. At any time the amount of water in storage is the integration of the moisture content through depth. It is

equivalent to

$$\hat{D}(t) = [(\theta_1 + \theta_2 + \theta_3 + \ldots + \theta_n)/n]*T \qquad (3.6)$$

where,

$\hat{D}(t)$ = depth of water in storage at time, t

θ = volumetric moisture content at the i-th depth and time, t

n = number of readings in the profile

T = total thickness of the profile

Volumetric water content is the ratio of the volume of water in the soil to the total volume of soil. This quantity may be obtained by destructive sampling or with a neutron moisture logging. In this study, water content data was measured using a neutron probe down to a depth of 3 meters, at 0, 115, and 265 cm from the canopy of the Dalea scoparia.

The most elusive parameter to quantify is that of evapotranspiration. This term combines bare soil evaporation as well as plant transpiration. Due to difficulties in determining the actual evapotranspiration, potential evapotranspiration is sometimes mistakenly substituted. Actual evapotranspiration though, is some fraction of the potential rate. Potential evapotranspiration, represents evapotranspiration from a well-watered field and is characteristic of the climate and the field itself. It depends primarily on latitude, solar radiation, wind, and convection or surface roughness.

In studies of close-growing, well-watered stands, actual

evapotranspiration should approach the potential evapotranspiration rate during the active growing season (Hillel, 1980). In non-irrigated studies, actual evapotranspiration rates greatly deviate from the potential rates and must be determined independently. This may be accomplished by using weighing lysimeters and measuring water loss directly. However, lysimeters have finite boundaries and interfere with the indigenous flow field. For field projects of this scale (6m x 6m), a lysimeter would be difficult to install and prohibitively expensive. An alternative method is to calculate the remaining terms in the water balance equation and solve for evapotranspiration.

Geostatistical Investigation

Spatial variability within soil types, though long recognized, has only recently been investigated through field observations and stoichastic approaches (Byers and Stephens, 1983; Bresler and Dagan, 1983). Collection of information on the statistical behavior of unsaturated soils must begin with laboratory soil columns or small agricultural studies. These experiments are limited in that they are concerned with only the top few meters of soil. Nonetheless, understanding small scale water movement in the unsaturated zone is the basis for understanding and quantifying larger scale cases used for ground-water recharge evaluation and waste disposal management. In this study, the geostatistical method of kriging was applied in the

hopes of obtaining better estimates of the moisture content profile. The water content of the soil was predicted at various spatial and temporal locations based on observed measurements.

A structural analysis of the data must be conducted considering the scale of investigation and the assumptions of the model. The random field, in this case $\theta(x,t)$, is statistically isotropic and is described by a certain probability distribution function. The data set required to make a complete description of the joint probability distribution at any set of locations would be quite nearly impossible to obtain. The function may, locally, take on one of any equally probable values. The general procedure is to obtain descriptions of moments such as the mean, variance, and covariance relationship.

The expected value, or mean of $V(x)$, expressed as $E[V(x)]$, is the probability weighted average,

$$E\ (\ V(x)\ ) = \int_{-\infty}^{\infty} V_g\ (V : x)\ dV \tag{3.7}$$

(Where x represents a vector in 1, 2, or 3 space.)

The variogram is a function defined as the variance of the increment $[V(x_1)-V(x_2)]$ written as (Journel and Huijbregts, 1978),

$$\gamma\ (x_1\ ,\ x_2) = E(\ [V\ (x + y) - V(x)]\ )^2 \tag{3.8}$$

The covariance function is a measure of the statistical relationship of two observations at different points in space. It is defined as,

$$\text{Cov}\ (\ V(x_1)\ ,\ V(x_2)\ ) = E\ [\ (\ V(x_1) - \overline{V}(x_1)\ )\ *\ (\ (V(x_2) - \overline{V}(x_2)\ )\ ]\qquad (3.9)$$

where y is the separation distance, $x_1 - x_2$

Kriging interpolates measurements between sampling points based on the spatial correlation of the data using either C(y) or $\gamma(y)$. C(y) represents the covariance relationship of the function. $\gamma(y)$ is used in the statistically homogeneous and isotropic case where the covariance function may be defined by the separation vector, y, alone. A statistically homogenous medium has an unchanging variance so that the covariance function is independent of position. If V(x) is a random field having $V(x_1)$, $V(x_2)$, . . ., $V(x_n)$ with a constant, though unknown mean, then $V(x_o)$ can be estimated from a linear weighted average of the data,

$$\hat{V}\ (x_o) = \sum_{j=1}^{n} \lambda_j\ V(x_j)\qquad (3.10)$$

The λ_j's are kriging weights, solved for by a system of kriging equations,

$$\sum_{j=1}^{n} \lambda_j\ C\ (\ x_i - x_j\ ) - \mu = C\ (\ x_i - x_j\ )\qquad i = 1, 2, 3, \ldots, n\qquad (3.11)$$

subject to the constraint,

$$\sum_{j=1}^{n} \mu_j = 1\qquad (3.12)$$

The kriging variance, σ_k^2, measures the precision of the interpolation.

$$\sigma_k^2 = C(0) - \sum_{j=1}^{n} \lambda_j\ C\ (\ x_j - x\ ) + \mu\qquad (3.13)$$

μ is the lagrange multiplier which is also solved for in the system of equations. For the case of an intrinsic random function of order zero (IRF-0), C(0)=0, therefore $\gamma(y) = -C(y)$ may be substituted into equations 3.11-3.13. An IRF-0 is a random field where the increments are assumed to be statistically homogeneous.

The kriging estimates have several interesting and noteworthy properties (Gutjahr, 1985).

1. Unbiasedness which can be proven with equation (3.12).
2. Minimum mean squared error estimation, equation (3.13).
3. Exact interpolation, ie., $\hat{V}(x_j)=V(xj)$ at observation points.
4. The mean, m, although not used to calculate the estimate V(x), must have a known form, or be a constant.
5. The kriging weights, λ_j , lagrange multiplier, μ , and kriging variance, σ_k^2 , depend on the covariance function, or variogram, and locations, not the actual observed values.

To evaluate the covariance function, or variogram, an estimate is made at x_{jo} (an observed data location) by leaving out that observation and using the remaining points to develop the kriging equations. This procedure is repeated with the exclusion of each of the other remaining observation points. The average squared normalized difference,

$$[V_{jo}(x_{jo}) - V(x_{jo})]^2 / \sigma_k^2 \qquad (3.14)$$

is calculated for each omitted point, x_{jo}. On the average, this

value should approach one if the assumptions of the model hold and the correct estimate of the variogram is used.

RESULTS AND DISCUSSION

Analyses of Total Head and Moisture Content Data

The hydraulic head and moisture-content data used in this study was collected by means of porous-cup tensiometers and neutron logging. Due to the uniformity of the soil, the distance to the water table, and the distance to other vegetation it was possible to make certain assumptions concerning the movement of soil water. The assumptions are that water losses may be attributed to evaporation, transpiration by the plant, vertical seepage, and changes in storage. In order to examine the validity and significance of each of the assumptions, the data was arranged so that the two- and three- dimensional characteristics could be assessed.

Total Head Observations. Total hydraulic head data was used to examine if, and how, water extraction by plant roots affects soil pressures. It was observed that water uptake patterns are affected not only by root distribution, but also by topography and atmospheric conditions. Total head data may be used to estimate the soil-water potential, although anisotropy, created by non-uniform water contents and stratification, must be taken into consideration.

Figure 10 is a vertical cross-section of the total head field on August 1, 1985. (This figure, along with figures 12 -

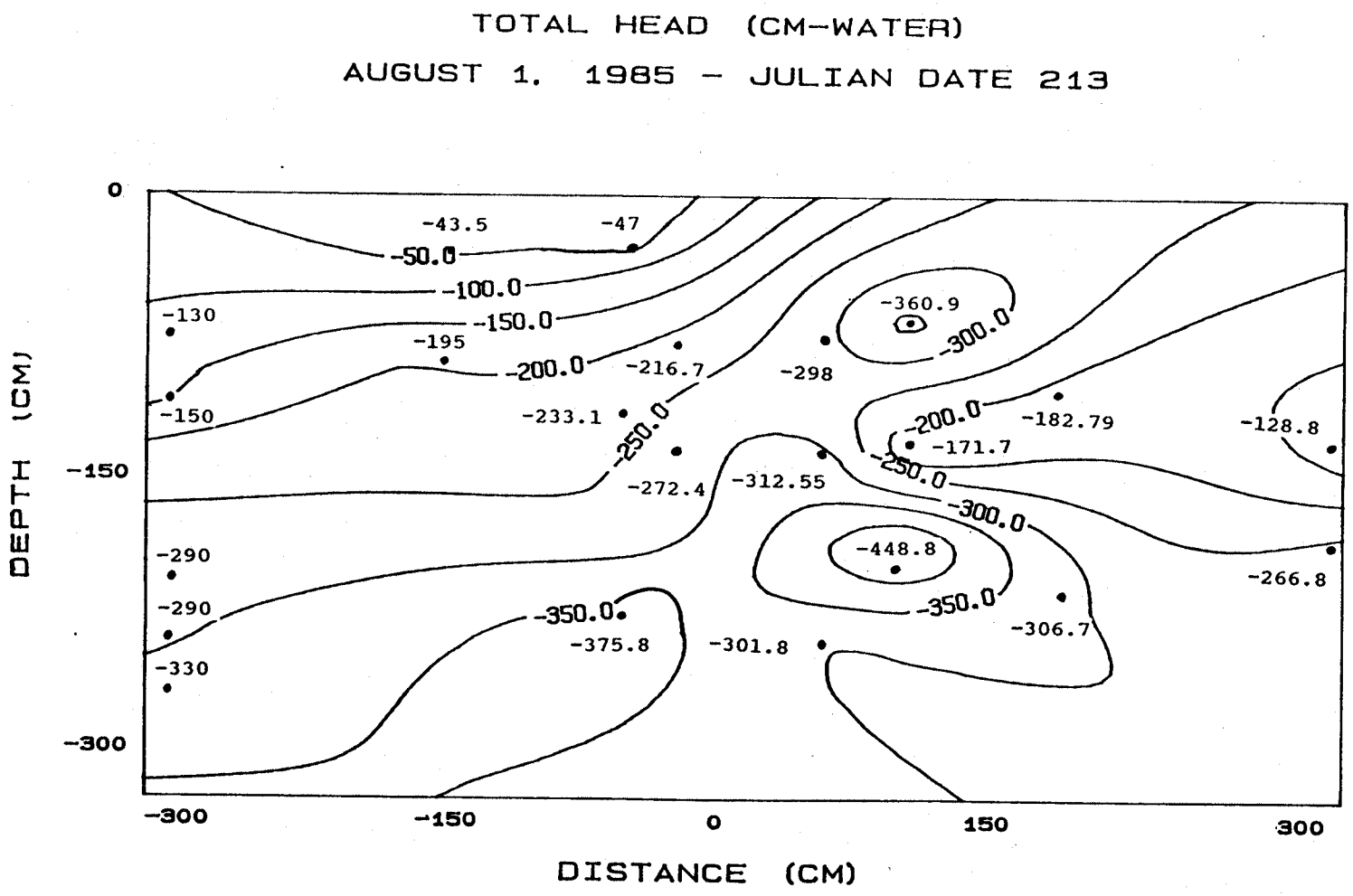

Figure 10. Vertical cross-section of total head on August 1, 1985. (Plant located in center of plot.)

15, displays no vertical exaggeration. The plant was located in the center of the plot, and the dune crest was towards the right side of the figure.) In general, the low hydraulic head values in the profile reflect the high temperatures and low precipitation throughout July and the fact that the Dalea scoparia was in full bloom. Hydraulic-head values were not uniformly distributed around the plant but instead were lowest on the dune side of the plant canopy where moisture was highest. During the late summer months, when overall soil-moisture was very low, plant roots appeared to withdraw water from where it was most available.

Soil-moisture tends to be greater at hillslope bases due to the change in surface gradient. According to the work of Zaslavsky and Sinai (1981) subsurface stormflow, or interflow, does not infiltrate vertically on hillslopes. Soil-moisture may follow a path which includes a horizontal flow component which is governed by the slope, rainfall intensity, antecedent moisture, and some coefficient of anisotropy. Figure 11 is a simulation of the surface of the dune area in three-dimensions and shows the location of the plant and neutron access tubes.

The late summer to early fall is characterized by frequent and heavy rainfalls in the semi-arid southwest. Precipitation during the first ten days of October alone was 32.0 mm. Low hydraulic head values recorded on October 11, 1985, indicate that plant roots were withdrawing water locally from the soil (figure 12). With abundant soil water, water withdrawal appeared to be

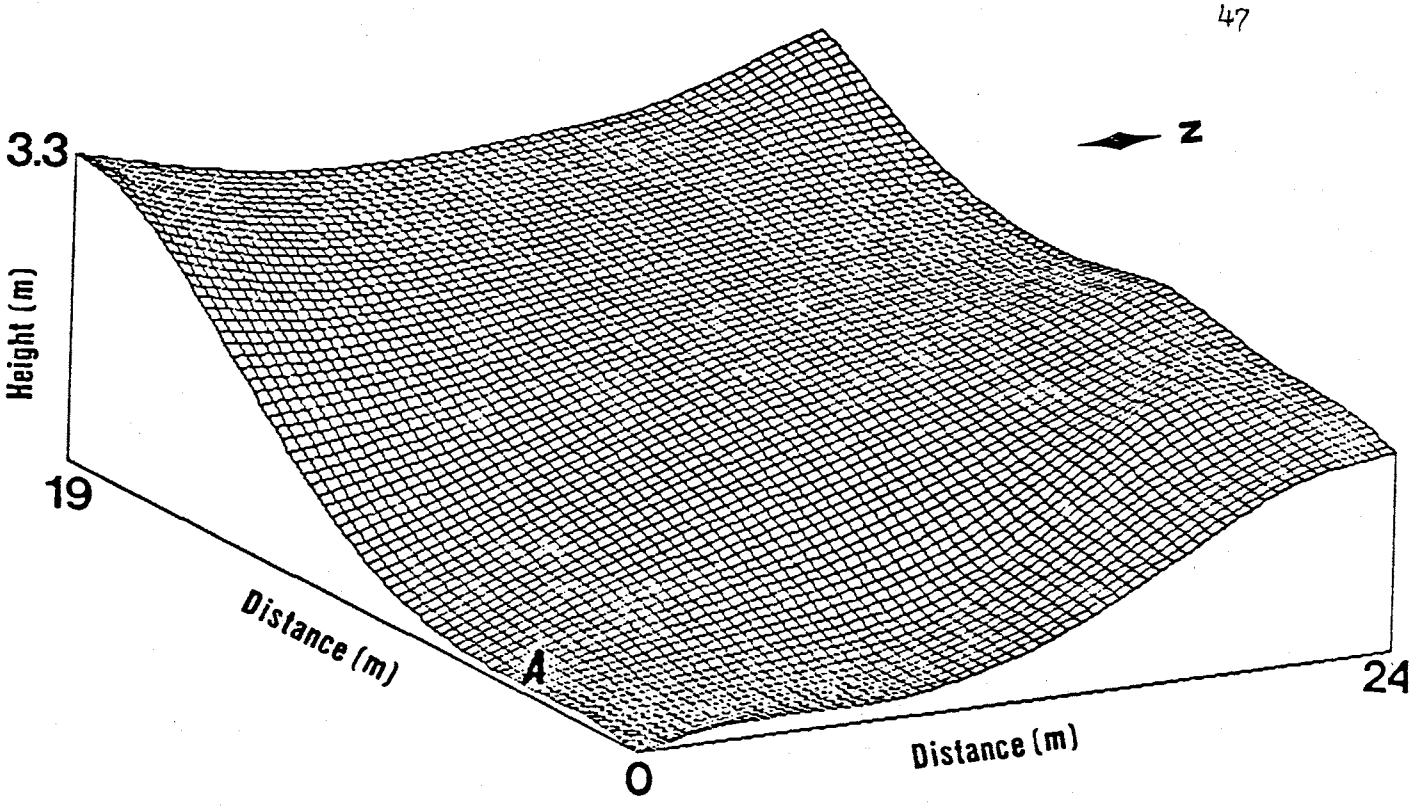

Figure 11a. Simulation of the dune surface. (Plant located at point A.)

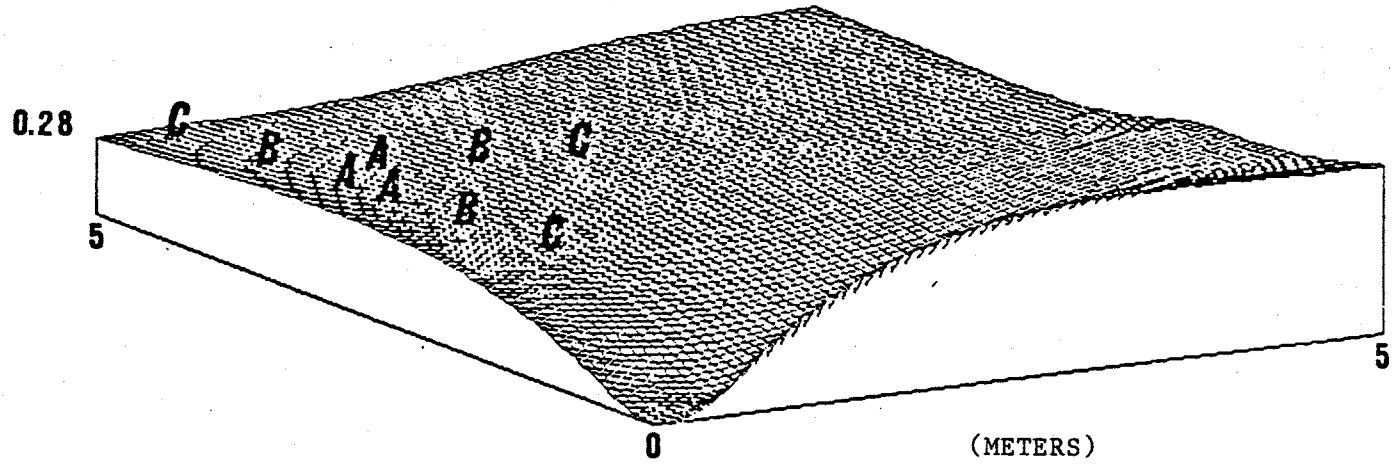

Figure 11b. Close-up of plant area and locations of neutron access tubes. (Vertical exaggeration 10x vertical scale of figure 11a.)

fairly uniform beneath the canopy of the plant in contrast to the drier, summer months represented by figure 10.

Throughout the plant's dormant season, which was approximately from November to April, a hydraulic head gradient of nearly unity existed in the soil surrounding the plant (figures 13, 14). The flow field was dominated by downward percolation and minor surface evaporation. By April of 1986, the plant stems had turned green again, which was evidence that the Dalea scoparia was transpiring.

On June 10, 1986 (figure 15) the hydraulic head gradient was about unity to the 150 cm depth. Below this depth, the gradient increased indicating water losses due to uptake by plant roots. Hydraulic head data proves that there was a downward liquid phase at all times of the year below ~30 cm and through the root zone. Water losses to surface evaporation were therefore primarily confined to depths less than 30 cm. Downslope from the plant the contours indicate a zone of greater suction. Unfortunately, this was based on only one tensiometer which had an extremely low head reading. It is possible that this reading is due to the nearby mesquite tree exerting extremely low pressures to the surrounding soil.

Minima in total head values indicate the zone(s) of maximum water withdrawal during each season (figure 16). Tensiometers, located directly beneath the plant, were used to monitor negative soil pressures at depths ranging from 30 to 240 cm throughout the study period. In the late spring and late fall, the lowest soil

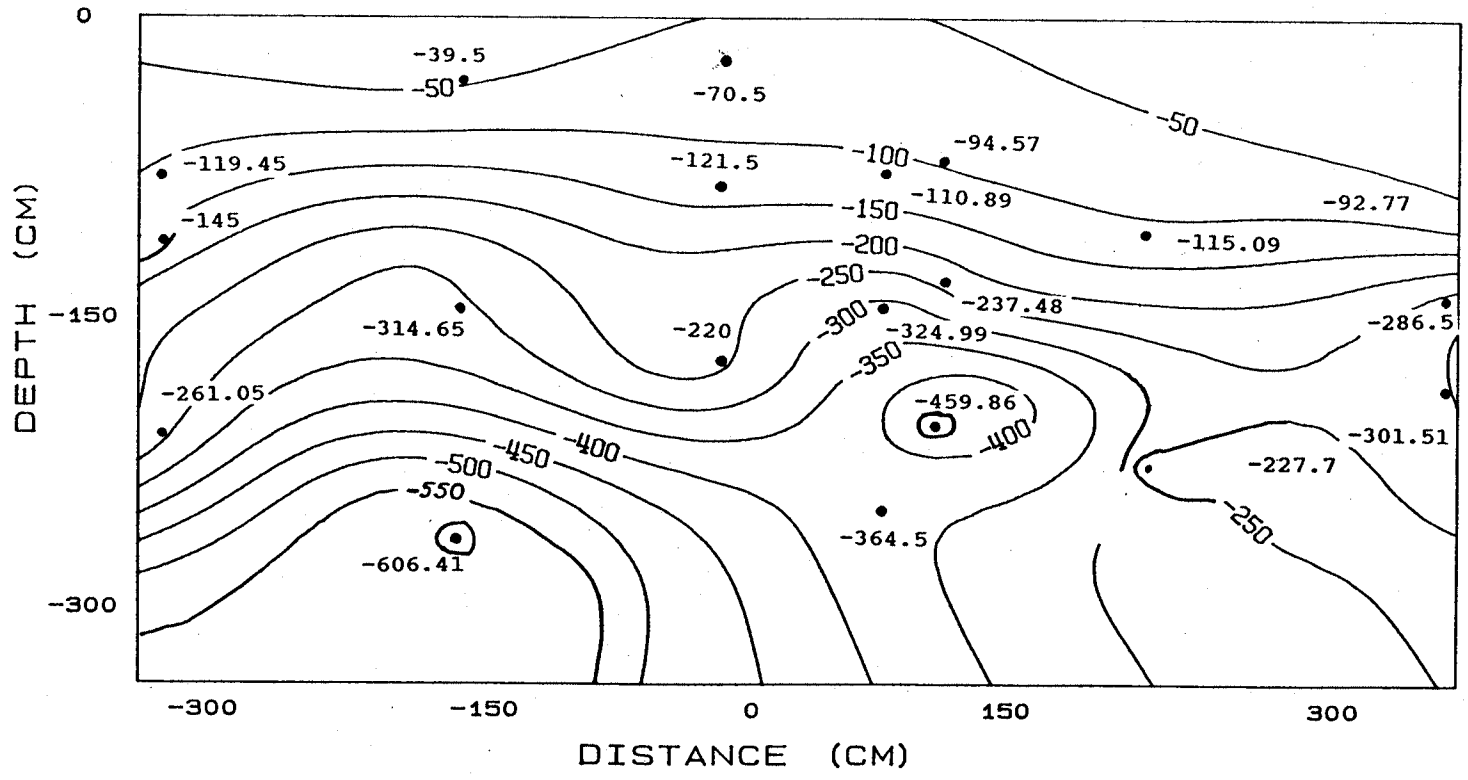

Figure 12. Vertical cross-section of total head on October 11, 1985. (Plant located in center of plot.)

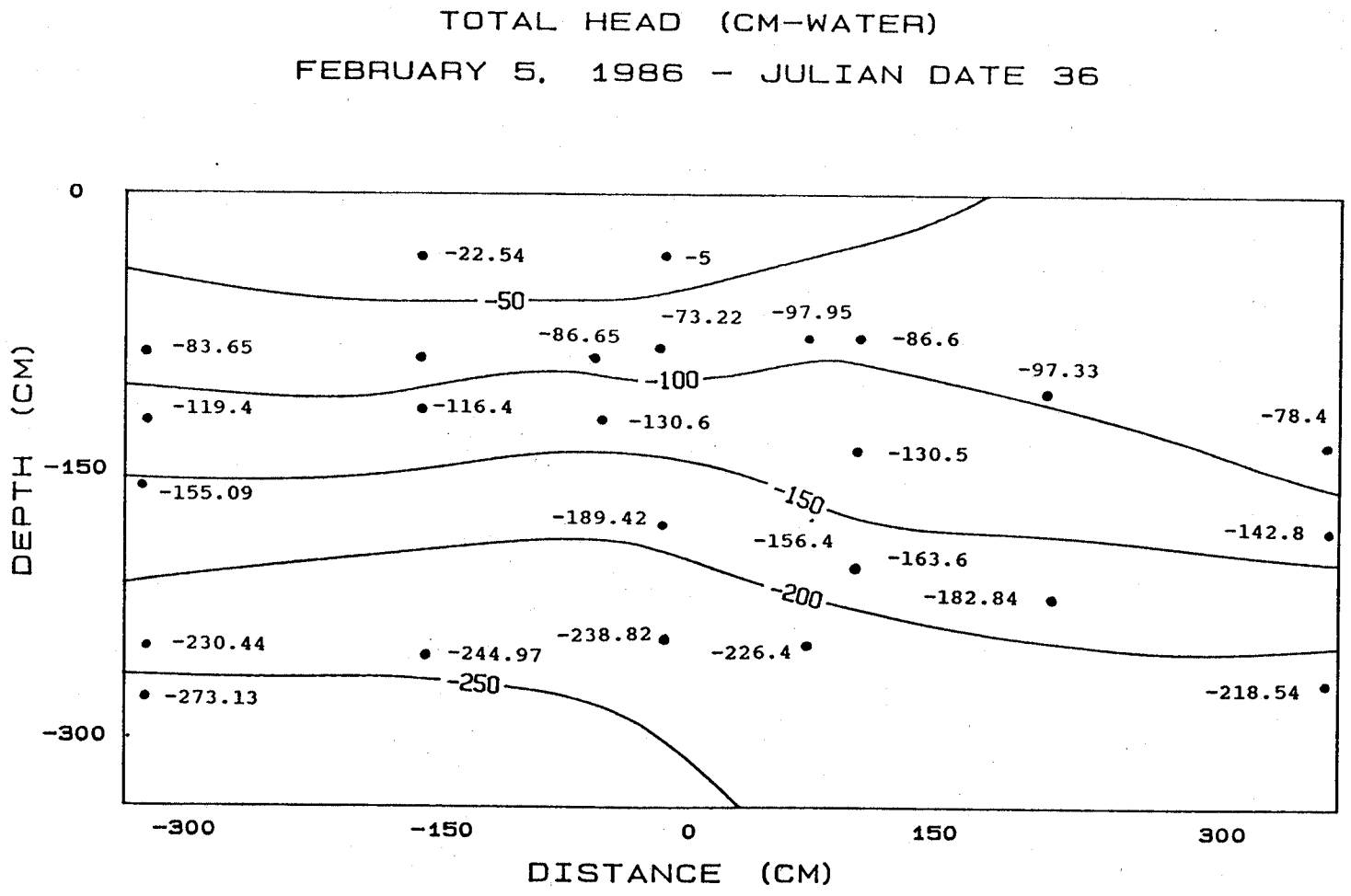

Figure 13. Vertical cross-section of total head on February 5, 1986. (Plant located in center of plot.)

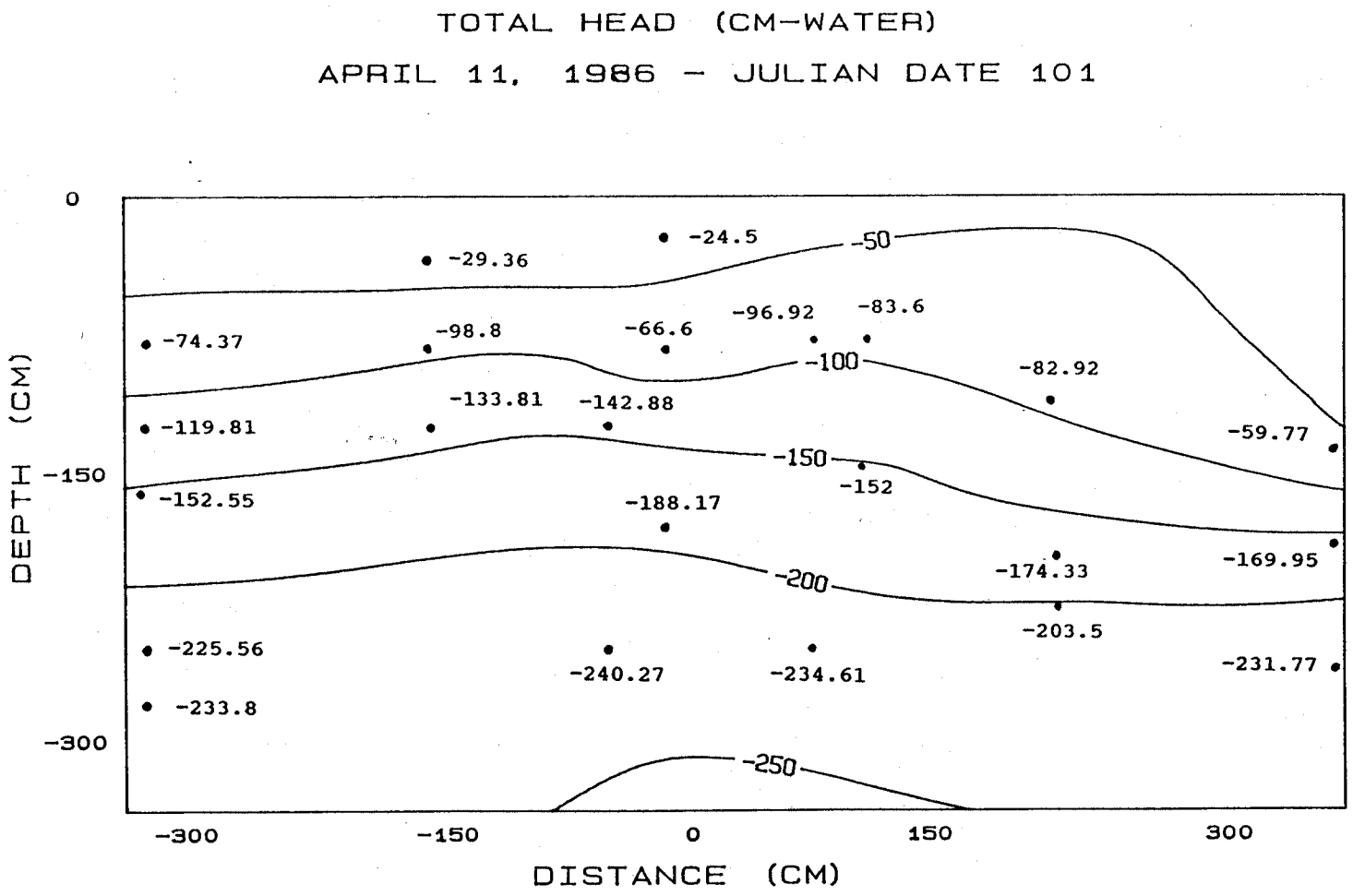

Figure 14. Vertical cross-section of total head on April 11, 1986. (Plant located in center of plot.)

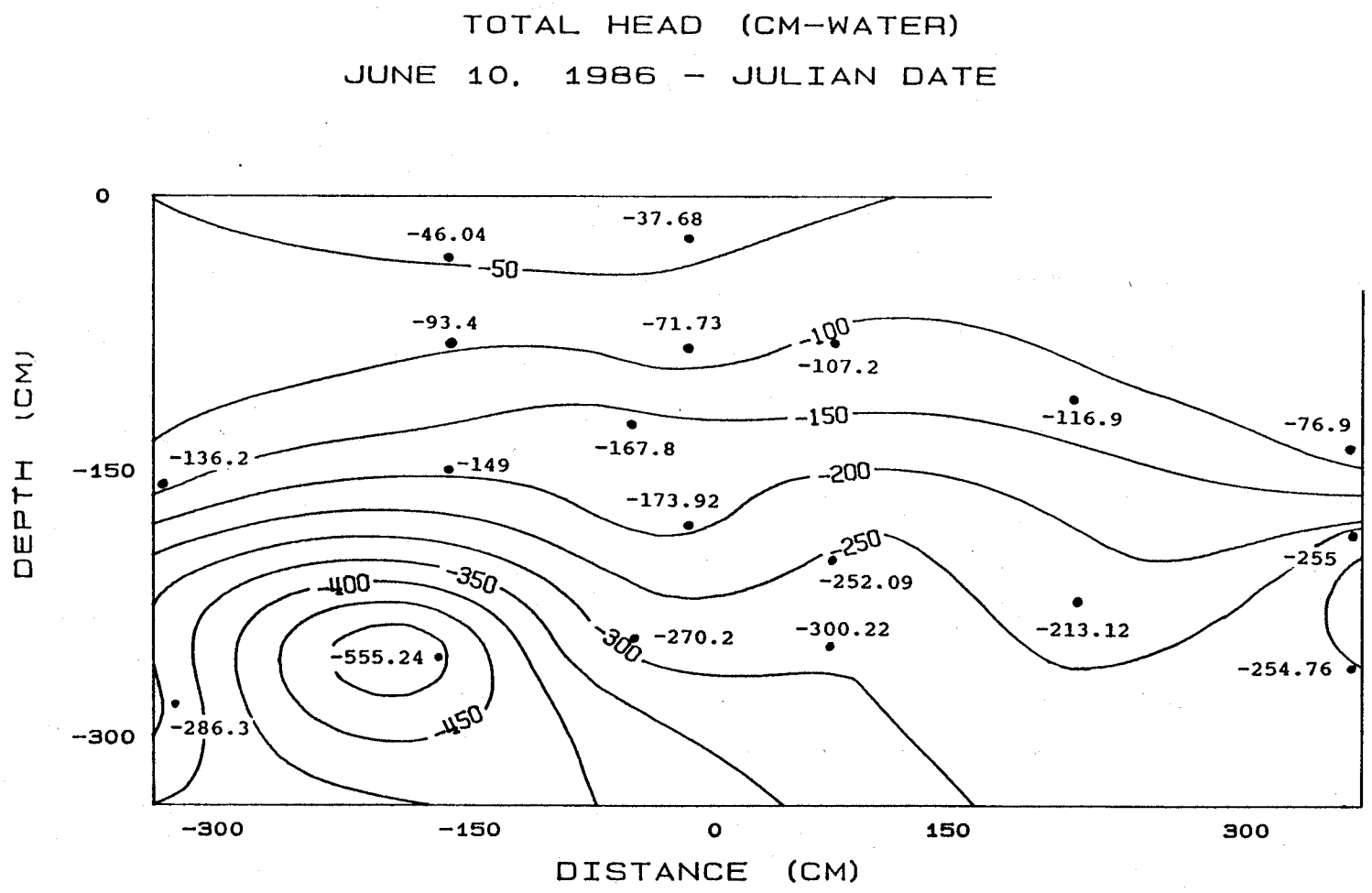

Figure 15. Vertical cross-section of total head on June 10, 1986.
(Plant located in center of plot.)

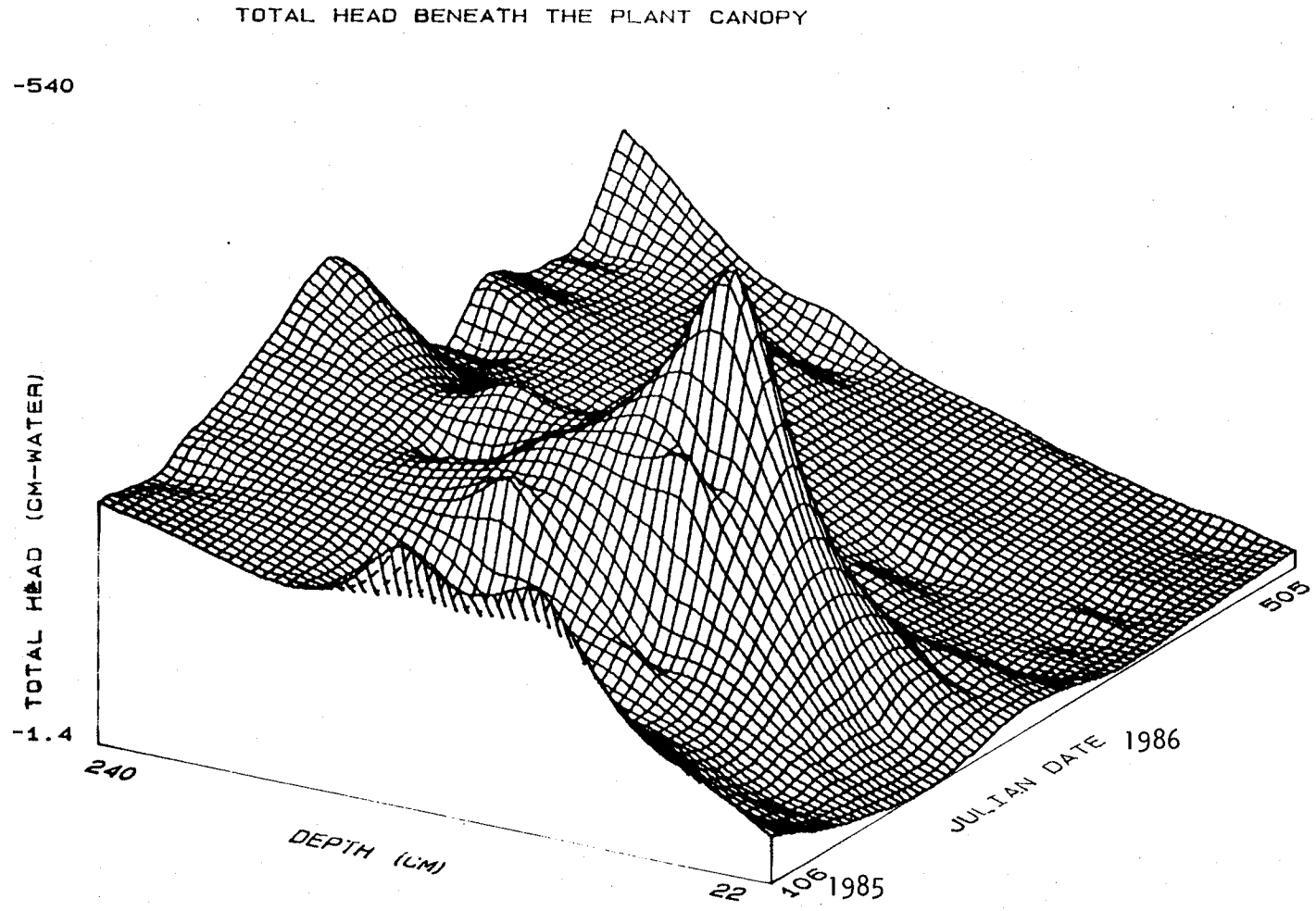

Figure 16. Total head beneath the canopy of the plant versus time and depth.

pressures were observed within the 180-240 cm depth. During the summer the lowest soil tensions were observed in the 90-150 cm interval indicating that lateral roots were actively withdrawing water. It appears that soil water extraction just prior to and after the dormant season occurred at greater depths than during the peak of the growing season. Moisture was highest deep in the profile and therefore more readily available for uptake by the main tap roots. The permeability of individual roots to soil-water was not constant spatially, nor temporally, as indicated by water withdrawal patterns.

Moisture Content Observations. Moisture content, although it is not a direct indicator of flow directions, does reveal information about moisture losses and gains. Observing changes in percent moisture throughout an entire year offers insights to the timing of infiltration, evaporation and redistribution of soil water.

The infiltration and redistribution processes may be seen graphically in figures 17a, b. The figures represent the moisture content at different points in time for drainage beneath the plant canopy (neutron tube West A, figure 8). As the summer season continues the profile becomes progressively drier. A precipitation event of 18.4 mm occurred on October 9, 1985 and by October 11, the wettting front had moved to approximately 100 cm below land surface. By November 8, the wetting front had only moved to 200 cm. During December, February, and March drainage

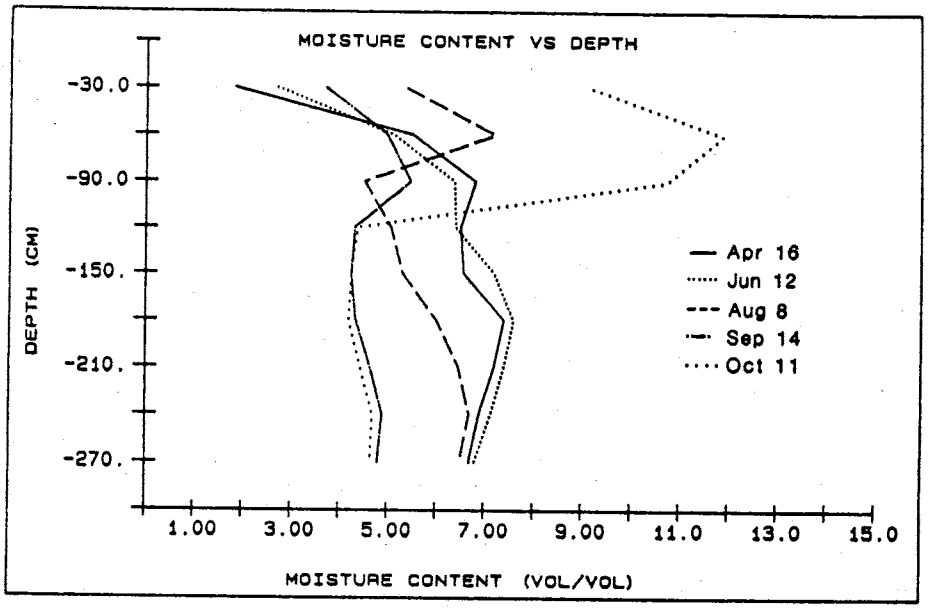

Figure 17a. Drainage beneath the plant canopy from April to October, 1985. (Neutron tube West A.)

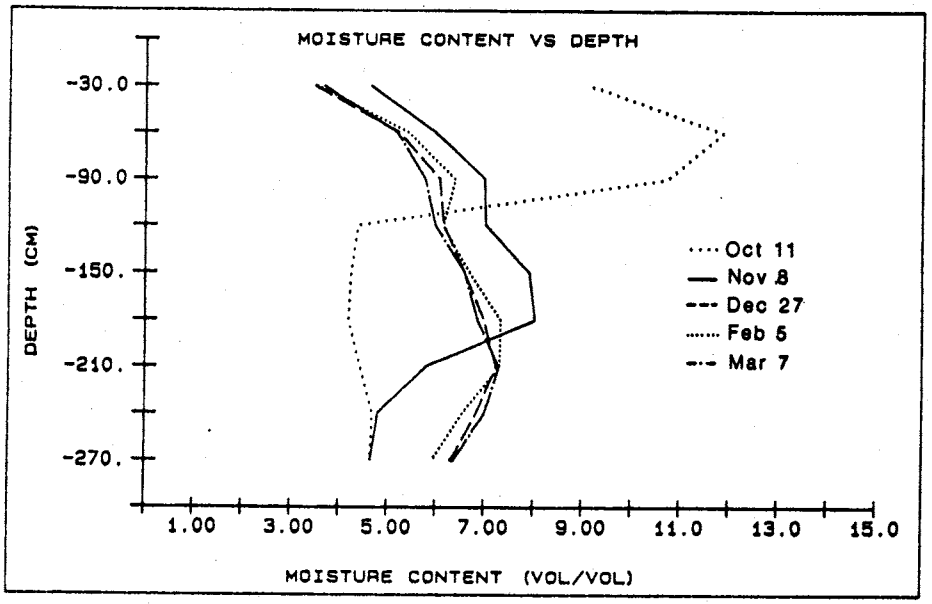

Figure 17b. Drainage beneath the plant canopy from October, 1985 to March, 1986. (Neutron tube West A.)

profiles show only slight redistribution above 2.7 m. There was very little net change in moisture, at 2.7 m, between April, 1985 (6.8%) and March, 1986 (6.3%). Drainage profiles for the neutron tube located 2.65 m from the canopy exhibit similar trends, yet higher overall water contents (figures 18a, b).

Water losses to evapotranspiration were greatest between June and September at depths upwards of 200 cm. This observation is illustrated in figure 19 where moisture beneath the plant canopy is plotted as a function of depth and time. Essentially, the vertical flux was followed as a point through time. The greatest variance in moisture content occurred during the summer and fall months when evapotranspiration and precipitation were most intense. During the dry winter and spring seasons, water was slowly redistributed throughout the profile. This figure graphically reflects the dynamic response of additions and subtractions to the soil with no significant net annual loss or gain to storage within the upper 2.70 m.

Evapotranspiration and precipitation have a pronounced effect on water content primarily during the summer months at depths less than 150 cm. Maxima in the moisture content data at the edge of the plant canopy (figures 19) represent specific precipitation events and may be traced through time and depth. Similarly, minima are representative of periods with intense evaporation and negligible precipitation. Eventually, the significance of each event disipates with time and depth. The moisture content remains fairly constant throughout the winter

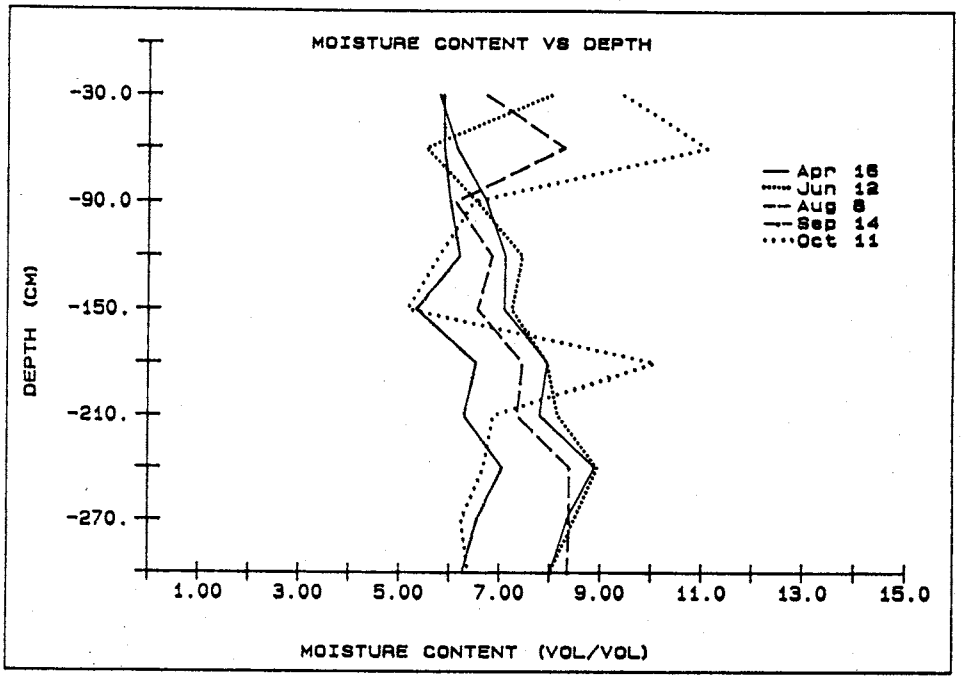

Figure 18a. Drainage 2.65 m from the plant from April to October, 1985. (Neutron tube West C.)

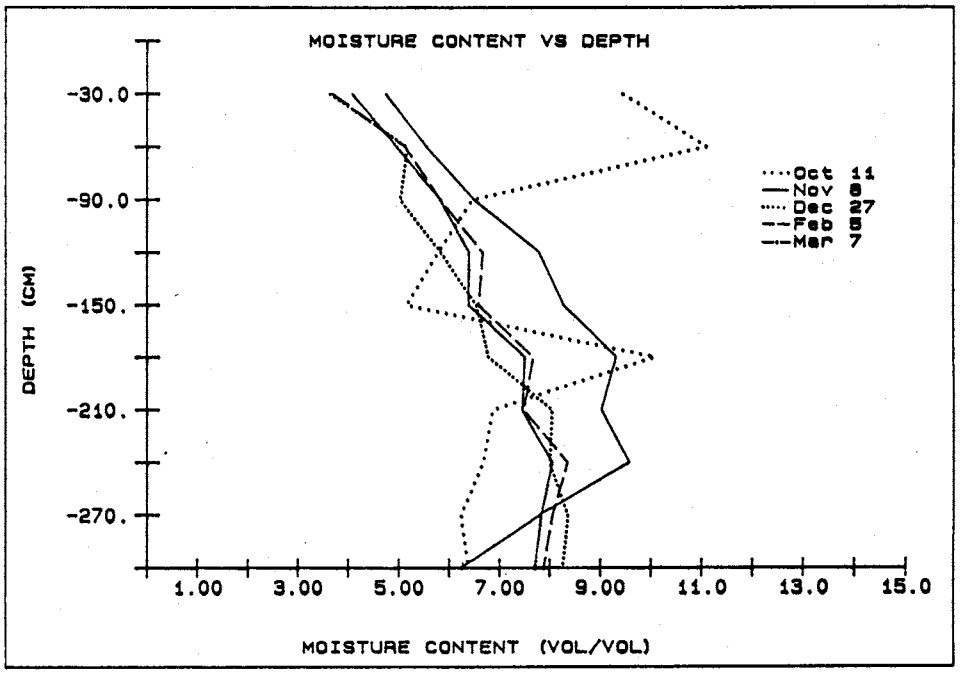

Figure 18b. Drainage 2.65 m from the plant from October, 1985 to March, 1986. (Neutron tube West C.)

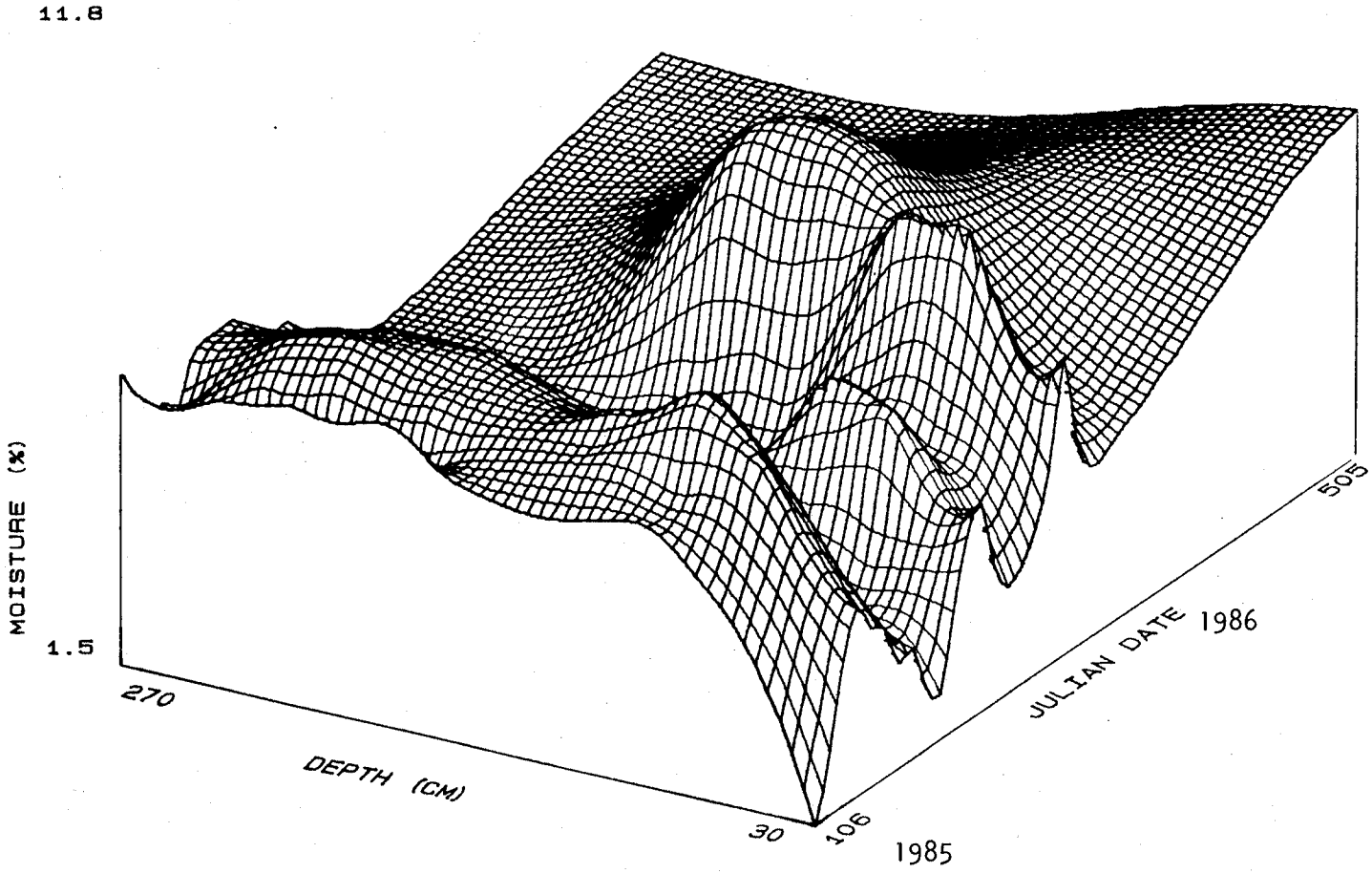

Figure 19. Moisture content versus time and depth at the edge of the canopy. (Neutron tube West A.)

months when transpiration, potential evaporation, and precipitation were negligible. However, during the summer months soil moisture losses were the greatest and also the most erratic. Water withdrawal by roots appears to be most active during this time especially at depths less than 150 cm. The cause of dryness at depth may have initially been related to intense surface evaporation or transpiration and have propagated vertically ahead of wetting fronts. Therefore it is difficult to make specific remarks on the structure of the root system.

An examination of the moisture field within a given plane revealed some anticipated and some surprising results. In figures 20 - 24, the areal distribution of moisture was plotted for depths of 60, 120, and 300 cm. The plant was located in the center of the plots and the high and low moisture values are indicated. These depths were chosen to examine the effects of surface evaporation, shallow lateral roots, and deep tap roots.

Figures 20-21a, b, c are an illustration of the rapid soil-water flux and the influence of topography within a shallow, sandy, vadose zone. Plant transpiration was probably the major source of moisture loss at all three depths during the late summer season. The rain that had fallen in late July, had infiltrated to the 60 and 120 cm depths by August 28, 1985. Moisture content steadily increased towards the flank of the dune. Soil-water tended to accumulate at the base of the hillslope where the change in surface gradient was largest.

In November, 1985, the moisture content at 60 cm was rather

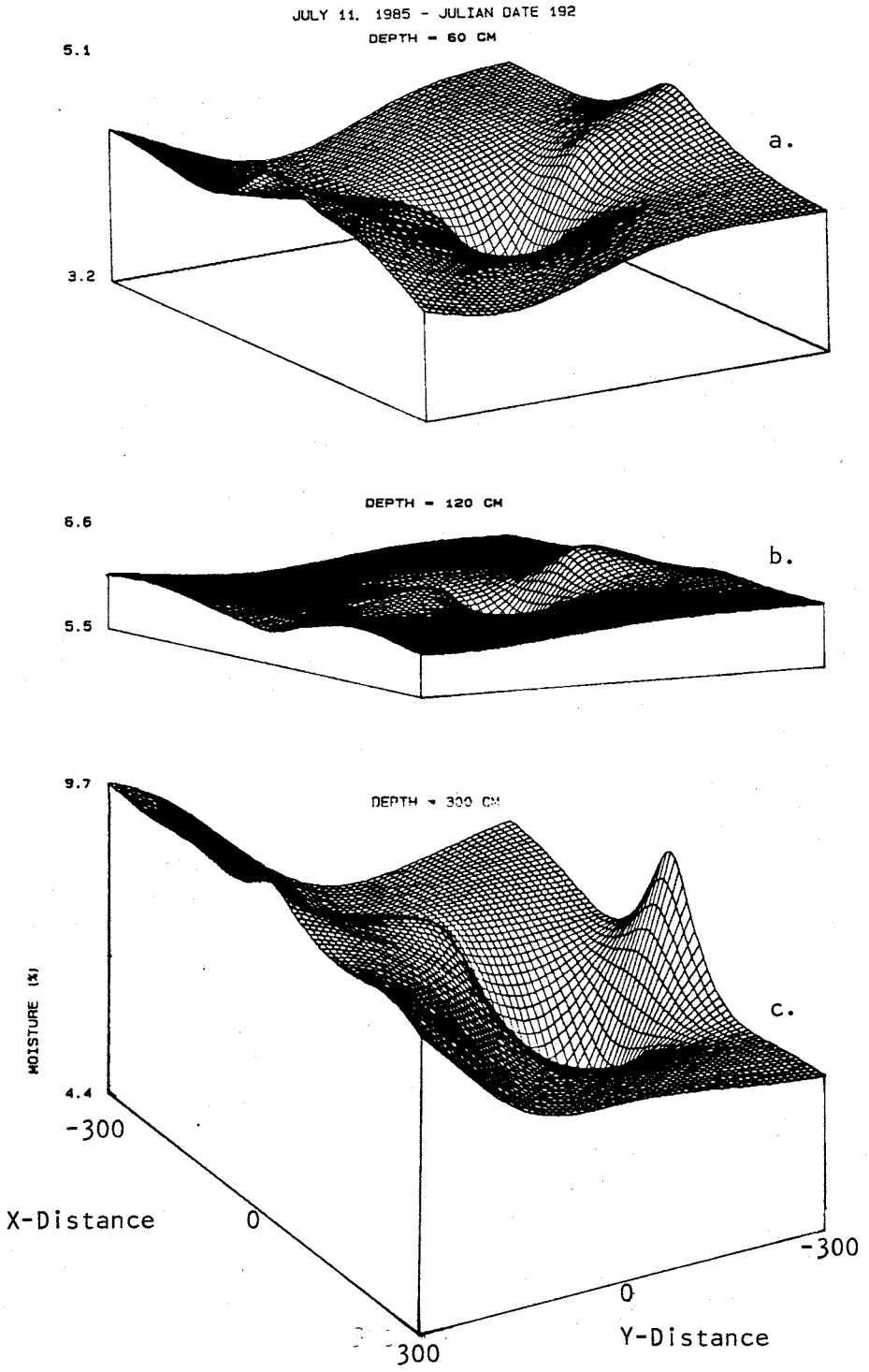

Figure 20. Moisture content on July 11, 1985, for 60, 120, and 300 cm depths. (Plant located in center at intersection of distance axes.)

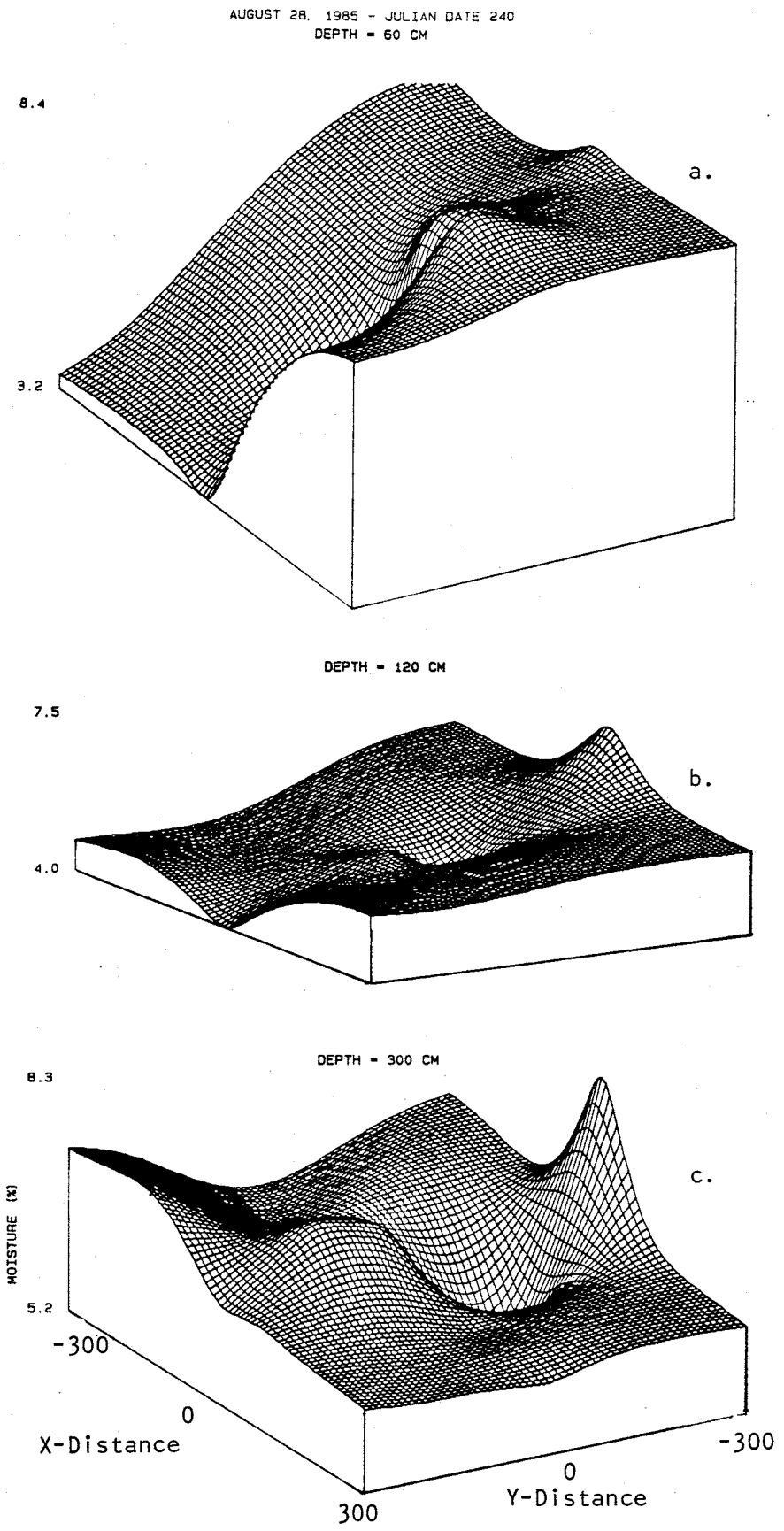

Figure 21. Moisture content on August 28, 1985, for 60, 120, and 300 cm depths. (Plant located in center at intersection of distance axes.)

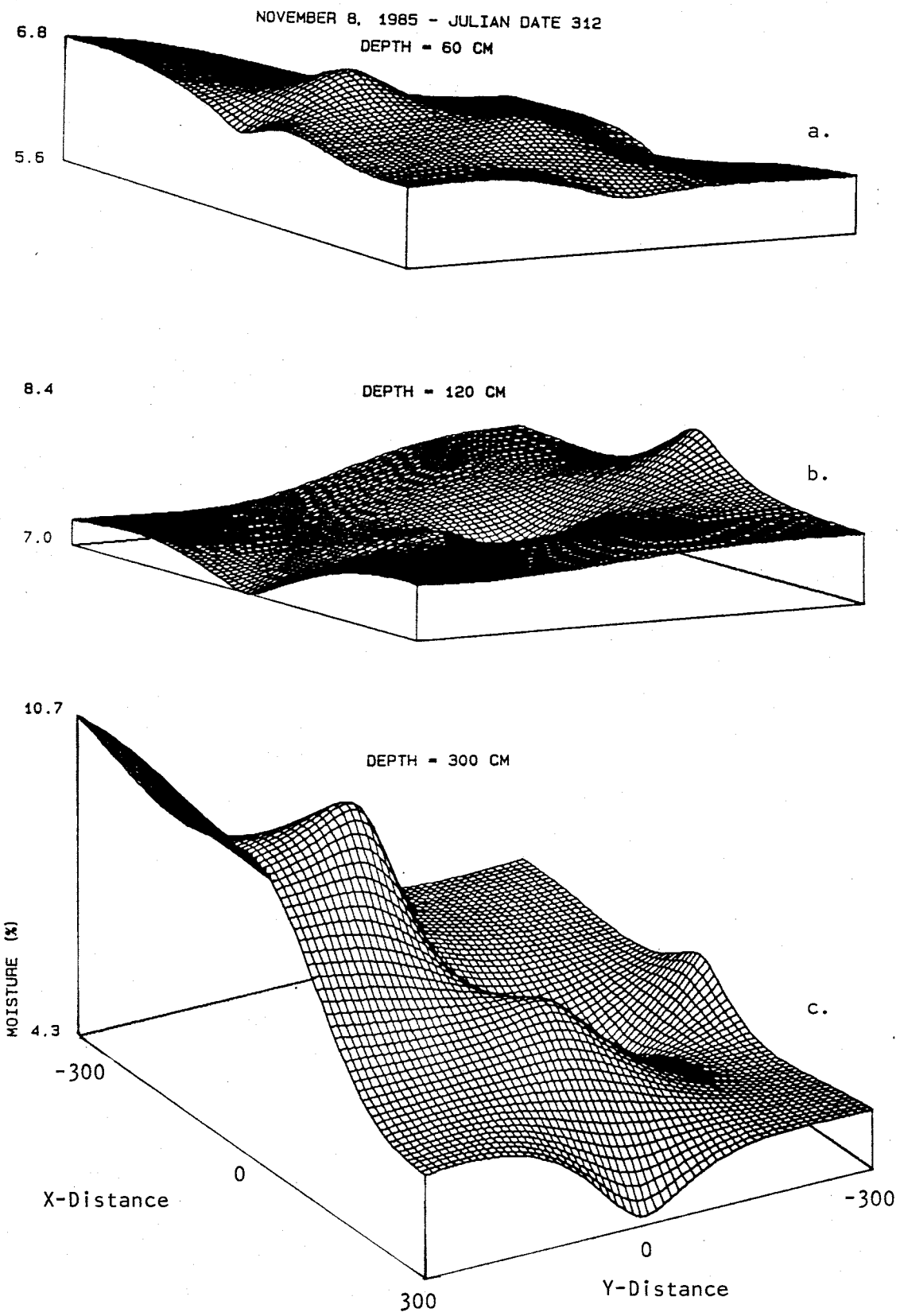

Figure 22. Moisture content on November 8, 1985, for 60, 120, and 300 cm depths. (Plant located in center at intersection of distance axes.)

uniform (figure 22a), as would be expected if the plant were dormant. Nevertheless, the moisture content at the 120 cm depth suggests some water loss to the plant (figure 22b). It is possible that the plant canopy may have shielded some rain from the soil surface creating the zone of low moisture beneath it. The cause of the dryness may have been related to evapotranspiration and have moved downward ahead of a wetting front. Decreasing water content towards the hillslope side of the dune is probably a result of an asymmetrical root distribution, or water uptake pattern (figure 22c). (The land surface slope increases in the direction of the Y-distance axis, as shown in figures 20 - 24.) Moisture losses were greatest where the roots appear to be most dense, or where moisture is most readily available. No direct evidence of the root density exists, yet based on root distributions of other Dalea scoparia plants rooting density rapidly decreases, vertically and horizontally, from the main tap roots.

On January 23, 1986, moisture was laterally uniform at the 60 and 120 cm depths (figures 23a, b). This reflected atmospheric conditions such as zero rainfall, low evaporation, and negligible transpiration. Redistribution of water content was slowly occurring at the 3 meter depth (figure 23c), yet the evidence of a tap root in the center of the plot may still be observed. By May 6, 1986, the plant was visibly showing signs of life on the surface, as well as, on the subsurface (figure 24a, b, c). Moisture content was lowest directly beneath the plant

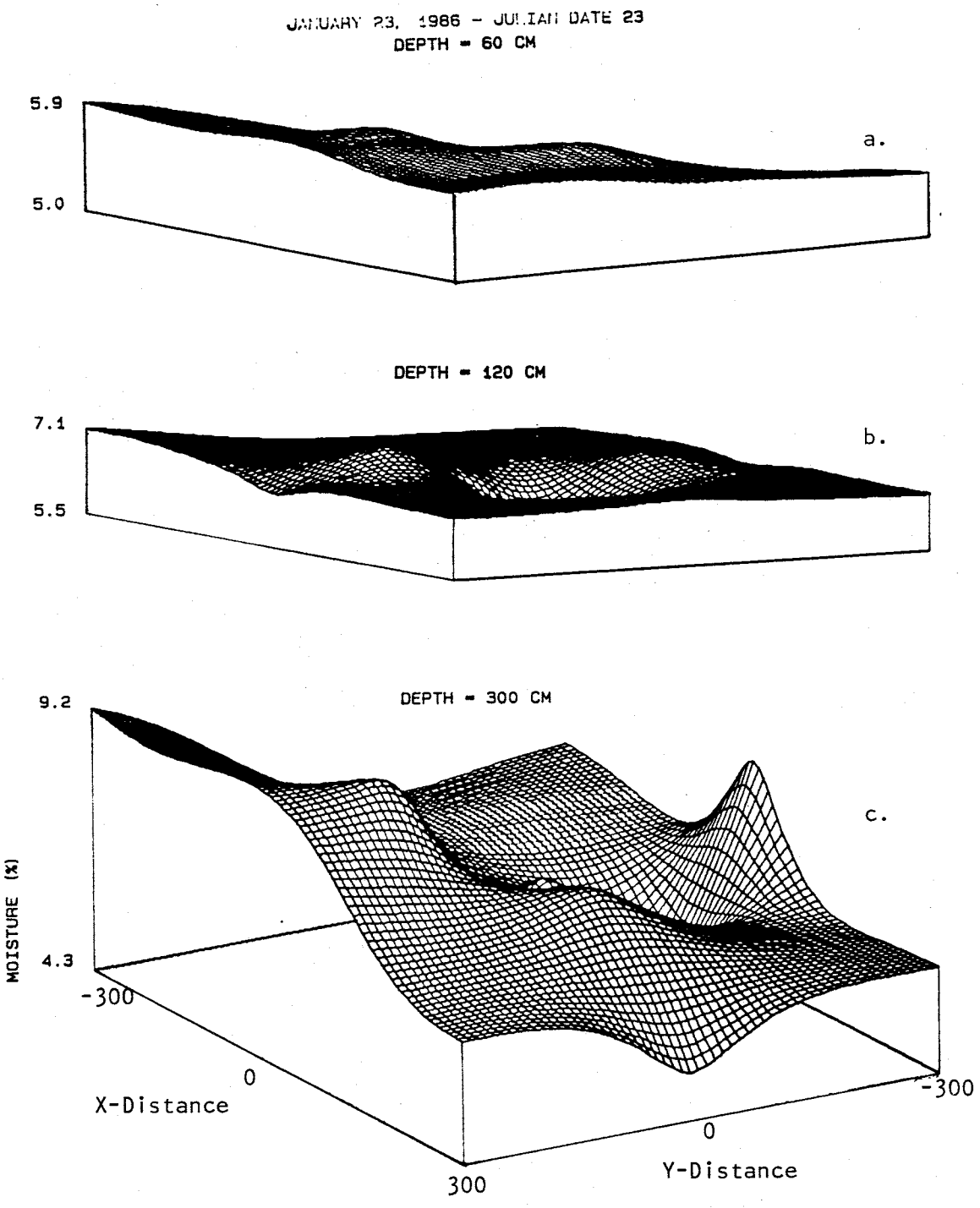

Figure 23. Moisture content on January 23, 1986, for 60, 120, and 300 cm depths. (Plant located in center at intersection of distance axes.)

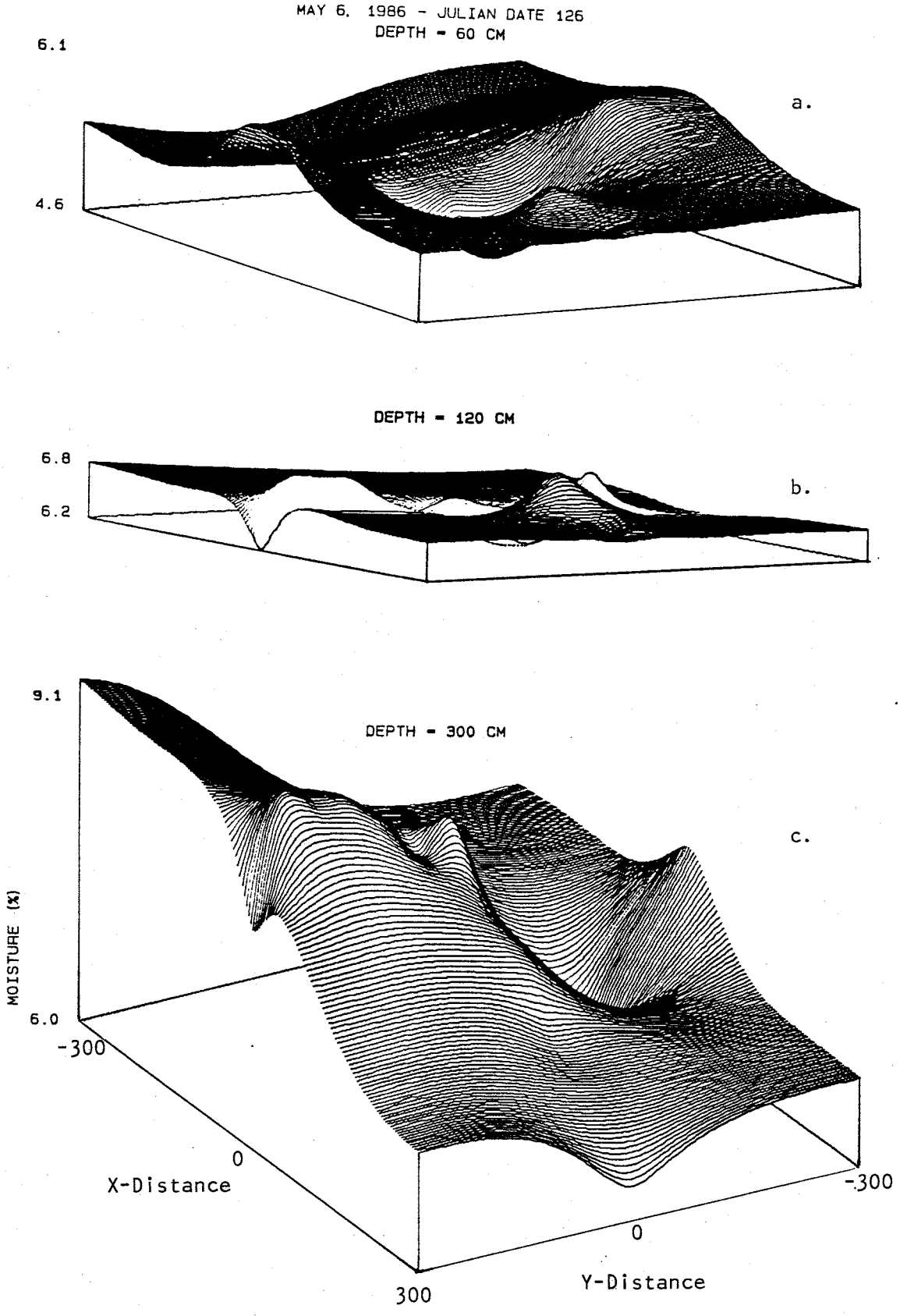

Figure 24. Moisture content on May 6, 1986, for 60, 120, and 300 cm depths. (Plant located in center at intersection of distance axes.)

canopy.

Soil moisture and hydraulic gradient indicate the pattern of water uptake by plant roots and possibly root distribution. The area, or zone, of maximum water withdrawal is primarily dependent on moisture content. Higher moisture contents apparently increase root permeability by decreasing the resistance of water flow across the soil-root interface. During the active growing season lateral roots contribute to the plant's soil water demand, whereas early and late in the season the tap roots provide the major water supply.

Water Balance Results

Meteorological conditions, moisture content and pressure-head were monitored for a period of one year. The data was used to evaluate the water balance in the soil surrounding the Dalea scoparia plant. Recharge, change in storage, and precipitation were determined and used to estimate the average evapotranspiration rate. Each of the major components were expressed in terms of a monthly rate.

Meteorological Data. Meteorological observations have been collected at the Sevilleta National Wildlife Refuge on a weekly basis since the winter of 1983. As previously mentioned, data, concerning precipitation, average wind speed, and standard pan evaporation for the period of this study have been included in

Appendix D. Rain gauge data were used in water balance accounting while wind and evaporation data were included as seasonal and climatological indicators.

Meteorological data reflect only the potential for evapotranspiration. For example, evaporation from open water is an indicator of the atmospheric potential to vaporize water. Actual bare soil evaporation is limited by the amount of moisture in the soil. The evaporation rates, as well as, solar output, were maximum during the summer months and minimum during the winter months (figure 25). During the spring season, average winds were the highest for the year in part as a result of large differences between nighttime and daytime temperatures (figure 26). High winds increase evapotranspiration rates by aiding evaporation from the soil surface and the leaf surface. Anemometer, or cumulative wind speed, data was collected in terms of total kilometers and then divided by the number of days between readings. The result was a weekly, average wind speed without recording the timing, duration, or actual speeds. Precipitation most frequently occurred during the late summer and autumn, and was characteristically of a short, though intense duration. Precipitation during the summer of 1985 was sparse, however the following summer, precipitation was far more abundant (figure 27).

Seepage Prediction. Drainage beyond the rooting zone, even in a semi-arid climate, must be considered in any accurate

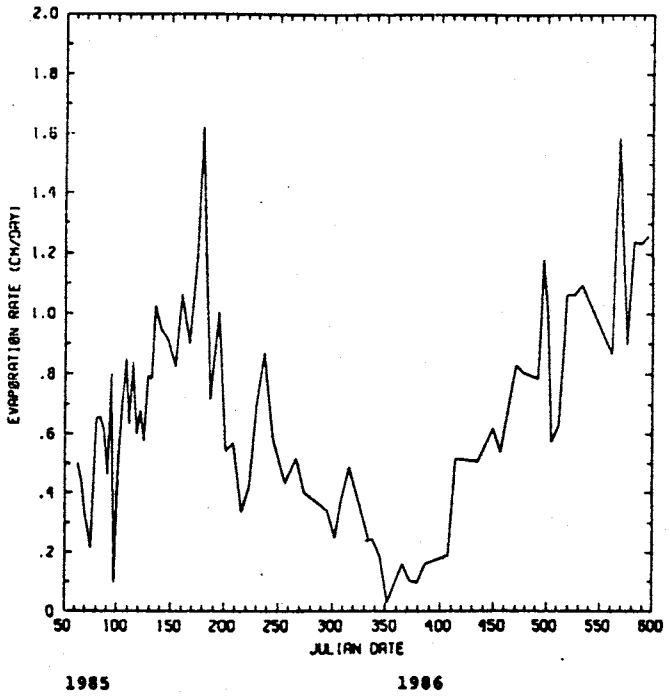

Figure 25. Class A pan evaporation.

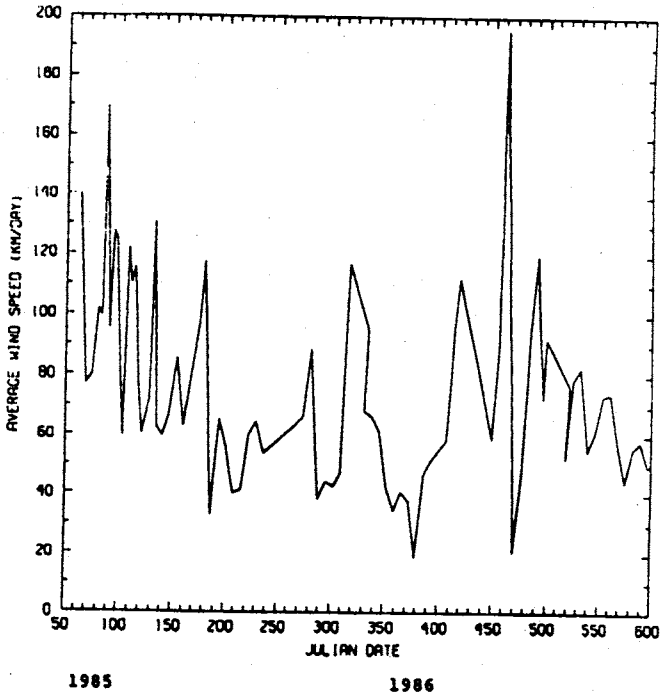

Figure 26. Average weekly wind velocity.

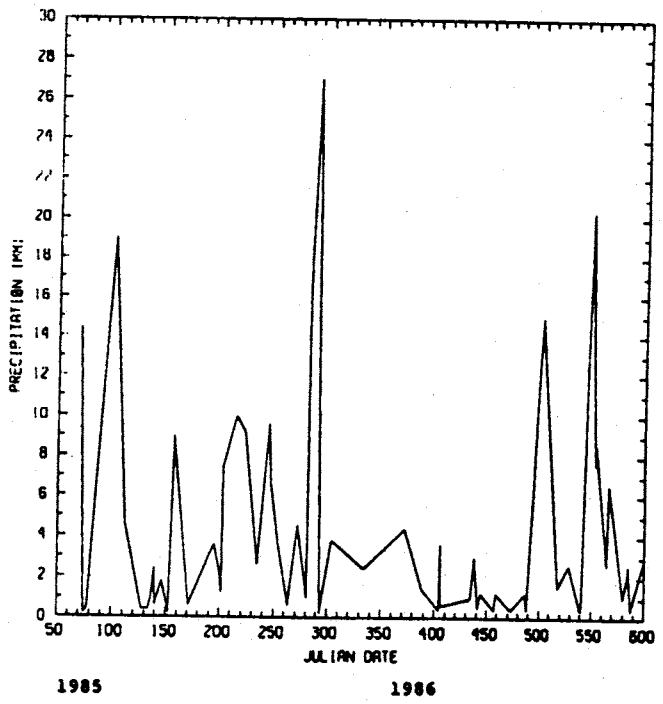

Figure 27. Precipitation events.

accounting of the water balance. Moisture content data and the resulting flux calculations determined that water movement occurs even directly beneath the canopy of the Dalea scoparia. For one-dimensional, unsaturated, vertical flow the Darcy flux is written in terms of pressure-head,

$$q = -K(\psi)\ i \qquad (4.1)$$

where i is the hydraulic head gradient,

or in terms of moisture content,

$$q = -K(\theta) \qquad (4.2)$$

assuming a unit hydraulic gradient.

Unsaturated hydraulic conductivity was calculated from the relationship between moisture content and pressure-head for the dune sand. Soil-moisture characteristic curves for the dune sands were derived from laboratory tests using Buchner funnel hanging columns and pressure plates (Appendix B-2 to B-8).

Van Genuchten (1978) developed a closed-form analytical solution to approximate the $K(\psi)$ - ψ relationship using a statistical model developed by Mualem (1976).

$$K_r = S_e^{-\frac{1}{2}} \left[\int_0^{S_e} \frac{1}{\psi(x)}\, dx \Big/ \int_0^{1} \frac{1}{\psi(x)}\, dx \right]^2 \qquad (4.3)$$

$K_r = K(\psi)/Ksat$ = Relative Hydraulic Conductivity [0]

ψ = Pressure Head [L]

S_e = moisture content [0]

A computer program by van Genuchten (1978) was employed to solve equation 4.3. Intially, the program solves for the empirical

constants and n. The parameters and n are obtained by a non-linear least squares fit to moisture retention data according to:

$$S_e = [\ 1/(1 + (\alpha\psi)^n)^m\ ] \qquad (4.4)$$

where ; $m = 1 - 1/n$ $\quad 0 < m < 1$ $\quad n > 2$

similarly,

$$K_r = S_e^{\,2}\ [\ 1 - (1 - S_e^{\,1/m})^m\ ] \qquad (4.5)$$

Using all of the available theta-psi data, wetting and drying curves were fit by the program to obtain the lines shown in figures 28, 29, based on the parameters in Table 2.

Compiling all of the theta-psi data (appendix B) was considered reasonable due to the uniformity of the soil. Particle-size analyses (appendix A) of samples collected during the installation of neutron tubes resulted in an average uniformity coefficient of 1.9432 (+/-0.338) and an average coefficient of curvature of 1.1789 (+/-0.3501). Variability in the theta - psi relationship may be related to some disturbance of the samples during collection, or subsequent handling, rather than soil properties alone.

Table 2. Moisture retention parameters in the Mualem model.

Numbers in parentheses represent standard error.

	Drainage	Imbibition
α	0.02912 (0.0018)	0.04320 (0.0044)
n	3.02687 (0.2616)	2.58385 (0.2555)

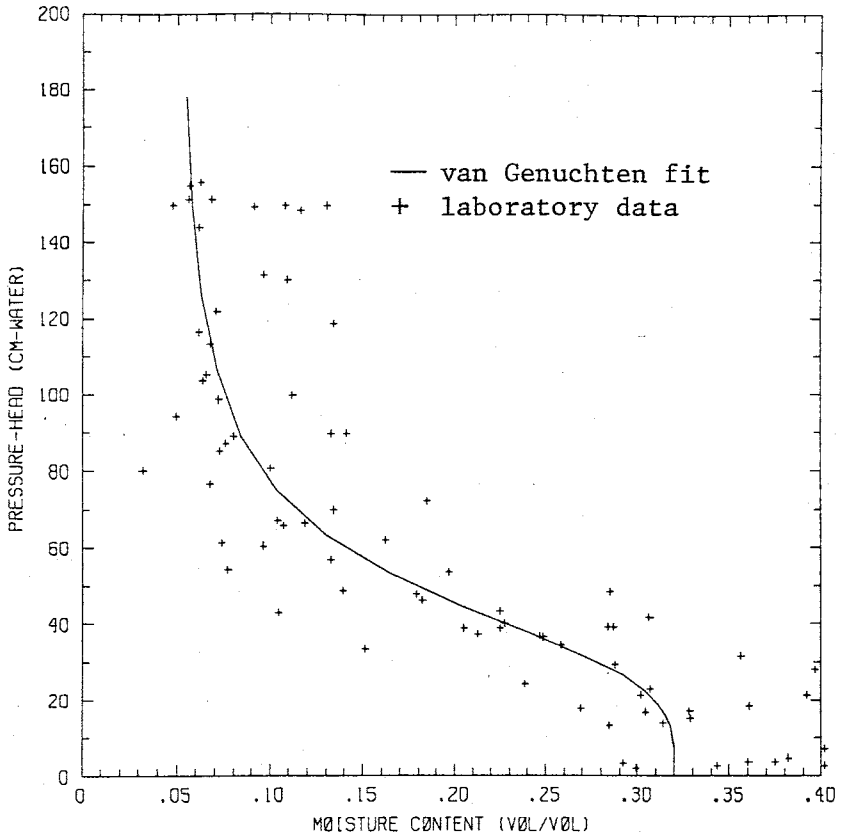

Figure 28. Moisture content versus pressure head for the drainage data.

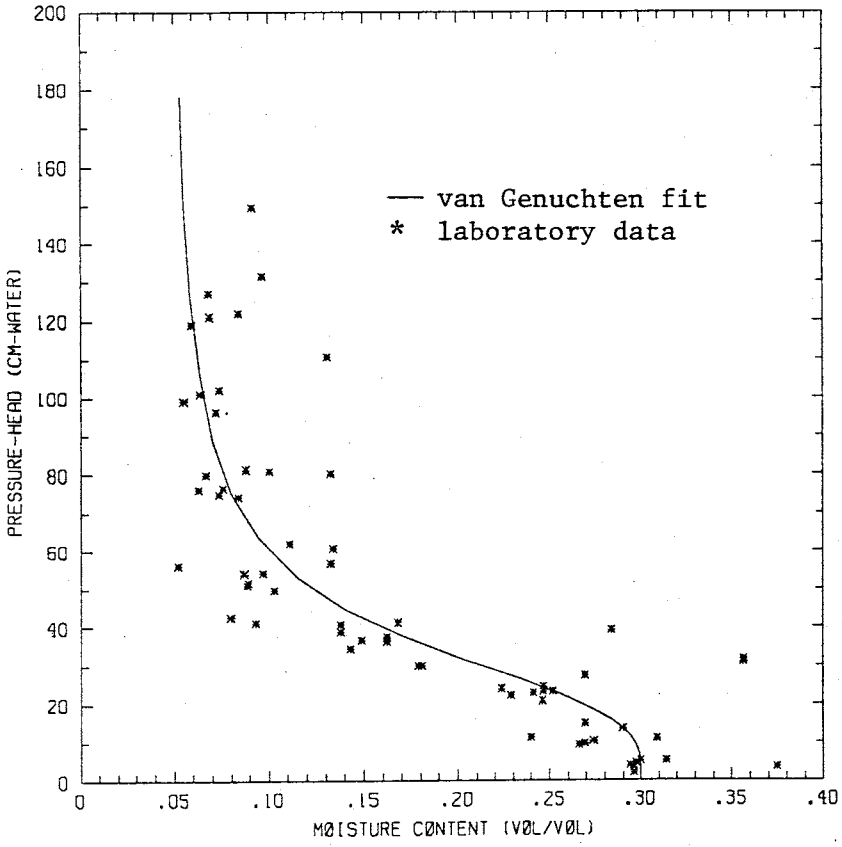

Figure 29. Moisture content versus pressure head for the imbibition data.

Unsaturated hydraulic conductivities corresponding to measured moisture-content and pressure-head data were derived and used to estimate deep drainage (table 3). In the dry zone, a one percent change of moisture content could result in an order of magnitude change in the hydraulic conductivity. Therefore, in dry soil conditions it is more appropriate to use pressurehead data which may be more sensitive to fluctuations in soilwater status.

Deep flux values from station 1 data (figure 3) for April, 1983 to May, 1984 are listed in table 4. Soil flux values using both pressure-head and moisture-content data were much smaller during that period than those calculated in this study. The average pressure-head and moisture-content values from the previous study were -96.2 and 5% respectively, and for the present study were -64.1 and 7%. The average precipitation rate during the 1985-86 season (0.043 cm/day) was 30% greater than that during 1983-84 (0.029 cm/day). Another factor to consider is that the soil at station 15 is more coarse than that at station 1, therefore the saturated hydrualic conductivity is greater.

Overall, hydraulic conductivity derived from pressurehead was greater than that derived from moisture content, especially during the winter months. The average monthly pressurehead and total hydraulic head gradient were calculated for depths between 180 and 240 cm and the corresponding hydraulic conductivity was determined from figure 30. During the winter months pres-

Table 3. Deep flux estimates using pressure-head and moisture-content data.

[1] Arthimetic average for 180, 210, 240, 270, 300 cm depths.
[2] Flux calculated using data collected at the edge of the canopy.
[3] Flux calculated using all of the available data.

	[1] Average Moisture	[2] q=K(theta) (cm/day)	[3] q=K(theta) (cm/day)	Average Gradient	Ave. psi (cm-water)	q=K(psi)*i (cm/day)	Precip (cm/day)
1985							
April	0.060	2.64E-02	3.52E-02	1.20	-58	3.850	0.033
May	0.076	2.75E-01	1.05E-01	0.95	-46	5.750	0.028
June	0.076	6.76E-02	7.45E-02	1.20	-64	4.550	0.069
July	0.075	5.87E-02	7.01E-02	1.06	-68	0.013	0.034
August	0.062	3.61E-02	4.20E-02	1.13	-138	0.007	0.038
September	0.053	2.69E-02	5.19E-02	0.40	-151	0.001	0.061
October	0.053	1.44E-02	4.61E-02	0.84	-185	12.830	0.131
November	0.065	2.35E-01	2.01E-01	1.60	-61	304.980	0.003
December	0.074	1.83E-01	1.84E-01	2.04	-22	148.400	0
1986							
January	0.072	8.76E-02	1.68E-01	1.01	-21	45.600	0.014
February	0.072	7.77E-02	1.65E-01	1.20	-29	41.660	0.001
March	0.072	7.63E-02	1.59E-01	1.12	-30	39.210	0.019
April	0.072	6.68E-02	1.61E-01	---	---	---	0.070
May	0.071	6.51E-02	1.33E-01	---	---	---	0.074

Table 4. Deep flux estimates using pressure-head and moisture-content data from the base of the dune (Stephens and Knowlton, 1986).

[1]For the 153 cm depth.
[2]Geometric mean.
[3]Harmonic mean.

	[1]Average Moisture	q=K(theta) (cm/day)	Average Gradient	Ave. psi (cm-water)	[2]q=K(psi)*i (cm/day)	[3]q=K(psi)*i (cm/day)	Precip (cm/day)
1983							
April	0.077	2.43E-02	0.94	-80	4.15E-03	4.07E-03	1.24E-02
May	0.070	1.22E-02	1.11	-85	2.49E-03	2.29E-03	2.55E-02
June	0.061	4.56E-03	1.58	-87	1.28E-03	3.25E-03	1.90E-02
July	0.049	1.22E-03	1.58	-99	1.20E-03	2.97E-04	3.78E-02
August	0.043	6.24E-04	1.13	-79	8.73E-04	3.83E-04	5.68E-02
September	0.056	2.69E-03	1.57	-95	8.52E-05	1.34E-06	1.86E-01
October	0.056	2.44E-03	1.22	-117	5.80E-05	9.42E-06	6.32E-02
November	0.054	1.71E-03	1.14	-111	5.90E-02	2.41E-04	3.34E-02
December	0.052	7.95E-04	1.15	-72	1.42E-02	1.11E-03	1.81E-02
1984							
January	0.056	1.87E-03	1.33	-115	2.19E-04	6.58E-10	2.58E-02
February	---	---	1.20	-95	2.51E-03	7.06E-07	6.89E-04
March	0.070	1.00E-02	1.31	-95	7.81E-03	9.42E-07	1.29E-03
April	0.073	1.58E-02	0.79	-83	1.81E-03	1.71E-06	2.00E-03
May	0.062	4.83E-03	1.18	-106	2.41E-05	1.99E-10	4.52E-03

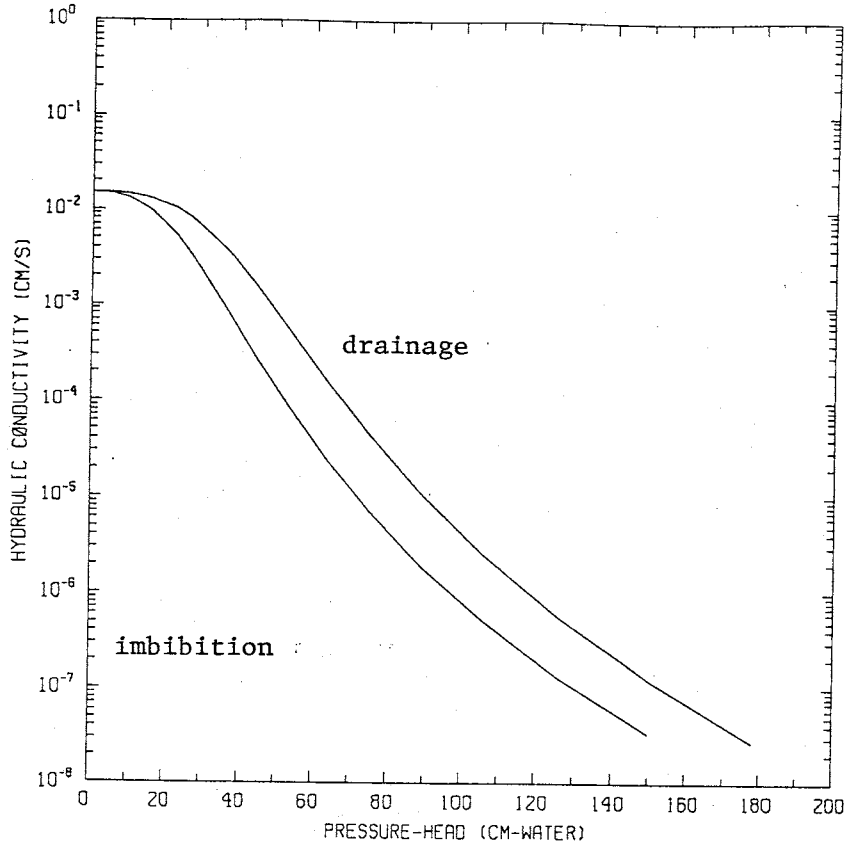

Figure 30. Hydraulic conductivity versus pressure head.

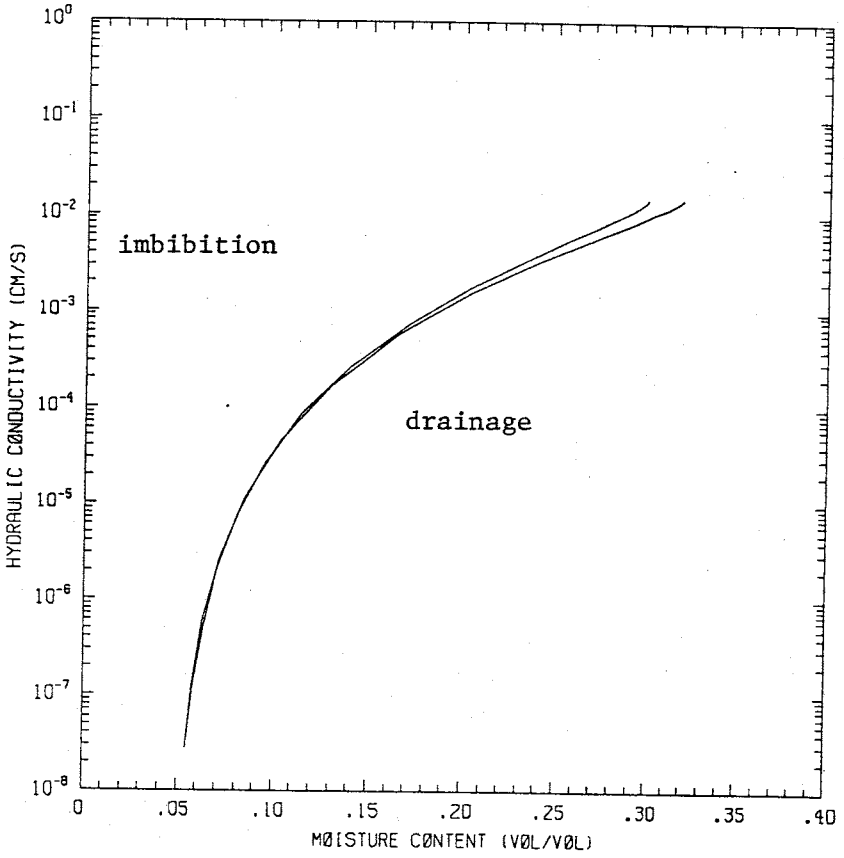

Figure 31. Hydraulic conductivity versus moisture content.

sure-head was much higher than would be predicted by the corresponding moisture content of the soil. This difference was probably due to inaccuracies in the moisture-content versus pressure-head relationship. It is also possible that the soil pressure-head was not determined accurately due to the 50% ethylene glycol solution that was used as an anti-freeze in the tensiometers. This organic liquid is considered to be non-wetting with respect to water and soil and is more dense than water. Although a density correction was made, when the ethylene glycol settled to the bottom of the tensiometer after a period of weeks there may not have been a good contact with the soil nor an accurate reading of the soil tension. Evidence is in the fact that this problem was most pronounced during the winter months when the ethylene glycol solution was in use. However, the ethylene glycol solution has been used in the past quite successfully.

Unsaturated hydraulic conductivity (figure 31) was also extrapolated using moisture content values measured at 210, 240, 270, and 300 cm depths, and an effective $K(\theta)$ value was calculated (Bakr et al., 1978; Gutjahr et al., 1978).

$$K_{eff} = K_{geom} \left(1 - \sigma_{\ln K_g}^{2} \right) \quad \text{(for 1-D)} \qquad (4.6)$$

$\sigma_{\ln K_g}^{2}$ = variance of the natural log of the geometric mean hydraulic conductivity

The geometric mean is expressed mathematically as,

(4.7)

The effective hydraulic conductivity incorporates the geometric mean and variance of the $\ln K(\theta)$. The natural logarithm of the hydraulic conductivity is examined because it has a normal distribution.

Mathematically, the effective, geometric hydraulic conductivity falls between the two extremes which are the arithmetic and harmonic means (figure 32). The harmonic mean,

$$K_{harm} = n \Big/ \sum_{i=1}^{n} 1/K_i \qquad (4.8)$$

weights the smallest value most heavily, therefore the hydraulic conductivity will only be as large as the least conductive layer. The arithmetic mean,

$$K_{arith} = \sum_{i=1}^{n} K_i / n \qquad (4.9)$$

which equally weights each layer, is analogous to flow along parallel layers.

The mean and variance of the logarithm of the hydraulic conductivity was calculated for the moisture content at the 210, 240, 270, and 300 cm depths. An effective hydraulic conductivity was calculated for each day of data collection and each neutron tube. The arithmetic average was used to estimate monthly seepage rates beneath the canopy of the plant and at 3 m away. The darcian flux beneath the edge of the canopy ranged between 20 and 190% of the flux 3 meters away, with an average of 82%.

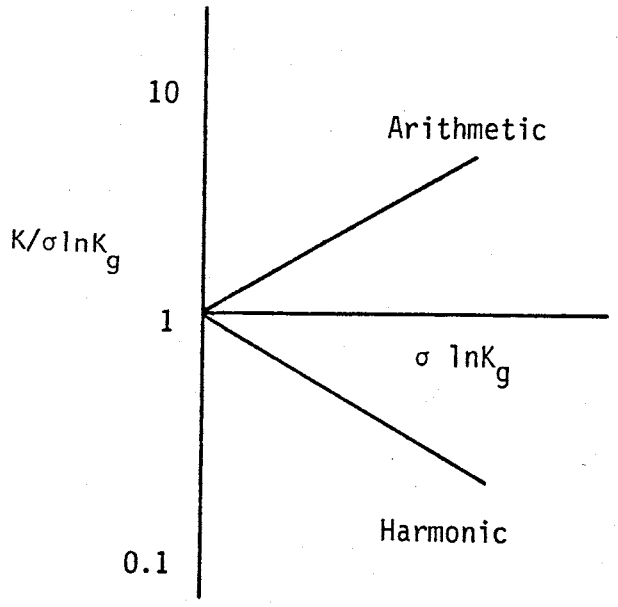

Figure 32. Variance of geometric mean hydraulic conductivity is intermediate to the variance of the arithmetic and harmonic means (Adapted from Gutjahr et al., 1978).

There is a large potential source of error in estimating the recharge beneath the plant canopy and the surrounding area. A very important source of error is the estimation of the unsaturated hydraulic conductivity. Although moisture contents corresponding to 2 and 15 bars of pressure were obtained to determine residual values (appendix B-8), most of the data used to calculate unsaturated hydraulic conductivity was much more moist than the average moisture contents observed at this site.

Changes in Storage Below the Root Zone. The change in moisture content integrated over depth and time is an indicator

of net losses, or gains to the system. Calculated for an extended time period, the net change generally approaches zero. Nonetheless, monthly or seasonally, storage changes have some significance. For example, in late summer the total profile was extremely dry due to high evaporation and low precipitation (figure 33). In contrast, by mid-autumn the late summer rains began to infiltrate beyond the 200 cm depth creating a positive storage change. The average cumulative monthly storage changes used in water balancing are listed in table 5, and the weekly changes in storage are tabulated in appendix C.

The total amount of moisture in storage increased with depth (figure 33). The shallow profile (0-1m) which was subjected to evaporation throughout the year remained fairly constant. The profile reached the lowest total cumulative moisture (0-3m) during the summer months and attained a nearly steady state value during the winter months. Changes in soil moisture during the summer months were due to the combined affects of evaporation and transpiration. Fall thunderstorms eventually replenished the moisture stored in the soil profile to that of the previous spring.

The error involved in determining soil-water storage changes is dependent on the accuracy of the neutron probe measurements. The decay of radioactive materials is a completely random process, therefore the error associated with neutron logging has a Poisson distribution. The expected value ($E(\theta)$), or mean, is equal to the variance ($Var(\theta)$). The counting time for the

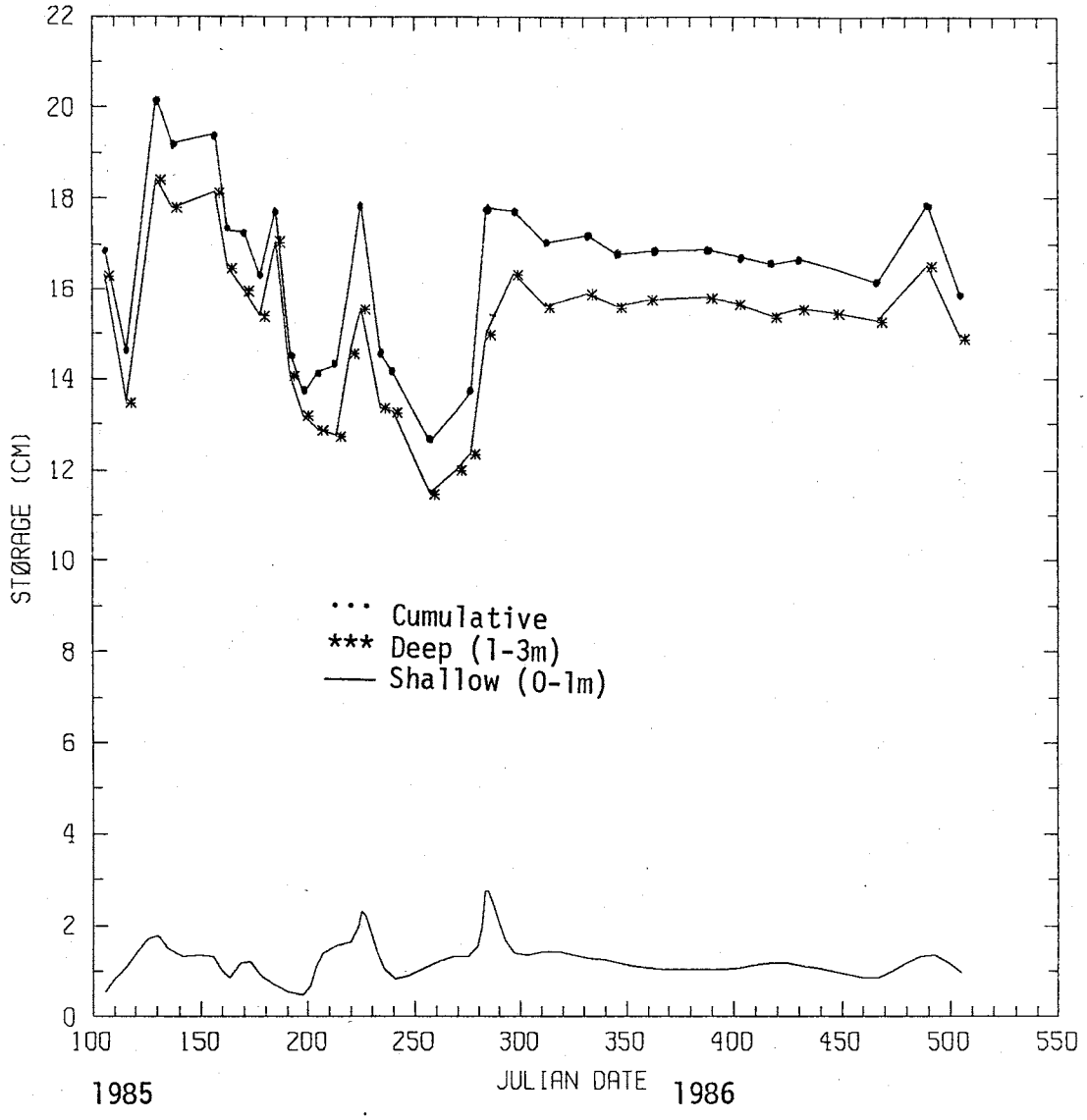

Figure 33. Cumulative storage rate versus time beneath the plant. (Neutron tube West A.)

Table 5. Summary of average monthly storage changes and precipitation.

+Changes in storage were calculated using the three neutron tubes at the edge of the canopy.
*Changes in storage were calculated using all nine neutron tubes.

	Change in Storage (cm/day)		Precipitation (cm/day)
	+Canopy	*Field	
1985			
April	-0.229		0.033
May	0.062	0.017	0.028
June	-0.052	0.008	0.069
July	-0.054	-0.103	0.034
August	-0.037	-0.035	0.038
September	-0.032	-0.032	0.061
October	0.211	0.211	0.131
November	-0.016	-0.022	0.003
December	-0.003	-0.028	0.000
1986			
January	-0.011	-0.003	0.014
February	-0.004	0.003	0.001
March	-0.042	-0.048	0.019
April	0.002	0.007	0.070
May	-0.029	-0.010	0.074

factory calibration was set for a count of 16 seconds. For field measurements in this study, a count of 32 seconds was used which reduced the variance by a factor of two.

$$E(\theta) = \theta_{ave} = Var(\theta_{16}) = 1/2\ Var(\theta_{32}) \qquad (4.10)$$

The variance is not constant, but rather it is dependent on the actual moisture recorded. For the small range of moisture contents encountered in this study, table 6 lists some standard errors involved. The reading on the neutron probe (Uncalibrated, θ) was entered into the site specific calibration equation to calculate the actual, $_{\theta}$.

Table 6. Moisture content after calibration adjustments (Calibrated,θ),and standard deviation.

Uncalibrated,θ	Calibrated,θ	Standard Deviation
6.1%	3.0%	0.073%
11.6	7.0	0.107
20.67	15.0	1.45

Evapotranspiration Estimates. The evapotranspiration rate of the Dalea scoparia plant was calculated by considering the balance of soil water within a 2.65 m radius from the edge of the plant canopy. The rates of inflows and outflows according to equation 3.1 were averaged over each monthly period and used to solve for an evapotranspiration rate (table 7). Evapotranspira-

Table 7. Estimated evapotranspiration using water balance accounting, equation 3.1.

ET calculated using the three A neutron tubes at the edge of the canopy.
ET calculated using all of the available data.
ET calculated using moisture-content derived flux.
ET calculated using pressure-head derived flux.
Evapotranspiration as a percent of precipitation.

	CANOPY				FIELD			
	K(theta)	ET/Px100	K(psi)	ET/Px100	K(theta)	ET/Px100	K(psi)	ET/Px100
1985								
May	-0.309				-0.094			
June	0.053	76.8			-0.153			
July	0.029	85.3	0.06	153.8	0.067	197.0	0.058	152.6
August	0.039	102.6	0.09	147.5	0.031	81.6	0.091	149.2
September	0.066	108.2			0.041	67.2	-0.080	
October	-0.094				-0.126			
November	-0.216				-0.176			
December	-0.180				-0.156			
1986								
January	-0.063				-0.151			
February	-0.073				-0.167			
March	-0.015				-0.092			
April	-0.062				-0.161			
May	0.038				-0.049			

tion rates were calculated using unsaturated hydraulic conductivities corresponding to both moisture content and pressure head and changes in soil-moisture storage over the whole field site and at the edge of the canopy. The negative values indicate an upward gradient or net loss of moisture.

The water balance method did not produce satisfactory results for calculating evapotranspiration. The cumulative error involved in calculating each variable in the water balance exceeded the expected evapotranspiration rate. The errors in this type of calculation include the accuracy of the neutron probe, the prediction of the soil-moisture retention curves, and to a small extent the rain gauge. An additional source of error involved the response-lag time between precipitation, changes in storage, and deep flux. This would in part account for some of the negative evapotranspiration rates recorded. As stated previously, the soil pressure-heads were underestimated during the winter months so predicted evapotranspiration at this time was not meaningful.

Without a direct measure of evapotranspiration, the water requirements of the plant, may only be roughly estimated through an accounting of the water balance. From all of the soil moisture data it appears that the active season of the plant ran approximately from May through October and the highest evapotranspiration rate estimated at the canopy edge occurred in September, 1985. Evapotranspiration (within a radius of 2.65m around the canopy of the Dalea scoparia), using moisture-content

data, accounted for between 77 and 154% of the precipitation rate during the growing season.

It was possible to estimate the rate of the evapotranspiration using water balance only during the active growing season from May to October. Although evapotranspiration accounts for a large percentage of precipitation the actual magnitude is a small number. During the period of this study, soil moisture was high which increased some of the errors involved. According to Passouri (1981), desert legumes such as the Dalea scoparia, typically transpire rapidly during the short active season and almost negligibly during all other times of the year. As a result, the magnitude of the errors involved may be greater than the actual evapotranspiration rate during those times of the year.

An adequate measurement of evapotranspiration using the water balance method is difficult without disturbing the natural flow field such as with a field or laboratory lysimeter. Laboratory experiments would produce reliable evapotranspiration rates, albeit with contrived solar input, average wind speeds, and measured precipitation. As one of the objectives of the study was to examine a natural setting this would not have satisfied all of the requirements. Water balance accounting was successful in illustrating the seasonal variations in the rate of evapotranspiration.

Direct Measurement of Transpiration Rates and Stem Potentials

A direct and nondestructive method of measuring transpiration rates is through the use of a portable steady state porometer (figure 34). A leaf (or leaves) is held within an open chamber and the rate of water vapor lost through the leaves is calculated (P. Kemp, Pers. Comm., New Mexico Museum of Natural History, 1986). A psychrometer detects the relative humidity of the chamber and the outside atmosphere, these in turn are used to determine the transpiration rate and stem resistance. The measurements are only point measurements which must be integrated over the total leaf area of the plant. A thermocouple within the chamber measures the leaf and chamber temperature. To calibrate each measurement, the leaf area within the chamber is estimated. In addition, a pyranometer mounted directly on to the porometer, records the solar radiation at each sampling location.

A pressure bomb system (Soilmoisture Equipment Corp., 1985), used in conjunction with the porometer, is a destructive method which measures the pressures exerted within plant stems (figure 35). Freshly cut stems are placed in an airtight chamber and a positive pressure is applied. It is assumed that the pressure necessary to force water out of plant stems is equal and opposite to the suction pressure necessary to transport water from the roots to leaves.

Leaf samples from the Dalea scoparia, Prosopis (mesquite), and Abronia (Sand verbena) were used to monitor diurnal patterns

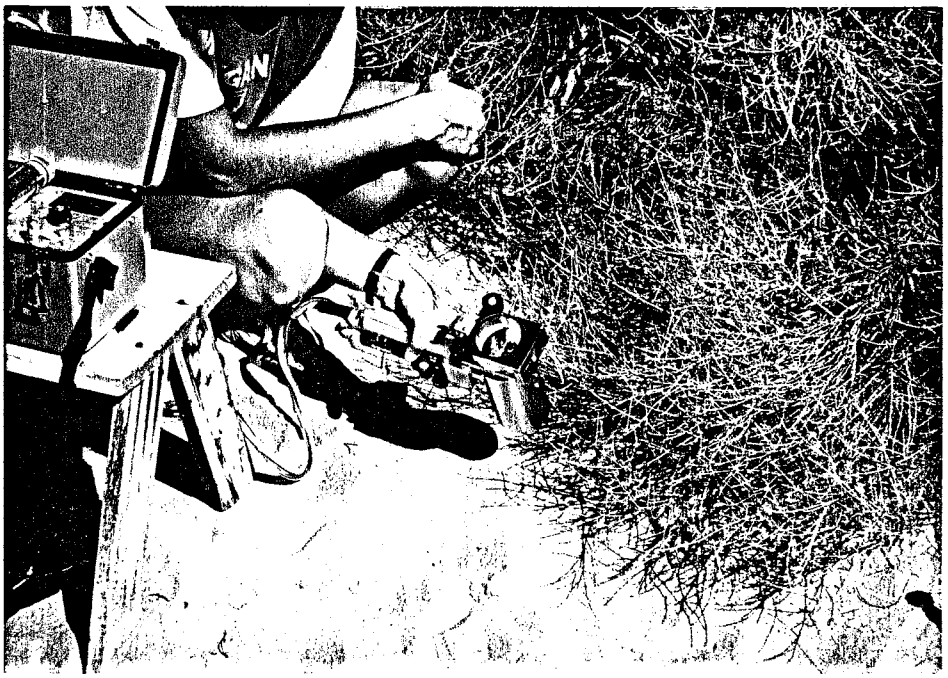

Figure 34. View of the open chamber porometer.

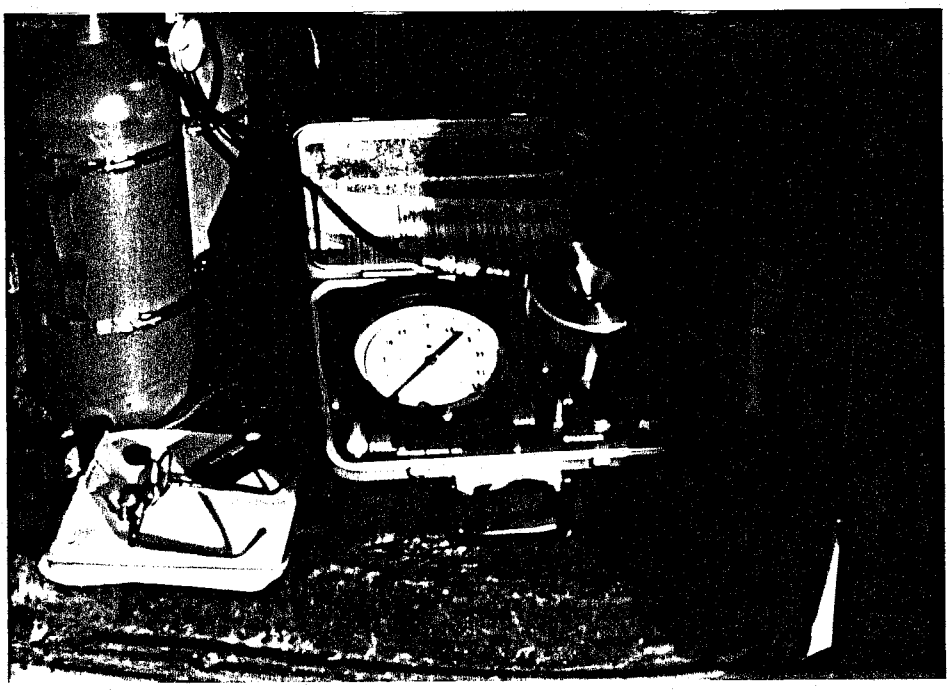

Figure 35. View of the pressure-bomb system.

of water use over a 24 hour period covering July 25-26, 1986. The porometer and pressure bomb systems were used to compare transpiration and stem potentials between those of a perennial, a deeply-rooted phreatophyte, and an annual plant. The transpiration rates and negative stem pressures were minimum at predawn and peaked in the early afternoon (figure 36). During the mid-day, solar radiation and the transpirational demand of plants is generally at a maximum. Higher transpiration rates induce larger gradients and resistance within the plant stems. Soil potentials have likewise been observed to decrease towards the mid-day and increase throughout the night (Rice, 1975). The data collected during the experiment were typical of plants growing in very moist soil. When plants are experiencing water stress, transpiration rates may decrease in response to partial, or total, stomatal closure which will in turn help to conserve a scarce water supply.

The recorded transpiration rates and stem potentials reflect the diurnal soil water requirements of three very different plant species. Negative stem potentials are much higher and transpiration rates are much lower for annual plants than for those of phreatophytes. Seeds from annual plants may lay dormant for years until conditions for rooting are favorable and then only survive while water is plentiful. In contrast to this, phreatophytes require a tremendous amount of water to support an extensive rooting system and canopy. The pressures within the stems must be extremely small in order to maintain a gradient

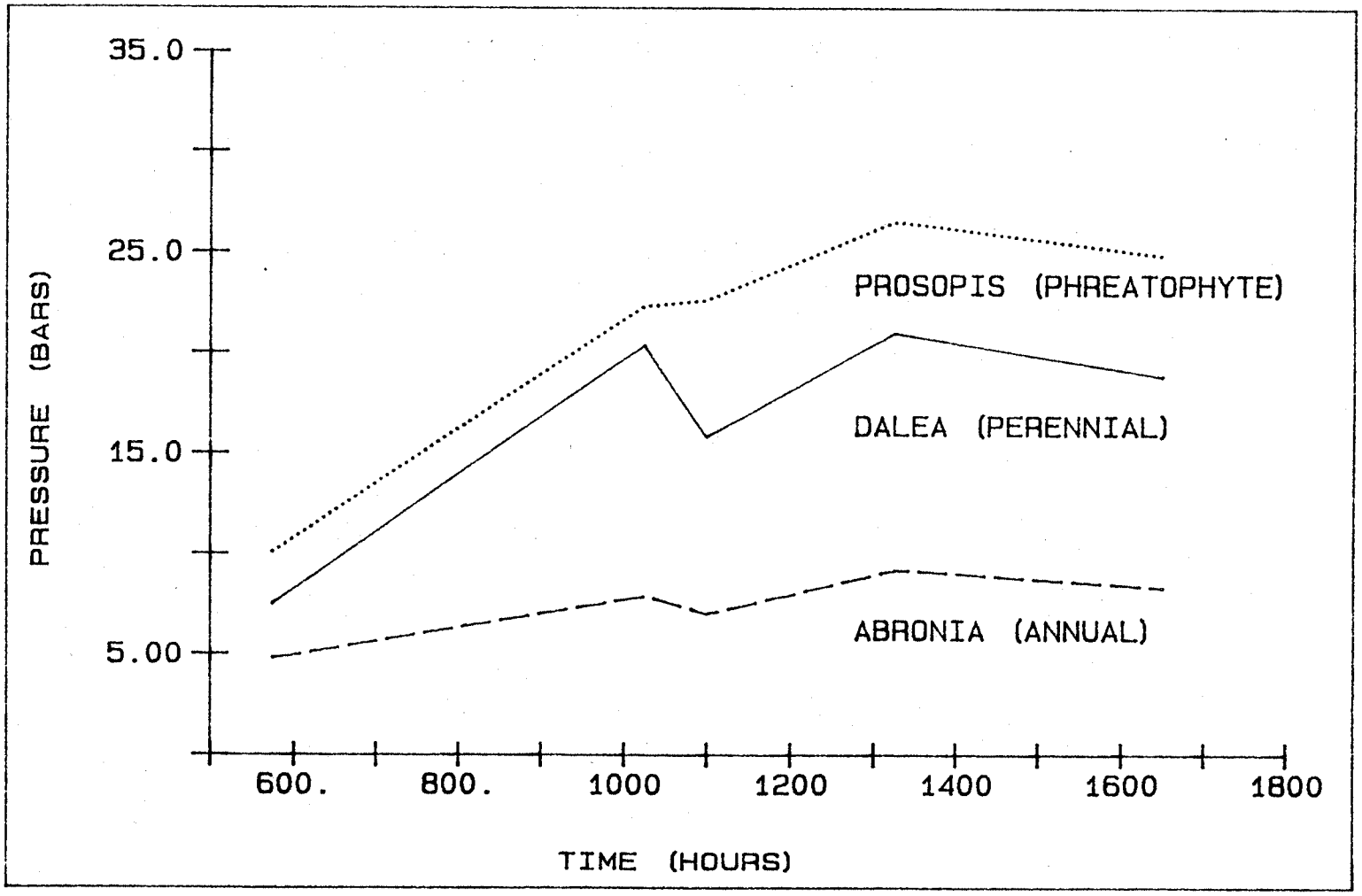

Figure 36. Average pressure bomb values over a 24 hour period.

between the small soil-suction and the rapid transpiration of the leaves. The Dalea scoparia plant is a perennial which is intermediate in size, rooting depth, transpiration rate, and stem potential to the annual, and the phreatophyte. This plant, as many other desert perennial plants, has adapted to grow under a variety of soil-moisture and atmospheric conditions. The data collected during this experiment was not typical of mid-summer soil moisture conditions because of the unusually high amount of precipitation that occurred in July, 1986 (appendix E).

Geostatistical Analyses

The geostatistical method of kriging was applied in the hopes of obtaining a more thorough, or perhaps smoothed, estimate of the moisture content in the soil surrounding the plant. Kriging is a method which interpolates measurements between sampling points based on temporal, or in this case spatial, correlations of the data. To characterize the intrinsic variance of the observations, several attempts were made to estimate the variogram.

Variogram Analysis. An examination was made of the behavior of the variance in one- and two-dimensions and through time. For the one-dimensional (depth) and time variograms there was not enough data to find conclusive results. The two-dimensional, linear variograms produced the most reliable and valid

variograms for the data.

The variance of the data in the vertical direction was examined by calculating the mean at each depth and subtracting this value from each of the other measurements.

$$\theta_{effective} = \sum_{i=1}^{10} [\, V(x_i) - \sum_{j=1}^{3} V(x_j)/k] \qquad (4.11)$$

i = 1, 2, 3, . . . , 10 ; number of vertical measurements

k = 3, neutron tubes on each transect

This resulted in a total of 100 points from each neutron tube to be used in the variogram. Rather than eradicate any trends, these variograms introduced them. The "nugget" effect, or error, appeared in all of the variograms and a quadratic or higher power variance appeared in several (figures 37a, b). This technique did not yield a consistent pattern between days or even between neutron tubes within the same day.

A second method used, was to study the variance of the mean zero moisture content at a given depth through time. The mean moisture content for a given depth was calculated then subtracted from each of the other values. This allowed the variation in moisture to be examined. A single variogram would then be calculated by averaging the three individual neutron tubes on each transect. With only one year of data available, the the resulting variogram could not be used to reliably predict moisture contents.

These time-variograms, with mean zero, were plotted for each

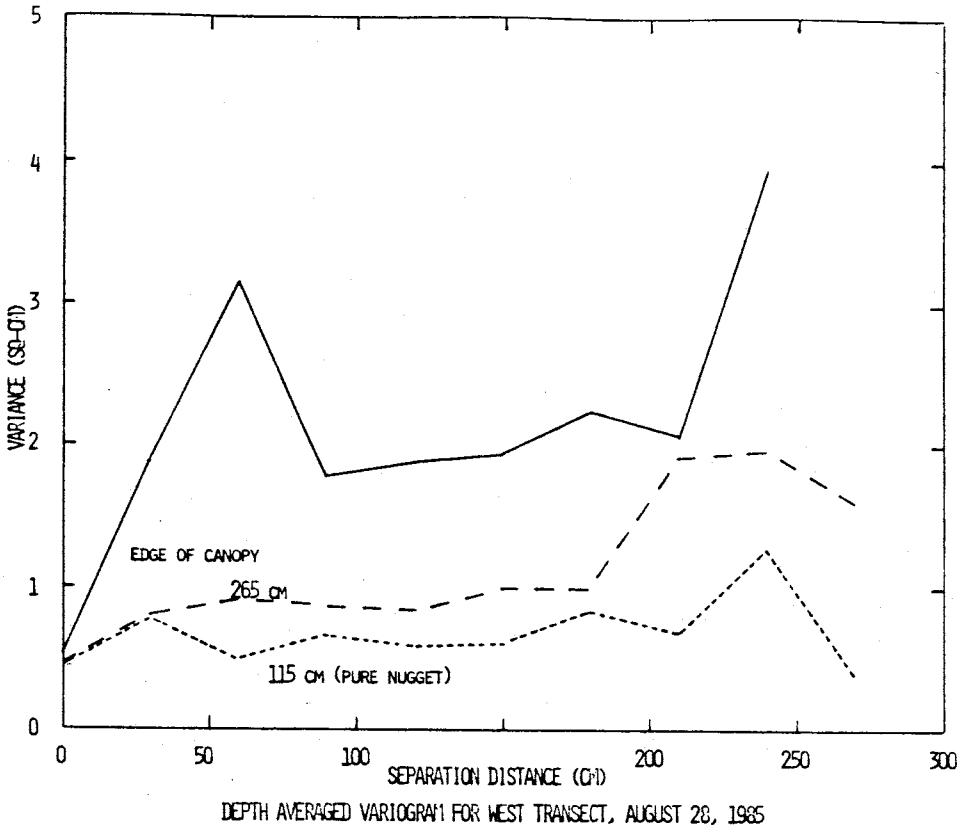

Figure 37a. Depth averaged variogram for the west transect, August 28, 1985.

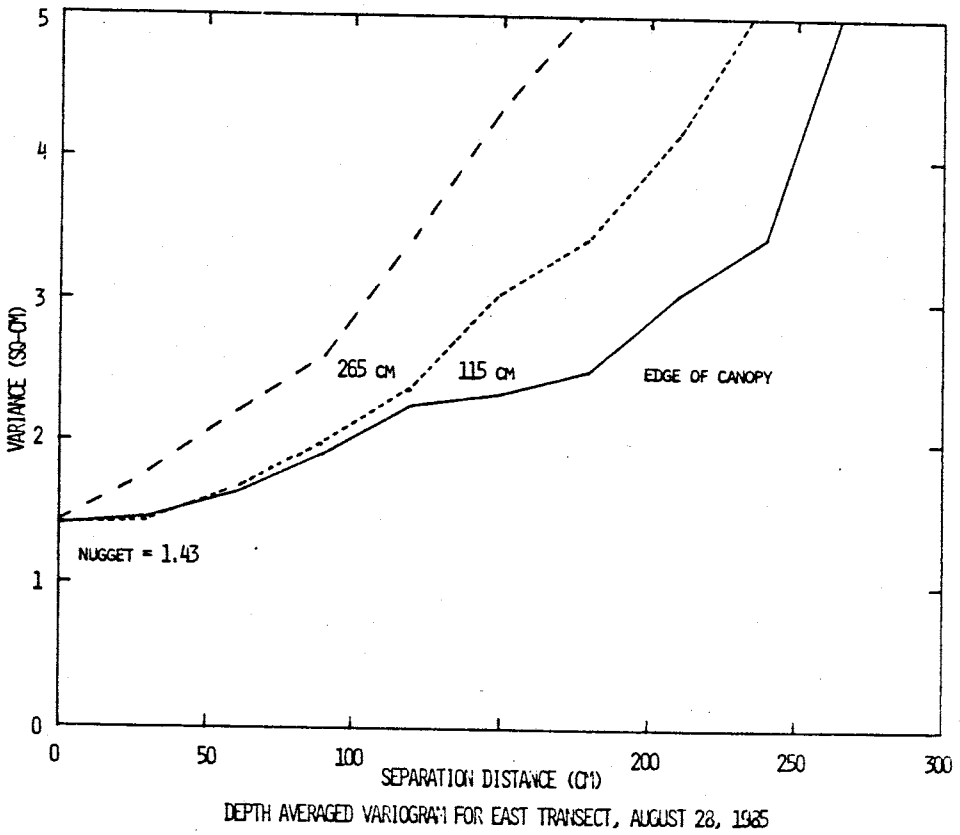

Figure 37b. Depth averaged variogram for the east transect, August 28, 1985.

neutron tube at 60 and 240 cm depths (figure 38a, b). At the Sevilleta National Wildlife Refuge, depths greater than 200 cm are generally considered to be below the major root zone with a net downward liquid and vapor flux (Stephens and Knowlton, 1986). Therefore daily fluctuations due to precipitation and evaporation would not affect the deeper measurements. In semi-arid to arid environments, soil-moisture flux at 60 cm may be dominated by upward vapor transport and water extraction by roots (Duval et al., 1985). Consistent with these observations, the 60 cm variogram shows that the moisture content has a higher and more erratic variance than the 240 cm variogram.

Two-dimensional variograms (depth versus horizontal distance) proved to have the most consistent variance. These variograms are representative of the variation in moisture content recorded at one point in time and were not detrended. The vertical distance between each data point was 30 cm and the horizontal spacing was 130 and 150 cm. A total of 30 points for each transect with a lag distance of 30 cm was used to develop the linear variograms used in kriging (figure 39 - 42).

It is an interesting point to note that the slope of the variogram generally increased from the beginning of the growing season to the end. For example, the slope of the March variogram is ~0.007 whereas that of October is ~0.05. One possible explanation is that the soil-water profile is relatively dry and uniform during the summer months. The fall rains create a large contrast in the percent saturation through the soil-water

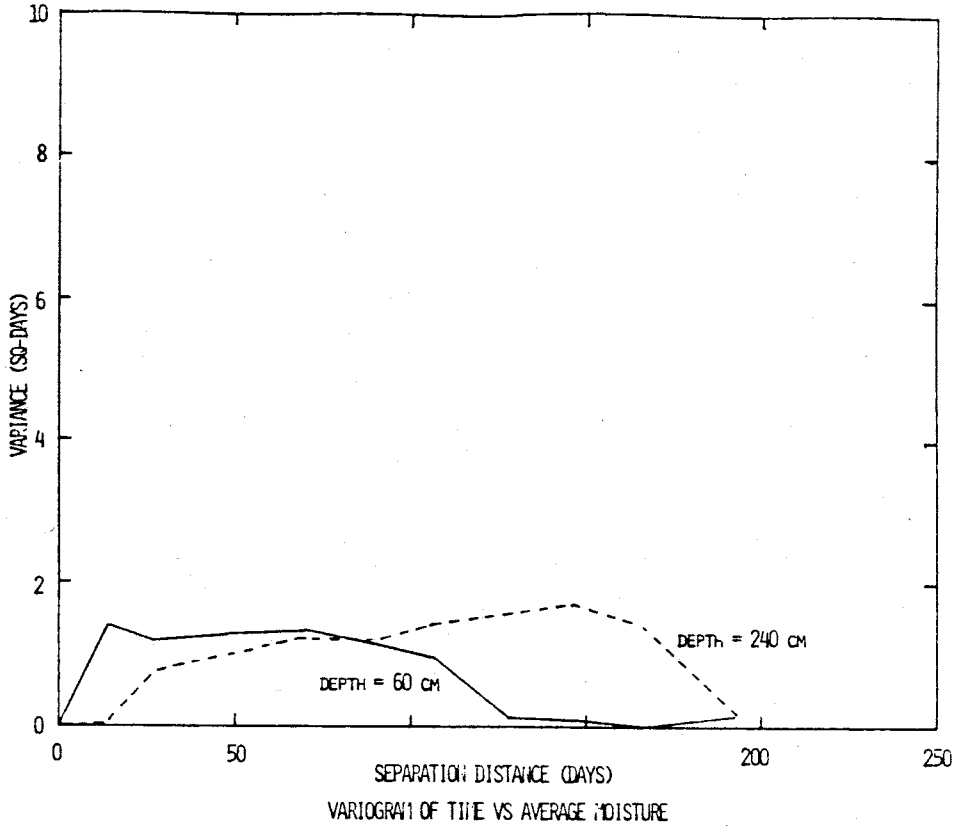

Figure 38a. Variogram of time versus mean zero moisture content, west transect, 2.65m from canopy.

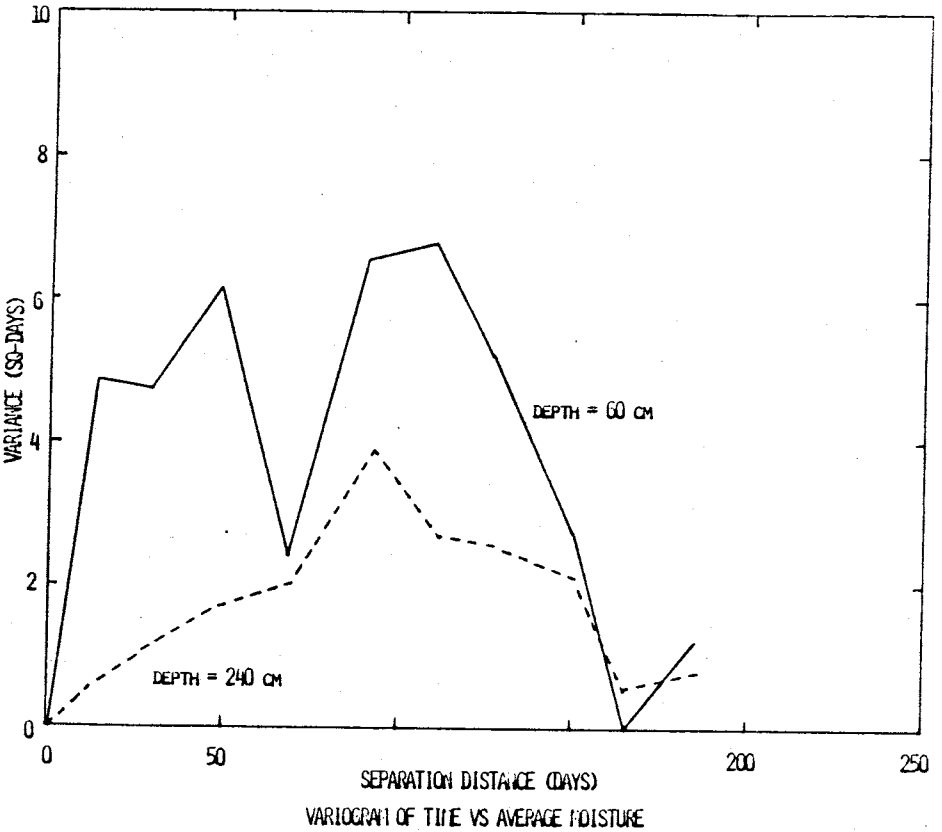

Figure 38b. Variogram of time versus mean zero moisture content, east transect, 2.65m from canopy.

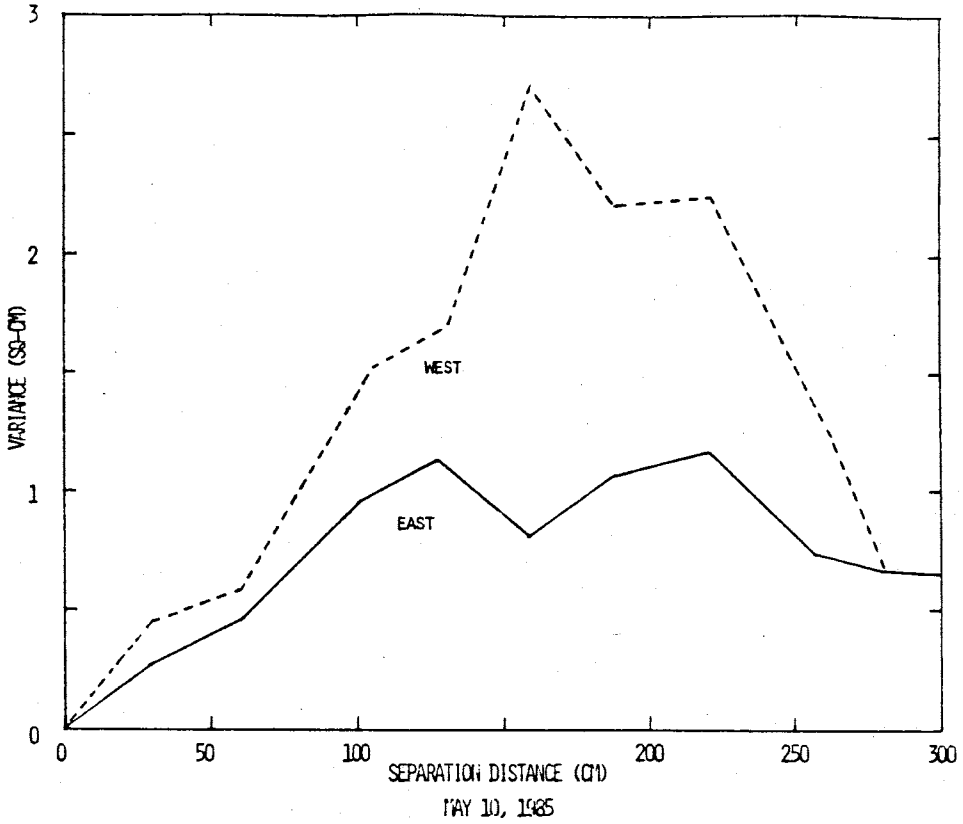

Figure 39. Linear variogram for May 10, 1985.

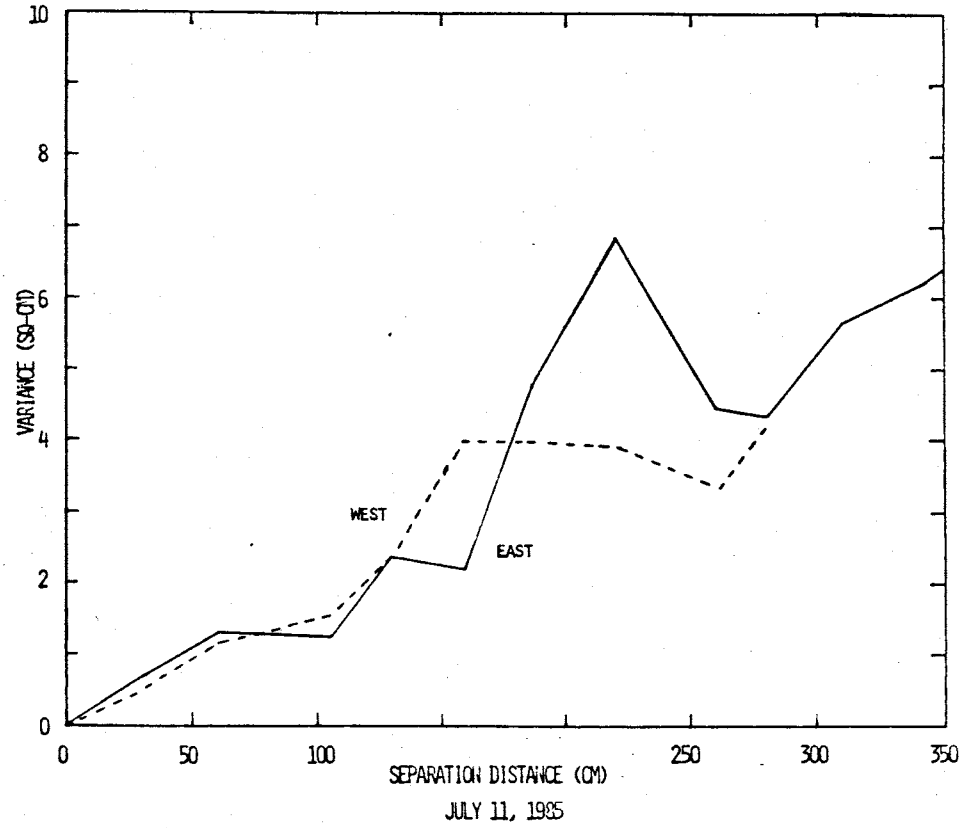

Figure 40. Linear variogram for July 11, 1985.

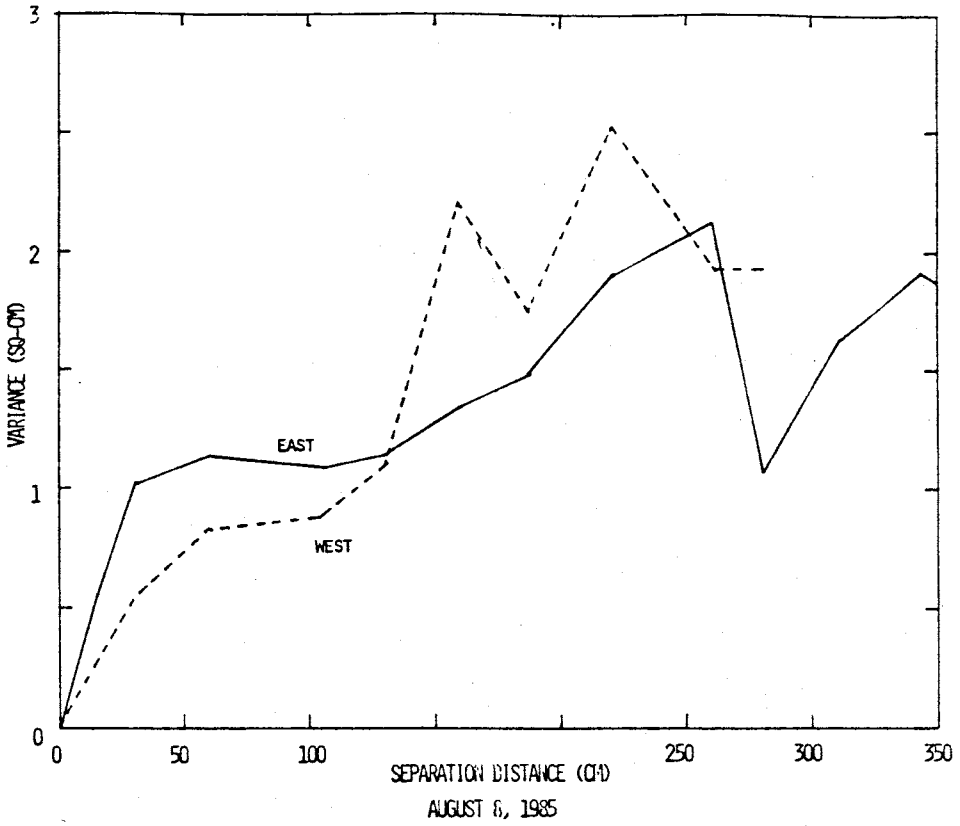

Figure 41. Linear variogram for August 13, 1985.

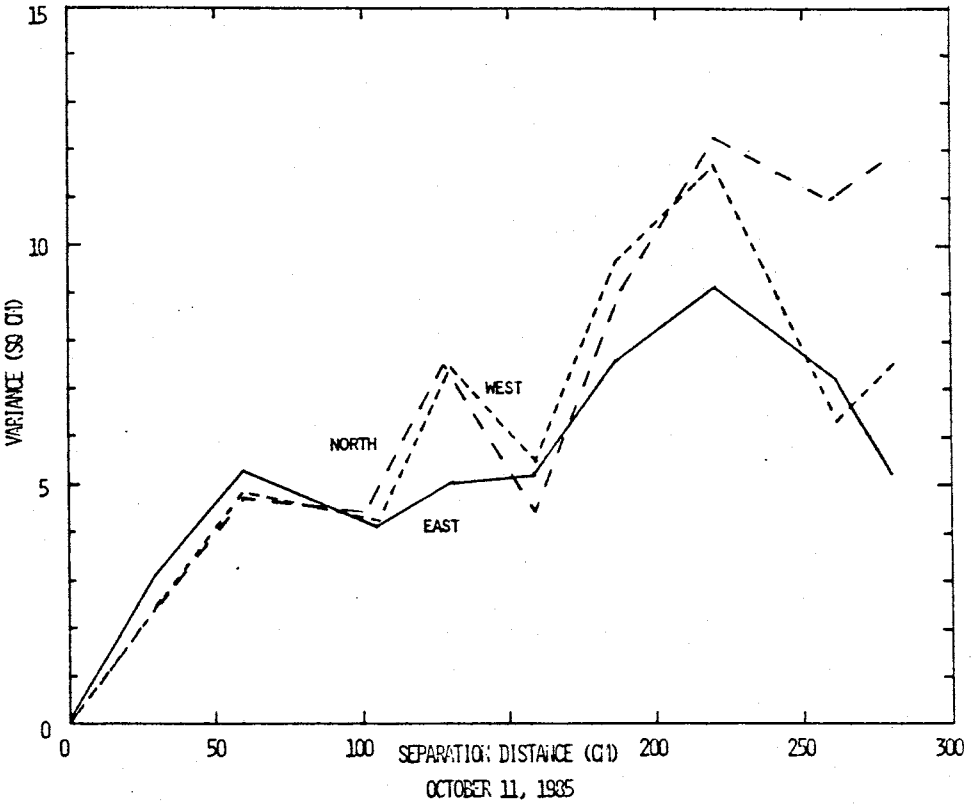

Figure 42. Linear variogram for October 11, 1985.

profile.

A validation program was used to verify each variogram. This is accomplished by neglecting the data, one point at a time, and using the remaining data to then predict it. It was found that predicted values correlated well with observed data. For the variogram estimates the mean difference between observed and predicted data points was +/- 0.02 and the mean squared errors between 0.9 and 1.1. An exact variogram would have a mean difference of zero and a mean squared error of one. The accuracy of these variograms may be explained by the fact that the distance between observed data points is small (<1.5 m), as are the spatial and temporal differences in moisture content (0-5%).

Kriging Results. Prediction locations were 30 cm apart in the vertical direction and 50 cm apart in the horizontal direction for a total of 50 "kriged" points on each transect from the plant (figure 43).

The figures which include the kriged points do not necessarily clarify moisture movement in the soil profile. It appears that using only the observed points there is adequate data for describing the moisture field. Figures 44-45a, b depict complete vertical cross-sections incorporating 100 kriged and 59 observed data points. Note that the plant was located in the center where horizontal distance equals zero. Figure 45c illustrates how the variance in the predicted moisture content decreases towards the

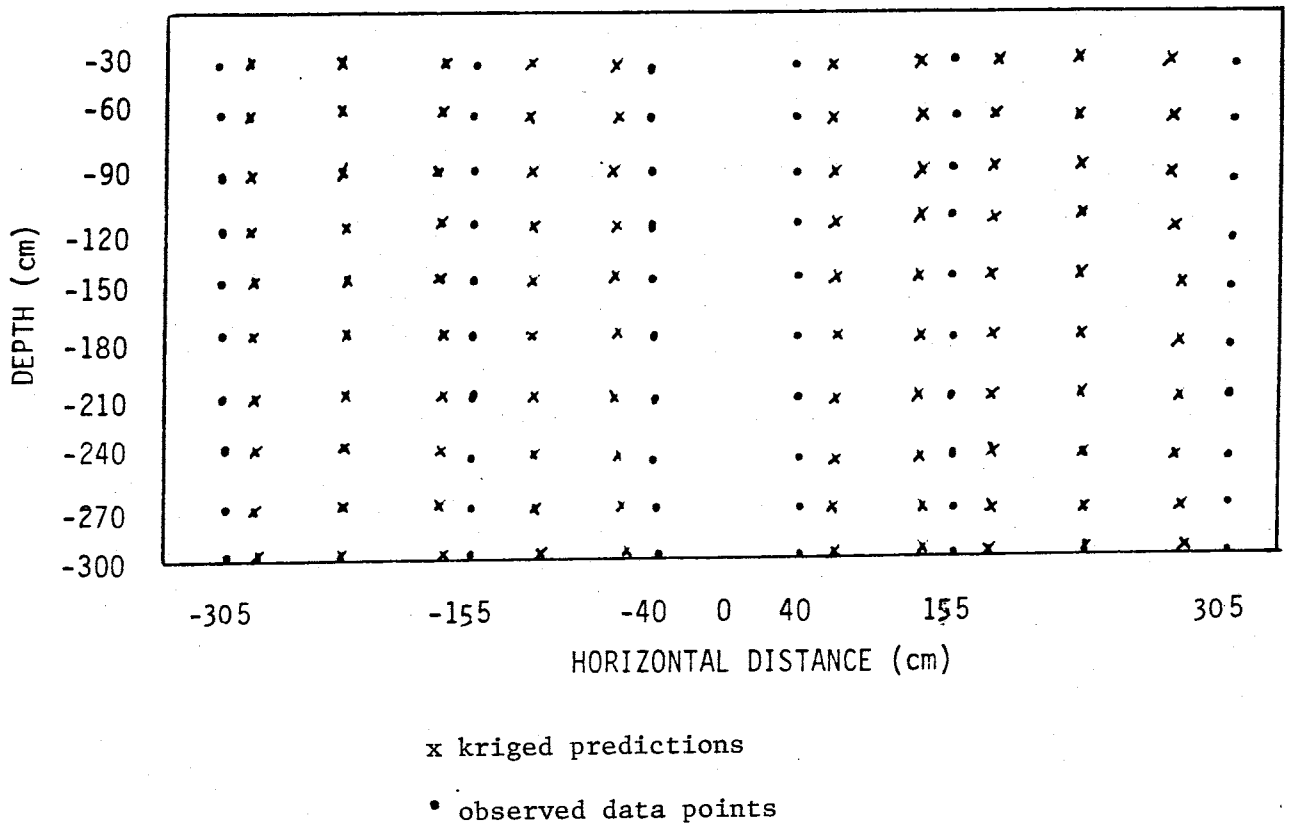

Figure 43. Location of kriged and observed data points.

locations of the neutron tubes. Including the kriged data points did not necessarily detract from, or add to, the observed moisture content cross-section. Considering the time and work involved kriging in this study did not prove to be a beneficial tool. Kriged estimates of the data should be used to improve, not neccessarily replace, actual field data.

One reason kriging did not improve the predictions of the water content profiles may have been due to the scale of investigation. The soil in the plot was very homogeneous and the total size of the plot was small given the number of sample points. Moisture content values primarily varied between 4 and 9%, so the variation in percent moisture may have been too small for the precision of the equations. In addition, the variogram that was ultimately used on the kriging equations was linear. Kriging in this case, though it incorporated weighted averages, served only as a straight-line interpolater between data points.

Another reason for the failure of the kriged estimates may have been a result of an anisotropic variance. The variogram may have been dependent on direction rather than merely the separation vector. As it was shown previously, the soil-moisture flux is not one-dimensional throughout the year. The set of kriging equations is derived assuming the variance function is statistically homogeneous and isotropic. Based on total hydraulic head and moisture-content projections there is evidence that the plant does not withdraw water symmetrically, or uniformly, throughout

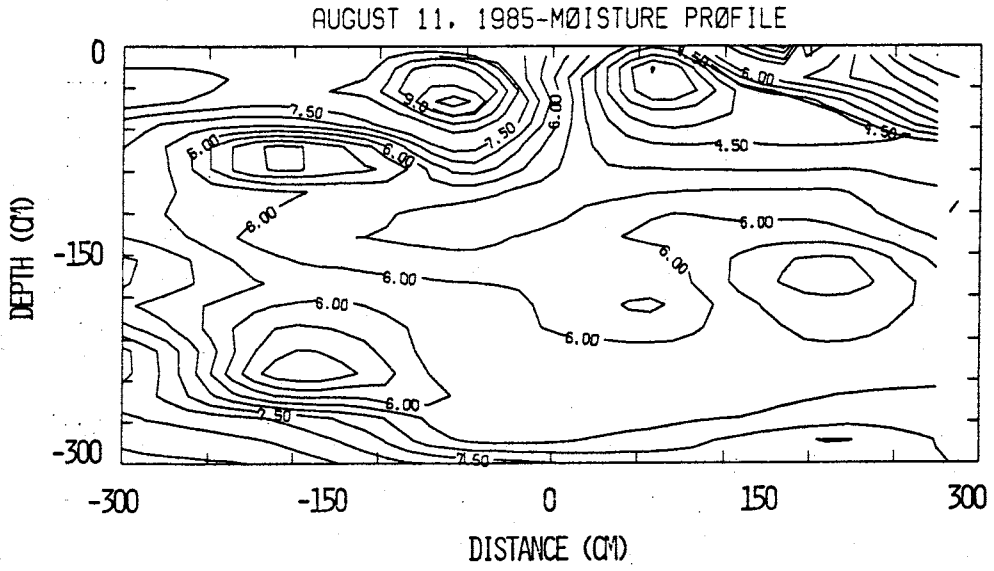

Figure 44a. Vertical cross-section of moisture content on August 11, 1985.

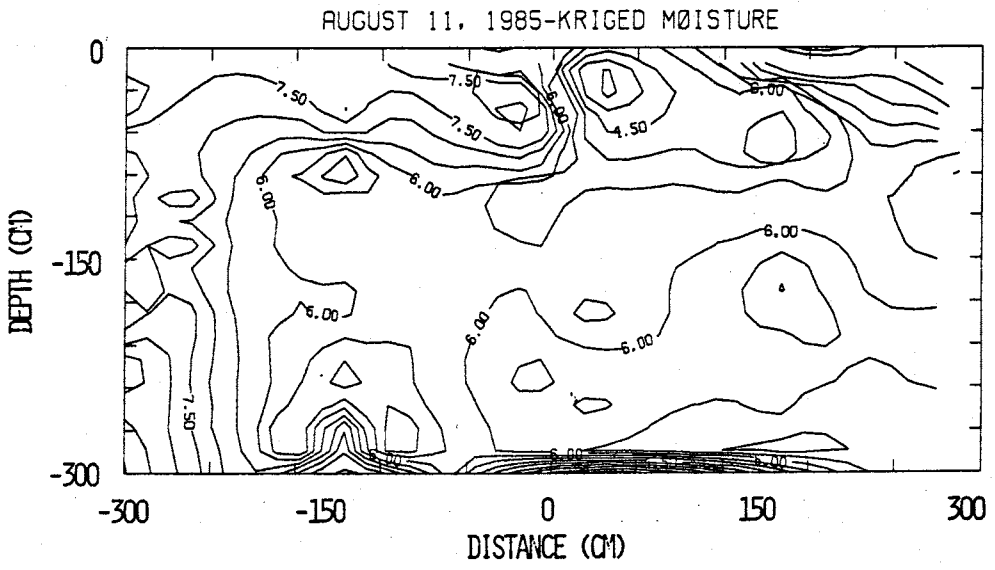

Figure 44b. Vertical cross-section of moisture content including kriged data points on August 11, 1985.

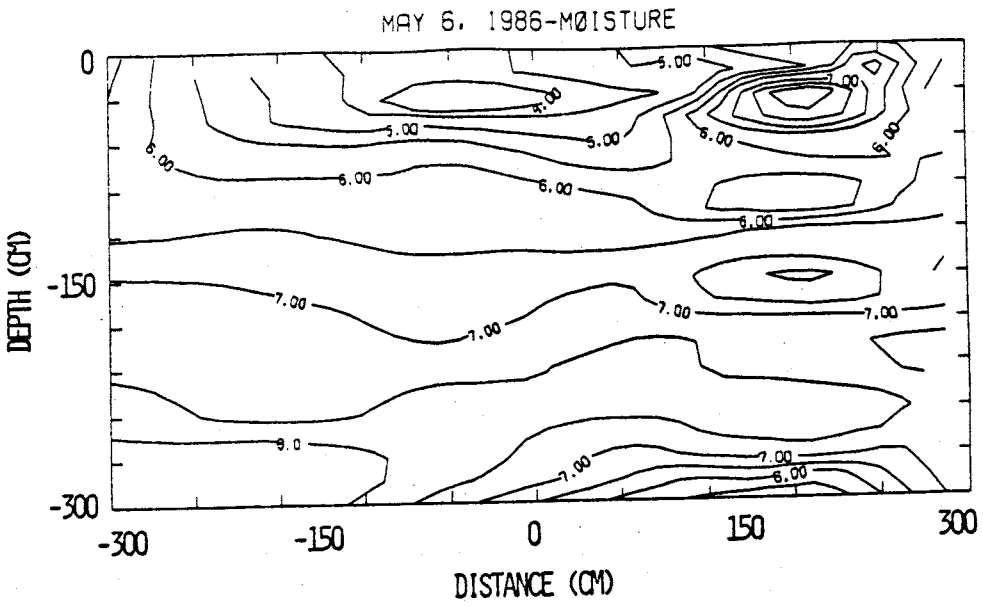

Figure 45a. Vertical cross-section of moisture content on May 6, 1986.

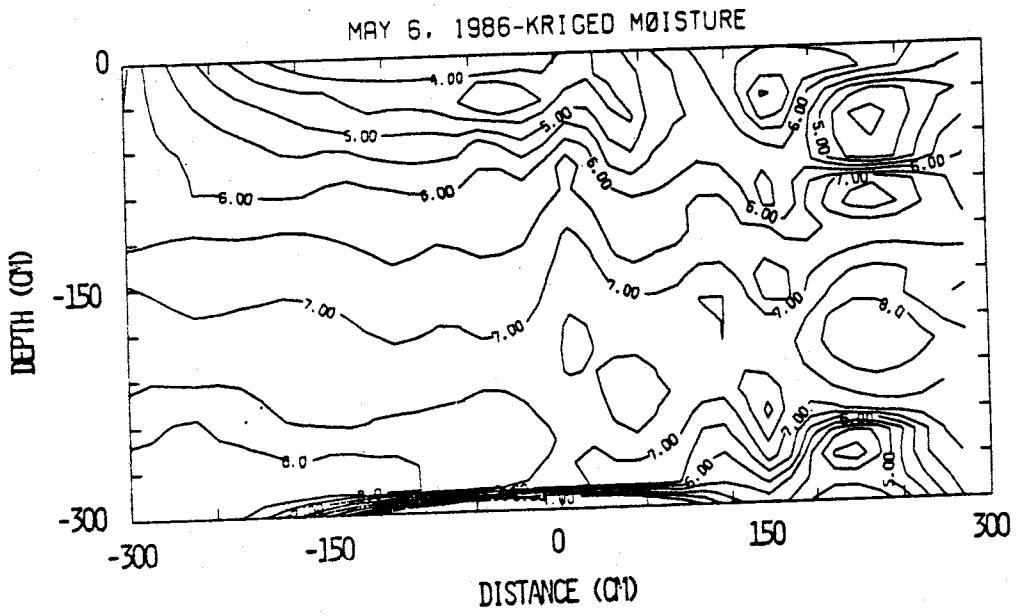

Figure 45b. Vertical cross-section of moisture content including kriged data points on May 6, 1986.

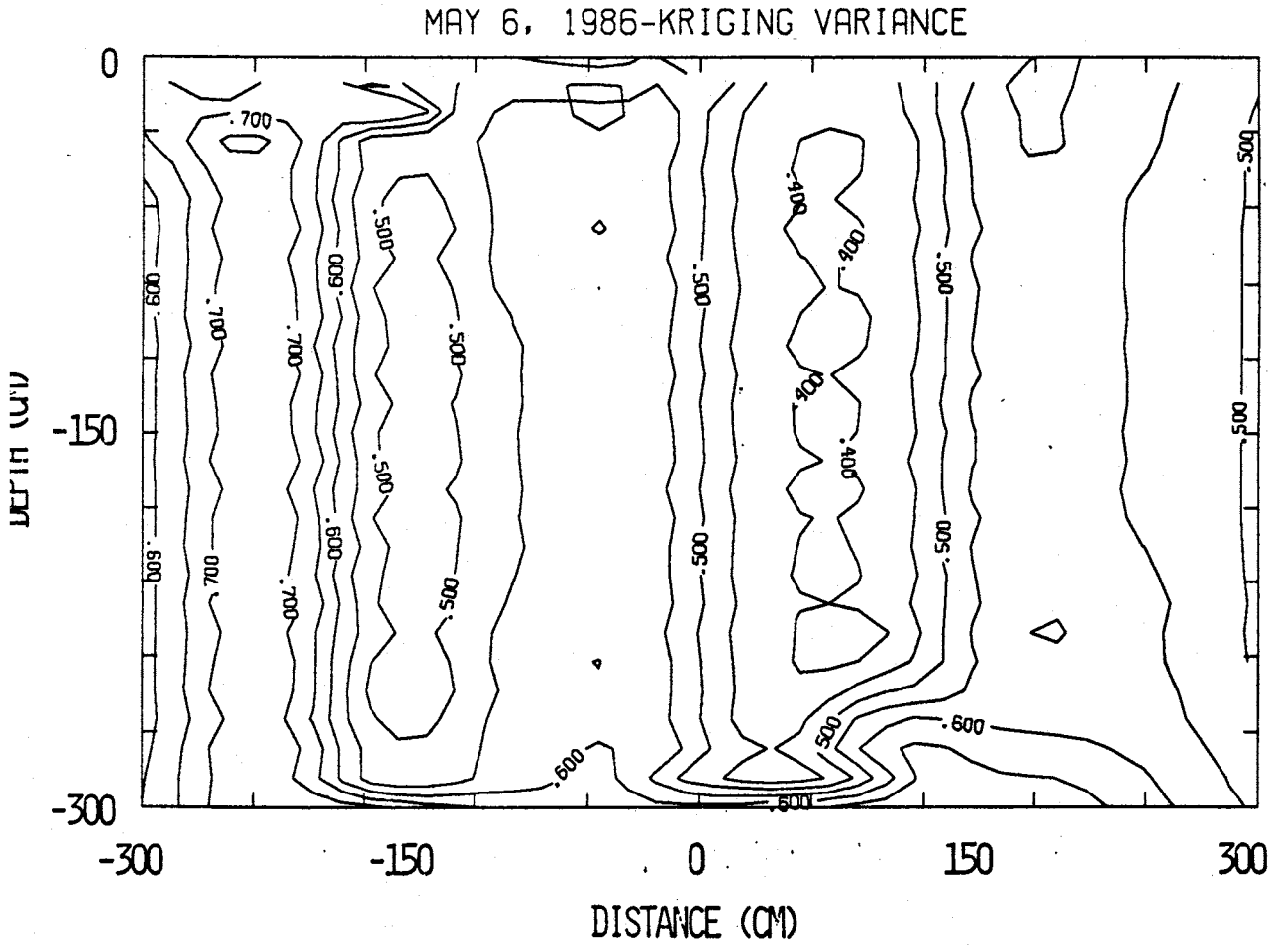

Figure 45c. Kriging variances for May 6, 1986.

the profile. Also, the transpirational demand and resulting plant-water use is seasonal.

SUMMARY OF CONCLUSIONS

1. A combination of total head and moisture content data may be used to analyze the water uptake pattern of plants. It was observed that topographic, seasonal, and meteorological changes each had profound effects on the gradient and soil-water content around the plant.

2. This study produced evidence that water withdrawal by roots was not uniform spatially, or temporally. Root distribution is not necessarily an indicator of water-use distribution.

3. Soil water gradients and moisture must be recorded over an extended period in order to investigate trends and identify inconsistencies.

4. The water balance method proved to be inadequate for estimating the monthly rate of evapotranspiration. The major problem was in compensating for the response-time lag between precipitation, changes in storage, and deep flux. However, this method was used to detect the seasonal variations in water use and to estimate evapotranspiration during the growing season as a percent of precipitation.

6. Soil moisture moves downward beneath the plant. For depths greater than 50 cm, plant transpiration and surface evaporation

did not remove soil water below laboratory residual values. Infiltration rates were observed to vary significantly immediately around the plant indicating that one-dimensional, vertical flow assumptions may be invalid.

7. Kriged estimates of the moisture content data were incorporated with the hopes of smoothing the observed data. This did not appear to improve the predictions of the moisture content field between observed data points. The problems associated to the method may have been due to the small variation in moisture content over the entire area.

RECOMENDATIONS FOR FUTURE WORK

1. A study to examine the inter-relationships of different plant species. Compare the transpiration rates and water withdrawal patterns of a perennial, an annual, and a phreatophyte growing closely together under the same atmospheric conditions.

2. Certain instrumentation would enhance the findings of a future study. These include: mini-lysimeters near the study site to directly examine bare soil evaporation, temperature blocks to investigate the effects of thermal gradients, and soil psychrometers to measure the soil pressures at depths less than 30 cm.

3. Regular monitoring of the plant's transpiration rate, using a portable porometer, along with moisture and hydraulic head measurements. A comparison could be made of the water balance method with that of the open chamber psychrometer.

4. Emplacement of soluble, or insoluble, tracers to monitor the movement, or immobilization, of contaminants due to plant activity. Directly examine plant material to reveal the amount of tracer retained within plant-cell tissues.

5. The problem of determining unsaturated hydraulic conductivity at small moisture contents should be addressed. More extensive

laboratory tests to examine moisture contents at high pressures (such as those which use centrifugal force, pressure plates) could reveal some important information. Considering the uniformity of the soil on the dune laboratory tests provide a fairly accurate estimate of insitu conditions.

REFERENCES

Advances in Evapotranspiration, 1985, In Proceedings of the National Conference on Advances in Evapotranspiration, American Society of Agricultural Engineers.

Al-Khafaf, S., Wierenga, P.J., Williams, B.C., 1977, A Floatation Method for Determining Root Mass in Soil, Agronomy Journal, Volume 69, pp. 1025 - 6.

Alley, William M., 1984, On the Treatment of Evapotranspiration, Soil Moisture Accounting, and Aquifer Recharge in Monthly Water Balance Models, Water Resources Research, Volume 20, No. 8, pp. 1137 - 1149.

Bakr, A.A., Gelhar, L., Gutjahr, A., MacMillan, J., 1978, Stochastic Analysis of Spatial Variability in Subsurface Flows 1. Comparison of One- and Three-Dimensional Flows, Water Resources Research, 14(2), pp. 263 - 271.

Belmans, C., Fegen, J., Hillel, D., 1979, An Attempt at Experimental Validations of Macroscopic-scale Models of Soil Moisture Extraction By Roots, Soil Science, Volume 127, No. 3,, pp. 174 - 186.

Bernard, Nelson T., Godfrey, Dan, 1984, In Wildflowers Along Forest and Mesa Trails, University of New Mexico Press, Albuquerque, 157 pages.

Black, T.A., Gardner, W.R., Thurtell, G.W., 1969, The Prediction of Evaporation, Drainage, and Soil Water Storage for a Bare Soil, Soil Science Society of America Proceedings, Volume 33, pp. 655 - 660.

Bresler,E., Dagan, G., 1979, Solute dispersion in unsaturated heterogeneous soil at field scale: II. Applications. Soil Science Society of America Journal, Volume 43, pp. 467 - 472.

Boonyatharokul, W., Walker, W.R., 1979, Evapotranspiration Under Depleting Soil Moisture, Journal of the Irrigation and Drainage Division, American Society of Civil Engineers, IR4, pp. 391 - 402.

Byers, E., Stephens, D.B., 1983, Statistical and Stoichastic Analyses of Hydraulic Conductivity and Particle Size in a Fluvial Sand, Soil Science Society of America Proceedings, 47(6), pp. 1072 - 1080.

Camillo, P., Schmugge, T.J., 1983, Estimating Soil Moisture Storage in the Root Zone from Surface Measurements, Soil

Science, Volume 135, No. 5, pp. 245 - 264.

Cline, J.F., Uresk, D.W., Rickard, W.H., 1977, Comparison of Soil Water Used by a Sagebrush-Bunchgrass and Cheatgrass Community, Journal of Range Management, Volume 30 No. 3, pp. 199 - 201.

Day, P.R., 1965, Particle Fractionization and Particle-Size Analysis, In Black, C.A. (ed) Methods of Soil Analysis, Agronomy 9: 545-566, American Society of Agronomy, Madison, WI.

Denmead, O.T., 1984, Plant Physiological Methods for Studying Evapotranspiration: Problems of Telling the Forest From the Trees, Agricultural Water Management, Volume 8, pp. 167 - 189.

Doorenbos, J., Pruitt, W.O., 1977, Guidelines for Predicting Crop Water Requirements, Food and Agriculture Organization of the United Nations, FAO Irrigation and Drainage Paper, No. 24.

Driess, S., Anderson, L., 1985, Estimating Vertical Soil-Moisture Flux at a Land Treatment Site, Ground Water, Volume 23, No. 4, pp. 503 - 511.

Duval, T., Phillips, F., Mattick, J., 1985, Tracing Soil-water movements with Bomb Chlorine-36 and Tritium in an Arid Zone, In The Joint Proceedings of the Fifth Annual AGU Hydrology Days Coloroado State University, Fort Collins, CO, pp 54 -76.

Evans, K., Thames, J.L., 1981, In Water in Desert Ecosystems, Dowden, Hutchinson & Ross, Inc., Stroudsburg, PA, 280 pp.

Feddes, R.A., Rijtema, P.E., 1972, Water Withdrawal By Plant Roots, Journal of Hydrology, Volume 17, pp. 3 - 59.

Fukuda, H., 1956, Diffusion of Water Vapor and its Exchange Between Condensation and Evaporation in Soil, Soil Science Society of America Proceedings, Volume 81, No. 2, pp.81 - 95.

Gardner, W.R., 1960, Dynamic Aspects of Water Availability to Plants, Soil Science, Volume 89, No. 2, pp. 63 -73.

Gardner, W.R., 1964, Relation of Root Distribution to Water Uptake and Availibility, Agronomy Journal, Volume 56, pp. 35 - 41.

Gardner, W.R., Ehlig, C.F., 1963, The Influence of Soil Water on Transportation By Plants, Journal of Geophysical Re-

search, Volume 68, No. 20, pp 5719 - 5724.

Gardner, W.R., Ehlig, C.F., 1963, Some Observations on the Movement of Water to Plant Roots, Agronomy Journal, pp. 453 - 456.

Gee, G., Heller, P., 1985, Unsaturated Water Flow at the Hanford Site: A Review of Literature & Annotated Bibliography, Batelle Pacific NW Labs for U.S. DOE, PNL-5428 UC 70.

Gee, G.W., Kirkham, R.R., 1984, Arid Site Water Balance: Evapotranspiration Modeling and Measurements, Batelle Pacific NW Laboratory for US DOE, PNL-5177 UC 70.

Greulach, V.A., Adams, J.E., 1967, In Plants: An Introduction to Modern Botany, John Wiley and Sons; New York, 630 pp.

Gutjahr, A., 1985, In Soil Spatial Variability; Spatial Variability: Geostatistical Methods, Workshop of the ISSA and SSSA; Pudoc Wageningen, pp. 9 - 34.

Gutjahr, A., Gelhar, L., Bakr, A. Mac Millan, R., 1978, 2. Evaluation and Application, Water Resources Research, Volume 14, No. 5, pp. 953 - 959.

Hainsworth, J.M., Aylmore, L.A.G., 1986, Water Extraction By Single Plant Roots, Soil Science Society of America Journal, Volume 50, No. 4, pp. 841 - 848.

Hillel, D., 1980, In Applications of Soil Physics, Academic Press; New York, 385 pp.

Holmes, J.W., 1984, Measuring Evapotranspiration By Hydrological Methods, Agricultural Water Management, Volume 8, pp. 20-40.

Journel, A.G., Huibregts, C.J., 1978, In Mining Geostatistics, Academic Press; London, 600 pp.

Kirkham, G., Gee, G., 1983, Measurement of Unsaturated Flow Below the Root Zone at an Arid Site, NWWA Conference on Characterization & Monitoring of the Vadose Zone, Batelle NW Laboratory for the DOE.

Klemt, W.B., 1981, Evaluating the Ground-Water Resources of the High Plains of Texas - Neutron Probe Measurements of Deep Soil Moisture as an Indication of Aquifer Recharge Rates, Texas Department of Water Resources.

Klute, A., 1965, Laboratory Measurement of Hydraulic Conductivity of a Saturated Soil, In Black, C.A. (ed) Methods of Soil Analysis, Agronomy 9: 210 - 220, American Society of

Agronomy, Madison, WI.

Klute, A., 1965, Laboratory Measurement of Hydraulic Conductivity of an Unsaturated Soil, In Black, C.A. (ed) Methods of Soil Analysis, Agronomy 9: 253 - 261, American Society of Agronomy, Madison, WI.

Klute, A., Danielson, R., Hamaker, P., 1972, Ground Water Recharge as Affected by Surface Vegetation & Management, Colorado State University, Ft. Collins, CO, Colorado Water Resource Research Institute, Completion Report No. 41.

Kreutzer, K., Strebel, O., Ranger, M., 1980, Field Measurement of Seepage and Evapotranspiration Rate for a Soil Under Plant Cover: A Comparison of Soil Water Balance and Tritium Labeling Procedure, Journal of Hydrology, Volume 48, pp 137 - 146.

Lane, L.J., Romney, E.M., Hakonson, T.E., 1984, Water Balance Calculations and Net Production of Perennial Vegetation in the Northern Mojave Desert, Journal of Range Management, Volume 37, No. 1, pp. 12 - 18.

Leavitt, M.L., 1987, Spatial Variability and Hydrologic Parameters at the Sevilleta National Wildlife Refuge, Unpublished Independent Study Paper, New Mexico Institute of Mining and Technology, Socorro, NM.

Miller, D.R., Smith, D.A., 1981, Modeling Evapotranspiration from Different Land Use Cover Types, Progress Report to the USGS, Water Resources Division and Connecticut Dept. of Environmental Protection, Report No. 5171-0119-112.

Machette, M.C., 1978, Geologic Map of the San Acacia Quadrangle, Socorro County, New Mexico, Map GQ-1415 USGS, Washington, DC

Molz, F.J., 1971, Interaction of Water Uptake and Root Distribution, Agronomy Journal, Volume 63, pp. 608 - 610.

Molz, F.J., 1981, Models of Water Transport in the Soil-Plant System: A Review, Water Resources Research, Volume 17, No. 5, pp. 1245 - 1260.

Molz, F.J., Remsen, I., 1971, Application of an Extraction Term Model to the Study of Moisture Flow to Plant Roots, Agronomy Journal, Volume 63, pp. 72 - 77.

Narasimhan, T.N., Witherspoon, P.A., 1977, Numerical Model for Saturated-Unsaturated Flow in Deformable Porous Media 1. Theory, Water Resources Research, Volume 13, No. 3, pp. 657 - 664.

Nielson, R.P., 1986, High-Resolution Climatic Analysis and

Southwest Biogeography, Science, Volume 232, pp. 27 - 34.

Nelson, W.W., Allmoras, R.R., 1969, An Improved Monolith Method for Excavating and Describing Roots, Agronomy Journal, Volume 61, pp. 751 - 754.

Neuman, S.P., Feddes, R.A., Bresler, E., 1975, Finite Element Analysis of Two-Dimensional Flow in Soils Considering Water Uptake By Roots: I. Theory, II. Field Applications, Soil Science Society of America Proceedings, Volume 39, pp. 224 - 237.

Nimah, M.N., Hanks, R.J., 1973, Model for Estimating Soil Water, Plant, and Atmospheric Interrelations: I. Description and Sensitivity. II. Field Test of Model, Soil Science Society of America Proceedings, Volume 37, pp. 522 - 532.

Nixon, P.R., Lawless, G.P., 1960, Translocation of Moisture With Time in Unsaturated Soil Profiles, Journal of Geophysical Research, 65(2), pp. 655 - 661.

Ogata, G., Richards, L.A., Gardner, W., 1960, Transpiration of Alfalfa Determined From Soil Water Content Changes, Soil Science, Volume 89, No. 4, pp. 179 - 182.

Passiour, J.B., 1981, Water Collection By Roots, In Physiology and Biochemistry of Drought Resistance in Plants, Editors: L.G. Paley & D. Aspinall, Academic Press, Sydney, pp. 39 - 53.

Penman, H.L., 1956, Estimating Evaporation, American Geophysical Union, Transactions, Volume 37, No. 1, pp. 43 - 50.

Perkins, B., De Poorter, G.L., 1985, Plants and Their Relationship to Soil Moisture and Tracer Movements, Los Alamos National Laboratories, New Mexico, Department of Energy, 71 pp.

Rice, R.C., 1975, Diurnal and Seasonal Soil-Water Uptake and Flux, Soil Science Society of America Proceedings, Volume 39, pp. 394 -398.

Rose, C.W., Stern, W.R., 1967, Determination of Withdrawal of Water From Soil By Crop Roots as a Function of Depth and Time, Australian Journal of Soil Research, Volume 5, pp 11 - 19.

Sammis, T.W., 1974, The Microenvironment of a Desert Hackberry Plant (Celtis Pallida), Unpublished Doctoral Thesis, University of Arizona, 159 pp.

Sammis, T.W., Evans, D.D., Warrick, A.W., 1982, Compari-

son of Methods to Estimate Deep Percolation Rates, Water Resources Research Bulletin, Volume 18, No. 3, pp. 465 - 470.

Scholl, D.G., 1976, Soil-Moisture Flux and Evapotranspiration Determined from Soil Hydraulic Properties in a Chaparral Stand, Soil Science Society of America Proceedings, Volume 40, pp. 14-18._

Schuurman, J.J., Goedewaagen, M.A.J., 1965, In Methods for the Examination of Root Systems and Roots, Centre for Agricultural Publications and Documentation, Wageningen, 84 pp.

Sharp, R.G., Davies, W.J., 1985, Root Growth and Water Uptake By Maize Plants, Journal of Experimental Botany, Volume 36, No. 170, pp. 1441 - 1446.

Slayter, R.O., 1967, In Plant - Water Relationships, Academic Press; London, 366 pp.

Stephens, D.B., Knowlton R.G., 1986, Soil Water Movement and Recharge Through Sand at a Semiarid Site in New Mexico, Water Resources Research, Volume 22, No. 6, pp.881 - 889.

Tapia, L.S., Lugg, D.G., 1986, Evaluation of Six Legumes Under Different Irrigation and Nitrogen Fertilization Levels in North-Central New Mexico, Agricultural Experiment Station, New Mexico State University, Research Report 590, 6 pp.

Taylor, S., 1952, Estimating the Integrated Soil Moisture Tension in the Root Zone of Growing Crops, Soil Science, Volume 73, No. 5, pp. 331 - 339.

Van Bavel, C.H.M., Stirk, G.B., Brust, K.J., 1968, Hydraulic Properties of a Clay Loam Soil and the Field Measurement of Water Uptake By Roots: I. Interpretation of Water Content and Pressure Profiles. II. The Water Balance of the Root Zone. III. Comparison of Field and Laboratory Data on Retention and Measured and Calculated Conductivities, Soil Science Society of American Proceedings, Volume 32, pp. 310 - 326.

Van Genuchten, R., 1978, Calculating the Unsaturated Hydraulic Conductivity With a New Closed-form Analytical Model, Research Report 78-WR-08, Water Resources Program, Dept. of Civil Engineering, Princeton University, Princeton, NJ.

Whitford, W.G., 1986, Adaptive Strategies of Desert Shrubs, In Patterns and Processes in Desert Ecosystems, University of New Mexico Press; Albuquerque, pp. 5 - 50.

Wilkins, M., 1984, In Advanced Plant Physiology, Pitman; New

York, 514 pp.

Yeh, T.C.J., Gelhar, L., Gutjahr, A., 1985, Stochastic Analysis of Unsaturated Flow in Heterogeneous Soils, 1. Statistically Isotropic Media, 2. Applications and Evaluation, Water Resources Research, Volume 21, No. 4, pp. 447 - 456.

Zaslavsky, D., Sinai, G., 1981, Surface Hydrology: III - Causes of Lateral Flow, Journal of the Hydraulics Division, American Society of Civil Engineers, HY1, pp. 37 - 52.

APPENDIX A

Particle-size distribution, uniformity coefficient, and coefficient of curvature for several core samples collected on the dune were determined following American Society of Testing and Measures (ASTM) standards (Day, 1965). Several plots of percent finer versus particle-size were plotted. None of the samples had more than 10% mass weight passing the #200 sieve (0.074 mm) therefore hydrometer analysis was not necessary. Uniformity coefficient, C_u, is defined as D_{60}/D_{10} and coefficient of curvature, C_c, is $D_{60}*D_{10}/(D_{30})^2$. D_n indicates that n% of the sample is smaller than this particle diameter. Uniformity coefficient and coefficient of curvature values which approach one are common for very uniform soils.

SEVILLETA DUNE SAND PARTICLE-SIZE ANALYSES

SAMPLE: E1-35cm DATE:6/27/85

SAMPLE WEIGHT WET (gm	78.09
SAMPLE WEIGHT DRY (gm	76.09
WATER WEIGHT (gm)	2.00
MASS WETNESS (%)	2.63
COEFF OF CURVATURE	0.83
UNIFORMITY COEFF	1.875
10% FINER (mm)	0.16

SIEVE NUMBER	DIAMETER (mm)	WT. RETAINED	CUM WT. RETAINED	WT PASSING	% PASSING
16	1.180	0.04	0.04	76.35	99.95
30	0.600	3.90	3.94	72.45	94.84
60	0.250	34.94	38.88	37.51	49.10
100	0.150	28.40	67.28	9.11	8.39
200	0.075	8.64	75.92	0.47	0.62
PAN		0.47	76.39		

SAMPLE: EA-58cm DEPTH: 6/27/85

SAMPLE WT WET (gm)	86.54
SAMPLE WT DRY (gm)	81.75
WATER WT (gm)	4.79
MASS WETNESS (%)	5.85
COEFF OF CURVATURE	1.667
UNIFORMITY COEFF	0.864
10% FINER (mm)	0.15

SIEVE NUMBER	DIAMETER (mm)	WT. RETAINED	CUM WT. RETAINED	WT PASSING	% PASSING
16	1.180	0.06	0.06	81.64	99.93
30	0.600	2.96	3.20	78.68	96.30
60	0.250	31.58	34.60	47.10	57.65
100	0.150	37.77	72.37	9.33	11.42
200	0.075	8.60	80.97	0.73	0.89
PAN		0.73	81.70		

SAMPLE: E1-80cm DATE: 6/27/85

SAMPLE WT WET (gm)	82.70
SAMPLE WT DRY (gm)	79.40
WATER WEIGHT	3.30
MASS WETNESS (%)	4.16
COEFF OF CURVATURE	0.85
UNIFORMITY COEFF	1.623
10% FINER (mm)	0.15

SIEVE NUMBER	DIAMETER (mm)	WT. RETAINED	CUM WT. RETAINED	WT PASSING	% PASSING
30	0.600	0.17	0.17	79.79	99.79
40	0.425	1.42	1.59	78.37	98.01
60	0.250	29.27	30.86	49.10	61.41
100	0.150	41.10	71.96	8.00	10.01
200	0.075	7.63	79.59	0.37	0.46
PAN		0.37	79.96		

SAMPLE: E1-110cm DATE: 6/27/85

SAMPLE WT WET (gm)	83.93
SAMPLE WT DRY (gm)	79.98
WATER WT (gm)	3.95
MASS WETNESS (%)	4.94
COEFF OF CURVATURE	0.90
UNIFORMITY COEFF	1.6
10% FINER (mm)	0.15

SIEVE NUMBER	DIAMETER (mm)	WT. RETAINED	CUM WT. RETAINED	WT PASSING	% PASSING
30	0.600	3.75	3.75	79.79	95.36
40	0.425	2.68	6.43	78.37	92.04
60	0.250	18.22	24.65	49.10	69.46
100	0.150	42.60	67.25	8.00	16.67
200	0.075	12.80	80.05	0.37	0.81
PAN		0.65	80.70		

SAMPLE: E1-150cm DATE: 6/27/85

SAMPLE WT WET (gm)	92.88
SAMPLE WT DRY (gm)	89.05
WATER WT (gm)	3.83
MASS WETNESS (%)	4.41
COEFF OF CURVATURE	1.01
UNIFORMITY COEFF	2.09
10% FINER (mm)	0.11

SIEVE NUMBER	DIAMETER (mm)	WT. RETAINED	CUM WT. RETAINED	WT PASSING	% PASSING
30	0.600	0.67	0.67	88.38	99.25
40	0.425	2.97	3.64	85.41	95.91
60	0.250	30.90	34.54	54.51	61.21
100	0.150	40.05	74.59	14.46	16.24
200	0.075	13.27	87.86	1.19	1.34
PAN		1.19	89.05		

SAMPLE: E1-195cm DATE: 6/27/85

SAMPLE WT WET (gm)	85.30
SAMPLE WT DRY (gm)	81.16
WATER WT (gm)	4.14
MASS WETNESS (%)	5.10
COEFF OF CURVATURE	1.73
UNIFORMITY COEFF	2
10% FINER (mm)	0.13

SIEVE NUMBER	DIAMETER (mm)	WT. RETAINED	CUM WT. RETAINED	WT PASSING	% PASSING
30	0.600	0.94	0.94	80.22	98.85
40	0.425	3.71	4.65	76.51	94.32
60	0.250	34.38	39.03	42.13	52.34
100	0.150	31.85	70.88	10.28	13.45
200	0.075	10.00	80.88	0.28	1.24
PAN		1.02	81.90		

SAMPLE: E1-212cm DATE: 6/27/85

TOTAL SAMPLE WT. (wet	90.93
TOTAL SAMPLE WT. (dry	85.92
WATER WT (gm)	5.01
MASS WETNESS (%)	5.51
COEFF OF CURVATURE	1.44
UNIFORMITY COEFF	2.5
10% FINER (mm)	0.1

SIEVE NUMBER	DIAMETER (mm)	WT. RETAINED	CUM WT. RETAINED	WT PASSING	% PASSING
30	0.600	0.73	0.73	85.80	98.93
40	0.425	3.78	4.51	82.02	94.79
60	0.250	31.54	36.05	50.48	58.34
100	0.150	35.14	71.19	15.34	17.73
200	0.075	13.61	84.80	1.73	2.00
PAN		1.73	86.53		

SAMPLE: E1-242 DATE:

SAMPLE WT WET (gm)	89.44
SAMPLE WT DRY (gm)	84.91
WATER WT (gm)	4.53
MASS WETNESS (%)	5.34
COEFF OF CURVATURE	1.39
UNIFORMITY COEFF	1.92
10% FINER (mm)	0.13

SIEVE NUMBER	DIAMETER (mm)	WT. RETAINED	CUM WT. RETAINED	WT PASSING	% PASSING
30	0.600	0.92	0.92	84.55	98.92
40	0.425	3.95	4.87	80.60	94.30
60	0.250	31.00	35.87	49.60	58.03
100	0.150	34.87	70.74	14.73	17.23
200	0.075	13.08	83.82	1.65	1.93
PAN		1.65	85.47		

SAMPLE: E1-268cm DATE: 6/27/85

SAMPLE WT WET (gm)	98.90
SAMPLE WT DRY (gm)	94.52
WATER WT (gm)	4.38
MASS WETNESS (%)	4.64
COEFF OF CURVATURE	0.93
UNIFORMITY COEFF	2.27
10% FINER (mm)	0.11

SIEVE NUMBER	DIAMETER (mm)	WT. RETAINED	CUM WT. RETAINED	WT PASSING	% PASSING
30	0.600	1.09	1.09	93.52	98.85
40	0.425	5.00	6.09	88.52	93.56
60	0.250	35.00	41.09	53.52	56.57
100	0.150	37.60	78.69	15.92	16.83
200	0.075	13.76	92.45	2.16	2.28
PAN		2.16	94.61		

SAMPLE: E1-290cm DATE: 6/27/85

SAMPLE WT WET (gm)	92.66
SAMPLE WT DRY (gm)	89.36
WATER WT (gm)	3.30
MASS WETNESS (%)	3.69
COEFF OF CURVATURE	0.89
UNIFORMITY COEFF	2
10% FINER (mm)	0.15

SIEVE NUMBER	DIAMETER (mm)	WT. RETAINED	CUM WT. RETAINED	WT PASSING	% PASSING
30	0.600	1.60	1.60	87.55	98.21
40	0.425	9.46	11.06	78.09	87.59
60	0.250	34.45	45.51	43.64	48.95
100	0.150	31.12	76.63	12.52	14.04
200	0.075	11.07	87.70	1.45	1.63
PAN		1.45	89.15		

SAMPLE: E1-330cm DATE:

SAMPLE WT WET (gm)	95.13
SAMPLE WT DRY (gm)	90.20
WATER WT (gm)	4.93
MASS WETNESS (%)	5.47
COEFF OF CURVATURE	1.25
UNIFORMITY COEFF	2
10% FINER (mm)	0.12

SIEVE NUMBER	DIAMETER (mm)	WT. RETAINED	CUM WT. RETAINED	WT PASSING	% PASSING
30	0.600	1.68	1.68	89.08	98.15
40	0.425	4.00	5.68	85.08	93.74
60	0.250	28.50	34.18	56.58	62.34
100	0.150	41.48	75.66	15.10	16.64
200	0.075	13.87	89.53	1.23	1.36
PAN		1.23	90.76		

SEVILLETA DUNE SAMPLES

SAMPLE : WEST 1C DEPTH : (CM) 30.00

TOTAL WEIGHT WET (GM)	73.30
TOTAL WEIGHT DRY (GM)	69.70
WATER WEIGHT (GM)	3.60
MASS WETNESS (GM/GM)	5.16
COEFFICIENT OF CURVATURE	1.12
UNIFORMITY COEFFICIENT	2.04
10% FINER (MM)	0.16

SIEVE NUMBER	DIAMETER (MM)	WEIGHT RETAINED	CUM. WT. RETAINED	% FINER
8	2.360	0.00	0.00	100.00
16	1.180	0.11	0.11	99.80
30	0.600	0.31	0.42	99.40
60	0.250	47.06	47.48	32.10
100	0.150	18.70	66.18	5.30
200	0.075	3.58	69.76	0.20
PAN		0.11	69.87	

SAMPLE : WEST 2C DEPTH : (CM) 60.00

TOTAL WEIGHT WET (GM)	80.92
TOTAL WEIGHT DRY (GM)	77.27
WATER WEIGHT (GM)	3.65
MASS WETNESS (GM/GM)	4.72
COEFFICIENT OF CURVATURE	0.90
UNIFORMITY COEFFICIENT	1.83
10% FINER (MM)	0.14

SIEVE NUMBER	DIAMETER (MM)	WEIGHT RETAINED	CUM. WT. RETAINED	% FINER
8	2.360	0.00	0.00	100.00
16	1.180	0.90	0.90	98.86
30	0.600	0.50	1.40	98.22
60	0.250	33.68	35.08	55.45
100	0.150	35.65	70.73	10.17
200	0.075	7.52	78.25	0.62
PAN		0.49	78.74	

SEVILLETA DUNE SAMPLES

SAMPLE : WEST 3C DEPTH : (CM) 90.00

TOTAL WEIGHT WET (GM)	80.15
TOTAL WEIGHT DRY (GM)	75.92
WATER WEIGHT (GM)	4.23
MASS WETNESS (GM/GM)	5.57
COEFFICIENT OF CURVATURE	0.89
UNIFORMITY COEFFICIENT	2.00
10% FINER (MM)	0.12

SIEVE NUMBER	DIAMETER (MM)	WEIGHT RETAINED	CUM. WT. RETAINED	% FINER
8	2.360	0.00	0.00	100.00
16	1.180	0.04	0.04	99.95
30	0.600	0.74	0.78	98.98
60	0.250	24.65	25.43	66.75
100	0.150	36.22	61.65	19.39
200	0.075	13.58	75.23	1.63
PAN		1.25	76.48	

SAMPLE : WEST 4C DEPTH : (CM) 120.00

TOTAL WEIGHT WET (GM)	86.49
TOTAL WEIGHT DRY (GM)	83.37
WATER WEIGHT (GM)	4.12
MASS WETNESS (GM/GM)	4.94
COEFFICIENT OF CURVATURE	1.07
UNIFORMITY COEFFICIENT	2.23
10% FINER (MM)	0.11

SIEVE NUMBER	DIAMETER (MM)	WEIGHT RETAINED	CUM. WT. RETAINED	% FINER
8	2.360	0.00	0.00	100.00
16	1.180	0.05	0.05	99.94
30	0.600	0.68	0.73	99.11
60	0.250	28.89	29.62	63.86
100	0.150	37.40	67.02	18.22
200	0.075	13.81	80.83	1.37
PAN		1.12	81.95	

SEVILLETA DUNE SAMPLES

SAMPLE : WEST 5C DEPTH : (CM) 150.00

TOTAL WEIGHT WET (GM)	79.95
TOTAL WEIGHT DRY (GM)	76.43
WATER WEIGHT (GM)	3.52
MASS WETNESS (GM/GM)	4.60
COEFFICIENT OF CURVATURE	0.91
UNIFORMITY COEFFICIENT	1.89
10% FINER (MM)	0.13

SIEVE NUMBER	DIAMETER (MM)	WEIGHT RETAINED	CUM. WT. RETAINED	% FINER
8	2.360	0.00	0.00	100.00
16	1.180	0.02	0.02	99.97
30	0.600	0.27	0.29	99.62
60	0.250	28.50	28.79	62.56
100	0.150	36.43	65.22	15.18
200	0.075	10.77	75.99	1.17
PAN		0.90	76.89	

SAMPLE : WEST 6C DEPTH : (CM) 180.00

TOTAL WEIGHT WET (GM)	77.25
TOTAL WEIGHT DRY (GM)	73.18
WATER WEIGHT (GM)	4.07
MASS WETNESS (GM/GM)	5.56
COEFFICIENT OF CURVATURE	1.18
UNIFORMITY COEFFICIENT	2.27
10% FINER (MM)	0.11

SIEVE NUMBER	DIAMETER (MM)	WEIGHT RETAINED	CUM. WT. RETAINED	% FINER
8	2.360	0.00	0.00	100.00
16	1.180	0.04	0.04	99.95
30	0.600	0.42	0.46	99.37
60	0.250	27.31	27.77	62.02
100	0.150	32.29	60.06	17.86
200	0.075	11.67	71.73	1.90
PAN		1.39	73.12	

SEVILLETA DUNE SAMPLES

SAMPLE : WEST 9C DEPTH : (CM) 270.00

TOTAL WEIGHT WET (GM)	79.11
TOTAL WEIGHT DRY (GM)	75.12
WATER WEIGHT (GM)	3.99
MASS WETNESS (GM/GM)	5.30
COEFFICIENT OF CURVATURE	2.00
UNIFORMITY COEFFICIENT	2.00
10% FINER (MM)	0.11

SIEVE NUMBER	DIAMETER (MM)	WEIGHT RETAINED	CUM. WT. RETAINED	% FINER
8	2.360	0.00	0.00	100.00
16	1.180	0.01	0.01	99.99
30	0.600	0.69	0.70	99.07
60	0.250	24.60	25.30	66.44
100	0.150	37.09	62.39	17.24
200	0.075	11.84	74.23	1.54
PAN		1.16	75.39	

SAMPLE : WEST 10C DEPTH : (CM) 300.00

TOTAL WEIGHT WET (GM)	75.82
TOTAL WEIGHT DRY (GM)	72.14
WATER WEIGHT (GM)	3.68
MASS WETNESS (GM/GM)	5.10
COEFFICIENT OF CURVATURE	0.89
UNIFORMITY COEFFICIENT	1.92
10% FINER (MM)	0.13

SIEVE NUMBER	DIAMETER (MM)	WEIGHT RETAINED	CUM. WT. RETAINED	% FINER
8	2.360	0.00	0.00	100.00
16	1.180	0.01	0.01	99.99
30	0.600	1.10	1.11	98.46
60	0.250	24.50	25.61	64.44
100	0.150	33.42	59.03	18.04
200	0.075	11.80	70.83	1.65
PAN		1.19	72.02	

SEVILLETA DUNE SAMPLES

SAMPLE : NORTH 1C DEPTH : (CM) 33.00

TOTAL WEIGHT WET (GM)	
TOTAL WEIGHT DRY (GM)	133.14
WATER WEIGHT (GM)	
MOISTURE CONTENT (%)	

SIEVE NUMBER	DIAMETER (MM)	WEIGHT RETAINED	CUM. WT. RETAINED	% FINER
20	0.850	0.06	0.06	99.95
40	0.425	0.57	0.63	99.50
60	0.250	40.55	41.18	86.90
100	0.150	78.19	119.37	9.90
140	0.106	12.32	131.69	0.60
200	0.075	1.43	132.12	0.30
PAN		0.28	132.48	

SAMPLE : NORTH 2C DEPTH : (CM) 64.00

TOTAL WEIGHT WET (GM)	
TOTAL WEIGHT DRY (GM)	136.90
WATER WEIGHT (GM)	
MOISTURE CONTENT (%)	

SIEVE NUMBER	DIAMETER (MM)	WEIGHT RETAINED	CUM. WT. RETAINED	% FINER
20	0.850	0.90	0.90	99.30
40	0.425	5.63	6.53	95.20
60	0.250	42.36	48.89	64.30
100	0.150	63.83	111.72	18.40
140	0.106	18.25	129.97	5.10
200	0.075	4.82	134.79	1.50
PAN		2.11	136.90	

SEVILLETA DUNE SAMPLES

SAMPLE : NORTH 3C DEPTH : (CM) 93.00

TOTAL WEIGHT WET (GM)	
TOTAL WEIGHT DRY (GM)	132.41
WATER WEIGHT (GM)	
MOISTURE CONTENT (%)	

SIEVE NUMBER	DIAMETER (MM)	WEIGHT RETAINED	CUM. WT. RETAINED	% FINER
20	0.850	0.10	0.10	99.90
40	0.425	4.28	4.38	96.84
60	0.250	30.83	35.21	74.60
100	0.150	83.29	118.50	14.40
140	0.106	16.50	135.00	2.50
200	0.075	2.67	137.67	0.50
PAN		0.75	138.42	

SAMPLE : NORTH 4C DEPTH : (CM) 124.00

TOTAL WEIGHT WET (GM)	
TOTAL WEIGHT DRY (GM)	139.65
WATER WEIGHT (GM)	
MOISTURE CONTENT (%)	

SIEVE NUMBER	DIAMETER (MM)	WEIGHT RETAINED	CUM. WT. RETAINED	% FINER
20	0.850	0.31	0.31	99.80
40	0.425	4.60	4.91	96.50
60	0.250	45.75	50.66	63.70
100	0.150	64.56	115.22	17.50
140	0.106	17.61	132.83	4.90
200	0.075	4.76	137.79	1.30
PAN		1.86	139.65	

SEVILLETA DUNE SAMPLES

SAMPLE : NORTH 5C DEPTH : (CM) 155.00

TOTAL WEIGHT WET (GM)	
TOTAL WEIGHT DRY (GM)	141.19
WATER WEIGHT (GM)	
MOISTURE CONTENT (%)	

SIEVE NUMBER	DIAMETER (MM)	WEIGHT RETAINED	CUM. WT. RETAINED	% FINER
20	0.850	0.14	0.14	99.90
40	0.425	6.12	6.26	95.60
60	0.250	42.88	49.14	65.25
100	0.150	65.02	114.16	19.28
140	0.106	18.97	133.13	5.90
200	0.075	5.44	138.57	2.02
PAN		2.86	141.43	

SAMPLE : NORTH 7C DEPTH : (CM) 216.00

TOTAL WEIGHT WET (GM)	
TOTAL WEIGHT DRY (GM)	139.35
WATER WEIGHT (GM)	
MOISTURE CONTENT (%)	

SIEVE NUMBER	DIAMETER (MM)	WEIGHT RETAINED	CUM. WT. RETAINED	% FINER
20	0.850	0.24	0.24	99.80
40	0.425	5.43	5.67	95.90
60	0.250	39.59	45.26	67.60
100	0.150	66.52	111.78	19.90
140	0.106	18.43	130.21	6.70
200	0.075	5.76	135.97	2.50
PAN		3.54	139.51	

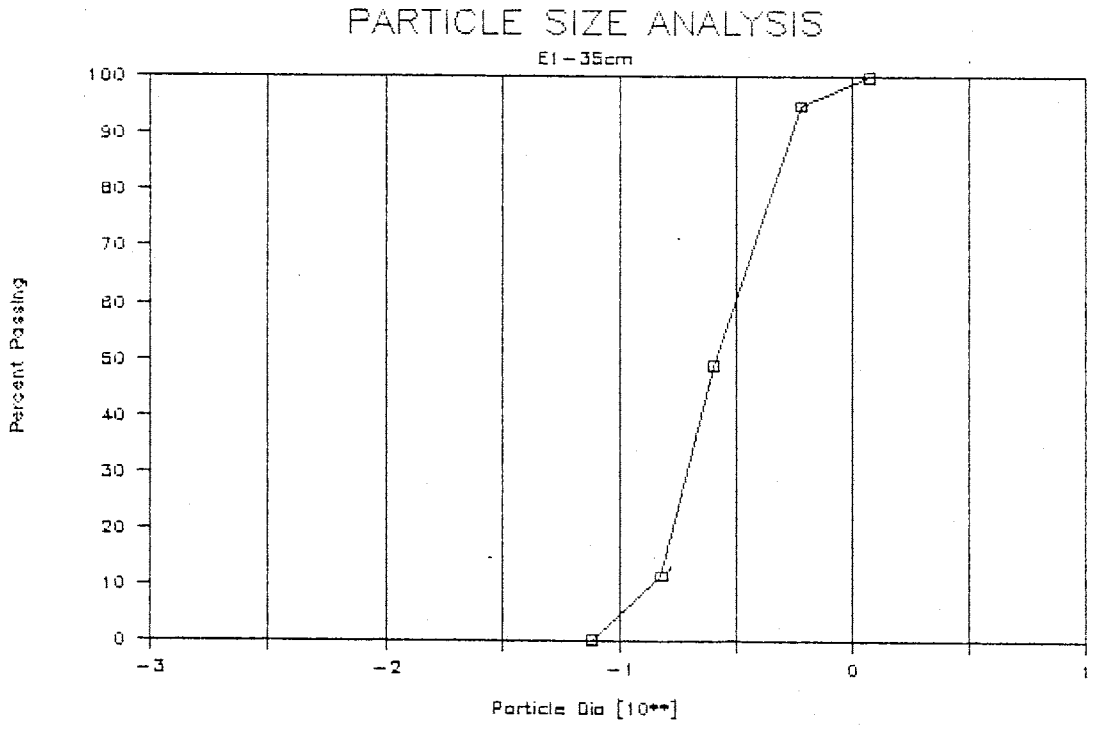
PARTICLE SIZE ANALYSIS
E1-35cm
Percent Passing
100
90
80
70
60
50
40
30
20
10
0
-3
-2
-1
0
1
Particle Dia [10**]

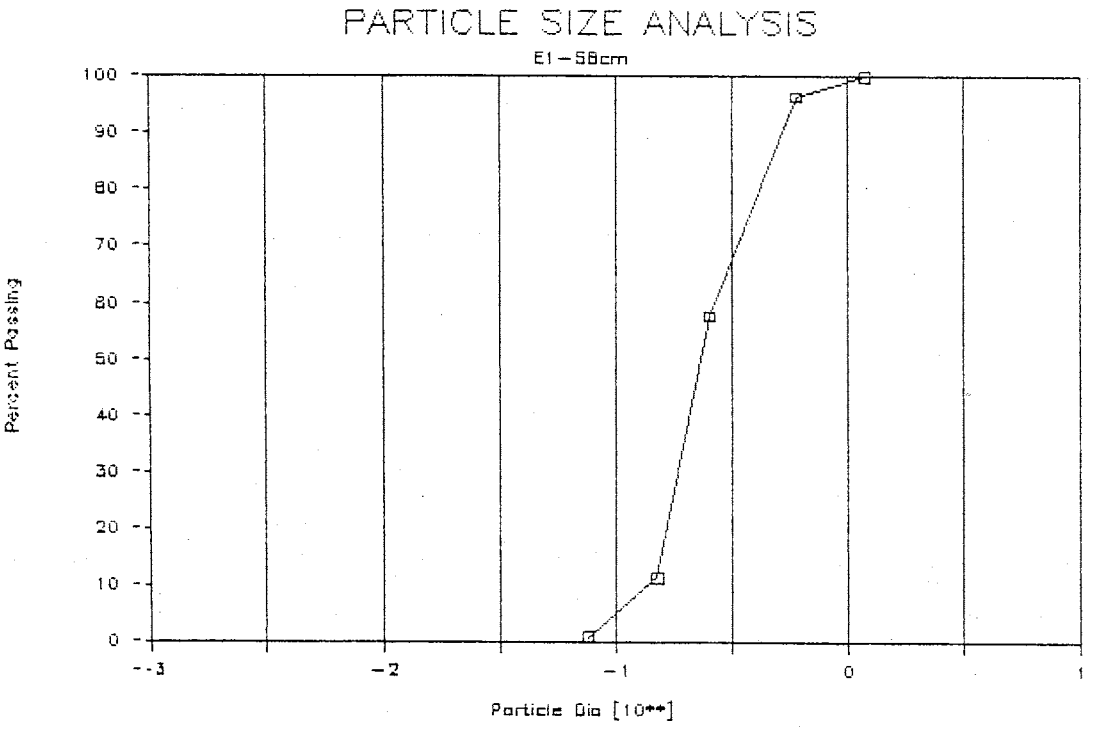
PARTICLE SIZE ANALYSIS
E1-58cm
Percent Passing
100
90
80
70
60
50
40
30
20
10
0
-3
-2
-1
0
1
Particle Dia [10**]

PARTICLE SIZE ANALYSIS

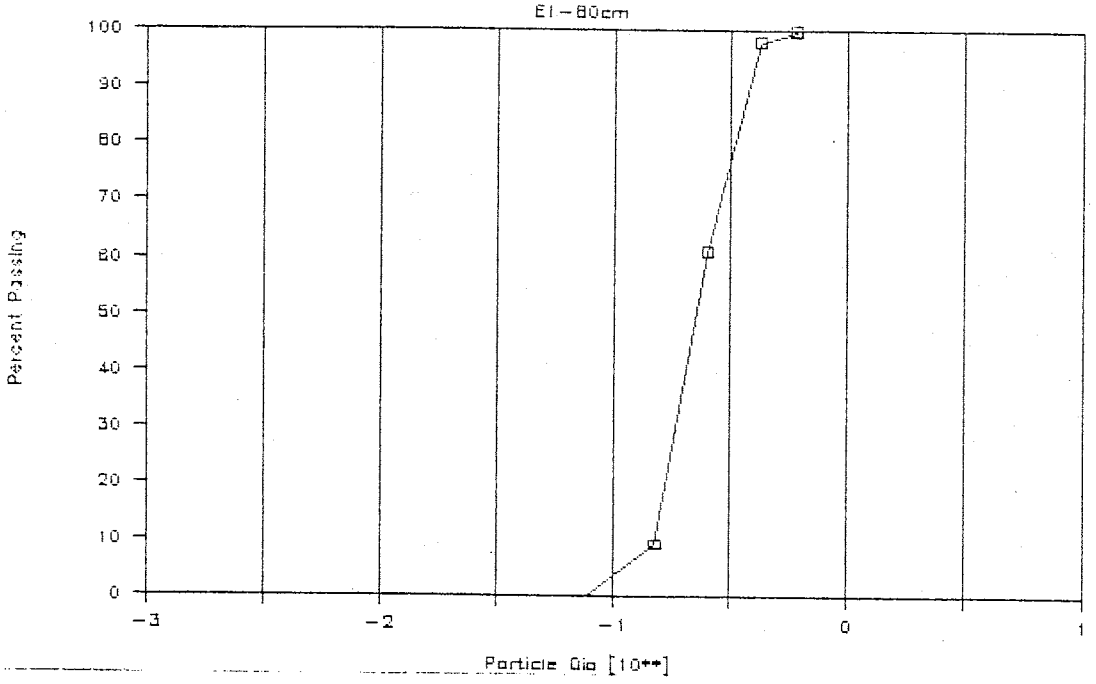

PARTICLE SIZE ANALYSIS

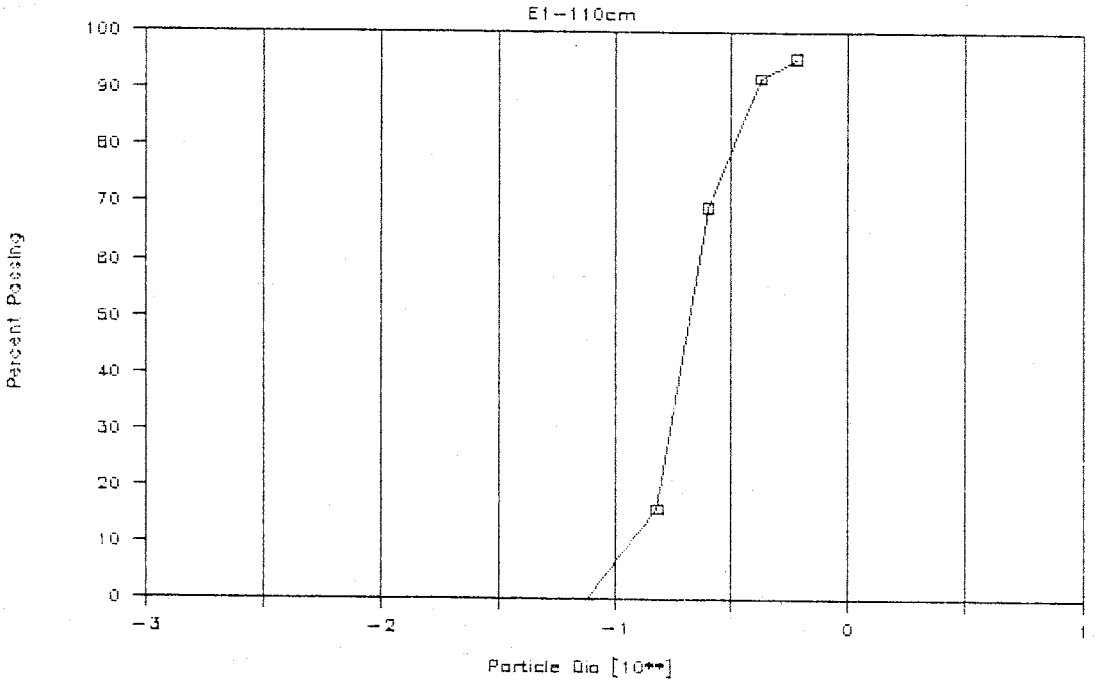

PARTICLE SIZE ANALYSIS

E1-150cm

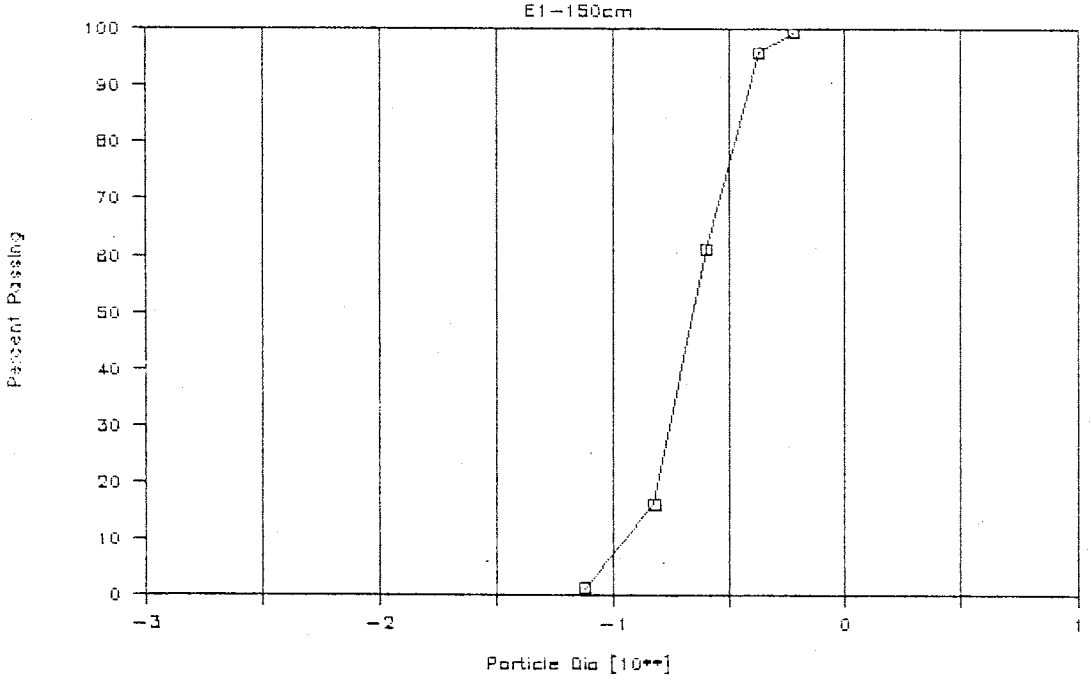

PARTICLE SIZE ANALYSIS

E1-195cm

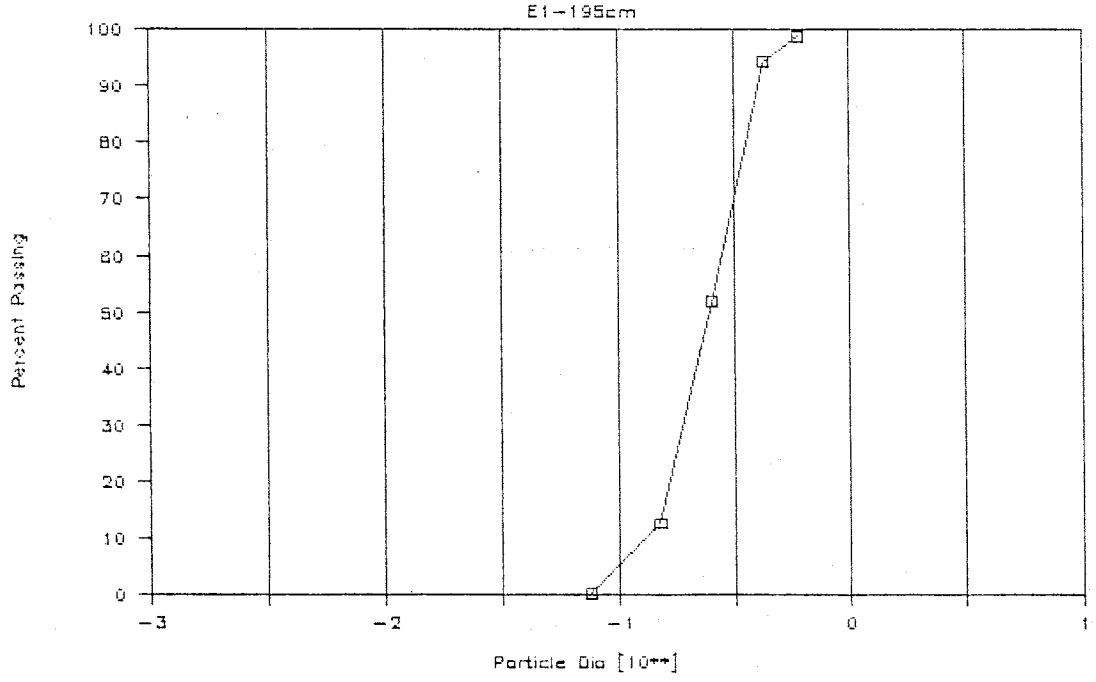

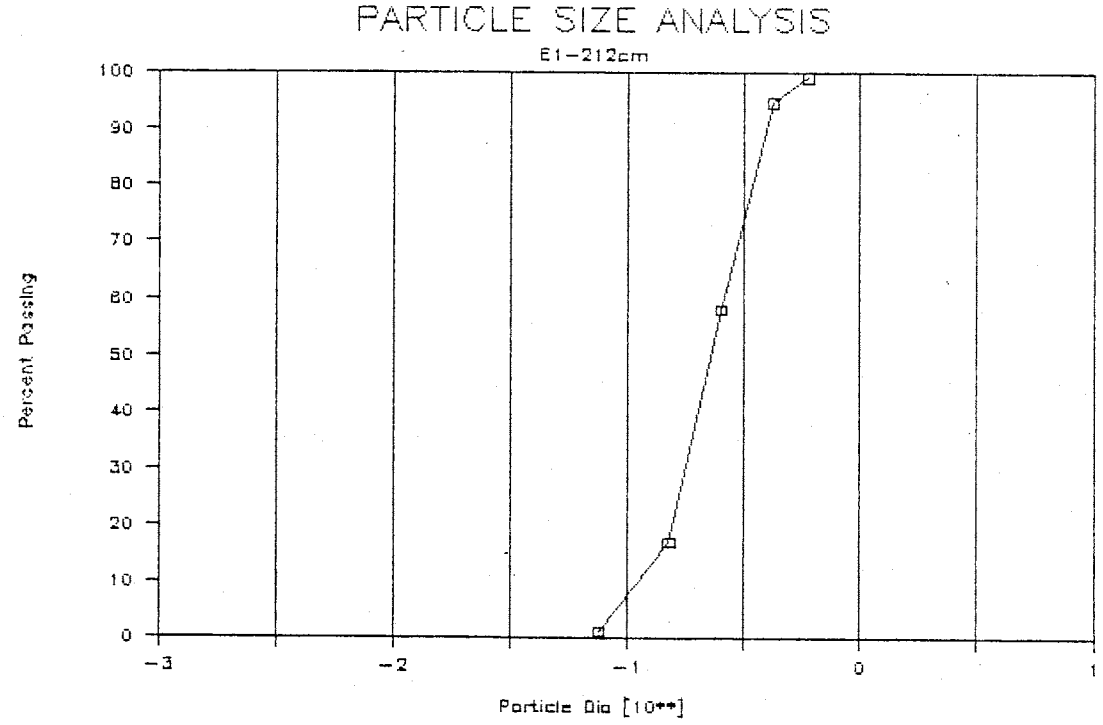
PARTICLE SIZE ANALYSIS
E1-212cm
Percent Passing
100
90
80
70
60
50
40
30
20
10
0
-3
-2
-1
0
1
Particle Dia [10**]

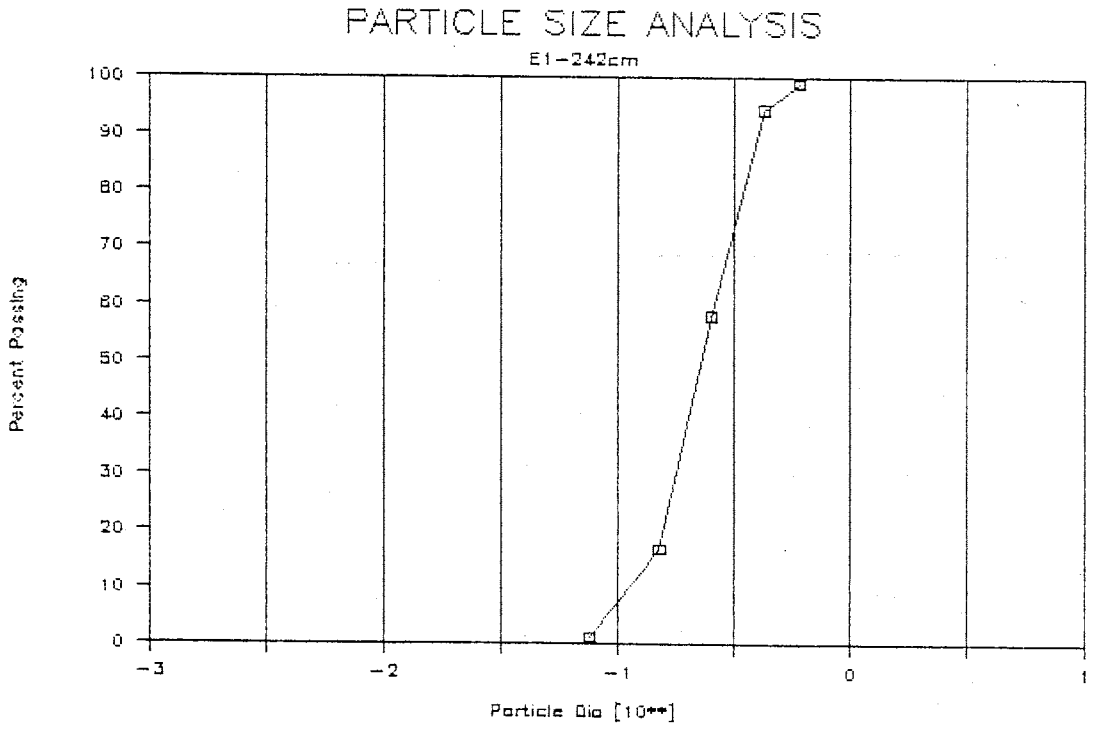
PARTICLE SIZE ANALYSIS
E1-242cm
Percent Passing
100
90
80
70
60
50
40
30
20
10
0
-3
-2
-1
0
1
Particle Dia [10**]

PARTICLE SIZE ANALYSIS

E1-288cm

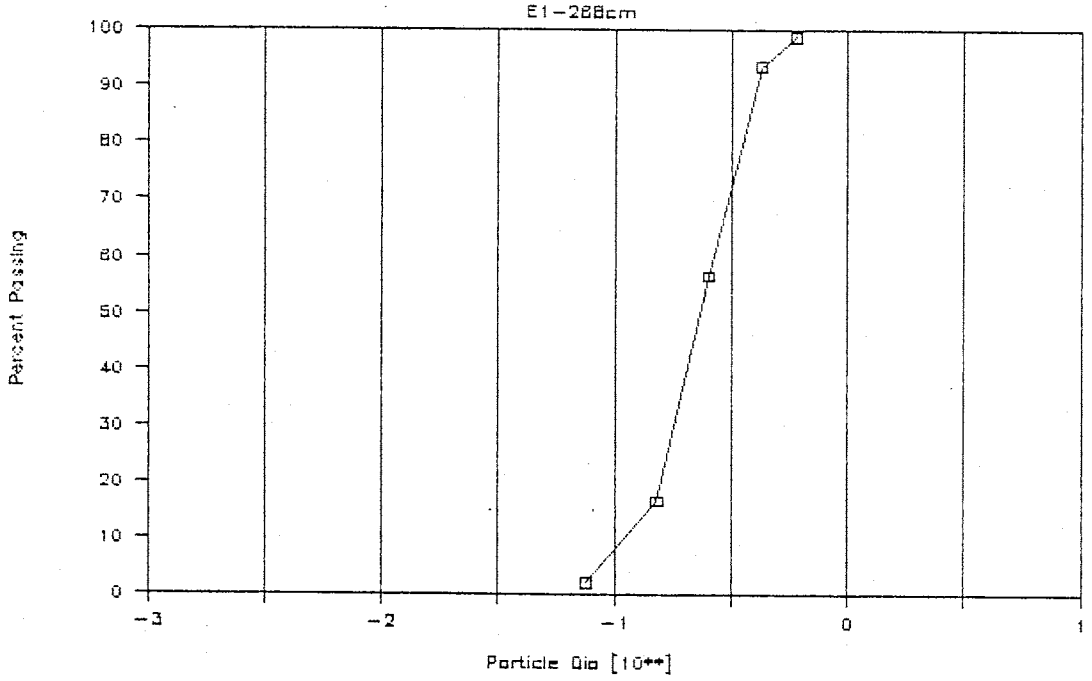

PARTICLE SIZE ANALYSIS

E1-290cm

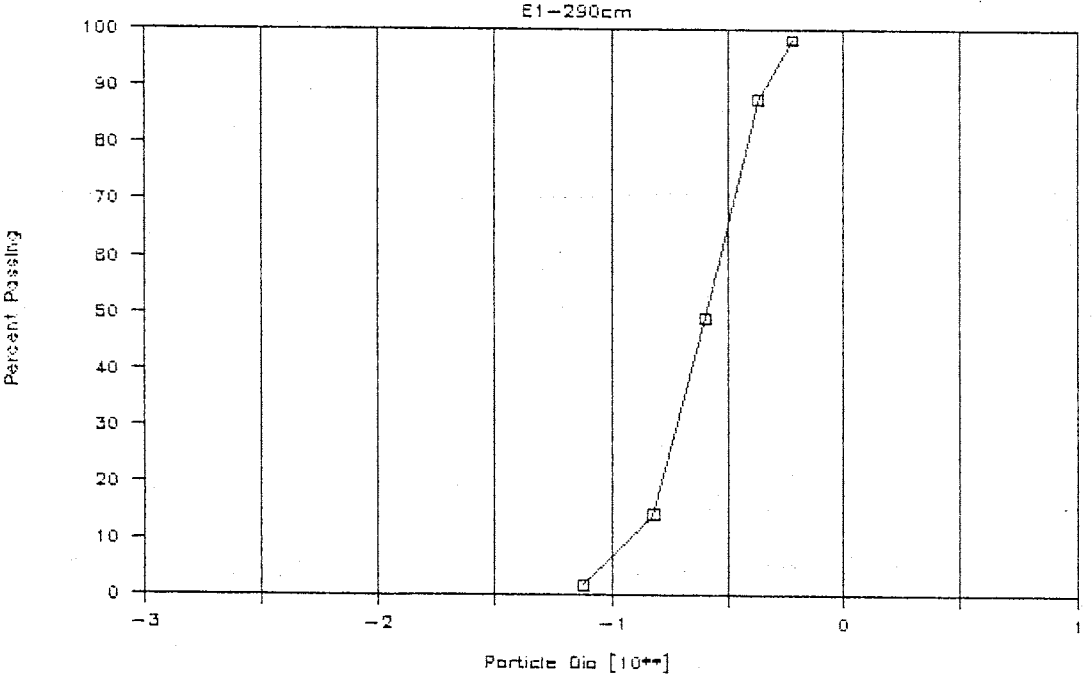

PARTICLE SIZE ANALYSIS

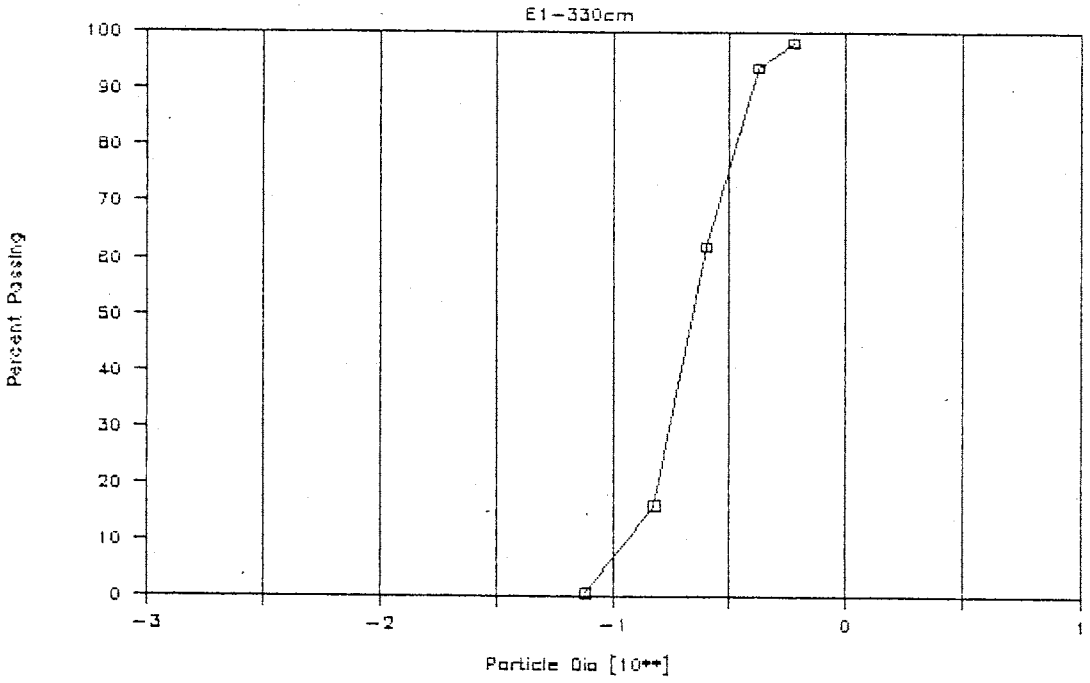

APPENDIX B

The relationship between pressure-head and moisture content of the dune sand was derived in the laboratory using Buchner funnel hanging columns and pressure plate apparatuses. Core samples, with 2.5 cm diameters, were placed on saturated porous plates and moisture contents were determined for each pressure applied. Hanging columns were used to examine pressures less than 200 cm, whereas pressure plates determined moisture content for pressures of 2 and 15 bars. The laboratory procedures followed are outlined in Vomocil (1965). Saturated hydraulic conductivities were determined using a constant-head permeameter to simulate Darcy's law. The method and theory are explained in Klute (1965).

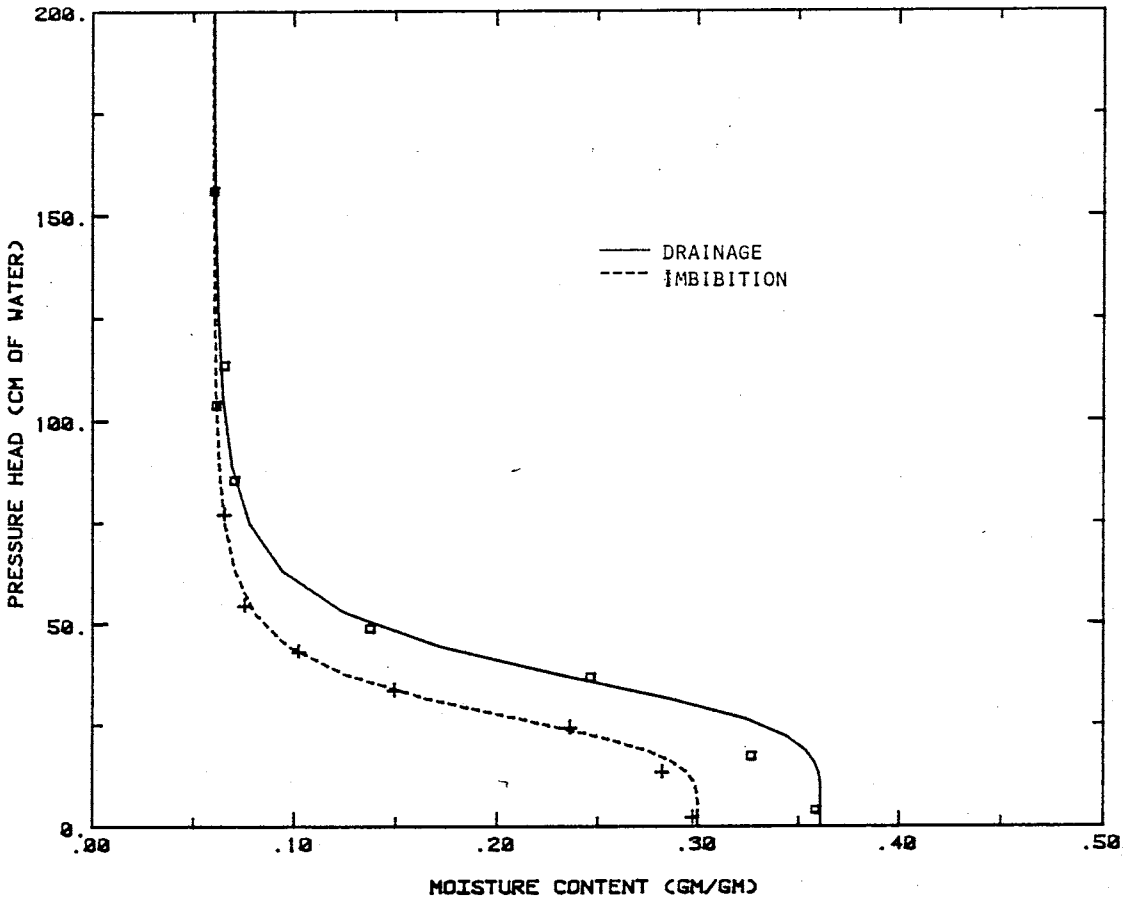

NORTH B, DEPTH = 58CM

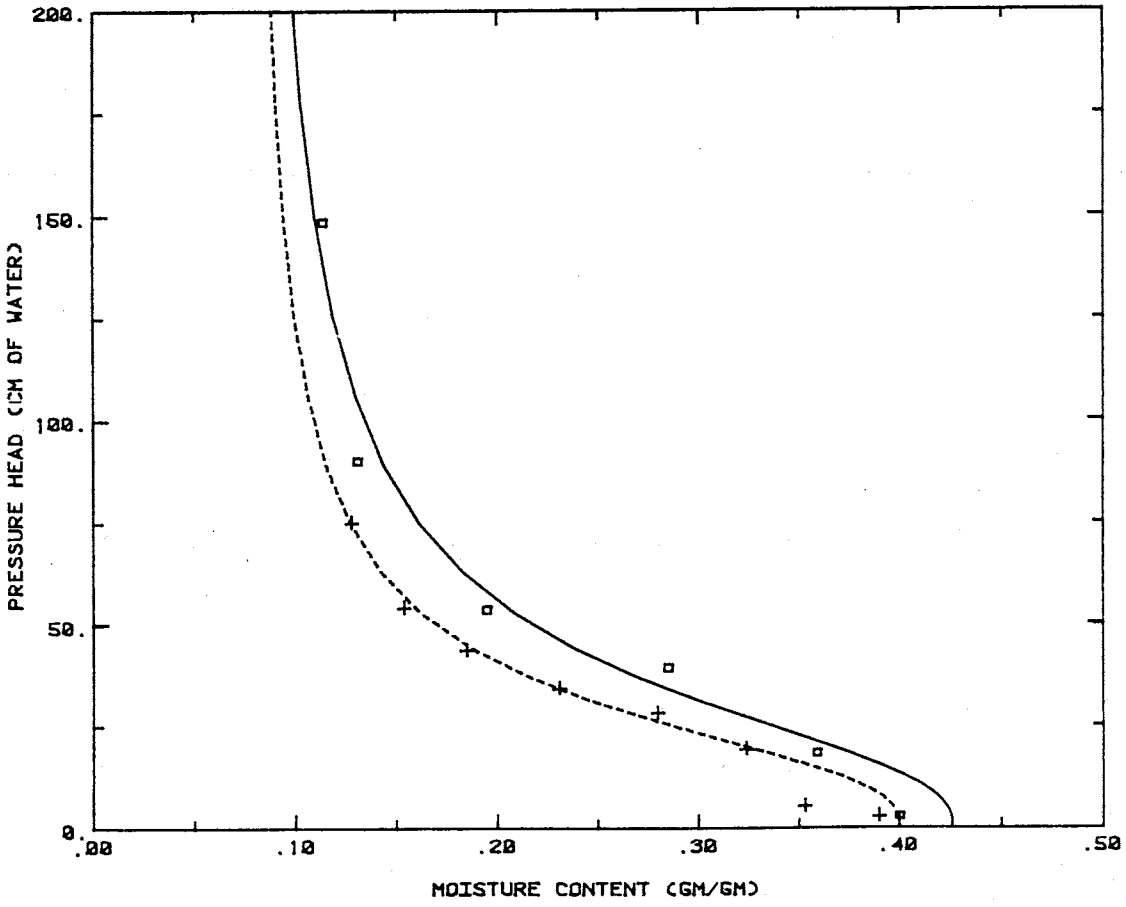

NORTH B, DEPTH = 95 CM

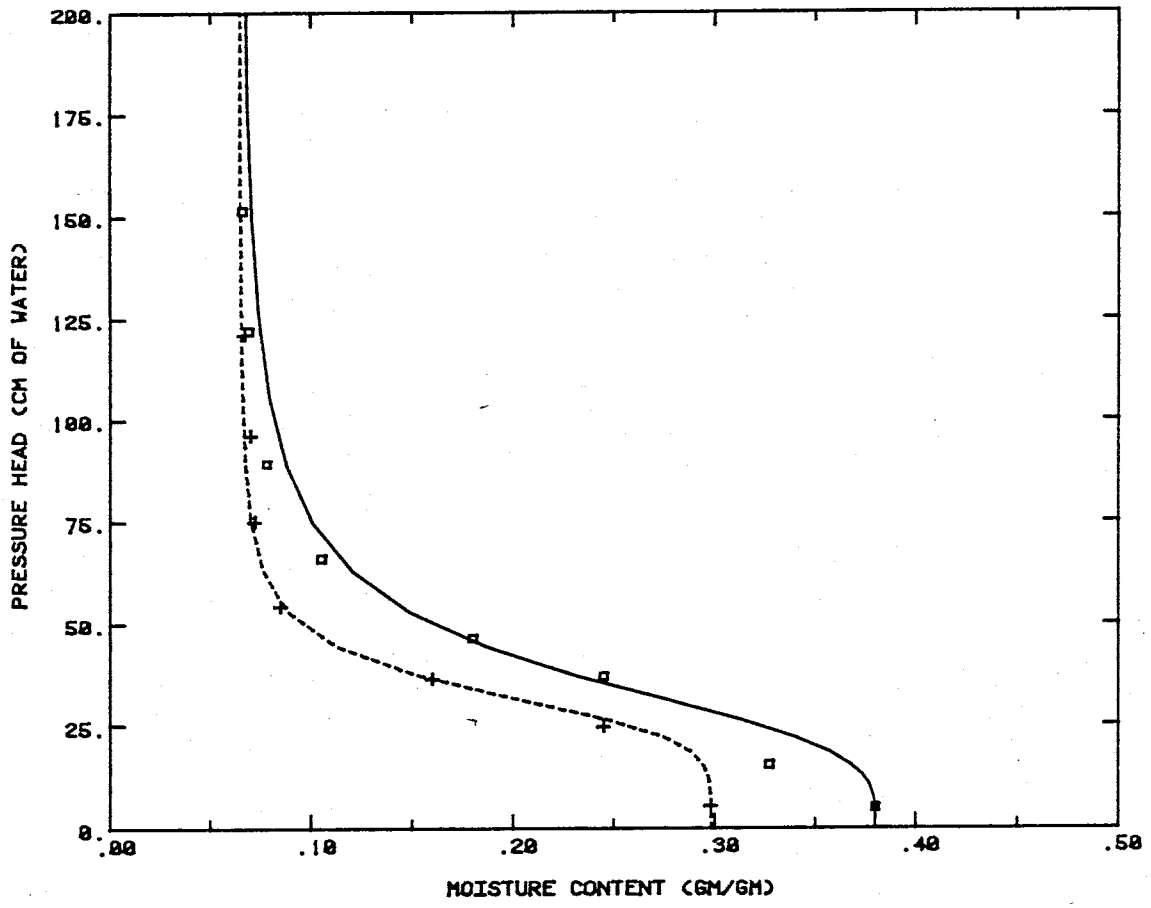

NORTH B, DEPTH = 130 CM

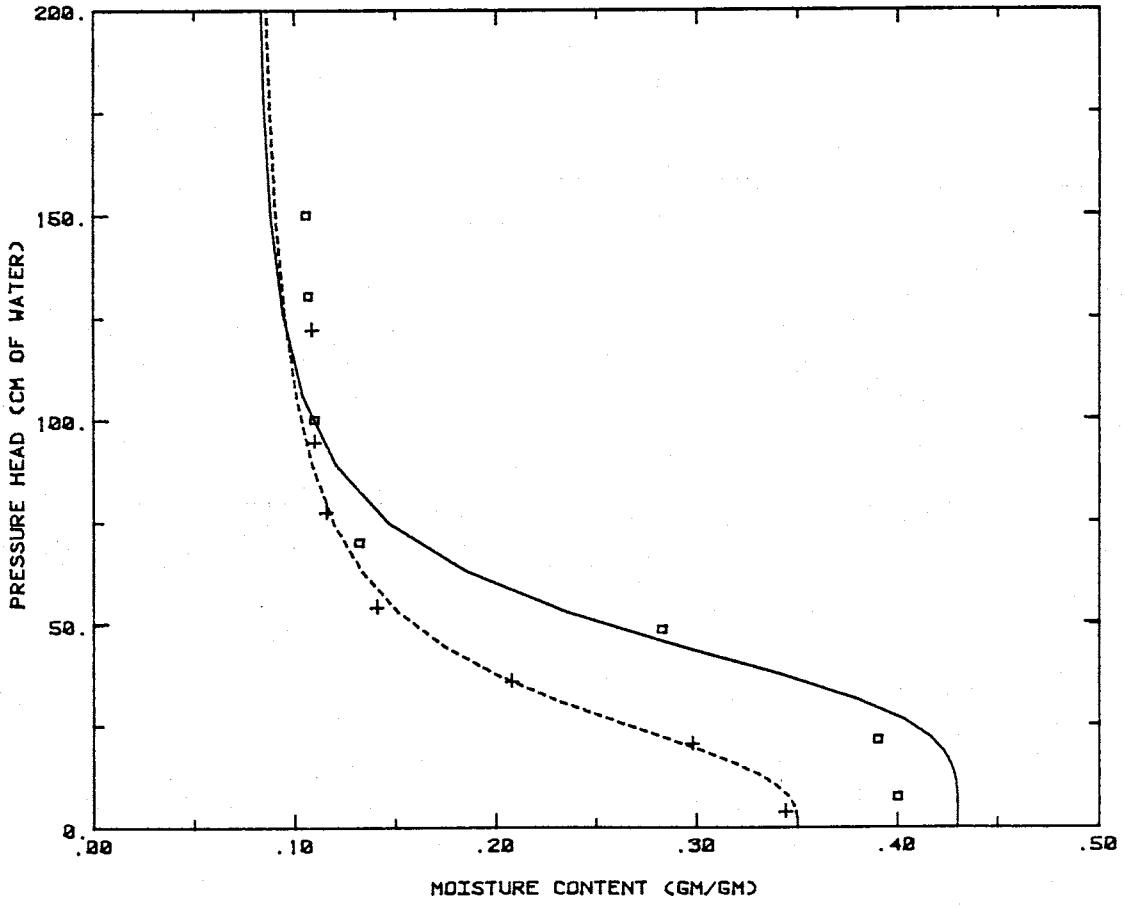

NORTH B, DEPTH = 157 CM

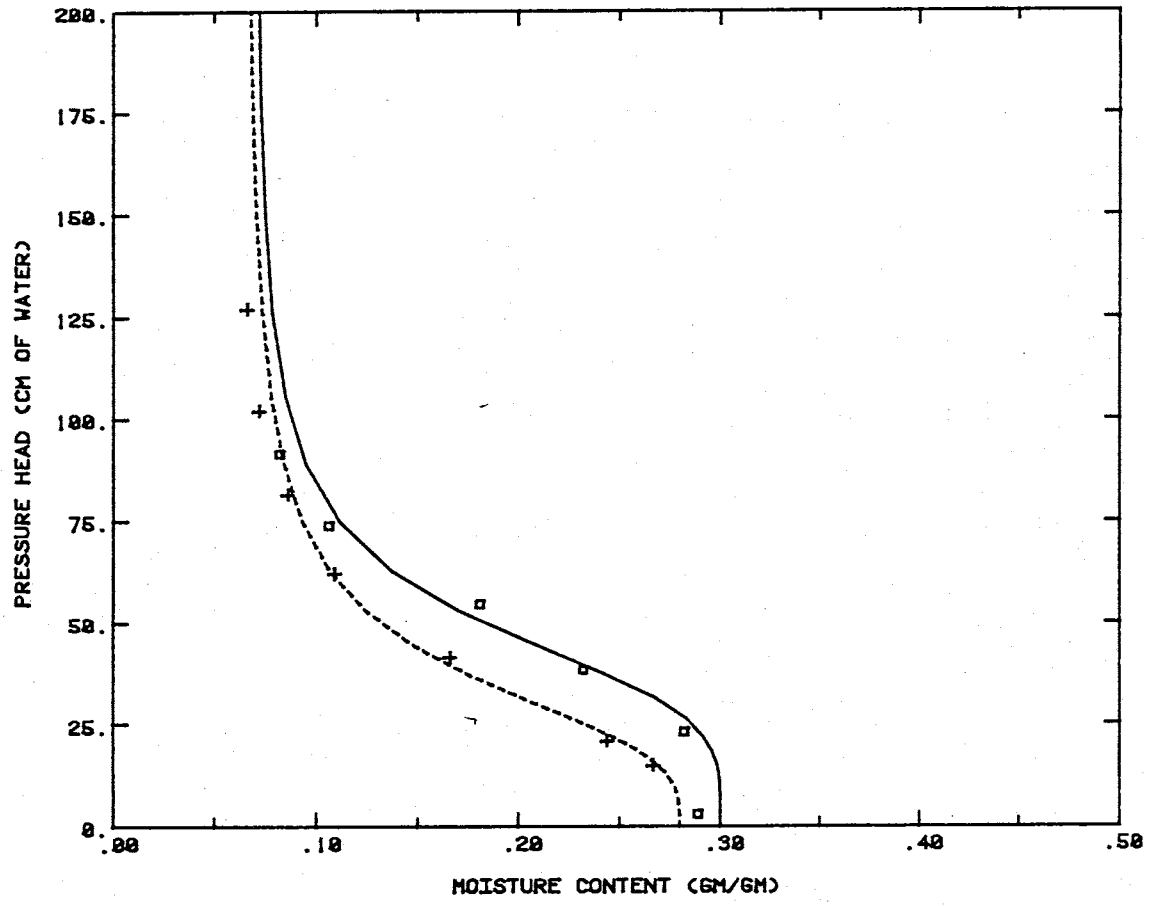

NORTH B, DEPTH = 260 CM

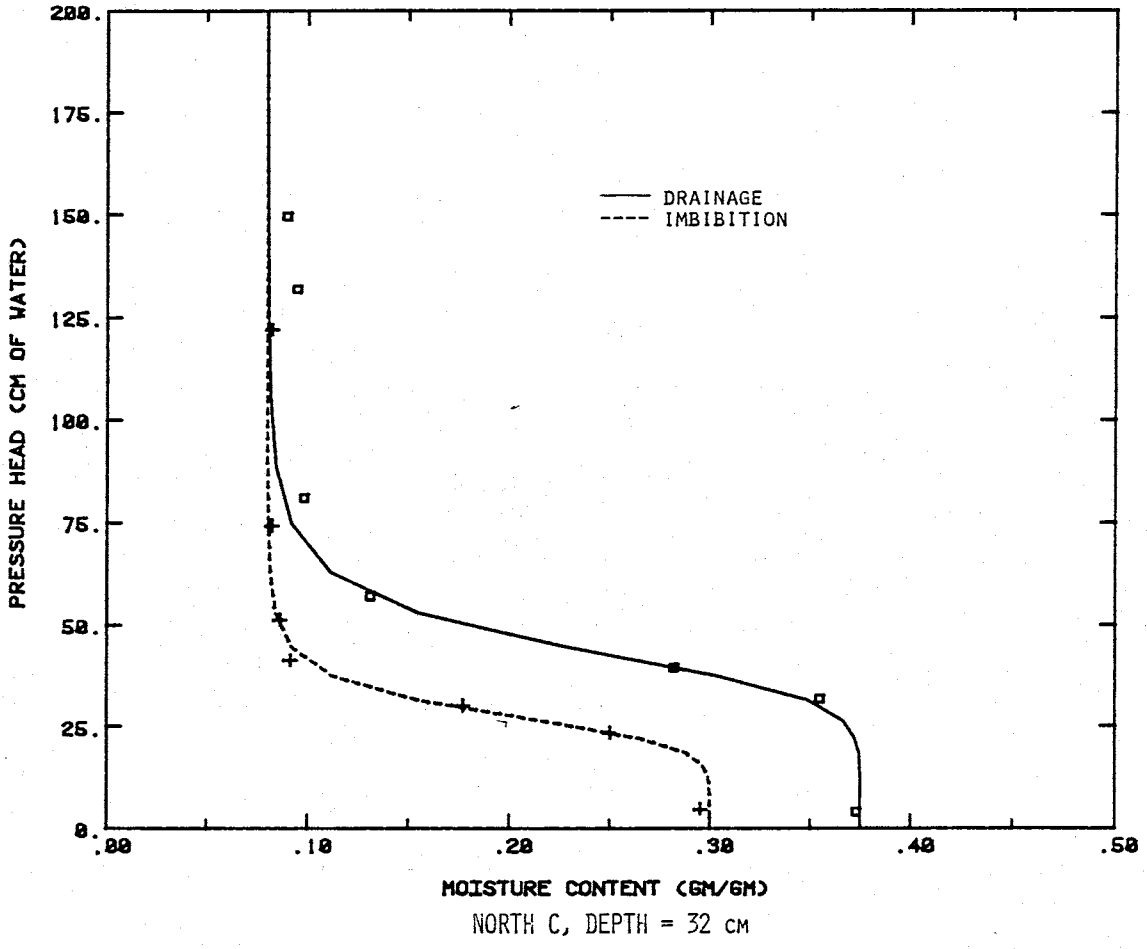

NORTH C, DEPTH = 32 CM

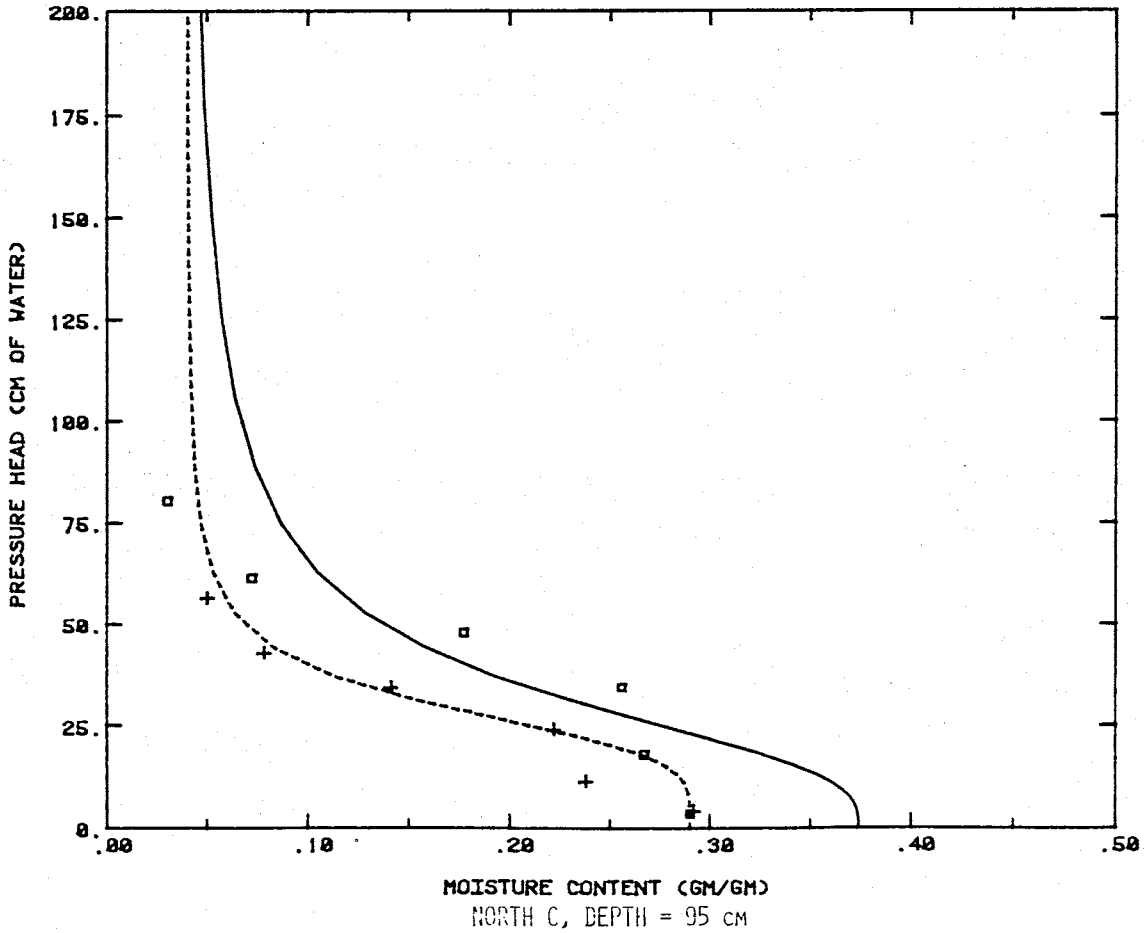

NORTH C, DEPTH = 95 CM

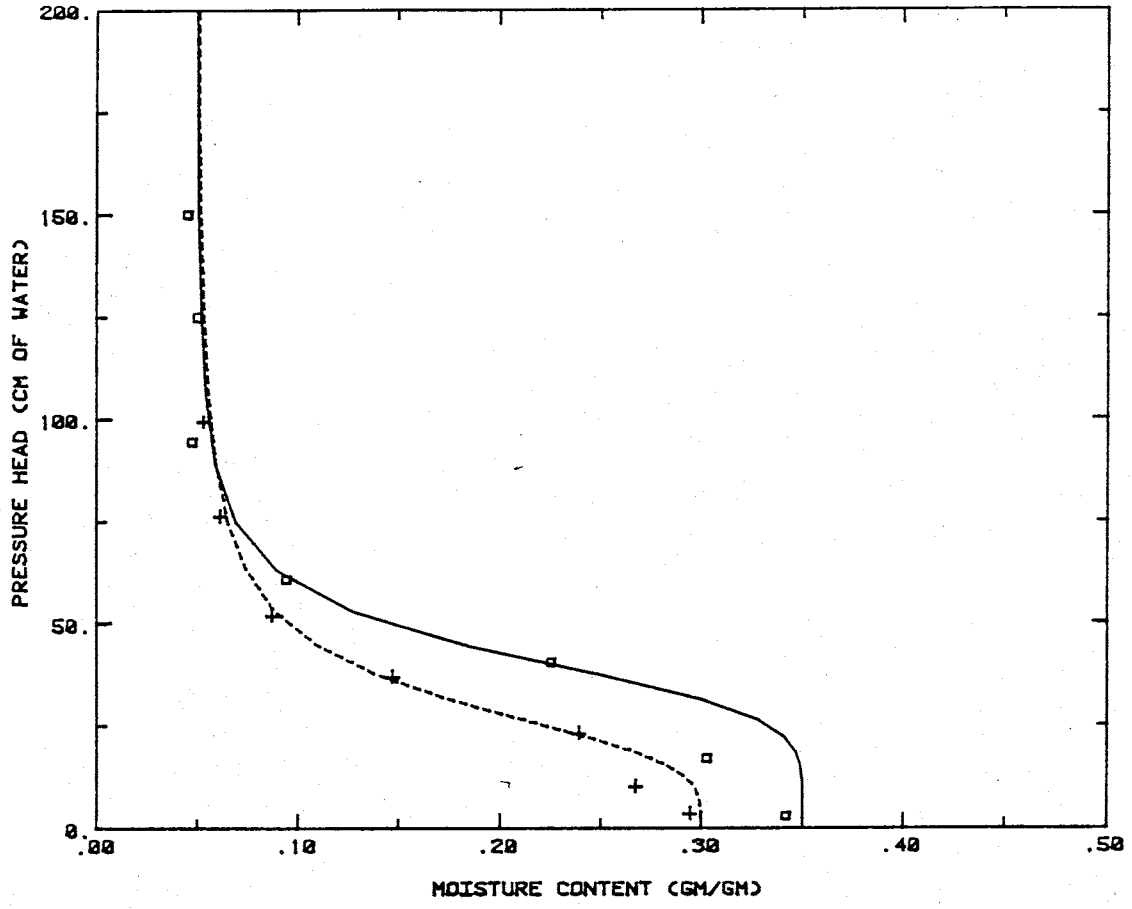

NORTH C, DEPTH = 124 CM

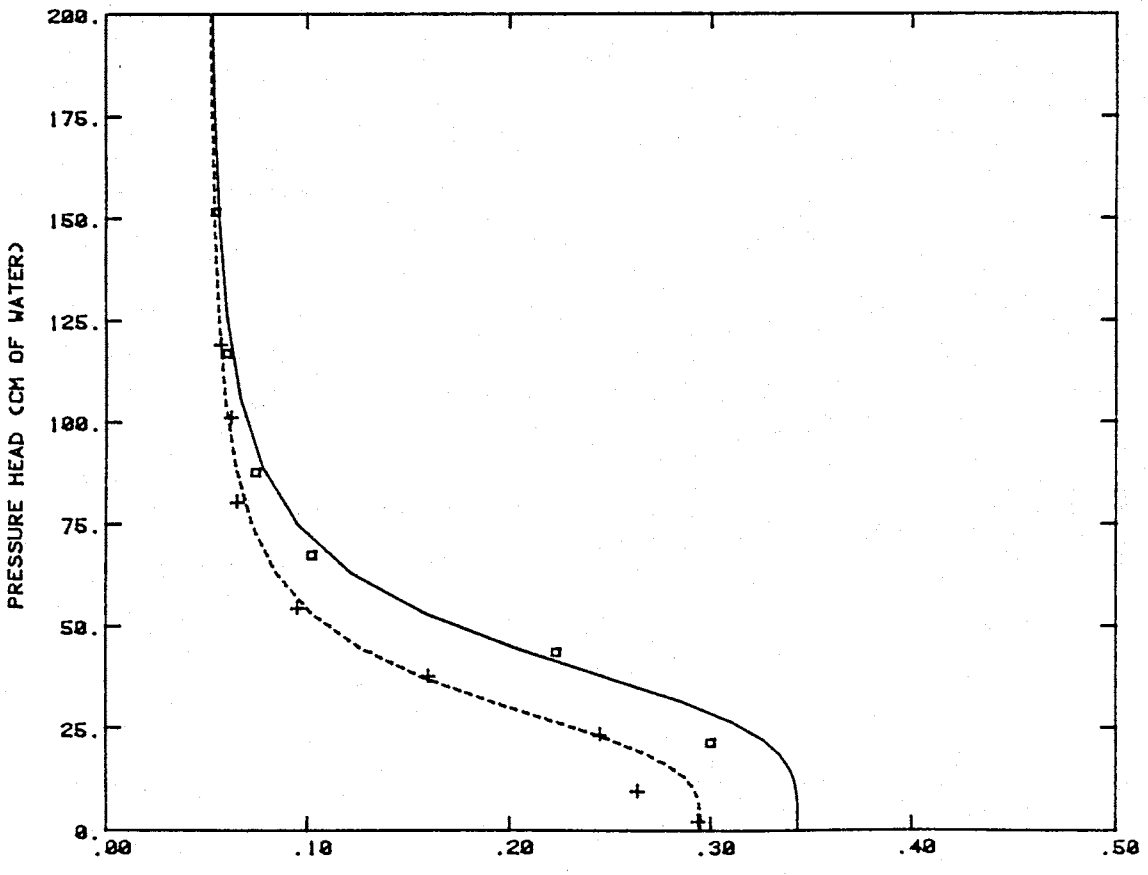

NORTH C, DEPTH = 152 CM

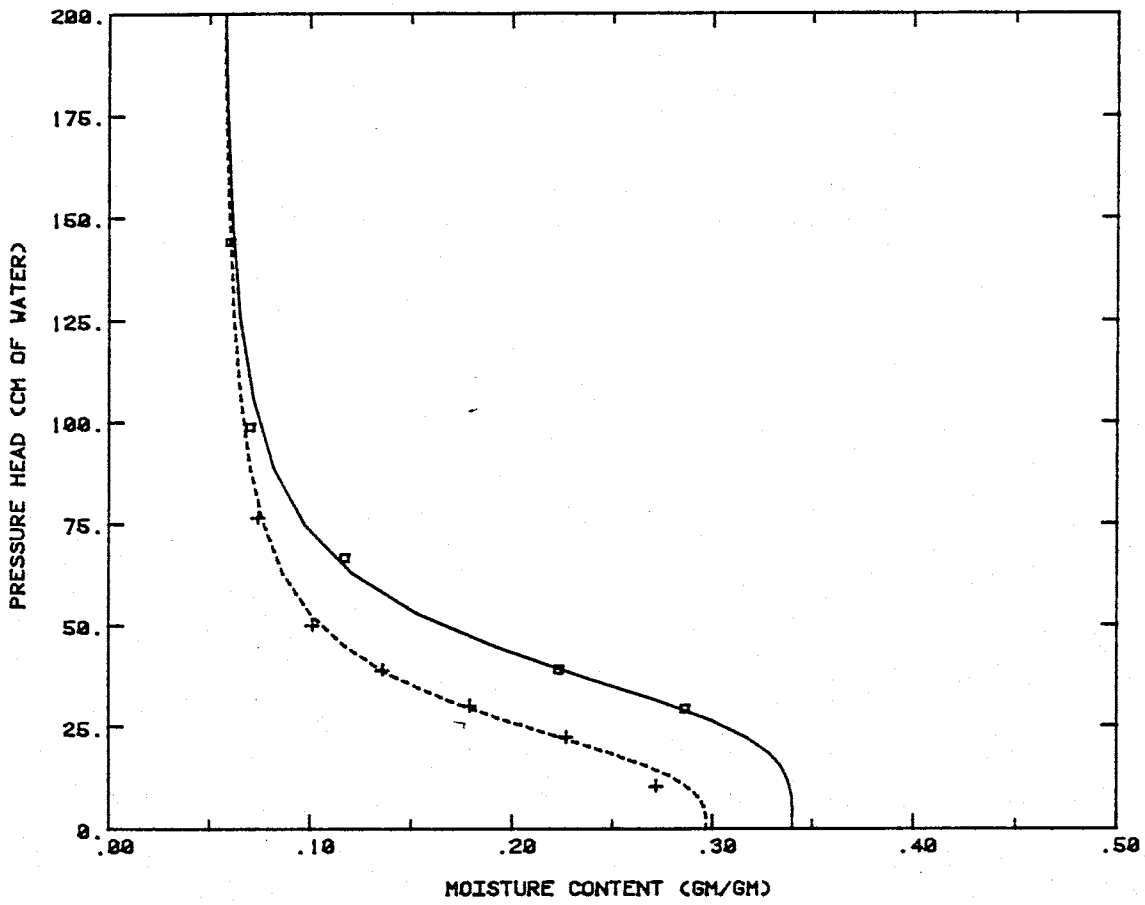

NORTH C, DEPTH = 215 CM

PRESSURE PLATE RESULTS
(Samples collected beneath plant canopy)

DEPTH (cm)	SATURATED MOISTURE CONTENT (%vol)	MOISTURE CONTENT 2 BARS (%vol)	MOISTURE CONTENT 15 BARS (%vol)
45	36.9	3.67	3.34
70	35.6	4.83	4.47
95	37.3	5.01	4.79
130	38.9	5.90	5.39
157	38.9	5.33	4.72
225	38.1	6.05	5.60
265	35.8	5.11	5.11
310	34.71	5.55	5.08
	ave = 37.03	ave = 5.09	ave = 4.87

SATURATED HYDRAULIC CONDUCTIVITY
Results of Constant Head Permeameter

LOCATION: NORTH B

SAMPLE #	DEPTH (CM)	KSAT (CM/S)
1B	35	6.48E-02
2B	58	3.57E-02
3B	97	9.96E-03
4B	130	2.90E-02
5B	157	8.95E-02
6B	202	1.54E-01
7B	257	4.49E-02

LOCATION: NORTH C

SAMPLE #	DEPTH (CM)	KSAT (CM/S)
1C	33	1.03E-02
2C	63	4.03E-03
3C	94	1.84E-02
4C	124	4.27E-03
5C	155	2.62E-02
7C	215	5.64E-02
9C	276	1.01E-02
10C	307	3.68E-02

```
C*************************************************************
C*                                                           *
C*       SOIL HYDRAULIC PROPERTIES:                          *
C*       NON-LINEAR LEAST-SQUARES ANALYSIS                   *
C*                                                           *
C*       --------------- INPUT INFORMATION ---------------   *
C*       CARDS 1,2,3: THREE INFORMATION CARDS                *
C*       CARD 4: MODEL NUMBER (MODE), NUMBER OF COEFFICIENTS (NP),*
C*               MAXIMUM NUMBER OF ITERATIONS (MIT), RATIO OF *
C*               COEFFICIENTS CRITERION (STOPCR), RESIDUAL MOISTU-*
C*               RE CONTENT (IF MODE=2) (WCR), SATURATED MOISTURE *
C*               CONTENT (WCS), CONDUCTIVITY AT SATURATION (SATK) *
C*               (3I10,4F10.0)                               *
C*       CARD 5: INITIAL ESTIMATES OF THE COEFFICIENTS (3F10.0)  *
C*       CARD 6: NAMES OF THE COEFFICIENTS; 3(A4,A2,4X)      *
C*       CARD 7, ETC: EXPERIMENTAL DATA: MOISTURE CONTENT AND *
C*               PRESSURE HEAD, RESPECTIVELY; (2F10.0)       *
C*       LAST CARD IS BLANK                                  *
C*                                                           *
C*       THIS SLIGHTLY MODIFIED VERSION WILL PROMPT THE USER *
C*       FOR NAMES OF THE "REL. K VS PRESSURE" AND           *
C*       "ABS. K VS PRESSURE" AND                            *
C*       "PRESSURE VS THETA" FILES THAT THIS PROGRAM GENERATES *
C*       FOR EASY PLOTTING.  RICH R.                         *
C*************************************************************

      DOUBLE PRECISION FLNI, FLNO, FLNM, flnf
      DIMENSION X(300),Y(300),R(300),F(300),DELZ(300,4),LSORT(300),
     1B(3),BI(6),E(3),P(3),PHI(3),Q(3),TB(3),A(3,3),D(3,3),
     1TITLE(20),TH(3)

      ----------
      TYPE 13
   3  FORMAT(1X,'INPUT FILE NAME: ',$)
      READ(5,9)flnf
      open (unit=1,access='seqin',file=flnf)
      TYPE 5
   5  FORMAT(1X, 'REL. K VS PRESSURE FILE NAME:',$)
      READ(5,9)FLNI
   9  FORMAT(A10)
      OPEN (UNIT=21, DEVICE='DSK', FILE=FLNI, ACCESS='SEQOUT')
      TYPE 11
  11  FORMAT(1X, 'ABS. K VS PRESSURE FILE NAME: ',$)
      READ(5,9)FLNM
      OPEN (UNIT=23, DEVICE='DSK', FILE=FLNM, ACCESS='SEQOUT')
      TYPE 7
   7  FORMAT(1X,'PRESSURE VS THETA FILE NAME:',$)
      READ(5,9)FLNO
      OPEN (UNIT=22, DEVICE='DSK', FILE=FLNO, ACCESS='SEQOUT')
      WRITE(3,1000)
      DO 2 I=1,3
      READ(1,1001) TITLE
   2  write(3,1002) TITLE
      write(3,1003)

      ----- READ INPUT PARAMETERS -----
      read(1,*) MODE,NP,MIT,STOPCR,WCR,WCS,SATK
```

```
      write(3,1005) MODE,NP,MIT,STOPCR,WCR,WCS,SATK

      ----- READ INITIAL ESTIMATES -----
       READ(1,1006)  (B(I),I=1,NP)
      READ(1,*)  (B(I),I=1,NP)

      ----- READ COEFFICIENTS NAMES -----
      NBI=2*NP
      READ(1,1007)  (BI(I),I=1,NBI)

      ----- READ AND WRITE EXPERIMENTAL DATA -----
      write(3,1008)
      I=0
    4 I=I+1
      READ(1,*,END=6) Y(I),X(I)
      write(3,1011) I,X(I),Y(I)
        GOTO 4
       IF(X(I).EQ.0.) GO TO 6
       GO TO 4
    6 NOB=I-1

      ----------
      DO 8 I=1,NP
    8 TH(I)=B(I)
      IF((NP-2)*(NP-3)) 12,14,12
   12 write(3,1016)
      GO TO 142
   14 GA=0.02
      CALL MODEL(TH,F,NOB,X,WCS,MODE,NP,WCR)
      SSQ=0.
      DO 32 I=1,NOB
      R(I)=Y(I)-F(I)
   32 SSQ=SSQ+R(I)*R(I)
      NIT=0
      write(3,1030)
      IF(MODE.EQ.2) write(3,1026) NIT,WCR,B(1),B(2),SSQ,MODE
      IF(MODE.NE.2) write(3,1026) NIT,B(1),B(2),B(3),SSQ,MODE

      ----- BEGIN OF ITERATION -----
   34 NIT=NIT+1
      GA=0.1*GA
      DO 38 J=1,NP
      TEMP=TH(J)
      TH(J)=1.01*TH(J)
      Q(J)=0
      CALL MODEL(TH,DELZ(1,J),NOB,X,WCS,MODE,NP,WCR)
      DO 36 I=1,NOB
      DELZ(I,J)=DELZ(I,J)-F(I)
   36 Q(J)=Q(J)+DELZ(I,J)*R(I)
      Q(J)=100.*Q(J)/TH(J)

      ----- STEEPEST DESCENT -----
   38 TH(J)=TEMP
      DO 44 I=1,NP
      DO 42 J=1,I
      SUM=0
      DO 40 K=1,NOB
   40 SUM=SUM+DELZ(K,I)*DELZ(K,J)
      D(I,J)=10000.*SUM/(TH(I)*TH(J))
   42 D(J,I)=D(I,J)
```

```
      ----- D = MOMENT MATRIX -----
   44 E(I)=SQRT(D(I,I))
   50 DO 52 I=1,NP
      DO 52 J=1,NP
   52 A(I,J)=D(I,J)/(E(I)*E(J))

      ----- A IS THE SCALED MOMENT MATRIX -----
      DO 54 I=1,NP
      P(I)=Q(I)/E(I)
      PHI(I)=P(I)
   54 A(I,I)=A(I,I)+GA
      CALL MATINV(A,NP,P)

      ----- P/E IS THE CORRECTION VECTOR -----
      STEP=1.0
   56 DO 58 I=1,NP
   58 TB(I)=P(I)*STEP/E(I)+TH(I)
      DO 62 I=1,NP
      IF(TH(I)*TB(I))66,66,62
   62 CONTINUE
      SUMB=0.0
      CALL MODEL(TB,F,NOB,X,WCS,MODE,NP,WCR)
      DO 64 I=1,NOB
      R(I)=Y(I)-F(I)
   64 SUMB=SUMB+R(I)*R(I)
   66 SUM1=0.0
      SUM2=0.0
      SUM3=0.0
      DO 68 I=1,NP
      SUM1=SUM1+P(I)*PHI(I)
      SUM2=SUM2+P(I)*P(I)
   68 SUM3=SUM3+PHI(I)*PHI(I)
      ANGLE=57.29578*ACOS(SUM1/SQRT(SUM2*SUM3))

      ----------
      DO 72 I=1,NP
      IF(TH(I)*TB(I))74,74,72
   72 CONTINUE
      IF(SUMB/SSQ-1.0)80,80,74
   74 IF(ANGLE-30.0)76,76,78
   76 STEP=STEP/2.0
      GO TO 56
   78 GA=10.*GA
      GO TO 50

      ----- PRINT COEFFICIENTS AFTER EACH ITERATION -----
   80 CONTINUE
      DO 82 I=1,NP
   82 TH(I)=TB(I)
      IF(MODE.EQ.2) write(3,1026) NIT,WCR,TH(1),TH(2),SUMB,MODE
      IF(MODE.NE.2) write(3,1026) NIT,TH(1),TH(2),TH(3),SUMB,MODE
      DO 92 I=1,NP
      IF(ABS(P(I)*STEP/E(I))/(1.0E-20+ABS(TH(I)))-STOPCR) 92,92,94
   92 CONTINUE
      GO TO 96
   94 SSQ=SUMB
      IF(NIT-MIT) 34,34,96

      ----- END OF ITERATION LOOP -----
```

```
6 IDF=NOB-NP
  CALL MATINV(D,NP,P)

  ----- WRITE CORRELATION MATRIX -----
  DO 98 I=1,NP
8 E(I)=SQRT(D(I,I))
  write(3,1044) (I,I=1,NP)
  DO 102 I=1,NP
  DO 100 J=1,I
0 A(J,I)=D(J,I)/(E(I)*E(J))
2 write(3,1048) I,(A(J,I),J=1,I)

  ----- CALCULATE 95% CONFIDENCE INTERVAL -----
  RMS=SUMB/FLOAT(IDF)
  SDEV=SQRT(RMS)
  write(3,1052)
  TVAR=TTEST(IDF)
  DO 108 I=1,NP
  SECOEF= E(I)*SDEV
  TVALUE= TH(I)/SECOEF
  TSEC=TVAR*SECOEF
  TMCOE=TH(I)-TSEC
  TPCOE=TH(I)+TSEC
  K=2*I
  J=K-1
8 write(3,1058) BI(J),BI(K),TH(I),SECOEF,TVALUE,TMCOE,TPCOE

  ----- PREPARE FINAL OUTPUT -----
  LSORT(1)=1
  DO 116 J=2,NOB
  TEMP=R(J)
  K=J-1
  DO 111 L=1,K
  LL=LSORT(L)
  IF(TEMP-R(LL)) 112,112,111
1 CONTINUE
  LSORT(J)=J
  GO TO 116
2 KK=J
3 KK=KK-1
  LSORT(KK+1)=LSORT(KK)
  IF(KK-L) 115,115,113
5 LSORT(L)=J
6 CONTINUE
  write(3,1066)
  DO 118 I=1,NOB
  J=LSORT(NOB+1-I)
8 write(3,1068) I,X(I),Y(I),F(I),R(I),J,X(J),Y(J),F(J),R(J)

  ----- WRITE SOIL HYDRAULIC PROPERTIES -----
  write(3,1069)
  PRESS=1.18850
  RN1=0.0
  RKLN=1.0
  write(3,1072) RN1,WCS,RKLN,SATK
  WRITE(21,1073)RN1, RKLN
  WRITE(22,1074)WCS, RN1
  WRITE(23,1073)RN1, SATK
  DO 140 I=1,75
  IF(RKLN.LT.(-16.)) GO TO 142
```

```
      PRESS=1.18850*PRESS
      IF(MODE-2) 120,122,120
 120  WCR=TH(1)
      ALPHA=TH(2)
      RN=TH(3)
      GO TO 124
 122  ALPHA=TH(1)
      RN=TH(2)
 124  RM=1.-1./RN
      IF(MODE.EQ.3) RM=1.-2./RN
      RN1=RM*RN
      RWC=1./(1.+(ALPHA*PRESS)**RN)**RM
      WC=WCR+(WCS-WCR)*RWC
      TERM=1.-RWC*(ALPHA*PRESS)**RN1
      IF(RWC.LT.0.06) TERM=RM*RWC**(1./RM)
      IF(MODE.EQ.3) RK=RWC*RWC*TERM
      IF(MODE.NE.3) RK=SQRT(RWC)*TERM*TERM
      TERM=ALPHA*RN1*(WCS-WCR)*RWC*RWC**(1./RM)*(ALPHA*PRESS)**(RN-1.)
      AK=SATK*RK
      DIFFUS=AK/TERM
      PRLN=ALOG10(PRESS)
      AKLN=ALOG10(AK)
      RKLN=ALOG10(RK)
      DIFLN=ALOG10(DIFFUS)
      WRITE(21,1073)PRESS, RK
      WRITE(22,1074)WC, PRESS
      WRITE(23,1073)PRESS, AK
 150  write(3,1070) PRESS,PRLN,WC,RK,RKLN,AK,AKLN,DIFFUS,DIFLN
 152  CONTINUE

      ----- END OF PROBLEM -----
 1000 FORMAT(1H1,10X,82(1H*)/11X,1H*,80X,1H*/11X,1H*, 9X,'NON-LINEAR LEA
     1ST SQUARES ANALYSIS',38X,1H*/11X,1H*,80X,1H*)
 1001 FORMAT(20A4)
 1002 FORMAT(11X,1H*,20A4,1H*)
 1003 FORMAT(11X,1H*,80X,1H*/11X,82(1H*))
 1004 FORMAT(3I10,5F10.0)
 1005 FORMAT(//11X,'INPUT PARAMETERS'/11X,16(1H=)/
     211X,'MODEL NUMBER.....',I3/
     311X,'NUMBER OF COEFFICIENTS.....',I3/
     411X,'MAXIMUM NUMBER OF ITERATIONS.....',I3/
     511X,'RATIO OF COEFFICIENTS CRITERION.....',F10.4/
     611X,'RESIDUAL MOISTURE CONTENT (FOR MODEL 2).....',F10.4/
     711X,'SATURATED MOISTURE CONTENT.....',F10.4/
     811X,'SATURATED HYDRAULIC CONDUCTIVITY.....',F10.4)
 1006 FORMAT(4F10.0)
 1007 FORMAT(4(A4,A2,4X))
 1008 FORMAT(//11X,'OBSERVED DATA',/11X,13(1H=)/11X,'OBS. NO.',4X,'PRESS
     1URE HEAD',2X,'MOISTURE CONTENT')
 1011 FORMAT(11X,I5,5X,F12.2,4X,F12.4)
 1016 FORMAT(//5X,10(1H*),' ERROR: INCORRECT NUMBER OF COEFFICIENTS')
 1026 FORMAT(15X,I2,10X,F8.4,3X,F10.6,2X,F10.4,5X,F12.7,4X,I4)
 1030 FORMAT(1H1,10X,'ITERATION NO',8X,'WCR',8X,'ALPHA',10X,'N',13X,'SSQ
     1',8X,'MODEL')
 1034 FORMAT(//11X,'CORRELATION MATRIX'/11X,18(1H=)/14X,10(4X,I2,5X))
 1038 FORMAT(11X,I3,10(2X,F7.4,2X))
 1052 FORMAT(//11X,'NON-LINEAR LEAST-SQUARES ANALYSIS: FINAL RESULTS'/
     111X,48(1H=)/64X,'95% CONFIDENCE LIMITS'/11X,'VARIABLE',8X,'VALUE',
     27X,'S.E.COEFF.',3X,'T-VALUE',6X,'LOWER',10X,'UPPER')
 1058 FORMAT(13X,A4,A2,4X,F10.5,5X,F9.4,5X,F6.2,4X,F9.4,5X,F9.4)
```

```
56 FORMAT(//10X,8(1H-),'ORDERED BY COMPUTER INPUT', 8(1H-), 7X,10(1H-
  1),'ORDERED BY RESIDUALS',10(1H-)/26X,'MOISTURE CONTENT',3X,'RESI-'
  1,24X,'MOISTURE CONTENT',3X,'RESI-'/10X,'NO',3X,'PRESSURE',5X,'OBS'
  2,4X,'FITTED',4X,'DUAL', 9X,'NO',3X,'PRESSURE',5X,'OBS',4X,'FITTED'
  3,4X,'DUAL')
58 FORMAT(10X,I2,F10.2,1X,3F9.4,8X,I2,E10.2,1X,3F9.4)
59 FORMAT(1H1,10X,'PRESSURE',4X,'LOG P',6X,'WC',7X,'REL K',5X,'LOG RK
  1',6X,'ABS K',4X,'LOG KA',5X,'DIFFUS',5X,'LOG D')
70 FORMAT(10X,E10.3,F8.3,F10.4,3(E13.3,F8.3))
72 FORMAT(10X,E10.3,8X,F10.4,E13.3,8X,E13.3)
73 FORMAT(1X,E10.3,1X,E10.3)
74 FORMAT(1X,F6.4,1X,E10.3)
   STOP
   END
   SUBROUTINE MODEL(B,FY,NOB,X,WCS,MODE,NP,WCR)
   DIMENSION B(3),FY(40),X(40)

   MODE=1 : MUALEM THEORY WITH THREE COEFFICIENTS
   MODE=2 : MUALEM THEORY WITH TWO COEFFICIENTS
   MODE=3 : BURDINE THEORY WITH THREE COEFFICIENTS

   IF(MODE-2) 10,20,30
10 CONTINUE
   DO 12 J=1,NOB
12 FY(J)=B(1)+(WCS-B(1))/(1.+(B(2)*X(J))**B(3))**(1.-1./B(3))
   RETURN
20 CONTINUE
   DO 22 J=1,NOB
22 FY(J)=WCR+(WCS-WCR)/(1.+(B(1)*X(J))**B(2))**(1.-1./B(2))
   RETURN
30 CONTINUE
   DO 32 J=1,NOB
32 FY(J)=B(1)+(WCS-B(1))/(1.+(B(2)*X(J))**B(3))**(1.-2./B(3))
   RETURN
   END
   FUNCTION TTEST(IDF)
   DIMENSION TA(30)
   DATA TA/12.706,4.303,3.182,2.776,2.571,2.447,2.365,2.306,2.262,
  12.228,2.201,2.179,2.160,2.145,2.131,2.120,2.110,2.101,2.093,2.086,
  22.080,2.074,2.069,2.064,2.060,2.056,2.052,2.048,2.045,2.042/
   IF(IDF-30)10,10,11
10 TTEST=TA(IDF)
   RETURN
11 IF(IDF-120)12,12,13
13 TTEST=1.96
   RETURN
12 IF(IDF-40)14,14,15
14 TTEST=2.042-0.021*FLOAT(IDF-30)/10.0
   RETURN
15 IF(IDF-60)16,16,17
16 TTEST=2.021-0.021*FLOAT(IDF-40)/20.0
   RETURN
17 TTEST=2.000-0.002*FLOAT(IDF-60)/60.0
   RETURN
   END
   SUBROUTINE MATINV(A,NP,B)
   DIMENSION A(3,3),B(3),INDEX(3,2)
   DO 2 J=1,4
 2 INDEX(J,1)=0
   I=0
```

```
 4 AMAX=-1.0
   DO 10 J=1,NP
   IF(INDEX(J,1)) 10,6,10
 6 DO 10 K=1,NP
   IF(INDEX(K,1)) 10,8,10
 8 P=ABS(A(J,K))
   IF(P.LE.AMAX) GO TO 10
   IR=J
   IC=K
   AMAX=P
.0 CONTINUE
   IF(AMAX) 30,30,14
.4 INDEX(IC,1)=IR
   IF(IR.EQ.IC) GO TO 18
   DO 16 L=1,NP
   P=A(IR,L)
   A(IR,L)=A(IC,L)
.6 A(IC,L)=P
   P=B(IR)
   B(IR)=B(IC)
   B(IC)=P
   I=I+1
   INDEX(I,2)=IC
.8 P=1./A(IC,IC)
   A(IC,IC)=1.0
   DO 20 L=1,NP
:0 A(IC,L)=A(IC,L)*P
   B(IC)=B(IC)*P
   DO 24 K=1,NP
   IF(K.EQ.IC) GO TO 24
   P=A(K,IC)
   A(K,IC)=0.0
   DO 22 L=1,NP
:2 A(K,L)=A(K,L)-A(IC,L)*P
   B(K)=B(K)-B(IC)*P
:4 CONTINUE
   GO TO 4
:6 IC=INDEX(I,2)
   IR=INDEX(IC,1)
   DO 28 K=1,NP
   P=A(K,IR)
   A(K,IR)=A(K,IC)
:8 A(K,IC)=P
   I=I-1
.0 IF(I) 26,32,26
.2 RETURN
   END
```

```
*****************************************************************************
*                                                                           *
*          NON-LINEAR LEAST SQUARES ANALYSIS                                *
*                                                                           *
*SEVILLETA DUNE SANDS                                                       *
*CUMULATIVE LABORATORY DATA                                                 *
*DRYING CURVE                                                               *
*                                                                           *
*****************************************************************************
```

INPUT PARAMETERS
==========

MODEL NUMBER	2
NUMBER OF COEFFICIENTS	2
MAXIMUM NUMBER OF ITERATIONS	20
RATIO OF COEFFICIENTS CRITERION	0.0001
RESIDUAL MOISTURE CONTENT (FOR MODEL 2)	0.0490
SATURATED MOISTURE CONTENT	0.3700
SATURATED HYDRAULIC CONDUCTIVITY	0.0150

OBSERVED DATA
==========

OBS. NO.	PRESSURE HEAD	MOISTURE CONTENT
1	7.50	0.4000
2	21.50	0.3900
3	48.60	0.2830
4	70.00	0.1320
5	100.00	0.1100
6	130.20	0.1070
7	150.00	0.1060
8	3.00	0.3415
9	17.00	0.3025
10	40.40	0.2255
11	60.70	0.0945
12	94.50	0.0475
13	150.00	0.0455
14	3.00	0.4000
15	18.50	0.3590
16	39.30	0.2850
17	53.70	0.1950
18	90.00	0.1310
19	148.50	0.1140
20	4.00	0.3584
21	17.30	0.3204
22	36.70	0.2464
23	49.00	0.1374
24	85.40	0.0704
25	113.50	0.0654
26	156.00	0.0604
27	103.70	0.0614
28	77.00	0.0654
29	54.60	0.0754
30	43.20	0.1024
31	33.60	0.1494
32	24.30	0.2364
33	13.40	0.2824
34	2.30	0.2974
35	28.30	0.3946

36	42.00	0.3046
37	72.50	0.1826
38	105.50	0.0636
39	155.00	0.0546
40	29.40	0.2859
41	39.00	0.2230
42	66.50	0.1170
43	98.80	0.0700
44	144.00	0.0600
45	21.50	0.2998
46	43.60	0.2230
47	67.30	0.1020
48	87.50	0.0740
49	116.70	0.0600
50	151.50	0.0540
51	3.50	0.2900
52	18.00	0.2670
53	34.50	0.2560
54	48.00	0.1770
55	61.40	0.0720
56	80.30	0.0300
57	5.00	0.3800
58	15.50	0.3270
59	37.00	0.2450
60	46.50	0.1800
61	66.00	0.1050
62	89.30	0.0780
63	122.00	0.0690
64	151.50	0.0660
65	14.00	0.3120
66	23.00	0.3050
67	37.50	0.2110
68	39.00	0.2030
69	62.00	0.1600
70	90.00	0.1390
71	118.70	0.1320
72	150.00	0.1280
73	4.00	0.3730
74	31.70	0.3544
75	39.50	0.2820
76	57.00	0.1310
77	81.00	0.0980
78	131.70	0.0944
79	149.50	0.0894
80	2000.00	0.0510

ITERATION NO	WCR	ALPHA	N	SSQ	MODEL
0	0.0490	0.002000	2.5000	3.5469543	2
1	0.0490	0.003551	1.6260	3.1565135	2
2	0.0490	0.007142	1.2707	2.9055828	2
3	0.0490	0.046843	1.5994	0.4417107	2
4	0.0490	0.024658	2.1053	0.3946205	2
5	0.0490	0.033100	2.4992	0.1745554	2
6	0.0490	0.029341	2.8606	0.1665000	2
7	0.0490	0.029320	2.9925	0.1648466	2
8	0.0490	0.029161	3.0201	0.1648182	2
9	0.0490	0.029121	3.0267	0.1648170	2
10	0.0490	0.029119	3.0269	0.1648170	2

CORRELATION MATRIX

	1	2
1	1.0000	
2	-0.7588	1.0000

NON-LINEAR LEAST-SQUARES ANALYSIS: FINAL RESULTS

VARIABLE	VALUE	S.E.COEFF.	T-VALUE	95% CONFIDENCE LIMITS LOWER	UPPER
ALPHA	0.02912	0.0018	15.92	0.0255	0.0328
N	3.02687	0.2616	11.57	2.5038	3.5499

ORDERED BY COMPUTER INPUT

NO	PRESSURE	MOISTURE CONTENT OBS	FITTED	RESIDUAL
1	7.50	0.4000	0.3679	0.0321
2	21.50	0.3900	0.3266	0.0634
3	48.60	0.2830	0.1789	0.1041
4	70.00	0.1320	0.1194	0.0126
5	100.00	0.1100	0.0848	0.0252
6	130.20	0.1070	0.0703	0.0367
7	150.00	0.1060	0.0650	0.0410
8	3.00	0.3415	0.3699	-0.0284
9	17.00	0.3025	0.3467	-0.0442
10	40.10	0.2255	0.2168	0.0087
11	60.70	0.0945	0.1397	-0.0452
12	94.50	0.0475	0.0890	-0.0415
13	150.00	0.0455	0.0650	-0.0195
14	3.00	0.4000	0.3699	0.0301
15	18.50	0.3590	0.3407	0.0183
16	39.30	0.2850	0.2226	0.0624
17	53.70	0.1950	0.1602	0.0348
18	90.00	0.1310	0.0930	0.0380
19	148.50	0.1140	0.0654	0.0486
20	4.00	0.3584	0.3697	-0.0113
21	17.30	0.3264	0.3456	-0.0192
22	36.70	0.2464	0.2370	0.0094
23	49.00	0.1374	0.1773	-0.0399
24	85.40	0.0704	0.0976	-0.0272
25	113.50	0.0654	0.0770	-0.0116
26	156.00	0.0604	0.0638	-0.0034
27	103.70	0.0614	0.0824	-0.0210
28	77.00	0.0654	0.1081	-0.0427

ORDERED BY RESIDUALS

NO	PRESSURE	MOISTURE CONTENT OBS	FITTED	RESIDUAL
35	28.30	0.3946	0.2877	0.1069
3	48.60	0.2830	0.1789	0.1041
36	42.00	0.3046	0.2086	0.0960
74	31.70	0.3544	0.2668	0.0876
37	72.50	0.1826	0.1151	0.0675
2	21.50	0.3900	0.3266	0.0634
72	150.00	0.1280	0.0650	0.0630
16	39.30	0.2850	0.2226	0.0624
75	39.50	0.2820	0.2215	0.0605
71	118.70	0.1320	0.0746	0.0574
19	148.50	0.1140	0.0654	0.0486
70	90.00	0.1390	0.0930	0.0460
7	150.00	0.1060	0.0650	0.0410
18	90.00	0.1310	0.0930	0.0380
6	130.20	0.1070	0.0703	0.0367
17	53.70	0.1950	0.1602	0.0348
1	7.50	0.4000	0.3679	0.0321
14	3.00	0.4000	0.3699	0.0301
5	100.00	0.1100	0.0848	0.0252
78	131.70	0.0944	0.0698	0.0246
79	149.50	0.0894	0.0652	0.0242
69	62.00	0.1600	0.1364	0.0236
46	43.60	0.2230	0.2008	0.0222
15	18.50	0.3590	0.3407	0.0183
4	70.00	0.1320	0.1194	0.0126
57	5.00	0.3800	0.3694	0.0106
59	37.00	0.2450	0.2353	0.0097
22	36.70	0.2464	0.2370	0.0094

29	54.60	0.0754	0.1573	-0.0819
30	43.20	0.1024	0.2027	-0.1003
31	33.60	0.1494	0.2552	-0.1058
32	24.30	0.2364	0.3114	-0.0750
33	13.40	0.2824	0.3581	-0.0757
34	2.30	0.2974	0.3699	-0.0725
35	28.30	0.3946	0.2877	0.1069
36	42.00	0.3016	0.2086	0.0960
37	72.50	0.1826	0.1151	0.0675
38	105.50	0.0636	0.0813	-0.0177
39	155.00	0.0516	0.0640	-0.0094
40	29.40	0.2859	0.2809	0.0050
41	39.00	0.2230	0.2242	-0.0012
42	66.50	0.1170	0.1262	-0.0092
43	98.80	0.0700	0.0857	-0.0157
44	141.00	0.0600	0.0664	-0.0064
45	21.50	0.2998	0.3266	-0.0268
46	43.60	0.2230	0.2008	0.0222
47	67.30	0.1020	0.1246	-0.0226
48	87.50	0.0740	0.0954	-0.0214
49	116.70	0.0600	0.0755	-0.0155
50	151.50	0.0540	0.0647	-0.0107
51	3.50	0.2900	0.3698	-0.0798
52	18.00	0.2670	0.3428	-0.0758
53	34.50	0.2560	0.2499	0.0061
54	48.00	0.1770	0.1813	-0.0043
55	61.40	0.0720	0.1379	-0.0659
56	80.30	0.0300	0.1036	-0.0736
57	5.00	0.3800	0.3694	0.0106
58	15.50	0.3270	0.3520	-0.0250
59	37.00	0.2450	0.2353	0.0097
60	46.50	0.1800	0.1877	-0.0077
61	66.00	0.1050	0.1273	-0.0223
62	89.30	0.0780	0.0936	-0.0156
63	122.00	0.0690	0.0732	-0.0042
64	151.50	0.0660	0.0647	0.0013
65	14.00	0.3120	0.3565	-0.0445
66	23.00	0.3050	0.3187	-0.0137
67	37.50	0.2110	0.2325	-0.0215
68	39.00	0.2030	0.2242	-0.0212
69	62.00	0.1600	0.1364	0.0236
70	90.00	0.1390	0.0930	0.0460
71	118.70	0.1320	0.0746	0.0574
72	150.00	0.1230	0.0650	0.0630
73	4.00	0.3730	0.3697	0.0033
74	31.70	0.3514	0.2668	0.0876
75	39.50	0.2820	0.2215	0.0605
76	57.00	0.1310	0.1498	-0.0188
77	81.00	0.0980	0.1027	-0.0047
78	131.70	0.0944	0.0698	0.0246
79	149.50	0.0894	0.0652	0.0242
80	2000.00	0.0510	0.0491	0.0019

10	40.10	0.2255	0.2168	0.0087
53	34.50	0.2560	0.2499	0.0061
40	29.40	0.2859	0.2809	0.0050
73	4.00	0.3730	0.3697	0.0033
80	2000.00	0.0510	0.0491	0.0019
64	151.50	0.0660	0.0647	0.0013
41	39.00	0.2230	0.2242	-0.0012
26	156.00	0.0604	0.0638	-0.0034
63	122.00	0.0690	0.0732	-0.0042
54	48.00	0.1770	0.1813	-0.0043
77	81.00	0.0980	0.1027	-0.0047
44	141.00	0.0600	0.0664	-0.0064
60	16.50	0.1800	0.1877	-0.0077
42	66.50	0.1170	0.1262	-0.0092
39	155.00	0.0546	0.0640	-0.0094
50	151.50	0.0540	0.0647	-0.0107
20	4.00	0.3584	0.3697	-0.0113
25	113.50	0.0654	0.0770	-0.0116
66	23.00	0.3050	0.3187	-0.0137
49	116.70	0.0600	0.0755	-0.0155
62	89.30	0.0780	0.0936	-0.0156
43	98.80	0.0700	0.0857	-0.0157
38	105.50	0.0636	0.0813	-0.0177
76	57.00	0.1310	0.1498	-0.0188
21	17.30	0.3264	0.3456	-0.0192
13	150.00	0.0455	0.0650	-0.0195
27	103.70	0.0614	0.0824	-0.0210
68	39.00	0.2030	0.2242	-0.0212
48	87.50	0.0740	0.0954	-0.0214
67	37.50	0.2110	0.2325	-0.0215
61	66.00	0.1050	0.1273	-0.0223
47	67.30	0.1020	0.1246	-0.0226
58	15.50	0.3270	0.3520	-0.0250
45	21.50	0.2998	0.3266	-0.0268
24	85.40	0.0704	0.0976	-0.0272
8	3.00	0.3415	0.3699	-0.0284
23	49.00	0.1374	0.1773	-0.0399
12	94.50	0.0475	0.0890	-0.0415
28	77.00	0.0654	0.1081	-0.0427
9	17.00	0.3025	0.3467	-0.0442
65	14.00	0.3120	0.3565	-0.0445
11	60.70	0.0945	0.1397	-0.0452
55	61.40	0.0720	0.1379	-0.0659
34	2.30	0.2974	0.3699	-0.0725
56	80.30	0.0300	0.1036	-0.0736
32	24.30	0.2364	0.3114	-0.0750
33	13.40	0.2824	0.3581	-0.0757
52	18.00	0.2670	0.3428	-0.0758
51	3.50	0.2900	0.3698	-0.0798
29	54.60	0.0754	0.1573	-0.0819
30	43.20	0.1024	0.2027	-0.1003
31	33.60	0.1494	0.2552	-0.1058

PRESSURE	LOG P	WC	REL K	LOG RK	ABS K	LOG KA	DIFFUS	LOG D
0.000E+00		0.3700	0.100E+01		0.150E-01			
0.141E+01	0.150	0.3700	0.997E+00	-0.001	0.150E-01	-1.825	0.508E+03	2.706
0.168E+01	0.225	0.3700	0.996E+00	-0.002	0.149E-01	-1.826	0.358E+03	2.554
0.200E+01	0.300	0.3700	0.994E+00	-0.003	0.149E-01	-1.827	0.252E+03	2.401
0.237E+01	0.375	0.3699	0.991E+00	-0.004	0.149E-01	-1.828	0.177E+03	2.248
0.282E+01	0.450	0.3699	0.987E+00	-0.006	0.148E-01	-1.829	0.124E+03	2.094
0.335E+01	0.525	0.3698	0.982E+00	-0.009	0.147E-01	-1.832	0.871E+02	1.940
0.398E+01	0.600	0.3697	0.974E+00	-0.011	0.146E-01	-1.835	0.610E+02	1.785
0.473E+01	0.675	0.3695	0.964E+00	-0.016	0.145E-01	-1.840	0.426E+02	1.629
0.562E+01	0.750	0.3691	0.948E+00	-0.023	0.142E-01	-1.847	0.296E+02	1.471
0.668E+01	0.825	0.3685	0.927E+00	-0.033	0.139E-01	-1.857	0.205E+02	1.311
0.794E+01	0.900	0.3675	0.897E+00	-0.047	0.135E-01	-1.871	0.141E+02	1.149
0.941E+01	0.975	0.3658	0.855E+00	-0.068	0.128E-01	-1.892	0.959E+01	0.982
0.112E+02	1.050	0.3629	0.799E+00	-0.098	0.120E-01	-1.922	0.645E+01	0.810
0.133E+02	1.125	0.3583	0.723E+00	-0.141	0.108E-01	-1.965	0.427E+01	0.631
0.158E+02	1.200	0.3508	0.627E+00	-0.203	0.940E-02	-2.027	0.277E+01	0.443
0.188E+02	1.275	0.3392	0.510E+00	-0.292	0.765E-02	-2.116	0.175E+01	0.244
0.224E+02	1.350	0.3220	0.381E+00	-0.419	0.571E-02	-2.243	0.108E+01	0.032
0.266E+02	1.425	0.2979	0.255E+00	-0.594	0.382E-02	-2.418	0.637E+00	-0.196
0.316E+02	1.500	0.2673	0.149E+00	-0.827	0.223E-02	-2.651	0.364E+00	-0.439
0.376E+02	1.575	0.2320	0.751E-01	-1.124	0.113E-02	-2.948	0.201E+00	-0.697
0.447E+02	1.650	0.1958	0.330E-01	-1.482	0.494E-03	-3.306	0.108E+00	-0.968
0.531E+02	1.725	0.1623	0.128E-01	-1.893	0.192E-03	-3.717	0.563E-01	-1.250
0.631E+02	1.800	0.1338	0.453E-02	-2.344	0.680E-04	-4.168	0.289E-01	-1.539
0.750E+02	1.875	0.1111	0.150E-02	-2.824	0.225E-04	-4.648	0.147E-01	-1.833
0.891E+02	1.950	0.0938	0.476E-03	-3.323	0.714E-05	-5.146	0.740E-02	-2.131
0.106E+03	2.025	0.0810	0.147E-03	-3.834	0.220E-05	-5.658	0.371E-02	-2.431
0.126E+03	2.100	0.0718	0.444E-04	-4.352	0.667E-06	-6.176	0.185E-02	-2.732
0.150E+03	2.175	0.0651	0.133E-04	-4.877	0.199E-06	-6.701	0.922E-03	-3.035
0.178E+03	2.250	0.0604	0.396E-05	-5.402	0.594E-07	-7.226	0.460E-03	-3.337
0.211E+03	2.325	0.0571	0.118E-05	-5.930	0.176E-07	-7.753	0.229E-03	-3.639
0.251E+03	2.400	0.0547	0.348E-06	-6.458	0.523E-08	-8.282	0.114E-03	-3.942
0.299E+03	2.475	0.0530	0.103E-06	-6.987	0.155E-08	-8.811	0.569E-04	-4.245
0.355E+03	2.550	0.0518	0.305E-07	-7.516	0.457E-09	-9.340	0.283E-04	-4.547
0.422E+03	2.625	0.0510	0.899E-08	-8.046	0.135E-09	-9.870	0.141E-04	-4.850
0.501E+03	2.700	0.0504	0.266E-08	-8.576	0.398E-10	-10.400	0.702E-05	-5.153
0.596E+03	2.775	0.0500	0.784E-09	-9.106	0.118E-10	-10.930	0.350E-05	-5.456
0.708E+03	2.850	0.0497	0.231E-09	-9.636	0.347E-11	-11.460	0.174E-05	-5.759
0.841E+03	2.925	0.0495	0.683E-10	-10.166	0.102E-11	-11.990	0.866E-06	-6.062
0.100E+04	3.000	0.0493	0.201E-10	-10.696	0.302E-12	-12.520	0.431E-06	-6.365
0.119E+04	3.075	0.0492	0.595E-11	-11.226	0.892E-13	-13.050	0.215E-06	-6.668
0.141E+04	3.150	0.0492	0.175E-11	-11.756	0.263E-13	-13.580	0.107E-06	-6.971
0.168E+04	3.225	0.0491	0.518E-12	-12.286	0.777E-14	-14.110	0.532E-07	-7.274
0.200E+04	3.300	0.0491	0.153E-12	-12.816	0.229E-14	-14.640	0.265E-07	-7.577
0.237E+04	3.375	0.0491	0.451E-13	-13.346	0.676E-15	-15.170	0.132E-07	-7.880
0.282E+04	3.450	0.0490	0.133E-13	-13.876	0.200E-15	-15.700	0.656E-08	-8.183
0.335E+04	3.525	0.0490	0.393E-14	-14.406	0.589E-16	-16.230	0.326E-08	-8.487
0.398E+04	3.600	0.0490	0.116E-14	-14.936	0.174E-16	-16.760	0.162E-08	-8.790
0.473E+04	3.675	0.0490	0.342E-15	-15.466	0.513E-17	-17.290	0.808E-09	-9.093
0.562E+04	3.750	0.0490	0.101E-15	-15.996	0.151E-17	-17.820	0.402E-09	-9.396
0.668E+04	3.825	0.0490	0.298E-16	-16.526	0.447E-18	-18.350	0.200E-09	-9.699

```
*********************************************************************************
*                                                                               *
*          NON-LINEAR LEAST SQUARES ANALYSIS                                    *
*                                                                               *
*SEVILLETA-LAVENDER BUSH                                                        *
*CUMULATIVE DATA SET                                                            *
*WETTING CURVE                                                                  *
*                                                                               *
*********************************************************************************
```

INPUT PARAMETERS

MODEL NUMBER	2
NUMBER OF COEFFICIENTS	2
MAXIMUM NUMBER OF ITERATIONS	20
RATIO OF COEFFICIENTS CRITERION	0.0001
RESIDUAL MOISTURE CONTENT (FOR MODEL 2)	0.0490
SATURATED MOISTURE CONTENT	0.3400
SATURATED HYDRAULIC CONDUCTIVITY	0.0150

OBSERVED DATA

Obs. No.	PRESSURE HEAD	MOISTURE CONTENT
1	5.50	0.2980
2	24.80	0.2450
3	36.60	0.1600
4	54.30	0.0850
5	75.00	0.0720
6	96.30	0.0700
7	121.20	0.0670
8	5.50	0.3120
9	11.30	0.3070
10	13.70	0.2880
11	27.70	0.2670
12	40.90	0.1360
13	61.00	0.1320
14	80.50	0.1310
15	110.70	0.1290
16	15.00	0.2670
17	21.00	0.2440
18	41.50	0.1660
19	62.20	0.1090
20	81.50	0.0860
21	102.10	0.0720
22	127.00	0.0660
23	4.00	0.3730
24	31.00	0.3544
25	4.00	0.3730
26	31.70	0.3544
27	39.50	0.2820
28	57.00	0.1310
29	81.00	0.0980
30	131.70	0.0944
31	149.50	0.0894
32	4.80	0.2954
33	23.50	0.2500
34	30.10	0.1770
35	41.10	0.0914

36	51.30	0.0864
37	71.20	0.0824
38	122.00	0.0824
39	4.30	0.2920
40	11.60	0.2380
41	24.20	0.2220
42	34.50	0.1410
43	43.00	0.0780
44	56.50	0.0500
45	99.40	0.0530
46	76.20	0.0610
47	51.90	0.0870
48	36.80	0.1470
49	23.20	0.2390
50	10.10	0.2670
51	3.50	0.2940
52	119.00	0.0570
53	101.10	0.0620
54	80.20	0.0650
55	54.40	0.0950
56	37.80	0.1600
57	23.40	0.2450
58	9.70	0.2640
59	2.40	0.2940
60	10.50	0.2720
61	22.50	0.2270
62	30.10	0.1790
63	39.00	0.1360
64	50.00	0.1010
65	76.50	0.0740

ITERATION NO	WCR	ALPHA	N	SSQ	MODEL
0	0.0490	0.002000	2.5000	2.3625359	2
1	0.0490	0.002305	1.1119	2.3265884	2
2	0.0490	0.068726	4.2098	0.5090305	2
3	0.0490	0.067380	2.6757	0.2498826	2
4	0.0490	0.058561	1.7318	0.2146661	2
5	0.0490	0.043394	2.2028	0.1543911	2
6	0.0490	0.044856	2.4792	0.1328321	2
7	0.0490	0.043874	2.5477	0.1325873	2
8	0.0490	0.043473	2.5694	0.1325584	2
9	0.0490	0.043311	2.5780	0.1325528	2
10	0.0490	0.043246	2.5815	0.1325515	2
11	0.0490	0.043219	2.5829	0.1325511	2
12	0.0490	0.043208	2.5835	0.1325510	2
13	0.0490	0.043203	2.5838	0.1325509	2
14	0.0490	0.043201	2.5838	0.1325509	2

CORRELATION MATRIX

	1	2
1	1.0000	
2	-0.8270	1.0000

NON-LINEAR LEAST-SQUARES ANALYSIS: FINAL RESULTS

VARIABLE	VALUE	S.E.COEFF.	T-VALUE	95% CONFIDENCE LIMITS LOWER	UPPER
ALPHA	0.04320	0.0044	9.72	0.0343	0.0521
	2.58385	0.2555	10.11	2.0730	3.0947

ORDERED BY COMPUTER INPUT

NO	PPESSURE	MOISTURE CONTENT OBS	FITTED	RESI-QUAL
1	5.50	0.2980	0.3357	-0.0377
2	24.80	0.2450	0.2287	0.0163
3	36.60	0.1600	0.1686	-0.0086
4	54.30	0.0850	0.1197	-0.0347
5	75.00	0.0720	0.0929	-0.0209
6	96.30	0.0700	0.0790	-0.0090
7	121.20	0.0670	0.0700	-0.0030
8	5.50	0.3120	0.3357	-0.0237
9	11.30	0.3070	0.3151	-0.0081
10	13.70	0.2880	0.3018	-0.0138
11	27.70	0.2670	0.2114	0.0556
12	40.90	0.1360	0.1531	-0.0171
13	61.00	0.1320	0.1088	0.0232
14	80.50	0.1310	0.0885	0.0425
15	110.70	0.1290	0.0731	0.0559
16	15.00	0.2670	0.2938	-0.0268
17	21.00	0.2440	0.2535	-0.0095
18	41.50	0.1660	0.1511	0.0149
19	62.20	0.1090	0.1071	0.0019
20	81.50	0.0860	0.0877	-0.0017
21	102.10	0.0720	0.0764	-0.0044
22	127.00	0.0660	0.0685	-0.0025
23	4.00	0.3730	0.3381	0.0349
24	31.00	0.3544	0.1937	0.1607

ORDERED BY RESIDUALS

NO	PRESSURE	MOISTURE CONTENT OBS	FITTED	RESI-DUAL
26	31.70	0.3544	0.1902	0.1642
24	31.00	0.3544	0.1937	0.1607
27	39.50	0.2820	0.1578	0.1242
15	110.70	0.1290	0.0731	0.0559
11	27.70	0.2670	0.2114	0.0556
14	80.50	0.1310	0.0885	0.0425
23	4.00	0.3730	0.3381	0.0349
25	4.00	0.3730	0.3381	0.0349
30	131.70	0.0944	0.0674	0.0270
31	149.50	0.0894	0.0641	0.0253
13	61.00	0.1320	0.1088	0.0232
2	24.80	0.2450	0.2287	0.0163
28	57.00	0.1310	0.1150	0.0160
18	41.50	0.1660	0.1511	0.0149
33	23.50	0.2500	0.2370	0.0130
38	122.00	0.0824	0.0697	0.0127
29	81.00	0.0980	0.0881	0.0099
57	23.40	0.2450	0.2376	0.0074
19	62.20	0.1090	0.1071	0.0019
49	23.20	0.2390	0.2389	0.0001
20	81.50	0.0860	0.0877	-0.0017
22	127.00	0.0660	0.0685	-0.0025
7	121.20	0.0670	0.0700	-0.0030
56	37.80	0.1600	0.1639	-0.0039

25	4.00	0.3730	0.3381	0.0349	21	102.10	0.0720	0.0764	-0.0044
26	31.70	0.3544	0.1902	0.1642	9	11.30	0.3070	0.3151	-0.0081
27	39.50	0.2820	0.1578	0.1242	3	36.60	0.1600	0.1686	-0.0086
28	57.00	0.1310	0.1150	0.0160	6	96.30	0.0700	0.0790	-0.0090
29	91.00	0.0980	0.0881	0.0099	17	21.00	0.2440	0.2535	-0.0095
30	131.70	0.0944	0.0674	0.0270	11	24.20	0.2220	0.2325	-0.0105
31	149.50	0.0894	0.0641	0.0253	37	74.20	0.0824	0.0936	-0.0112
32	4.80	0.2954	0.3370	-0.0416	52	119.00	0.0570	0.0706	-0.0136
33	23.50	0.2500	0.2370	0.0130	10	13.70	0.2880	0.3018	-0.0138
34	30.10	0.1770	0.1983	-0.0213	53	101.10	0.0620	0.0768	-0.0148
35	41.40	0.0914	0.1514	-0.0600	61	22.50	0.2270	0.2435	-0.0165
36	51.30	0.0864	0.1256	-0.0392	12	40.90	0.1360	0.1531	-0.0171
37	74.20	0.0824	0.0936	-0.0112	65	76.50	0.0740	0.0916	-0.0176
38	122.00	0.0824	0.0697	0.0127	62	30.10	0.1790	0.1983	-0.0193
39	4.30	0.2920	0.3377	-0.0457	48	36.80	0.1470	0.1678	-0.0208
40	11.60	0.2380	0.3136	-0.0756	5	75.00	0.0720	0.0929	-0.0209
41	24.20	0.2220	0.2325	-0.0105	34	30.10	0.1770	0.1983	-0.0213
42	34.50	0.1410	0.1773	-0.0363	63	39.00	0.1360	0.1596	-0.0236
43	43.00	0.0780	0.1465	-0.0685	54	80.20	0.0650	0.0887	-0.0237
44	56.50	0.0500	0.1158	-0.0658	8	5.50	0.3120	0.3357	-0.0237
45	99.40	0.0530	0.0775	-0.0245	55	54.40	0.0950	0.1195	-0.0245
46	76.20	0.0610	0.0919	-0.0309	45	99.40	0.0530	0.0775	-0.0245
47	51.90	0.0870	0.1244	-0.0374	16	15.00	0.2670	0.2938	-0.0268
48	36.80	0.1470	0.1678	-0.0208	64	50.00	0.1010	0.1284	-0.0274
49	23.20	0.2390	0.2389	0.0001	46	76.20	0.0610	0.0919	-0.0309
50	10.10	0.2670	0.3209	-0.0539	4	54.30	0.0850	0.1197	-0.0347
51	3.50	0.2940	0.3387	-0.0447	42	31.50	0.1410	0.1773	-0.0363
52	119.00	0.0570	0.0706	-0.0136	47	51.90	0.0870	0.1244	-0.0374
53	101.10	0.0620	0.0768	-0.0148	1	5.50	0.2980	0.3357	-0.0377
54	80.20	0.0650	0.0887	-0.0237	36	51.30	0.0864	0.1256	-0.0392
55	54.40	0.0950	0.1195	-0.0245	32	4.80	0.2954	0.3370	-0.0416
56	37.80	0.1600	0.1639	-0.0039	51	3.50	0.2940	0.3387	-0.0447
57	23.40	0.2450	0.2376	0.0074	59	2.40	0.2940	0.3395	-0.0455
58	9.70	0.2640	0.3226	-0.0586	39	4.30	0.2920	0.3377	-0.0457
59	2.40	0.2940	0.3395	-0.0455	60	10.50	0.2720	0.3190	-0.0470
60	10.50	0.2720	0.3190	-0.0470	50	10.10	0.2670	0.3209	-0.0539
61	22.50	0.2270	0.2435	-0.0165	58	9.70	0.2640	0.3226	-0.0586
62	30.10	0.1790	0.1983	-0.0193	35	41.40	0.0914	0.1514	-0.0600
63	39.00	0.1360	0.1596	-0.0236	44	56.50	0.0500	0.1158	-0.0658
64	50.00	0.1010	0.1284	-0.0274	43	43.00	0.0780	0.1465	-0.0685
65	76.50	0.0740	0.0916	-0.0176	40	11.60	0.2380	0.3136	-0.0756

PRESSURE	LOG P	MC	REL K	LOG RK	ABS K	LOG KA	DIFFUS	LOG D
0.000E+00		0.3400	0.100E+01		0.150E-01			
0.111E+01	0.150	0.3399	0.976E+00	-0.011	0.146E-01	-1.834	0.617E+02	1.791
0.168E+01	0.225	0.3398	0.969E+00	-0.014	0.145E-01	-1.838	0.466E+02	1.669
0.200E+01	0.300	0.3397	0.959E+00	-0.018	0.144E-01	-1.842	0.352E+02	1.546
0.237E+01	0.375	0.3395	0.946E+00	-0.024	0.142E-01	-1.848	0.264E+02	1.422
0.282E+01	0.450	0.3392	0.929E+00	-0.032	0.139E-01	-1.856	0.198E+02	1.296
0.335E+01	0.525	0.3388	0.907E+00	-0.042	0.136E-01	-1.866	0.148E+02	1.169
0.398E+01	0.600	0.3381	0.879E+00	-0.056	0.132E-01	-1.880	0.109E+02	1.039
0.473E+01	0.675	0.3371	0.842E+00	-0.075	0.126E-01	-1.899	0.805E+01	0.906
0.562E+01	0.750	0.3355	0.795E+00	-0.099	0.119E-01	-1.923	0.587E+01	0.769
0.668E+01	0.825	0.3330	0.737E+00	-0.133	0.111E-01	-1.957	0.423E+01	0.627
0.794E+01	0.900	0.3293	0.665E+00	-0.177	0.997E-02	-2.001	0.301E+01	0.478
0.944E+01	0.975	0.3237	0.579E+00	-0.237	0.868E-02	-2.061	0.210E+01	0.322
0.112E+02	1.050	0.3155	0.481E+00	-0.318	0.722E-02	-2.142	0.144E+01	0.158
0.133E+02	1.125	0.3040	0.376E+00	-0.424	0.565E-02	-2.248	0.962E+00	-0.017
0.158E+02	1.200	0.2883	0.273E+00	-0.564	0.409E-02	-2.388	0.627E+00	-0.203
0.188E+02	1.275	0.2682	0.181E+00	-0.743	0.271E-02	-2.567	0.398E+00	-0.400
0.224E+02	1.350	0.2443	0.108E+00	-0.965	0.162E-02	-2.789	0.246E+00	-0.609
0.266E+02	1.425	0.2177	0.585E-01	-1.233	0.877E-03	-3.057	0.148E+00	-0.829
0.316E+02	1.500	0.1906	0.286E-01	-1.543	0.429E-03	-3.367	0.876E-01	-1.058
0.376E+02	1.575	0.1648	0.129E-01	-1.891	0.193E-03	-3.714	0.509E-01	-1.294
0.447E+02	1.650	0.1417	0.541E-02	-2.267	0.811E-04	-4.091	0.292E-01	-1.535
0.531E+02	1.725	0.1220	0.216E-02	-2.666	0.324E-04	-4.490	0.166E-01	-1.780
0.631E+02	1.800	0.1059	0.830E-03	-3.081	0.125E-04	-4.905	0.938E-02	-2.028
0.750E+02	1.875	0.0929	0.312E-03	-3.506	0.467E-05	-5.330	0.528E-02	-2.278
0.891E+02	1.950	0.0828	0.115E-03	-3.940	0.172E-05	-5.763	0.296E-02	-2.529
0.106E+03	2.025	0.0749	0.419E-04	-4.378	0.629E-06	-6.201	0.166E-02	-2.780
0.126E+03	2.100	0.0688	0.152E-04	-4.819	0.228E-06	-6.643	0.928E-03	-3.033
0.150E+03	2.175	0.0641	0.545E-05	-5.263	0.818E-07	-7.087	0.517E-03	-3.287
0.178E+03	2.250	0.0605	0.196E-05	-5.707	0.294E-07	-7.531	0.289E-03	-3.539
0.211E+03	2.325	0.0577	0.701E-06	-6.152	0.105E-07	-7.976	0.162E-03	-3.791
0.251E+03	2.400	0.0557	0.252E-06	-6.598	0.378E-08	-8.422	0.903E-04	-4.044
0.299E+03	2.475	0.0541	0.903E-07	-7.044	0.135E-08	-8.868	0.504E-04	-4.297
0.355E+03	2.550	0.0529	0.323E-07	-7.491	0.484E-09	-9.315	0.282E-04	-4.550
0.422E+03	2.625	0.0519	0.115E-07	-7.938	0.173E-09	-9.761	0.157E-04	-4.803
0.501E+03	2.700	0.0512	0.413E-08	-8.384	0.619E-10	-10.208	0.878E-05	-5.056
0.596E+03	2.775	0.0507	0.148E-08	-8.831	0.221E-10	-10.655	0.490E-05	-5.310
0.708E+03	2.850	0.0503	0.527E-09	-9.278	0.791E-11	-11.102	0.274E-05	-5.563
0.841E+03	2.925	0.0500	0.188E-09	-9.725	0.283E-11	-11.549	0.153E-05	-5.816
0.100E+04	3.000	0.0497	0.673E-10	-10.172	0.101E-11	-11.996	0.853E-06	-6.069
0.119E+04	3.075	0.0496	0.241E-10	-10.619	0.361E-12	-12.443	0.476E-06	-6.322
0.141E+04	3.150	0.0494	0.859E-11	-11.066	0.129E-12	-12.890	0.266E-06	-6.575
0.168E+04	3.225	0.0493	0.307E-11	-11.513	0.461E-13	-13.337	0.148E-06	-6.829
0.200E+04	3.300	0.0493	0.110E-11	-11.960	0.165E-13	-13.784	0.828E-07	-7.082
0.237E+04	3.375	0.0492	0.392E-12	-12.407	0.588E-14	-14.231	0.462E-07	-7.335
0.282E+04	3.450	0.0491	0.140E-12	-12.854	0.210E-14	-14.678	0.258E-07	-7.588
0.335E+04	3.525	0.0491	0.500E-13	-13.301	0.751E-15	-15.125	0.144E-07	-7.841
0.398E+04	3.600	0.0491	0.179E-13	-13.748	0.268E-15	-15.571	0.804E-08	-8.095
0.473E+04	3.675	0.0491	0.639E-14	-14.195	0.958E-16	-16.018	0.449E-08	-8.348
0.562E+04	3.750	0.0490	0.228E-14	-14.642	0.342E-16	-16.465	0.251E-08	-8.601
0.668E+04	3.825	0.0490	0.816E-15	-15.088	0.122E-16	-16.912	0.140E-08	-8.854
0.794E+04	3.900	0.0490	0.291E-15	-15.535	0.437E-17	-17.359	0.781E-09	-9.107
0.944E+04	3.975	0.0490	0.104E-15	-15.982	0.156E-17	-17.806	0.436E-09	-9.360
0.112E+05	4.050	0.0490	0.372E-16	-16.429	0.558E-18	-18.253	0.243E-09	-9.614

APPENDIX C

This appendix includes moisture content data collected throughout the study period by neutron logging. Changes in soil-moisture storage and the fortran code used to compute it (Mc Cord, 1986) are also included.

ılian Date	Total Profile Storage (cm)	Total Profile Change in Storage	Shallow Profile Storage (cm)	Shallow Profile Change in Storage	Deep Profile Storage (cm)	Deep Profile Change in Storage
106	16.88	0.00	0.56	0.00	16.32	0.00
116	14.59	-2.29	1.11	0.55	13.48	-2.84
130	20.21	5.62	1.78	0.68	18.43	4.94
137	19.20	-1.01	1.39	-0.39	17.81	-0.62
157	19.43	0.23	1.27	-0.12	18.15	0.34
163	17.31	-2.12	0.81	-0.46	16.49	-1.66
171	17.26	-0.05	1.28	0.47	15.98	-0.52
178	16.29	-0.97	0.88	-0.40	15.41	-0.56
185	17.77	1.47	0.70	-0.18	17.06	1.65
192	14.61	-3.15	0.52	-0.19	14.10	-2.97
198	13.67	-0.94	0.47	-0.05	13.20	-0.90
205	14.15	0.48	1.25	0.78	12.91	-0.29
213	14.30	0.14	1.55	0.30	12.75	-0.15
220	16.21	1.92	1.64	0.09	14.58	1.83
225	17.90	1.69	2.32	0.69	15.58	1.00
234	14.55	-3.35	1.18	-1.15	13.37	-2.21
240	14.12	-0.43	0.84	-0.33	13.27	-0.10
257	12.61	-1.51	1.13	0.29	11.48	-1.80
270	13.34	0.73	1.32	0.19	12.02	0.54
277	13.72	0.39	1.36	0.04	12.37	0.35
284	17.80	4.08	2.81	1.45	15.00	2.63
297	17.71	-0.09	1.38	-1.43	16.34	1.34
312	17.02	-0.69	1.41	0.04	15.61	-0.73
332	17.20	0.18	1.30	-0.12	15.90	0.30
346	16.79	-0.41	1.18	-0.12	15.61	-0.29
360	16.84	0.05	1.07	-0.10	15.77	0.16
388	16.87	0.02	1.04	-0.04	15.83	0.06
401	16.73	-0.13	1.06	0.02	15.67	-0.16
418	16.57	-0.16	1.18	0.12	15.39	-0.28
431	16.68	0.11	1.12	-0.06	15.56	0.17
447	16.45	-0.23	0.99	-0.13	15.47	-0.10
467	16.15	-0.31	0.86	-0.12	15.28	-0.18
490	17.87	1.72	1.36	0.49	16.51	1.23
505	15.86	-2.01	0.95	-0.41	14.92	-1.60

lian Date	Total Profile Storage (cm)	Total Profile Change in Storage	Shallow Profile Storage (cm)	Shallow Profile Change in Storage	Deep Profile Storage (cm)	Deep Profile Change in Storage
185	18.99	0.00	0.63	0.00	18.36	0.00
192	19.91	0.92	0.65	0.02	19.26	0.91
198	19.73	-0.18	0.76	0.11	18.98	-0.29
205	18.67	-1.07	0.84	0.08	17.83	-1.15
213	19.04	0.37	0.96	0.12	18.08	0.25
220	17.43	-1.61	1.33	0.37	16.10	-1.98
225	16.46	-0.97	1.50	0.17	14.97	-1.14
234	16.09	-0.37	1.01	-0.49	15.08	0.11
240	15.35	-0.74	0.85	-0.16	14.50	-0.58
257	13.34	-2.01	0.72	-0.13	12.62	-1.88
270	13.63	0.29	0.90	0.18	12.73	0.12
277	12.71	-0.92	0.78	-0.12	11.93	-0.80
284	15.22	2.51	2.83	2.05	12.39	0.46
297	20.45	5.23	1.72	-1.11	18.73	6.34
312	20.50	0.04	1.56	-0.16	18.93	0.20
332	19.94	-0.55	1.36	-0.21	18.59	-0.35
346	20.18	0.23	1.31	-0.04	18.86	0.27
360	20.14	-0.04	1.28	-0.03	18.85	-0.01
388	19.73	-0.41	1.32	0.03	18.41	-0.44
401	20.16	0.43	1.28	-0.04	18.88	0.47
418	20.26	0.10	1.37	0.09	18.89	0.01
431	18.61	-1.65	1.28	-0.08	17.33	-1.56
447	20.16	1.54	1.21	-0.08	18.95	1.62
467	19.77	-0.39	1.04	-0.17	18.73	-0.22
490	19.61	-0.15	0.95	-0.08	18.66	-0.07
505	18.58	-1.04	0.76	-0.19	17.81	-0.85

lian Date	Total Profile Storage (cm)	Total Profile Change in Storage	Shallow Profile Storage (cm)	Shallow Profile Change in Storage	Deep Profile Storage (cm)	Deep Profile Change in Storage
346	22.05	0.00	1.27	0.00	20.78	0.00
401	20.59	-1.46	1.21	-0.06	19.38	-1.40
418	20.30	-0.29	1.28	0.07	19.02	-0.36
431	20.20	-0.10	1.18	-0.11	19.02	0.01
447	19.82	-0.39	1.03	-0.14	18.78	-0.24
467	19.56	-0.26	0.83	-0.21	18.73	-0.05
490	19.44	-0.11	1.23	0.40	18.22	-0.51
505	18.91	-0.53	0.93	-0.29	17.98	-0.24

lian Date	Total Profile Storage (cm)	Total Profile Change in Storage	Shallow Profile Storage (cm)	Shallow Profile Change in Storage	Deep Profile Storage (cm)	Deep Profile Change in Storage
116	15.95	0.00	1.11	0.00	14.84	0.00
130	17.46	1.51	1.97	0.86	15.49	0.64
137	17.07	-0.38	1.54	-0.43	15.53	0.04
157	16.52	-0.56	1.27	-0.27	15.25	-0.28
163	16.15	-0.37	1.17	-0.10	14.98	-0.26
171	16.40	0.25	1.44	0.27	14.96	-0.02
178	16.12	-0.28	1.19	-0.24	14.93	-0.04
185	15.47	-0.65	1.06	-0.13	14.41	-0.52
192	15.61	0.14	0.99	-0.07	14.62	0.21
198	16.20	0.59	1.04	0.05	15.15	0.54
205	14.76	-1.44	1.15	0.10	13.62	-1.54
213	17.23	2.47	2.23	1.08	15.00	1.39
220	16.34	-0.89	1.98	-0.25	14.36	-0.65
225	17.84	1.50	2.38	0.40	15.46	1.10
234	16.06	-1.78	1.72	-0.67	14.34	-1.12
240	15.95	-0.10	1.44	-0.27	14.51	0.17
257	17.11	1.16	2.01	0.57	15.10	0.59
270	14.81	-2.30	1.98	-0.04	12.84	-2.26
277	14.89	0.07	1.82	-0.15	13.06	0.23
284	18.50	3.62	3.14	1.31	15.37	2.30
297	17.31	-1.20	1.58	-1.56	15.73	0.36
312	16.90	-0.41	1.62	0.04	15.28	-0.44
332	17.05	0.15	1.37	-0.25	15.68	0.39
346	16.78	-0.27	1.32	-0.05	15.46	-0.21
360	16.22	-0.56	1.18	-0.14	15.04	-0.42
388	17.35	1.12	1.22	0.04	16.13	1.09
401	17.60	0.25	1.22	0.00	16.38	0.24
418	17.74	0.14	1.18	-0.04	16.56	0.18
431	17.69	-0.04	1.14	-0.04	16.55	-0.01
447	17.63	-0.06	1.05	-0.09	16.58	0.03
467	17.75	0.11	0.97	-0.09	16.78	0.20
490	20.17	2.42	2.28	1.31	17.89	1.11
505	18.51	-1.66	1.61	-0.66	16.90	-1.00

ılian Date	Total Profile Storage (cm)	Total Profile Change in Storage	Shallow Profile Storage (cm)	Shallow Profile Change in Storage	Deep Profile Storage (cm)	Deep Profile Change in Storage
130	26.72	0.00	2.62	0.00	24.11	0.00
137	25.97	-0.75	2.04	-0.58	23.93	-0.17
157	22.59	-3.38	1.34	-0.70	21.25	-2.68
163	23.43	0.84	1.17	-0.17	22.26	1.01
171	22.34	-1.09	1.34	0.17	21.00	-1.26
178	22.28	-0.06	1.22	-0.12	21.05	0.06
185	21.78	-0.50	1.01	-0.21	20.77	-0.28
192	20.27	-1.51	0.69	-0.33	19.59	-1.18
198	19.03	-1.24	0.57	-0.11	18.46	-1.13
205	18.71	-0.32	0.93	0.36	17.78	-0.68
213	19.72	1.01	1.64	0.71	18.08	0.30
220	20.40	0.68	2.20	0.56	18.20	0.11
225	19.05	-1.35	2.50	0.30	16.55	-1.64
234	15.80	-3.24	1.39	-1.10	14.41	-2.14
240	15.29	-0.51	0.93	-0.47	14.37	-0.04
257	13.92	-1.37	1.12	0.19	12.80	-1.56
270	15.61	1.68	1.34	0.22	14.27	1.47
277	13.01	-2.60	1.31	-0.03	11.70	-2.57
284	17.81	4.80	3.75	2.45	14.06	2.36
297	25.63	7.82	1.84	-1.92	23.80	9.74
312	26.67	1.04	1.87	0.03	24.80	1.00
332	23.92	-2.75	1.34	-0.53	22.58	-2.22
346	20.18	-3.75	1.31	-0.03	18.86	-3.72
360	22.51	2.33	1.14	-0.17	21.37	2.51
388	21.95	-0.56	1.10	-0.04	20.84	-0.52
401	21.76	-0.19	1.07	-0.03	20.69	-0.16
418	21.53	-0.23	1.15	0.08	20.37	-0.32
431	20.16	-1.37	1.01	-0.14	19.15	-1.23
447	21.02	0.87	0.94	-0.07	20.09	0.94
467	20.46	-0.57	0.67	-0.27	19.79	-0.30
490	20.62	0.16	1.31	0.64	19.31	-0.48
505	19.22	-1.40	0.62	-0.69	18.60	-0.71

ılian Date	Total Profile Storage (cm)	Total Profile Change in Storage	Shallow Profile Storage (cm)	Shallow Profile Change in Storage	Deep Profile Storage (cm)	Deep Profile Change in Storage
220	17.06	0.00	1.45	0.00	15.60	0.00
234	18.23	1.18	1.27	-0.18	16.96	1.36
257	21.10	2.87	1.88	0.61	19.22	2.26
270	16.75	-4.35	1.43	-0.46	15.33	-3.89
277	18.65	1.90	1.74	0.32	16.91	1.58
284	20.77	2.11	2.68	0.94	18.08	1.17
297	23.72	2.95	1.43	-1.25	22.29	4.20
312	22.74	-0.98	1.28	-0.15	21.47	-0.82
332	21.46	-1.29	1.14	-0.14	20.31	-1.15
346	20.57	-0.88	1.03	-0.11	19.54	-0.77
360	20.25	-0.33	0.95	-0.08	19.29	-0.25
388	18.98	-1.26	1.04	0.08	17.94	-1.35
401	19.77	0.78	0.98	-0.06	18.79	0.85
418	19.50	-0.27	0.96	-0.01	18.53	-0.26
431	19.22	-0.28	0.83	-0.14	18.39	-0.14
447	18.86	-0.36	0.70	-0.13	18.16	-0.23
467	18.70	-0.16	0.55	-0.15	18.15	-0.01
490	19.54	0.84	1.34	0.78	18.20	0.05
505	19.39	-0.15	1.03	-0.31	18.36	0.16

lian Date	Total Profile Storage (cm)	Total Profile Change in Storage	Shallow Profile Storage (cm)	Shallow Profile Change in Storage	Deep Profile Storage (cm)	Deep Profile Change in Storage
130	22.52	0.00	1.77	0.00	20.75	0.00
137	22.61	0.09	1.52	-0.25	21.09	0.34
157	22.11	-0.50	1.31	-0.21	20.80	-0.29
163	23.25	1.14	2.44	1.14	20.81	0.00
171	21.90	-1.35	1.42	-1.02	20.48	-0.32
178	20.38	-1.52	1.36	-0.05	19.02	-1.46
185	22.39	2.01	1.39	0.02	21.01	1.99
192	22.78	0.39	1.50	0.11	21.29	0.28
198	20.38	-2.40	1.05	-0.45	19.33	-1.95
205	20.02	-0.36	1.33	0.28	18.70	-0.64
213	22.11	2.08	2.20	0.88	19.90	1.20
220	22.68	0.57	2.05	-0.16	20.63	0.73
225	23.62	0.94	2.27	0.22	21.35	0.72
234	23.19	-0.43	1.66	-0.61	21.53	0.18
240	19.94	-3.25	1.46	-0.20	18.49	-3.04
257	18.88	-1.06	1.79	0.33	17.09	-1.39
270	17.77	-1.11	1.78	-0.01	16.00	-1.10
277	17.71	-0.06	1.64	-0.14	16.07	0.07
284	21.11	3.40	2.88	1.24	18.23	2.16
297	22.56	1.45	1.50	-1.38	21.06	2.83
312	22.82	0.26	1.45	-0.05	21.38	0.31
332	22.25	-0.57	1.23	-0.21	21.02	-0.36
346	21.58	-0.67	1.16	-0.07	20.42	-0.60
360	20.02	-1.57	1.11	-0.05	18.91	-1.51
388	20.66	0.64	1.14	0.03	19.52	0.61
401	20.54	-0.12	1.13	-0.01	19.41	-0.11
418	20.22	-0.32	1.15	0.03	19.06	-0.35
431	20.19	-0.03	1.24	0.09	18.94	-0.12
447	19.85	-0.33	1.05	-0.19	18.80	-0.14
467	19.60	-0.26	0.95	-0.10	18.64	-0.16
490	19.98	0.38	1.70	0.75	18.27	-0.37
505	19.28	-0.70	1.30	-0.41	17.98	-0.30

ılian Date	Total Profile Storage (cm)	Total Profile Change in Storage	Shallow Profile Storage (cm)	Shallow Profile Change in Storage	Deep Profile Storage (cm)	Deep Profile Change in Storage
106	20.57	0.00	0.26	0.00	20.32	0.00
130	23.20	2.63	2.19	1.93	21.01	0.70
137	23.24	0.04	2.12	-0.06	21.12	0.10
144	22.52	-0.72	1.79	-0.34	20.74	-0.38
157	21.37	-1.16	0.54	-1.24	20.83	0.09
177	20.59	-0.78	1.25	0.71	19.34	-1.49
192	20.20	-0.39	0.82	-0.44	19.39	0.05
205	16.83	-3.38	0.82	0.01	16.01	-3.38
225	19.58	2.75	2.77	1.95	16.81	0.80
240	13.39	-6.18	0.20	-2.56	13.19	-3.62
249	15.13	1.74	0.95	0.75	14.18	0.99
257	15.77	0.64	0.82	-0.13	14.95	0.77
270	13.11	-2.66	0.79	-0.03	12.32	-2.63
277	14.35	1.24	1.89	1.10	12.46	0.14
291	24.88	10.53	3.13	1.24	21.75	9.29
326	23.77	-1.11	1.70	-1.43	22.07	0.32
410	20.93	-2.84	1.55	-0.15	19.37	-2.69
418	21.20	0.28	1.44	-0.12	19.77	0.39
424	21.66	0.46	1.80	0.36	19.86	0.10
431	20.19	-1.47	1.24	-0.55	18.94	-0.92
447	19.55	-0.64	0.28	-0.96	19.26	0.32
467	21.37	1.83	1.53	1.24	19.85	0.58
490	22.16	0.79	1.96	0.43	20.20	0.35
505	20.61	-1.55	1.53	-0.43	19.08	-1.12

lian Date	Total Profile Storage (cm)	Total Profile Change in Storage	Shallow Profile Storage (cm)	Shallow Profile Change in Storage	Deep Profile Storage (cm)	Deep Profile Change in Storage
234	17.89	0.00	1.40	0.00	16.49	0.00
257	18.27	0.38	1.71	0.31	16.56	0.07
270	17.29	-0.98	1.59	-0.12	15.71	-0.85
277	16.16	-1.13	1.50	-0.09	14.66	-1.04
284	19.01	2.85	2.80	1.30	16.21	1.55
297	18.01	-1.00	1.36	-1.44	16.66	0.44
312	17.50	-0.51	1.33	-0.03	16.17	-0.48
332	17.34	-0.16	1.13	-0.20	16.21	0.04
346	23.12	5.78	1.29	0.16	21.83	5.62
360	17.36	-5.76	1.05	-0.25	16.32	-5.52
388	17.61	0.24	1.10	0.05	16.51	0.19
401	17.56	-0.05	1.03	-0.07	16.53	0.03
418	17.77	0.21	1.04	0.02	16.73	0.20
431	15.65	-2.12	0.96	-0.08	14.69	-2.04
447	17.44	1.79	0.91	-0.05	16.53	1.84
467	17.24	-0.20	0.77	-0.15	16.47	-0.06
490	18.21	0.96	1.50	0.73	16.70	0.23
505	17.25	-0.96	1.23	-0.27	16.01	-0.69

M A S B A L 2

This program will do an incremental (w/respect to time) mass balance on volumetric moisture content profiles.

The program will use data file output by THETA.FOR.

Basically, D(t)=((01+02+03+...0n)/n)*T
where,
t=time,
0i=volumetric moisture content at the i'th depth,
n=number of readings in profile,
T=total thickness of profile,
D=depth of water in storage at time t.

Program written by James McCord with minor changes

```
double precision filnm,pfilnm,pflnm6,TABLE,PFL3T6,pflnmd
1,table2,NWFLNM

dimension theta(0:90),depth(0:90),deldep(90),D(0:90),d6(0:90),
1deldp6(90),DELSTO(90),DELST6(90),dshalo(90),dlstsh(90),DMED(90),
2DELMED(90),dpdeep(90),deleep(90),cumsto(90),cumst6(90),
3cummed(90),cumshl(90),ndays(90),deltmd(90),delshl(90)

real ngdlsh,ngdlmd,ngdldp

type 10
format(/' Enter desired data file name: ',$)
read(5,15)filnm
format(a10)
type 20
format(/' Enter desired deep profile plot file name: ',$)
read(5,15)pfilnm
type 22
format(/' Enter desired medium profile plot file name: ',$)
read(5,15)pflnm6
type 23
format(/' Enter desired shallow profile plot file name: ',$)
read(5,15)pfl3t6
type 231
format(/' Enter desired total profile plot file name: ',$)
read(5,15)pflnmd
TYPE 24
FORMAT(/' Enter desired table1 file name: ',$)
read(5,15)table
TYPE 241
FORMAT(/' Enter desired table2 file name: ',$)
read(5,15)table2

open(unit=1,file=filnm)
open(unit=2,file=pfilnm,device='dsk')
open(unit=3,file=pflnm6,device='dsk')
open(unit=7,file=pfl3t6,device='dsk')
open(unit=4,file=table,device='dsk')
open(unit=8,file=pflnmd,device='dsk')
```

```
open(unit=9,file=table2,device='dsk')
open(unit=57,file='shal.dat')
open(unit=56,file='med.dat')
open(unit=55,file='deep.dat')

type 30
format(/' Enter number of time increments: ',$)
read(5,*)incrt
type 40
format(/' Enter number of depths monitored at each time: ',$)
read(5,*)ndepth
type 42
format(/' Enter shallow depth: ',$)
read(5,*)shallo
type 422
format(/' Enter medium depth: ',$)
read(5,*)centre
TYPE 424
FORMAT(/' Enter total depth (in cm): ',$)
ACCEPT 47,ITD
type 44
Format(/' Is there a date heading involved? 1=yes,2=no: ',$)
accept 47,Kdate
formaT(I)
if(kdate.eq.1)icount=1

Initialize

delsto(1)=0.
delst6(1)=0.
D(0)=0.
ngdlsh=0.
ngdlmd=0.
ngdldp=0.
SHLLO=SHALLO*.30
CNTRE=CENTRE*.30
TD=ITD*.01

Write out table headings before computational algorythms

Write(4,26)
format(//2x,'Julian Date       Total Profile',5x,
1'Shallow Profile',7x,
1'Deep Profile'/
2'               Storage   Change in   Storage   ',
3'Change in   Storage  Change in'/
4'                  (cm)     Storage     (cm)'
5,6x,'Storage     (cm)     Storage'/2x,77('-'))

write(9,261)shllo,shllo,cntre,cntre,td
format(//15x,'Julian Date          Changes in St
lorage (cm)',/,
2'                              0-',F3.1,'m   ',F3.1,'-',F3.1,'
2m   ',F3.1,'-',F3.1,'m   Total',/,
315x,52('-'))


Begin computational algorythms

do 160 i=1,incrt
```

```
itest=((i-1)*ndepth)+i
if(Kdate.eq.1.and.itest.eq.icount)go to 90
continue
icount=icount+1
sumthe=0.0
sumth6=0.0
smthsh=0.0
smthmd=0.0
do 80 n=1,ndepth
icount=icount+1
read(1,45)depth(n),theta(n)
format(2f7.4)

d(theta)/dt

if(n.le.shallo)then
  smthsh=(smthsh+theta(n))/(ndays(i)-ndays(i-1))
  write(57,*)smthsh,ndays(i)
endif
if(n.gt.shallo.and.n.le.centre)then
   smthmd=(smthmd+theta(n))/(ndays(i)-ndays(i-1))
   write(56,*)smthmd,ndays(i)
endif
if(n.gt.centre)then
  sumth6=(sumth6+theta(n))/(ndays(i)-ndays(i-1))
  write(55,*)sumth6,ndays(i)
endif
continue
deep=depth(ndepth)-shallo

go to 99
read(1,91)ndays(i)
format(i4)
go to 43

(depth calc. in cm)

continue
d6(i)=(sumth6/(ndepth-(centre-1)))*(depth(ndepth)-(centre-1)
1)*30.48/100.
dshalo(i)=(smthsh/100.)*30.48
dmed(i)=(smthmd/100.)*30.48
dpdeep(i)=d6(i)+dmed(i)
D(i)=dshalo(i)+dpdeep(i)
format(i4)
format(f12.5,i4,f12.5)
datum=D(1)
datum6=d6(1)
datumd=dmed(1)
dtmshl=dshalo(1)
deldep(i)=D(i)-datum
deldp6(i)=d6(i)-datum6
deltmd(i)=dmed(i)-datumd
delshl(i)=dshalo(i)-dtmshl

Incremental change in profile storage

ii=i-1
if(ii.eq.0)go to 100
delsto(i)=d(i)-d(ii)
```

```
delst6(i)=d6(i)-D6(ii)
if(delst6(i).le.0.)ngdldp=ngdldp+delst6(i)
delmed(i)=dmed(i)-dmed(ii)
if(delmed(i).le.0.)ngdlmd=ngdlmd+delmed(i)
dlstsh(i)=dshalo(i)-dshalo(ii)
if(dlstsh(i).le.0.)ngdlsh=ngdlsh+dlstsh(i)
deleep(i)=dpdeep(i)-dpdeep(ii)

cumulative changes
cumsto(i)=cumsto(ii)+delsto(i)
cumst6(i)=cumst6(ii)+delst6(i)
cummed(i)=cummed(ii)+delmed(i)
cumshl(i)=cumshl(ii)+dlstsh(i)
continue

Normalize then Write Cumulative Storage Change
deldp6(i)=deldp6(i)/((depth(ndepth)-(centre-1))*.3048)
deltmd(i)=deltmd(i)/((centre-(shallo-1))*.3048)
delshl(i)=delshl(i)/((shallo-(depth(1)-1))*.3048)
write(2,105)ndays(i),deldp6(i)
write(3,105)ndays(i),deltmd(i)
write(7,105)ndays(i),delshl(i)
format(i4,1x,f8.4)

Output table

Write(4,150)ndays(i),d(i),delsto(i),dshalo(i),dlstsh(i),
ldpdeep(i),deleep(i)

write(9,151)ndays(i),dlstsh(i),delmed(i),delst6(i),delsto(i)
format(6x,i4,2x,f8.2,5(3x,f8.2))
format(17x,i4,3x,4f10.2)
continue

write(9,152)cumshl(incrt),cummed(incrt),cumst6(incrt),
lngdlsh,ngdlmd,ngdldp
format(29x,'-----',2(5x,'-----'),/
124x,3(1x,'Sum=',f5.1),/
212x,'Sum of Drainages=',3(f5.1,5x))

do 170 i=1,incrt
write(8,105)ndays(i),d(i)
continue
do 180 i=1,incrt
write(8,105)ndays(i),dpdeep(i)
continue
do 190 i=1,incrt
write(8,105)ndays(i),dshalo(i)
continue


stop
END
```

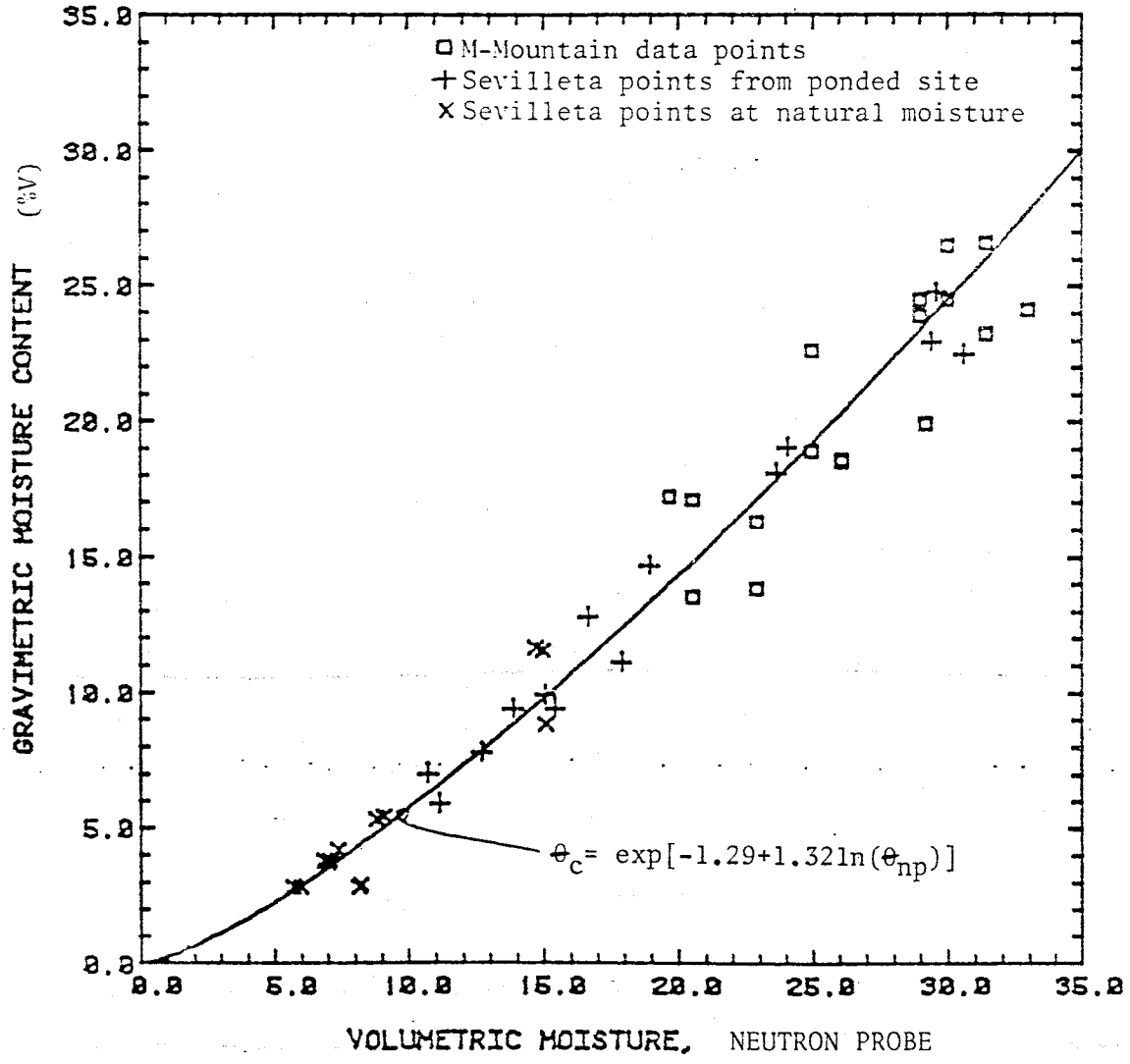

NEUTRON PROBE CALIBRATION

Moisture content data for West A neutron tube (edge of canopy)

Julian Date

106		163		198	
Depth	Theta				
30.0	1.83	30.0	2.67	30.0	1.54
60.0	5.48	60.0	5.09	60.0	3.13
90.0	6.82	90.0	6.37	90.0	4.21
120.0	6.48	120.0	6.44	120.0	5.29
150.0	6.57	150.0	7.21	150.0	5.74
180.0	7.37	180.0	7.63	180.0	5.94
210.0	7.20	210.0	7.42	210.0	6.41
240.0	6.91	240.0	7.13	240.0	6.47
270.0	6.70	270.0	6.81	270.0	6.11
116		171		205	
30.0	3.63	30.0	4.21	30.0	4.09
60.0	5.89	60.0	4.46	60.0	3.43
90.0	5.83	90.0	5.77	90.0	4.27
120.0	7.24	120.0	6.18	120.0	5.60
150.0	6.55	150.0	7.00	150.0	5.83
180.0	4.85	180.0	7.60	180.0	5.35
210.0	4.73	210.0	7.53	210.0	5.85
240.0	4.39	240.0	7.20	240.0	5.99
270.0	4.76	270.0	6.66	270.0	6.03
130		178		213	
30.0	5.84	30.0	2.89	30.0	5.07
60.0	8.26	60.0	3.91	60.0	3.18
90.0	8.49	90.0	5.37	90.0	4.35
120.0	6.68	120.0	6.18	120.0	5.76
150.0	7.18	150.0	6.78	150.0	5.72
180.0	7.51	180.0	7.33	180.0	5.79
210.0	7.83	210.0	7.46	210.0	5.53
240.0	7.62	240.0	6.88	240.0	5.74
270.0	6.88	270.0	6.66	270.0	5.76
137		185		220	
30.0	4.56	30.0	2.30	30.0	5.37
60.0	7.24	60.0	3.87	60.0	7.21
90.0	9.01	90.0	5.85	90.0	4.54
120.0	7.68	120.0	7.19	120.0	5.06
150.0	7.10	150.0	7.47	150.0	5.33
180.0	7.53	180.0	8.46	180.0	6.01
210.0	7.57	210.0	8.04	210.0	6.47
240.0	7.24	240.0	7.63	240.0	6.70
270.0	5.06	270.0	7.48	270.0	6.50
157		192		225	
30.0	4.18	30.0	1.69	30.0	7.62
60.0	6.41	60.0	3.22	60.0	8.65
90.0	8.09	90.0	4.78	90.0	6.89
120.0	7.53	120.0	5.52	120.0	5.39
150.0	7.33	150.0	6.03	150.0	5.47
180.0	7.32	180.0	6.88	180.0	6.00
210.0	7.97	210.0	6.90	210.0	6.21
240.0	7.61	240.0	6.58	240.0	6.40
270.0	7.29	270.0	6.34	270.0	6.10

234	
30.0	3.86
60.0	7.07
90.0	8.37
120.0	4.34
150.0	4.40
180.0	4.47
210.0	4.95
240.0	5.06
270.0	5.22

240	
30.0	2.77
60.0	5.81
90.0	7.87
120.0	4.84
150.0	4.66
180.0	4.78
210.0	4.89
240.0	5.29
270.0	5.42

257	
30.0	3.71
60.0	4.97
90.0	5.46
120.0	4.31
150.0	4.24
180.0	4.34
210.0	4.64
240.0	4.90
270.0	4.80

270	
30.0	4.33
60.0	6.81
90.0	6.10
120.0	4.33
150.0	4.13
180.0	4.17
210.0	4.49
240.0	4.57
270.0	4.81

277	
30.0	4.45
60.0	7.06
90.0	6.85
120.0	4.51
150.0	4.07
180.0	4.08
210.0	4.57
240.0	4.58
270.0	4.86

284	
30.0	9.20
60.0	11.88
90.0	10.72
120.0	4.38
150.0	4.24
180.0	4.19
210.0	4.44
240.0	4.69
270.0	4.65

297	
30.0	4.52
60.0	6.80
90.0	9.26
120.0	8.58
150.0	8.86
180.0	6.30
210.0	4.53
240.0	4.63
270.0	4.64

312	
30.0	4.64
60.0	5.97
90.0	7.00
120.0	7.03
150.0	7.92
180.0	8.03
210.0	5.79
240.0	4.81
270.0	4.66

332	
30.0	4.26
60.0	5.85
90.0	6.55
120.0	6.46
150.0	7.15
180.0	7.86
210.0	7.06
240.0	6.02
270.0	5.23

346	
30.0	3.87
60.0	5.54
90.0	6.32
120.0	6.26
150.0	6.83
180.0	7.53
210.0	7.04
240.0	6.18
270.0	5.52

360	
30.0	3.52
60.0	5.41
90.0	6.38
120.0	6.13
150.0	6.69
180.0	7.33
210.0	7.31
240.0	6.54
270.0	5.93

388	
30.0	3.40
60.0	5.27
90.0	5.84
120.0	6.11
150.0	6.63
180.0	6.91
210.0	7.28
240.0	6.77
270.0	7.12

401	
30.0	3.48
60.0	5.21
90.0	6.07
120.0	6.16
150.0	6.59
180.0	7.00
210.0	7.24
240.0	6.84
270.0	6.31

418	
30.0	3.87
60.0	5.21
90.0	5.87
120.0	6.01
150.0	6.42
180.0	6.92
210.0	6.95
240.0	6.85
270.0	6.29

431	
30.0	3.67
60.0	5.17
90.0	5.77
120.0	5.99
150.0	6.59
180.0	6.86
210.0	7.30
240.0	7.00
270.0	6.37

447	
30.0	3.24
60.0	5.11
90.0	5.71
120.0	5.96
150.0	6.49
180.0	7.03
210.0	6.97
240.0	6.95
270.0	6.53

467	
30.0	2.83
60.0	4.81
90.0	5.62
120.0	5.96
150.0	6.26
180.0	7.08
210.0	6.98
240.0	6.99
270.0	6.44

490	
30.0	4.45
60.0	5.18
90.0	6.15
120.0	6.37
150.0	7.00
180.0	7.21
210.0	7.66
240.0	7.59
270.0	7.00

505

30.0	3.11
60.0	5.43
90.0	5.16
120.0	5.70
150.0	6.13
180.0	6.56
210.0	6.81
240.0	6.85
270.0	6.29

Moisture content data for West B neutron tube (distance = 115 cm)

Julian Date
116

Depth	Theta
30.0	3.63
60.0	5.89
90.0	5.83
120.0	7.24
150.0	6.55
180.0	4.85
210.0	4.73
240.0	4.39
270.0	4.76
300.0	4.46

130

30.0	6.46
60.0	7.99
90.0	5.92
120.0	7.00
150.0	6.49
180.0	5.13
210.0	4.69
240.0	4.45
270.0	4.79
300.0	4.34

137

30.0	5.06
60.0	7.21
90.0	6.23
120.0	7.18
150.0	6.71
180.0	5.16
210.0	4.77
240.0	4.38
270.0	4.83
300.0	4.48

157

30.0	4.16
60.0	6.03
90.0	5.82
120.0	7.21
150.0	6.88
180.0	5.51
210.0	4.84
240.0	4.51
270.0	4.84
300.0	4.39

163

30.0	3.82
60.0	5.57
90.0	5.74
120.0	7.14
150.0	6.67
180.0	5.57
210.0	4.87
240.0	4.38
270.0	4.84
300.0	4.38

171

30.0	4.72
60.0	5.31
90.0	5.72
120.0	7.18
150.0	6.67
180.0	5.67
210.0	4.77
240.0	4.34
270.0	5.00
300.0	4.44

178

30.0	3.92
60.0	5.15
90.0	5.76
120.0	7.26
150.0	6.62
180.0	5.75
210.0	4.87
240.0	4.48
270.0	4.71
300.0	4.37

185

30.0	3.48
60.0	4.76
90.0	5.12
120.0	6.77
150.0	6.44
180.0	5.83
210.0	4.89
240.0	4.43
270.0	4.76
300.0	4.27

192

30.0	3.26
60.0	4.60
90.0	5.09
120.0	6.98
150.0	6.27
180.0	6.30
210.0	4.98
240.0	4.48
270.0	4.86
300.0	4.40

198

30.0	3.42
60.0	4.95
90.0	5.49
120.0	6.56
150.0	6.56
180.0	6.40
210.0	5.42
240.0	4.89
270.0	5.06
300.0	4.40

205

30.0	3.76
60.0	4.15
90.0	4.61
120.0	6.09
150.0	5.81
180.0	5.86
210.0	4.84
240.0	4.42
270.0	4.56
300.0	4.33

213

30.0	7.32
60.0	4.58
90.0	4.97
120.0	6.60
150.0	6.12
180.0	6.42
210.0	5.42
240.0	5.09
270.0	5.19
300.0	4.83

220

30.0	6.51
60.0	6.74
90.0	4.31
120.0	5.65
150.0	5.43
180.0	6.05
210.0	5.26
240.0	4.54
270.0	4.66
300.0	4.45

225

30.0	7.82
60.0	7.88
90.0	4.71
120.0	5.90
150.0	5.53
180.0	6.23
210.0	5.52

240.0	4.99
270.0	5.17
300.0	4.78
234	
30.0	5.63
60.0	7.10
90.0	4.90
120.0	5.61
150.0	5.14
180.0	5.86
210.0	5.15
240.0	4.42
270.0	4.66
300.0	4.21
240	
30.0	4.73
60.0	6.46
90.0	4.94
120.0	5.51
150.0	5.02
180.0	5.55
210.0	5.35
240.0	4.94
270.0	5.19
300.0	4.64
257	
30.0	6.61
60.0	6.53
90.0	4.97
120.0	6.12
150.0	4.89
180.0	5.14
210.0	5.92
240.0	5.49
270.0	5.62
300.0	4.86
270	
30.0	6.48
60.0	6.52
90.0	4.45
120.0	4.57
150.0	4.21
180.0	4.39
210.0	4.84
240.0	4.32
270.0	4.51
300.0	4.31
277	
30.0	5.98
60.0	6.81
90.0	4.72
120.0	4.61
150.0	4.22
180.0	4.49
210.0	4.79
240.0	4.37
270.0	4.58
300.0	4.27
284	
30.0	10.29
60.0	12.58
90.0	6.03
120.0	4.79
150.0	4.29
180.0	4.40
210.0	4.79
240.0	4.50
270.0	4.70
300.0	4.35
297	
30.0	5.19
60.0	6.93
90.0	7.16
120.0	8.92
150.0	5.56
180.0	4.60
210.0	4.82
240.0	4.64
270.0	4.68
300.0	4.27
312	
30.0	5.31
60.0	5.97
90.0	5.96
120.0	7.62
150.0	6.84
180.0	5.44
210.0	4.84
240.0	4.49
270.0	4.65
300.0	4.34
332	
30.0	4.50
60.0	5.76
90.0	5.58
120.0	7.42
150.0	6.98
180.0	6.68
210.0	5.52
240.0	4.48
270.0	4.73
300.0	4.28
346	
30.0	4.32
60.0	5.31
90.0	5.46
120.0	6.68
150.0	6.81
180.0	6.96
210.0	6.18
240.0	4.63
270.0	4.54
300.0	4.15
360	
30.0	3.87
60.0	5.28
90.0	5.43
120.0	6.52
150.0	6.99
180.0	6.83
210.0	4.84
240.0	4.62
270.0	4.62
300.0	4.23
388	
30.0	3.99
60.0	5.23
90.0	5.34
120.0	6.77
150.0	6.49
180.0	6.86
210.0	7.17
240.0	5.81
270.0	4.93
300.0	4.32
401	
30.0	4.00
60.0	5.26
90.0	5.35
120.0	6.66
150.0	6.44
180.0	7.03
210.0	7.31
240.0	6.27
270.0	5.04
300.0	4.37
418	
30.0	3.87
60.0	5.21
90.0	5.87
120.0	6.58
150.0	6.30
180.0	6.70
210.0	7.29
240.0	6.68
270.0	5.21
300.0	4.48
431	
30.0	3.75
60.0	5.16
90.0	5.23
120.0	6.51
150.0	6.13
180.0	6.89
210.0	7.36
240.0	6.95
270.0	5.64
300.0	4.43
447	
30.0	3.45
60.0	5.00
90.0	5.20
120.0	6.42
150.0	6.38
180.0	6.88
210.0	7.32
240.0	7.02
270.0	5.68
300.0	4.49
467	

30.0	3.17
60.0	5.03
90.0	5.23
120.0	6.55
150.0	6.23
180.0	6.68
210.0	7.38
240.0	7.23
270.0	6.29
300.0	4.44
490	
30.0	7.47
60.0	5.89
90.0	5.21
120.0	6.69
150.0	6.08
180.0	7.23
210.0	7.34
240.0	7.83
270.0	7.25
300.0	5.20
505	
30.0	5.29
60.0	5.54
90.0	4.84
120.0	5.99
150.0	6.16
180.0	6.53
210.0	7.40
240.0	7.30
270.0	6.77
300.0	4.89

Moisture content data for West C neutron tube (distance = 265 cm)

Julian Date
130

Depth	Theta
30.0	5.80
60.0	6.14
90.0	6.73
120.0	7.11
150.0	7.08
180.0	7.95
210.0	7.80
240.0	8.89
270.0	8.35
300.0	8.02

137

30.0	4.98
60.0	6.34
90.0	6.90
120.0	7.34
150.0	6.94
180.0	8.24
210.0	7.91
240.0	8.87
270.0	8.44
300.0	8.22

157

30.0	4.29
60.0	5.68
90.0	6.63
120.0	7.36
150.0	7.49
180.0	7.99
210.0	7.85
240.0	8.75
270.0	8.48
300.0	8.01

163

30.0	8.02
60.0	5.52
90.0	6.54
120.0	7.44
150.0	7.23
180.0	7.94
210.0	8.16
240.0	8.94
270.0	8.48
300.0	8.02

171

30.0	4.66
60.0	5.37
90.0	6.29
120.0	7.20
150.0	7.23
180.0	7.94
210.0	7.92
240.0	8.76
270.0	8.49
300.0	8.02

178

30.0	4.48
60.0	5.22
90.0	6.05
120.0	7.08
150.0	7.30
180.0	7.93
210.0	8.71
240.0	8.25
270.0	8.11
300.0	3.78

185

30.0	4.55
60.0	5.39
90.0	6.25
120.0	7.45
150.0	7.36
180.0	8.15
210.0	8.16
240.0	9.12
270.0	8.79
300.0	8.24

192

30.0	4.91
60.0	5.06
90.0	6.06
120.0	6.53
150.0	8.07
180.0	9.46
210.0	7.78
240.0	9.32
270.0	8.98
300.0	8.59

198

30.0	3.44
60.0	5.14
90.0	5.67
0.0	6.67
150.0	5.80
180.0	7.52
210.0	7.73
240.0	8.60
270.0	8.29
300.0	8.01

205

30.0	4.35
60.0	4.97
90.0	5.65
120.0	6.46
150.0	6.06
180.0	7.09
210.0	7.13
240.0	8.12
270.0	8.08
300.0	7.78

213

30.0	7.23
60.0	5.68
90.0	6.68
120.0	7.33
150.0	7.04
180.0	7.26
210.0	7.07
240.0	8.24
270.0	7.97
300.0	8.02

220

30.0	6.72
60.0	8.28
90.0	6.10
120.0	6.84
150.0	6.55
180.0	7.45
210.0	7.34
240.0	8.39
270.0	8.39
300.0	8.36

225

30.0	7.45
60.0	8.47
90.0	7.12
120.0	6.82
150.0	6.78
180.0	7.67
210.0	7.16
240.0	8.72
270.0	8.34
300.0	8.95

234

30.0	5.45
60.0	7.72
90.0	6.94
120.0	7.45
150.0	7.12
180.0	7.97
210.0	7.69

240.0	8.98
270.0	8.46
300.0	8.31
240	
30.0	4.79
60.0	6.85
90.0	6.67
120.0	6.34
150.0	6.03
180.0	6.75
210.0	6.68
240.0	7.75
270.0	7.24
300.0	6.34
257	
30.0	5.86
60.0	5.88
90.0	6.00
120.0	6.20
150.0	5.33
180.0	6.52
210.0	6.29
240.0	7.05
270.0	6.55
300.0	6.27
270	
30.0	5.83
60.0	5.43
90.0	5.81
120.0	5.61
150.0	5.62
180.0	5.52
210.0	5.04
240.0	6.46
270.0	6.37
300.0	6.61
277	
30.0	5.37
60.0	5.87
90.0	5.37
120.0	5.53
150.0	5.24
180.0	5.83
210.0	5.65
240.0	6.55
270.0	6.37
300.0	6.30
284	
30.0	9.45
60.0	11.10
90.0	6.45
120.0	5.77
150.0	5.14
180.0	6.04
210.0	5.65
240.0	6.78
270.0	6.41
300.0	6.45
297	
30.0	4.92
60.0	6.37
90.0	8.12
120.0	8.90
150.0	9.47
180.0	10.08
210.0	6.86
240.0	6.67
270.0	6.23
300.0	6.39
312	
30.0	4.75
60.0	5.55
90.0	6.50
120.0	7.80
150.0	8.28
180.0	9.32
210.0	9.03
240.0	9.58
270.0	7.81
300.0	6.26
332	
30.0	4.05
60.0	5.45
90.0	6.12
120.0	6.76
150.0	7.09
180.0	8.66
210.0	8.59
240.0	9.26
270.0	8.96
300.0	8.07
346	
30.0	3.82
60.0	5.12
90.0	5.90
120.0	6.85
150.0	7.10
180.0	8.39
210.0	8.07
240.0	8.71
270.0	8.62
300.0	8.25
360	
30.0	3.64
60.0	5.17
90.0	5.03
120.0	5.84
150.0	6.55
180.0	6.79
210.0	8.05
240.0	8.00
270.0	8.36
300.0	8.26
388	
30.0	3.73
60.0	5.00
90.0	5.89
120.0	6.46
150.0	6.55
180.0	7.74
210.0	7.70
240.0	8.37
270.0	7.97
300.0	8.36
401	
30.0	3.69
60.0	5.13
90.0	5.83
120.0	6.67
150.0	6.58
180.0	7.68
210.0	7.49
240.0	8.35
270.0	8.06
300.0	7.88
418	
30.0	3.78
60.0	4.99
90.0	5.79
120.0	6.61
150.0	6.65
180.0	7.36
210.0	7.56
240.0	8.11
270.0	7.75
300.0	7.74
431	
30.0	4.08
60.0	4.96
90.0	5.83
120.0	6.41
150.0	6.39
180.0	7.51
210.0	7.45
240.0	8.06
270.0	7.84
300.0	7.71
447	
30.0	3.45
60.0	4.95
90.0	5.74
120.0	6.62
150.0	6.48
180.0	7.40
210.0	7.24
240.0	8.11
270.0	7.62
300.0	7.54
467	
30.0	3.13
60.0	4.85
90.0	5.66
120.0	6.55
150.0	6.36
180.0	7.40
210.0	7.17
240.0	8.21
270.0	7.37
300.0	7.58
490	

30.0	5.59
60.0	4.93
90.0	5.73
120.0	6.29
150.0	6.50
180.0	7.16
210.0	6.90
240.0	7.75
270.0	7.37
300.0	7.32
505	
30.0	4.26
60.0	4.98
90.0	5.51
120.0	6.04
150.0	6.21
180.0	7.06
210.0	6.82
240.0	7.85
270.0	7.15
300.0	7.36

Moisture content data for East A neutron tube (edge of canopy)

Julian Date
185

Depth	Theta
30.0	2.07
60.0	3.93
90.0	5.85
120.0	6.08
150.0	6.71
180.0	6.89
210.0	7.46
240.0	7.64
270.0	7.66
300.0	8.00

192

30.0	2.12
60.0	4.24
90.0	6.08
120.0	6.55
150.0	7.04
180.0	7.49
210.0	7.16
240.0	8.04
270.0	8.21
300.0	8.38

198

30.0	2.48
60.0	4.28
90.0	5.96
120.0	6.38
150.0	7.04
180.0	7.20
210.0	7.42
240.0	7.85
270.0	7.88
300.0	8.24

205

30.0	2.76
60.0	4.05
90.0	5.53
120.0	5.58
150.0	6.79
180.0	6.85
210.0	7.09
240.0	7.45
270.0	7.42
300.0	7.73

213

30.0	3.15
60.0	4.12
90.0	5.79
120.0	6.31
150.0	7.06
180.0	6.58
210.0	6.86
240.0	7.35
270.0	7.49
300.0	7.75

220

30.0	4.35
60.0	3.38
90.0	4.68
120.0	5.48
150.0	6.41
180.0	6.01
210.0	5.93
240.0	6.47
270.0	7.06
300.0	7.42

225

30.0	4.92
60.0	3.46
90.0	4.38
120.0	5.15
150.0	5.90
180.0	5.79
210.0	5.52
240.0	6.22
270.0	6.05
300.0	6.62

234

30.0	3.32
60.0	3.77
90.0	4.25
120.0	5.37
150.0	5.98
180.0	5.80
210.0	5.55
240.0	6.08
270.0	6.03
300.0	6.65

240

30.0	2.79
60.0	4.28
90.0	4.62
120.0	5.14
150.0	5.77
180.0	5.63
210.0	5.43
240.0	5.68
270.0	5.40
300.0	5.62

257

30.0	2.36
60.0	3.58
90.0	4.02
120.0	4.30
150.0	4.89
180.0	4.81
210.0	4.73
240.0	4.85
270.0	4.97
300.0	5.25

270

30.0	2.95
60.0	3.18
90.0	3.74
120.0	4.23
150.0	4.64
180.0	4.58
210.0	4.38
240.0	5.71
270.0	5.65
300.0	5.67

277

30.0	2.56
60.0	3.22
90.0	3.84
120.0	4.12
150.0	4.53
180.0	4.57
210.0	4.38
240.0	4.76
270.0	4.67
300.0	5.06

284

30.0	9.28
60.0	3.63
90.0	3.82
120.0	4.61
150.0	4.61
180.0	4.55
210.0	4.48
240.0	4.92
270.0	4.84
300.0	5.19

297

30.0	5.65
60.0	7.29
90.0	9.93
120.0	9.17
150.0	9.55
180.0	6.61
210.0	4.30

240.0	4.68
270.0	4.73
300.0	5.19

312

30.0	5.12
60.0	6.29
90.0	8.02
120.0	7.44
150.0	8.15
180.0	8.54
210.0	7.88
240.0	5.25
270.0	5.03
300.0	5.52

332

30.0	4.45
60.0	6.10
90.0	7.53
120.0	6.88
150.0	7.60
180.0	7.66
210.0	8.23
240.0	6.49
270.0	5.23
300.0	5.27

346

30.0	4.31
60.0	5.77
90.0	7.27
120.0	6.85
150.0	7.50
180.0	7.72
210.0	8.13
240.0	7.48
270.0	6.00
300.0	5.17

360

30.0	4.21
60.0	5.79
90.0	7.03
120.0	6.55
150.0	7.20
180.0	7.37
210.0	7.93
240.0	7.79
270.0	6.58
300.0	5.61

388

30.0	4.33
60.0	5.49
90.0	6.81
120.0	6.51
150.0	7.00
180.0	7.31
210.0	7.82
240.0	6.26
270.0	7.20
300.0	6.00

401

30.0	4.21
60.0	5.58
90.0	6.95
120.0	6.38
150.0	6.37
180.0	7.15
210.0	7.65
240.0	7.95
270.0	7.39
300.0	6.52

418

30.0	4.49
60.0	5.44
90.0	6.76
120.0	6.56
150.0	6.85
180.0	7.07
210.0	7.56
240.0	7.70
270.0	7.53
300.0	6.50

431

30.0	4.21
60.0	5.46
90.0	6.73
120.0	0.50
150.0	6.95
180.0	7.32
210.0	7.57
240.0	7.75
270.0	7.70
300.0	6.86

447

30.0	3.96
60.0	5.54
90.0	6.62
120.0	6.20
150.0	6.82
180.0	6.90
210.0	7.57
240.0	7.70
270.0	7.81
300.0	7.00

467

30.0	3.40
60.0	5.37
90.0	6.47
120.0	6.10
150.0	6.62
180.0	6.94
210.0	7.32
240.0	7.82
270.0	7.53
300.0	7.28

490

30.0	3.13
60.0	5.31
90.0	6.19
120.0	6.15
150.0	6.69
180.0	6.85
210.0	7.18
240.0	7.61
270.0	7.77
300.0	7.47

505

30.0	2.51
60.0	4.35
90.0	5.91
120.0	6.20
150.0	6.42
180.0	6.40
210.0	7.04
240.0	7.34
270.0	7.53
300.0	7.24

Moisture content data for East B neutron tube (distance = 115 cm)

Julian Date
130

Depth	Theta
30.0	8.58
60.0	9.49
90.0	7.81
120.0	8.18
150.0	8.34
180.0	8.04
210.0	9.03
240.0	9.06
270.0	9.55
300.0	9.57

137

30.0	6.69
60.0	8.53
90.0	8.82
120.0	8.71
150.0	8.43
180.0	8.15
210.0	8.43
240.0	8.80
270.0	9.32
300.0	9.32

157

30.0	4.40
60.0	6.54
90.0	7.70
120.0	8.41
150.0	8.13
180.0	8.16
210.0	8.24
240.0	8.62
270.0	8.74
300.0	5.19

163

30.0	3.85
60.0	6.05
90.0	7.50
120.0	8.48
150.0	8.17
180.0	8.02
210.0	8.40
240.0	8.46
270.0	8.77
300.0	9.16

171

30.0	4.40
60.0	5.87
90.0	6.72
120.0	7.66
150.0	7.72
180.0	7.57
210.0	8.02
240.0	8.21
270.0	8.36
300.0	8.78

178

30.0	4.02
60.0	5.81
90.0	6.31
120.0	7.21
150.0	7.45
180.0	7.88
210.0	8.35
240.0	8.56
270.0	8.63
300.0	8.87

185

30.0	3.32
60.0	5.34
90.0	6.51
120.0	7.18
150.0	7.73
180.0	7.53
210.0	7.97
240.0	8.36
270.0	8.54
300.0	8.98

192

30.0	2.25
60.0	4.50
90.0	5.46
120.0	6.46
150.0	7.10
180.0	7.38
210.0	7.98
240.0	8.18
270.0	8.50
300.0	8.70

198

30.0	1.88
60.0	4.09
90.0	5.06
120.0	6.12
150.0	6.82
180.0	6.88
210.0	7.34
240.0	7.34
270.0	8.24
300.0	8.67

205

30.0	3.05
60.0	3.85
90.0	4.73
120.0	6.20
150.0	6.96
180.0	6.68
210.0	6.93
240.0	7.56
270.0	7.79
300.0	7.63

213

30.0	5.37
60.0	4.76
90.0	5.39
120.0	5.99
150.0	7.45
180.0	7.71
210.0	6.75
240.0	6.69
270.0	7.07
300.0	7.53

220

30.0	7.22
60.0	4.89
90.0	5.01
120.0	6.38
150.0	7.01
180.0	7.49
210.0	6.86
240.0	6.75
270.0	7.24
300.0	8.07

225

30.0	8.19
60.0	4.60
90.0	4.12
120.0	5.48
150.0	6.21
180.0	7.05
210.0	6.50
240.0	6.28
270.0	6.49
300.0	7.58

234

30.0	4.58
60.0	4.04
90.0	3.78
120.0	4.77
150.0	5.38
180.0	5.70
210.0	5.46

240.0 5.41
270.0 5.84
300.0 6.90

240

30.0 3.05
60.0 3.85
90.0 4.00
120.0 4.54
150.0 5.15
180.0 5.94
210.0 5.60
240.0 5.57
270.0 5.81
300.0 6.66

257

30.0 3.67
60.0 3.16
90.0 3.46
120.0 4.24
150.0 4.47
180.0 4.54
210.0 4.76
240.0 4.83
270.0 6.23
300.0 6.30

270

30.0 4.38
60.0 5.26
90.0 3.84
120.0 4.39
150.0 4.60
180.0 4.79
210.0 5.55
240.0 5.66
270.0 5.98
300.0 6.74

277

30.0 4.28
60.0 3.04
90.0 3.46
120.0 4.03
150.0 3.98
180.0 4.09
210.0 4.73
240.0 4.64
270.0 4.98
300.0 5.43

284

30.0 12.31
60.0 10.44
90.0 3.58
120.0 4.08
150.0 3.91
180.0 4.16
210.0 4.74
240.0 4.63
270.0 5.04
300.0 5.55

297

30.0 6.03
60.0 7.59
90.0 9.57
120.0 10.88
150.0 11.01
180.0 10.85
210.0 11.16
240.0 6.48
270.0 4.96
300.0 5.56

312

30.0 6.13
60.0 6.82
90.0 7.50
120.0 8.40
150.0 8.74
180.0 8.77
210.0 9.62
240.0 10.27
270.0 10.59
300.0 10.66

332

30.0 4.40
60.0 6.37
90.0 7.59
120.0 7.53
150.0 7.88
180.0 7.99
210.0 8.38
240.0 8.79
270.0 9.22
300.0 10.32

346

30.0 4.31
60.0 5.77
90.0 7.27
120.0 6.85
150.0 7.50
180.0 7.72
210.0 8.13
240.0 7.48
270.0 6.00
300.0 5.17

360

30.0 3.74
60.0 5.99
90.0 6.75
120.0 7.52
150.0 7.29
180.0 7.39
210.0 7.81
240.0 8.44
270.0 9.21
300.0 9.71

388

30.0 3.61
60.0 5.92
90.0 6.64
120.0 7.10
150.0 7.35
180.0 7.26
210.0 7.84
240.0 8.12
270.0 9.00
300.0 9.16

401

30.0 3.51
60.0 5.93
90.0 6.55
120.0 7.10
150.0 7.24
180.0 7.29
210.0 7.84
240.0 8.02
270.0 8.65
300.0 9.26

418

30.0 3.79
60.0 5.90
90.0 6.46
120.0 7.01
150.0 7.29
180.0 7.23
210.0 7.70
240.0 7.80
270.0 8.49
300.0 8.95

431

30.0 3.32
60.0 5.66
90.0 5.75
120.0 6.32
150.0 7.05
180.0 7.28
210.0 7.08
240.0 7.44
270.0 7.79
300.0 8.45

447

30.0 3.07
60.0 5.65
90.0 6.50
120.0 6.96
150.0 7.08
180.0 7.10
210.0 7.48
240.0 7.89
270.0 8.49
300.0 8.76

467

30.0 2.19
60.0 5.40
90.0 6.26
120.0 7.02
150.0 7.02
180.0 7.01
210.0 7.53
240.0 7.66
270.0 8.31
300.0 8.73

490

```
 30.0  4.30
 60.0  5.55
 90.0  6.23
120.0  6.51
150.0  6.88
180.0  7.07
210.0  7.20
240.0  7.32
270.0  8.15
300.0  8.44
    505
 30.0  2.05
 60.0  4.41
 90.0  5.39
120.0  5.97
150.0  6.41
180.0  6.60
210.0  7.25
240.0  8.03
270.0  8.31
300.0  8.66
```

Moisture content data for East C neutron tube (distance = 265 cm)

Julian Date
106

Depth	Theta
15.0	0.84
60.0	6.43
90.0	7.37
120.0	7.08
150.0	7.00
180.0	7.34
210.0	7.16
240.0	7.49
270.0	7.98
300.0	8.79

130

45.0	7.17
60.0	7.21
90.0	7.38
120.0	7.16
150.0	7.32
180.0	7.62
210.0	7.46
240.0	7.81
270.0	8.20
300.0	8.79

137

45.0	6.96
60.0	7.61
90.0	8.21
120.0	7.09
150.0	7.16
180.0	7.45
210.0	7.32
240.0	7.63
270.0	8.10
300.0	8.73

144

45.0	5.86
60.0	7.10
90.0	8.14
120.0	7.49
150.0	7.11
180.0	7.39
210.0	7.08
240.0	7.36
270.0	7.98
300.0	8.40

157

15.0	1.78
60.0	6.60
90.0	7.88
120.0	7.45
150.0	7.38
180.0	7.63
210.0	7.29
240.0	7.66
270.0	7.90
300.0	8.53

177

45.0	4.11
60.0	4.81
90.0	6.45
120.0	6.65
150.0	7.01
180.0	7.44
210.0	7.41
240.0	7.68
270.0	7.70
300.0	8.29

192

45.0	2.68
60.0	3.90
90.0	5.89
120.0	6.09
150.0	6.24
180.0	7.24
210.0	8.47
240.0	9.01
270.0	7.08
300.0	9.69

205

45.0	2.69
60.0	3.27
90.0	4.50
120.0	5.20
150.0	5.42
180.0	6.34
210.0	6.23
240.0	6.98
270.0	7.08
300.0	7.51

225

45.0	9.08
60.0	8.03
90.0	4.66
120.0	4.95
150.0	5.26
180.0	6.02
210.0	6.06
240.0	6.41
270.0	6.85
300.0	6.91

240

15.0	0.66
60.0	3.22
90.0	3.88
120.0	4.02
150.0	4.77
180.0	5.18
210.0	4.80
240.0	5.55
270.0	5.93
300.0	5.91

249

45.0	3.11
60.0	3.69
90.0	3.94
120.0	4.26
150.0	5.18
180.0	5.33
210.0	5.30
240.0	5.95
270.0	6.44
300.0	6.43

257

45.0	2.69
60.0	4.11
90.0	4.31
120.0	4.92
150.0	5.62
180.0	5.75
210.0	5.20
240.0	5.96
270.0	6.73
300.0	6.44

270

45.0	2.59
60.0	3.80
90.0	3.26
120.0	3.75
150.0	4.40
180.0	4.26
210.0	4.33
240.0	5.32
270.0	5.42
300.0	5.89

277

45.0	6.20
60.0	4.02
90.0	3.42
120.0	3.71
150.0	4.67
180.0	4.86
210.0	4.23

240.0 4.93
270.0 5.46
300.0 5.57
291
45.0 10.28
60.0 11.52
90.0 13.37
120.0 11.97
150.0 9.85
180.0 4.46
210.0 4.20
240.0 5.06
270.0 5.49
300.0 5.43
326
45.0 5.58
60.0 6.30
90.0 7.49
120.0 6.87
150.0 7.36
180.0 7.80
210.0 8.05
240.0 8.91
270.0 9.59
300.0 10.04
410
45.0 5.09
60.0 5.55
90.0 6.40
120.0 6.48
150.0 6.62
180.0 7.17
210.0 7.35
240.0 7.40
270.0 7.98
300.0 8.61
418
45.0 4.71
60.0 5.84
90.0 6.49
120.0 6.49
150.0 6.90
180.0 7.20
210.0 7.20
240.0 7.60
270.0 8.18
300.0 8.94
424
45.0 5.90
60.0 6.34
90.0 6.31
120.0 6.56
150.0 7.18
180.0 7.16
210.0 7.20
240.0 7.97
270.0 7.38
300.0 9.07
431
45.0 4.08
60.0 4.96
90.0 5.83
120.0 6.41
150.0 6.39
180.0 7.51
210.0 7.45
240.0 8.06
270.0 7.84
300.0 7.71
447
15.0 0.92
60.0 5.51
90.0 6.36
120.0 6.23
150.0 6.59
180.0 7.04
210.0 7.08
240.0 7.40
270.0 8.02
300.0 8.97
467
45.0 5.00
60.0 6.27
90.0 6.21
120.0 6.62
150.0 7.07
180.0 7.00
210.0 7.33
240.0 8.01
270.0 8.44
300.0 8.18
490
45.0 6.43
60.0 6.13
90.0 6.08
120.0 6.58
150.0 7.20
180.0 7.44
210.0 7.47
240.0 7.79
270.0 8.45
300.0 9.13
505
45.0 5.02
60.0 5.77
90.0 5.98
120.0 6.28
150.0 6.75
180.0 6.90
210.0 6.99
240.0 7.29
270.0 8.10
300.0 8.54

Moisture content data for North A neutron tube (edge of canopy)

Julian date

346	
Depth	Theta
30.0	4.17
60.0	5.70
90.0	6.43
120.0	7.14
150.0	7.35
180.0	7.37
210.0	7.82
240.0	8.62
270.0	8.66
300.0	9.09

401	
30.0	3.98
60.0	5.49
90.0	6.14
120.0	6.78
150.0	6.89
180.0	7.22
210.0	7.28
240.0	7.67
270.0	8.11
300.0	7.97

418	
30.0	4.21
60.0	5.42
90.0	6.13
120.0	6.54
150.0	6.66
180.0	6.78
210.0	7.28
240.0	7.72
270.0	8.06
300.0	7.81

431	
30.0	3.87
60.0	5.45
90.0	5.92
120.0	6.58
150.0	6.87
180.0	6.96
210.0	7.16
240.0	7.56
270.0	8.05
300.0	7.87

447	
30.0	3.39
60.0	5.46
90.0	5.88
120.0	6.51
150.0	6.62
180.0	6.92
210.0	7.15
240.0	7.49
270.0	7.78
300.0	7.82

467	
30.0	2.71
60.0	5.23
90.0	5.87
120.0	6.40
150.0	6.77
180.0	7.01
210.0	7.27
240.0	7.53
270.0	7.66
300.0	7.70

490	
30.0	4.02
60.0	4.65
90.0	5.68
120.0	6.18
150.0	6.62
180.0	6.70
210.0	7.08
240.0	7.40
270.0	7.84
300.0	7.62

505	
30.0	3.06
60.0	4.38
90.0	5.58
120.0	6.18
150.0	6.48
180.0	6.96
210.0	7.08
240.0	7.26
270.0	7.60
300.0	7.48

Moisture content data for North B neutron tube (distance = 115 cm)

Julian Date

220	
Depth	Theta
30.0	4.77
60.0	5.93
90.0	4.29
120.0	5.58
150.0	5.79
180.0	6.14
210.0	6.19
240.0	6.13
270.0	5.67
300.0	5.46

234	
30.0	4.16
60.0	8.43
90.0	5.52
120.0	5.60
150.0	6.16
180.0	6.36
210.0	6.34
240.0	6.06
270.0	5.68
300.0	5.49

257	
30.0	6.17
60.0	8.45
90.0	8.14
120.0	6.96
150.0	6.70
180.0	7.26
210.0	6.87
240.0	6.51
270.0	6.20
300.0	5.96

270	
30.0	4.68
60.0	7.62
90.0	6.94
120.0	5.35
150.0	5.49
180.0	5.41
210.0	5.15
240.0	4.95
270.0	4.70
300.0	4.67

277	
30.0	5.72
60.0	8.74
90.0	8.52
120.0	6.12
150.0	5.88
180.0	6.03
210.0	5.37
240.0	5.16
270.0	5.11
300.0	4.55

284	
30.0	8.81
60.0	12.38
90.0	10.83
120.0	5.96
150.0	5.17
180.0	5.52
210.0	5.11
240.0	5.02
270.0	4.86
300.0	4.50

297	
30.0	4.69
60.0	7.96
90.0	8.87
120.0	9.67
150.0	9.74
180.0	10.05
210.0	9.53
240.0	7.45
270.0	5.23
300.0	4.65

312	
30.0	4.19
60.0	6.56
90.0	6.58
120.0	7.47
150.0	7.78
180.0	8.41
210.0	8.87
240.0	8.86
270.0	8.21
300.0	7.69

332	
30.0	3.74
60.0	6.30
90.0	6.57
120.0	6.86
150.0	6.78
180.0	7.28
210.0	8.07
240.0	8.36
270.0	8.12
300.0	8.31

346	
30.0	3.39
60.0	6.13
90.0	6.14
120.0	6.55
150.0	6.65
180.0	7.26
210.0	7.77
240.0	7.74
270.0	7.74
300.0	8.13

360	
30.0	3.13
60.0	6.09
90.0	6.13
120.0	6.62
150.0	6.67
180.0	6.90
210.0	7.41
240.0	8.03
270.0	7.61
300.0	7.84

388	
30.0	3.41
60.0	5.89
90.0	3.07
120.0	6.47
150.0	6.47
180.0	6.66
210.0	7.24
240.0	7.80
270.0	7.48
300.0	7.80

401	
30.0	3.20
60.0	5.71
90.0	6.00
120.0	6.46
150.0	6.51
180.0	6.85
210.0	7.32
240.0	7.74
270.0	7.43
300.0	7.65

418	
30.0	3.16
60.0	5.74
90.0	5.93
120.0	6.44
150.0	6.39
180.0	6.70
210.0	7.20

240.0	7.73
270.0	7.17
300.0	7.50
431	
30.0	2.72
90.0	5.60
90.0	5.66
120.0	6.37
150.0	6.42
180.0	6.65
210.0	7.24
240.0	7.58
270.0	7.16
300.0	7.65
447	
30.0	2.30
60.0	5.52
90.0	5.74
120.0	6.32
150.0	6.35
180.0	6.77
210.0	7.19
240.0	7.32
270.0	7.14
300.0	7.23
467	
30.0	1.81
60.0	5.49
90.0	5.72
120.0	6.24
150.0	6.32
180.0	6.51
210.0	7.08
240.0	7.53
270.0	7.12
300.0	7.52
490	
30.0	4.38
60.0	5.73
90.0	5.42
120.0	6.83
150.0	6.59
180.0	6.56
210.0	7.34
240.0	7.70
270.0	6.91
300.0	6.62
505	
30.0	3.36
60.0	5.27
90.0	6.10
120.0	6.45
150.0	6.62
180.0	7.02
210.0	7.21
240.0	7.34
270.0	7.03
300.0	7.20

Moisture content data for North C neutron tube (distance = 265 cm)

Julian Date

234	
Depth	Theta
30.0	4.60
60.0	7.85
90.0	4.71
120.0	5.69
150.0	6.53
180.0	6.85
210.0	6.15
240.0	5.64
270.0	5.23
300.0	5.45

257	
30.0	5.61
60.0	7.50
90.0	5.46
120.0	5.80
150.0	6.57
180.0	7.39
210.0	5.77
240.0	5.76
270.0	5.24
300.0	4.84

270	
30.0	5.20
60.0	7.79
90.0	5.49
120.0	5.62
150.0	5.79
180.0	6.33
210.0	5.38
240.0	4.92
270.0	4.93
300.0	5.28

277	
30.0	4.91
60.0	7.31
90.0	5.37
120.0	5.14
150.0	5.88
180.0	5.82
210.0	5.03
240.0	4.53
270.0	4.43
300.0	4.59

284	
30.0	9.19
60.0	11.69
90.0	6.17
120.0	5.09
150.0	5.62
180.0	5.74
210.0	4.85
240.0	4.43
270.0	4.38
300.0	5.22

297	
30.0	4.45
60.0	6.99
90.0	8.04
120.0	8.50
150.0	6.93
180.0	5.89
210.0	4.79
240.0	4.51
270.0	4.40
300.0	4.60

312	
30.0	4.36
60.0	6.03
90.0	6.62
120.0	7.66
150.0	7.75
180.0	7.11
210.0	4.73
240.0	4.35
270.0	4.35
300.0	4.49

332	
30.0	3.71
60.0	5.87
90.0	6.12
120.0	7.09
150.0	7.36
180.0	7.24
210.0	5.50
240.0	4.60
270.0	4.66
300.0	4.75

346	
30.0	4.24
60.0	6.16
90.0	6.92
120.0	7.57
150.0	7.65
180.0	7.52
210.0	8.39
240.0	8.52
270.0	9.41
300.0	9.48

360	
30.0	3.44
60.0	5.53
90.0	6.13
120.0	6.85
150.0	7.04
180.0	7.12
210.0	6.20
240.0	4.89
270.0	4.78
300.0	4.98

388	
30.0	3.61
60.0	5.65
90.0	5.81
120.0	6.68
150.0	6.91
180.0	7.14
210.0	6.34
240.0	5.24
270.0	5.17
300.0	5.23

401	
30.0	3.36
60.0	5.37
90.0	5.82
120.0	6.67
150.0	6.89
180.0	7.17
210.0	6.47
240.0	5.31
270.0	5.22
300.0	5.32

418	
30.0	3.42
60.0	5.45
90.0	5.78
120.0	6.62
150.0	6.94
180.0	7.16
210.0	6.67
240.0	5.51
270.0	5.37
300.0	5.39

431	
30.0	3.16
60.0	5.45
90.0	5.68
120.0	0.30
150.0	6.69
180.0	7.10
210.0	6.63

240.0	5.56
270.0	5.36
300.0	5.41
447	
30.0	3.00
60.0	5.31
90.0	5.63
120.0	6.41
150.0	6.66
180.0	6.96
210.0	6.69
240.0	5.55
270.0	5.59
300.0	5.41
467	
30.0	2.52
60.0	5.36
90.0	5.68
120.0	6.46
150.0	6.59
180.0	6.92
210.0	6.74
240.0	5.88
270.0	4.89
300.0	5.51
490	
30.0	4.92
60.0	5.49
90.0	5.56
120.0	6.47
150.0	6.82
180.0	6.80
210.0	6.48
240.0	5.84
270.0	5.58
300.0	5.76
505	
30.0	4.04
60.0	5.40
90.0	5.26
120.0	6.12
150.0	6.48
180.0	6.69
210.0	6.05
240.0	5.38
270.0	5.61
300.0	5.55

APPENDIX D

Appendix D includes weekly average wind speed and class A pan evaporation and precipitation events for the study period March, 1985 through August, 1986. Data was collected at the New Mexico Institute of Mining and Technology weather station within the Sevilleta National Wildlife Refuge.

Precipitation recorded by a tipping bucket rain gauge, Sevilleta National Wildlife Refuge.

Date 1985	Julian Date	Precip (mm)
3-12	71	0.6
3-15	74	8.4
3-19	78	9
4-11	101	0.2
4-22	112	0.4
4-28	118	19
5-4	125	4.6
5-17	137	0.4
5-19	139	0.4
5-20	140	1
5-26	146	2.4
6-1	152	0.6
6-5	156	1.8
6-6	157	0.2
6-20	171	9
7-14	195	0.6
7-19	200	3.6
7-21	202	2.2
7-22	203	1.2
7-23	204	7.4
8-3	215	10
8-11	223	9.2
8-22	234	2.6
9-2	245	6.6
9-4	247	9.6
9-11	254	3.6
9-20	263	0.6
9-28	271	4.6
10-8	281	1
10-9	282	13.4
10-10	283	17.8
10-16	289	27
10-20	293	0.2
10-31	304	3.8
11-30	334	2.4

Date 1986	Julian Date	Precip (mm)
1-7	7	4.4
1-23	23	1.4
2-8	39	1.6
2-9	40	3.6
2-10	41	0.6
3-10	69	0.6
3-14	73	0.5
3-17	76	1.2
4-2	92	0.4
4-4	94	1.2
4-18	108	0.4
5-1	121	15
5-3	123	3
5-17	137	1.5
5-31	151	2.6
6-2	153	0.4
6-12	163	0.4
6-24	175	20.4
6-25	176	7.6
7-8	189	8.6
7-18	199	2.6
7-20	201	6.6
8-3	215	1
8-7	219	2
8-8	220	2.6
8-10	222	0.4
8-23	235	3
8-25	237	10
8-26	238	1.1

Average class A pan evaporation and averag wind speed data.

Date	Julian Date	Pan Evap (cm/d)	Wind Speed (km/d)
1985			
3-3	62	0.501	140.43
3-7	66	0.440	104.73
3-10	69	0.340	76.98
3-16	75	0.212	80.30
3-21	80	0.650	101.90
3-25	84	0.656	99.33
3-28	87	0.617	169.75
4-1	91	0.461	95.13
4-4	93	0.803	127.57
4-7	96	0.097	124.50
4-11	101	0.521	80.10
4-14	104	0.675	59.50
4-18	108	0.852	122.20
4-21	111	0.631	110.28
4-25	115	0.840	115.77
4-28	118	0.600	77.95
5-2	122	0.679	60.43
5-5	125	0.576	66.20
5-9	129	0.796	72.20
5-12	132	0.786	130.70
5-16	136	1.026	62.67
5-21	141	0.945	59.59
5-27	147	0.915	66.60
6-3	154	0.823	85.59
6-9	160	1.064	62.98
6-16	167	0.901	79.35
6-24	175	1.205	97.79
6-29	180	1.625	117.58
7-6	187	0.715	32.92
7-14	195	1.007	65.02
7-20	201	0.543	56.59
7-27	208	0.568	40.11
8-4	216	0.333	41.54
8-11	223	0.419	59.87
8-18	230	0.698	64.41
8-25	237	0.871	53.75
9-2	245	0.583	
9-13	256	0.432	
9-24	267	0.515	63.56
10-1	274	0.400	66.11
10-8	281		88.70
10-15	288		38.33

12-10	344	(.184)	61.37
12-17	351	0.029	42.00
12-24	358	0.097	34.47
12-31	365	0.161	40.84
1986			37.59
1-7	7	0.104	18.66
1-14	14	0.096	46.80
1-21	21	0.162	51.54
2-11	42	0.190	58.33
2-18	49	0.515	94.60
2-23	54		112.43
3-11	70	0.507	84.36
3-25	84	0.620	58.56
4-1	91	0.539	92.37
4-7	97		195.73
4-15	104	0.829	20.51
4-22	112	0.805	47.80
4-29	119	0.805	91.56
5-6	125	0.787	119.71
5-11	131	0.801	72.60
5-14	134	1.177	92.28
5-19	139	1.028	
5-26	146	0.573	
6-3	154	0.630	52.41
6-10	161	1.065	78.54
6-17	168	1.095	82.57
6-24	175	4.310	54.81
7-1	182		61.36
7-8	189		73.29
7-15	196	0.870	74.10
7-22	203	1.590	56.97
7-29	210	0.900	44.39
8-5	217	1.239	55.51
8-12	224	1.235	57.94
8-18	230	1.260	50.58

APPENDIX E

This appendix includes the results of the steady-state porometer and pressure bomb monitoring conducted July 25-26, 1986. This experiment was possible through the cooperation of Dr. Paul Kemp, curator of the National History Museum, Albuquerque, New Mexico.

Steady State Porometer
July 25-26, 1986
Sevilleta Wildlife Refuge

Plant: Dalea Scoparia Xerophyte Time 11:15	Sample 1	Sample 2	Sample 3	Sample 4
Aperature Set (sq cm)	1.5	1.41	0.75	
Chamber Temp (C)	30.2	31	32.2	33.4
Leaf Temp (C)	30.2	31	32.2	33.4
Rel. Humidity (%)	17.6	17.6	18	17.6
Quantum (mmol/s-sq m)	1860	1800	1870	1080
Resistance (s/cm)	5.9	1.4	1.66	2.15
Transpir (mg-sq cm/s)	4.18	17.43	15.27	13.02
Comments	stem		stem/leaf,1:1	

Plant: Dalea Scoparia Time 11:15	Sample 5	Sample 6	Sample 7	Sample 8
Aperature Set (sq cm)				0.75
Chamber Temp (C)	34	34	34.4	34
Leaf Temp (C)	33.9	34	34.4	34
Rel. Humidity (%)	18	17.6	17.6	17.6
Quantum (mmol/s-sq m)	1960	1650	2020	1040
Resistance (s/cm)	2.11	2.34	6.32	1.24
Transpir (mg-sq cm/s)	13.44	12.43	4.88	22.18
Comments			stem	

Plant: Dalea Scoparia Time 13:15	Sample 1	Sample 2	Sample 3	Sample 4
Aperature Set (sq cm)	1	0.6	0.8	1
Chamber Temp (C)	35.2	35	35	35
Leaf Temp (C)	35.2	34.6	34.9	35
Rel. Humidity (%)	10	9.6	10	9.6
Quantum (mmol/s-sq m)	2020	1970	1210	2040
Resistance (s/cm)	1.52	2.57	1.69	3.38
Transpir (mg-sq cm/s)	21.59	12.98	19.12	10.12
Comments				

Plant:
Dalea Scoparia

Time 13:15	Sample 5	Sample 6	Sample 7
Aperature Set (sq cm)	0.8	1	1
Chamber Temp (C)	35.2	35	35
Leaf Temp (C)	35.2	35	35
Rel. Humidity (%)	10	10	10
Quantum (mmol/s-sq m)	2090	2030	830
Resistance (s/cm)	1.3	6.39	5.96
Transpir (mg-sq cm/s)	24.91	5.44	5.81
Comments		stem	stem

Plant:
Dalea Scoparia

Time 16:30	Sample 1	Sample 2	Sample 3	Sample 4
Aperature Set (sq cm)				
Chamber Temp (C)	35.4	35.6	35.6	35.6
Leaf Temp (C)	35.5	35.7	35.6	35.6
Rel. Humidity (%)	10.4	10.4	10.8	10
Quantum (mmol/s-sq m)	1420	950	1400	1420
Resistance (s/cm)	1.25	2.93	1.62	3.55
Transpir (mg-sq cm/s)	25.85	11.87	20.52	9.99
Comments	leaves	leaves	leaves	leaves

Plant:
Dalea Scoparia

Time 16:30	Sample 5	Sample 6	Sample 7
Aperature Set (sq cm)			
Chamber Temp (C)	35.2	35.4	35.6
Leaf Temp (C)	35.2	35.3	35.6
Rel. Humidity (%)	10.4	10.8	11.2
Quantum (mmol/s-sq m)	930	950	610
Resistance (s/cm)	4.54	4.72	4.49
Transpir (mg-sq cm/s)	7.6	7.32	7.8
Comments	leaves	stem	stem

Plant:
Dalea Scoparia

Time 05:00	Sample 1	Sample 2	Sample 3	Sample 4
Aperature Set (sq cm)	0.8	0.5	0.3	0.5
Chamber Temp (C)	20.8	20.6	20.4	20.8
Leaf Temp (C)	20.8	20.5	20.4	20.8
Rel. Humidity (%)	18.8	19.6	19.6	18
Quantum (mmol/s-sq m)	0	0	0	0
Resistance (s/cm)	6.65	5.11	2.88	5.71
Transpir (mg-sq cm/s)	2.163	2.7	2.7	2.53
Comments				null adjust?

Plant:
Dalea Scoparia

Time 05:00	Sample 5	Sample 6
Aperature Set (sq cm)	0.85	0.65
Chamber Temp (C)	20.8	20.6
Leaf Temp (C)	20.8	20.6
Rel. Humidity (%)	17.2	14
Quantum (mmol/s-sq m)	0	0
Resistance (s/cm)	10.4	9.27
Transpir (mg-sq cm/s)	1.415	1.634
Comments	stem(n adj?)	stem

Plant:
Dalea Scoparia

Time 09:00	Sample 1	Sample 2	Sample 3	Sample 4
Aperature Set (sq cm)	0.85	0.45	0.65	0.5
Chamber Temp (C)	27.2	27.6	28.2	29
Leaf Temp (C)	27.1	27.6	28.4	29.2
Rel. Humidity (%)	12.4	12.4	12.4	12.4
Quantum (mmol/s-sq m)	1050	1260	205	1100
Resistance (s/cm)	1.3	0.96	3.43	0.99
Transpir (mg-sq cm/s)	15.55	21	6.807	22.26
Comments	stem	stem	leaves	leaves

Plant: Dalea Scoparia Time 09:00	Sample 5	Sample 6	Sample 7
Aperature Set (sq cm)	0.45	0.8	1
Chamber Temp (C)	30	30.4	31.4
Leaf Temp (C)	30.1	30.2	31.4
Rel. Humidity (%)	12	12	12
Quantum (mmol/s-sq m)	1300	81.99	1680
Resistance (s/cm)	3.49	5.57	4.55
Transpir (mg-sq cm/s)	7.33	4.82	6.118
Comments	stem	leaves	leaves

Plant: Prosopis Time 11:30	Phreatophyte Sample 1	Sample 2	Sample 3	Sample 4
Aperature Set (sq cm)	5	5	5	5
Chamber Temp (C)	34	34	33	32.8
Leaf Temp (C)	34	33.9	32.9	32.8
Rel. Humidity (%)	18.4	18.4	32.8	29.6
Quantum (mmol/s-sq m)	1600	1970	2070	1930
Resistance (s/cm)	1.79	1.74	0.6	0.72
Transpir (mg-sq cm/s)	15.99	16	31.26	28.35
Comments			null adj?	

Plant: Prosopis Time 11:30	Sample 5
Aperature Set (sq cm)	5
Chamber Temp (C)	33.2
Leaf Temp (C)	33.2
Rel. Humidity (%)	18.8
Quantum (mmol/s-sq m)	1040
Resistance (s/cm)	1.52
Transpir (mg-sq cm/s)	17.46
Comments	

Plant: Prosopis Time 13:15	Sample 1	Sample 2	Sample 3	Sample 4
Aperature Set (sq cm)	5	3	3	2.2
Chamber Temp (C)	35.2	35.6	35.8	36
Leaf Temp (C)	35.1	35.4	35.8	35.9
Rel. Humidity (%)	16.4	11.2	10	10
Quantum(mmol/s-sq m)	780	1070	2040	2070
Resistance (s/cm)	1.81	1.83	4.32	2.37
Transpir (mg-sq cm/s)	16.84	18.1	8.47	14.69
Comments	null adj?			

Plant:
Prosopis
Time 13:15 Sample 5

Aperature Set (sq cm)	2
Chamber Temp (C)	36.2
Leaf Temp (C)	36.1
Rel. Humidity (%)	9.6
Quantum (mmol/s-sq m)	2030
Resistance (s/cm)	3.03
Transpir (mg-sq cm/s)	11.8
Comments	

Plant:
Prosopis

Time 16:30	Sample 1	Sample 2	Sample 3	Sample 4
Aperature Set (sq cm)				
Chamber Temp (C)	34	34.6	34.6	34.8
Leaf Temp (C)	33.9	34.6	34.5	34.7
Rel. Humidity (%)	11.2	10	10.8	10.8
Quantum (mmol/s-sq m)	250	1230	1230	990
Resistance (s/cm)	1.73	1.33	1.4	2.69
Transpir (mg-sq cm/s)	17.54	23.34	22.05	12.16
Comments	leaves			

Plant:
Prosopis
Time 16:30 Sample 5

Aperature Set (sq cm)	
Chamber Temp (C)	34.8
Leaf Temp (C)	34.7
Rel. Humidity (%)	10.8
Quantum (mmol/s-sq m)	650
Resistance (s/cm)	2.43
Transpir (mg-sq cm/s)	13.38
Comments	

Plant:
Prosopis

Time 05:00	Sample 1	Sample 2	Sample 3
Aperature Set (sq cm)	2.6	1.6	2.75
Chamber Temp (C)	20.6	19.8	19.8
Leaf Temp (C)	20.6	19.8	19.8
Rel. Humidity (%)	17.2	16.4	16
Quantum (mmol/s-sq m)	0	0	0
Resistance (s/cm)	28.5	19.7	35.1
Transpir (mg-sq cm/s)	0.517	0.712	0.418
Comments			

Plant:
Prosopis
Time 09:00

	Sample 5
Aperature Set (sq cm)	1.5
Chamber Temp (C)	27
Leaf Temp (C)	26.5
Rel. Humidity (%)	12.4
Quantum (mmol/s-sq m)	1100
Resistance (s/cm)	1.8
Transpir (mg-sq cm/s)	10.8
Comments	

Plant:
Abronia
Annual
Time 13:15

	Sample 1	Sample 2	Sample 3	Sample 4
Aperature Set (sq cm)	3	2	2	2
Chamber Temp (C)	36	36.8	36.8	37
Leaf Temp (C)	36.1	36.7	36.6	36.8
Rel. Humidity (%)	10	10	10.4	10.4
Quantum (mmol/s-sq m)	1990	1920	1490	1500
Resistance (s/cm)	3.01	2.08	1.69	1.47
Transpir (mg-sq cm/s)	11.83	17.36	10.92	24.01
Comments				

Plant:
Abronia
Time 16:30

	Sample 1	Sample 2	Sample 3
Aperature Set (sq cm)	3	2	2
Chamber Temp (C)	35	35.2	35.2
Leaf Temp (C)	34.9	35.1	35.1
Rel. Humidity (%)	11.6	10.8	11.2
Quantum(mmol/s-sq m)	1300	1520	1890
Resistance (s/cm)	1.97	2.21	1.53
Transpir (mg-sq cm/s)	16.28	14.92	20.85
Comments			

Plant:
Abronia
Time 05:45

	Sample 1	Sample 2	Sample 3
Aperature Set (sq cm)	2	2	2
Chamber Temp (C)	18.8	19	19.6
Leaf Temp (C)	18.8	19	19.6
Rel. Humidity (%)	20.4	20	20
Quantum(mmol/s-sq m)	0	0	0
Resistance (s/cm)	7.29	10.6	12.3
Transpir (mg-sq cm/s)	1.723	1.214	1.087
Comments			

Plant:
Abronia

Time 09:00	Sample 1	Sample 2	Sample 3	Sample 4
Aperature Set (sq cm)	2	2	2	2
Chamber Temp (C)	28.8	28.8	29	29.2
Leaf Temp (C)	28.7	28.7	29	29.2
Rel. Humidity (%)	12.8	12.8	12.8	13.2
Quantum(mmol/s-sq m)	1350	1730	800	1420
Resistance (s/cm)	2.09	2.01	2.23	2.05
Transpir (mg-sq cm/s)	10.91	11.3	10.51	11.43
Comments				

Plant:
Abronia

Time 09:00	Sample 5	Sample 6
Aperature Set (sq cm)	2	2
Chamber Temp (C)	28.8	29.2
Leaf Temp (C)	28.7	29.2
Rel. Humidity (%)	13.2	13.2
Quantum(mmol/s-sq m)	370	1060
Resistance (s/cm)	1.81	1.95
Transpir (mg-sq cm/s)	12.39	11.98
Comments		

Stem Samples Taken for Leaf Area Calibration
Dalea

Time Sample	1115 Initial Weight	Final Weight	% Lost
1	0.03525	0.033	6.67
2	0.0302	0.02822	7.02
3	0.02615	0.02524	3.57
4	0.07797	0.0745	4.66
5	0.02734	0.02608	4.83
6	0.05841	0.05399	8.17
7	0.01553	0.01481	4.73
8	0.02616	0.02424	7.93

Portable Pressure Bomb
July 25-26, 1986
Sevilleta National Wildlife Refuge

Time	11:00			
Plant	Dalea	Prosopis	Abronia	Dithyrea
Pressure (bars)	17	19	8	13
	16	29	8	9
	17	20	5	12
	13	17		13
		28		

Time	13:15			
Plant	Dalea	Prosopis	Abronia	Atroplex
Pressure (bars)	23	25	9	29
	19	25.5	9	33
	23	27	10	32
	21	25	9	30.5
	19	30	9	28

Time	16:30			
Plant	Dalea	Prosopis	Abronia	Atroplex
Pressure (bars)	20	25	4	27
	21	24	9	33
	16	26	11	30
	18	24	9	31
	19			30

Time	05:45		
Plant	Dalea	Prosopis	Abronia
Pressure (bars)	6	9	5.5
	6	11	6
	9	11	3
	8	7	
	7	7	
	9	8	

Time	10:15			
Plant	Dalea	Prosopis	Abronia	Rabbitbrush
Pressure (bars)	24	24	9	24
	23	24	9.5	
	22	31	9.5	
	20	32	8.5	
	19	29	10	
	17	24	9	
	18			